

UNDERSTANDING ADIPOKINE SECRETION AND ADIPOCYTE-MACROPHAGE
CELLULAR INTERACTIONS, IN SEARCH FOR THE MOLECULAR BASIS OF INSULIN
SENSITIVITY AND RESISTANCE

by

LINGLIN XIE

M. D., Tongji Medical University, 2000
M. S., Kansas State University, 2004

AN ABSTRACT OF A DISSERTATION

submitted in partial fulfillment of the requirements for the degree

DOCTOR OF PHILOSOPHY

Division of Biology
College of Arts and Sciences

KANSAS STATE UNIVERSITY
Manhattan, Kansas

2008

Abstract

My work focused on understanding adipocyte function and regulation because of the importance to diabetes. In addition to being a fat storage depot, adipose tissue is an endocrine tissue. Adiponectin and leptin are two adipokines that control insulin sensitivity and energy balance. In spite of their importance, there are still questions about their secretion. I hypothesized that leptin and adiponectin follow different secretory routes. I found adiponectin localized in Golgi and the *trans* Golgi Network, while leptin mostly localized in ER during basal metabolisms. Common requirements for their secretion were the presence of class III Arf proteins and an intact Golgi apparatus, since BFA treatment inhibited secretion of both adiponectin and leptin. I found that trafficking of adiponectin is dependent on GGA1 coated vesicles. Endosomal inactivation significantly reduced adiponectin, but not leptin, secretion in both 3T3L1 and isolated rat adipocytes. Also, adiponectin, but not leptin, secretion was reduced in cells expressing non- functional form of Rab11 and Rab5 proteins. However, secretion of leptin, but not adiponectin was inhibited in cells expressing mutants of Protein Kinase D1. These results suggest that leptin and adiponectin secretion involve distinct intracellular compartments and pathways.

Insulin resistance is associated with macrophage infiltration into adipose tissue and elevated levels of IL-6, TNF- α and IL-1 β . Therefore, the second part of my dissertation tested the hypothesis that the interaction of macrophages and adipocytes causes insulin resistance. To test this hypothesis, I co-cultured macrophages and adipocytes. I found that mouse elicited peritoneal macrophages significantly decreased insulin-stimulated GLUT4 translocation to the

plasma membrane in a contact-independent manner. IL-6 was the most inhibitory cytokine in reducing GLUT4 translocation, GLUT4 expression, Akt phosphorylation and reducing adipocyte differentiation compared to TNF- α and IL-1 β . These data suggest that IL-6 is the most effective cytokine secreted by macrophages involved in insulin resistance. Lastly, I tested the impact of adipocytes on macrophage differentiation *in vitro* and *in vivo*. I found that C2D macrophages isolated from the peritoneal cavity had increased IL-6 transcript levels after co-culture with 3T3L1 adipocytes *in vitro*. After *i.p.* injection, C2D macrophages isolated from WAT increased expression of mature macrophage surface markers and transcript levels of proinflammatory cytokines compared to C2D cells *in vitro*. However, macrophages isolated from BAT expressed low levels of cytokines and macrophage surface markers.

UNDERSTANDING ADIPOKINE SECRETION AND ADIPOCYTE-MACROPHAGE
CELLULAR INTERACTIONS, IN SEARCH FOR THE MOLECULAR BASIS OF INSULIN
SENSITIVITY AND RESISTANCE

by

LINGLIN XIE

M. D., Tongji Medical University, 2000
M. S., Kansas State University, 2004

A DISSERTATION

submitted in partial fulfillment of the requirements for the degree

DOCTOR OF PHILOSOPHY

Division of Biology
College of Arts and Sciences

KANSAS STATE UNIVERSITY
Manhattan, Kansas

2008

Approved by:

Major Professor
Silvia Mora, Stephen K. Chapes

Abstract

My work focused on understanding adipocyte function and regulation because of the importance to diabetes. In addition to being a fat storage depot, adipose tissue is an endocrine tissue. Adiponectin and leptin are two adipokines that control insulin sensitivity and energy balance. In spite of their importance, there are still questions about their secretion. I hypothesized that leptin and adiponectin follow different secretory routes. I found adiponectin localized in Golgi and the *trans* Golgi Network, while leptin mostly localized in ER during basal metabolisms. Common requirements for their secretion were the presence of class III Arf proteins and an intact Golgi apparatus, since BFA treatment inhibited secretion of both adiponectin and leptin. I found that trafficking of adiponectin is dependent on GGA1 coated vesicles. Endosomal inactivation significantly reduced adiponectin, but not leptin, secretion in both 3T3L1 and isolated rat adipocytes. Also, adiponectin, but not leptin, secretion was reduced in cells expressing non-functional form of Rab11 and Rab5 proteins. However, secretion of leptin, but not adiponectin was inhibited in cells expressing mutants of Protein Kinase D1. These results suggest that leptin and adiponectin secretion involve distinct intracellular compartments and pathways.

Insulin resistance is associated with macrophage infiltration into adipose tissue and elevated levels of IL-6, TNF- α and IL-1 β . Therefore, the second part of my dissertation tested the hypothesis that the interaction of macrophages and adipocytes causes insulin resistance. To test this hypothesis, I co-cultured macrophages and adipocytes. I found that mouse elicited peritoneal macrophages significantly decreased insulin-stimulated GLUT4 translocation to the plasma membrane in a contact-independent manner. IL-6 was the most inhibitory cytokine in

reducing GLUT4 translocation, GLUT4 expression, Akt phosphorylation and reducing adipocyte differentiation compared to TNF- α and IL-1 β . These data suggest that IL-6 is the most effective cytokine secreted by macrophages involved in insulin resistance. Lastly, I tested the impact of adipocytes on macrophage differentiation *in vitro* and *in vivo*. I found that C2D macrophages isolated from the peritoneal cavity had increased IL-6 transcript levels after co-culture with 3T3L1 adipocytes *in vitro*. After *i.p.* injection, C2D macrophages isolated from WAT increased expression of mature macrophage surface markers and transcript levels of proinflammatory cytokines compared to C2D cells *in vitro*. However, macrophages isolated from BAT expressed low levels of cytokines and macrophage surface markers.

Table of Contents

TABLE OF CONTENTS.....	vii
LIST OF FIGURES	x
LIST OF TABLES	xii
ACKNOWLEDGEMENTS.....	xiii
CHAPTER 1 - Introduction	1
1. Diabetes.....	2
1.1 Classification of diabetes mellitus	2
1.1.1 Type 1 diabetes mellitus	2
1.1.2 Type 2 diabetes mellitus	3
1.1.3 Gestational diabetes mellitus	3
1.1.4 Other specific types of diabetes	4
1.2 Diabetes complications	4
1.3 Insulin	4
1.4 Glucose transporter proteins	6
1.4.1 Sodium-dependent glucose transporters (SGLT).....	6
1.4.2 Facilitative glucose transporters	6
1.4.2.1 Classification.....	6
1.4.2.2 Glucose uptake transporter 4 (GLUT4).....	7
1.4.3 insulin signaling in GLUT4 translocation.....	8
1.4.3.1 PI3K-dependent pathway.....	8
1.4.3.2 PI3K-independent pathway.....	11
2. Adipocytes as endocrine cells.....	12
2.1 White adipose tissue (WAT) vs. brown adipose tissue (BAT)	12
2.2 Adipocyte secreted hormones	14
2.2.1 Adiponectin	14
2.2.2 Leptin.....	18
2.2.3 Resistin	21
2.2.4 Visfatin	22

3. Role of macrophages and their interactions with adipocytes.....	23
3.1 Insulin resistance: an inflammatory disease.....	23
3.2 Characteristics of adipose tissue macrophages	24
3.3 Important cytokines involved in insulin resistance.....	25
3.3.1 TNF- α	26
3.3.2 IL-6	27
3.3.3 IL-1 β	29
3.4 Macrophage and adipocyte differentiation	30
4. Intracellular trafficking	31
4.1 Transport from the ER through the Golgi apparatus.....	32
4.1.1 Arf proteins	33
4.2 Transport from the <i>Trans</i> Golgi Nextwork (TGN) to the cell exterior.....	34
4.2.1 GGA proteins	35
4.2.2 Rab proteins	36
4.3 Constitutively vs. regulated secretory pathway in adipocytes.....	38
4.3.1 Regulated secretory pathway in adipocytes: intracellular trafficking of GLUT4	38
4.3.2 Constitutively secretory pathway in adipocytes: intracellular trafficking of leptin..	40
.....	40
CHAPTER 2 – Intracellular trafficking and secretion is dependent on	
GGA coated vesicles	42
Abstract	43
Introduction.....	44
Experimental procedures	47
Results.....	51
Discussion	67
CHAPTER 3 - Adiponectin and leptin are secreted through distinct	
trafficking pathways in adipocytes	69
Abstract	70
Introduction.....	71
Materials and Methods.....	74
Results.....	77

Discussion	93
CHAPTER 4 – Macrophage-derived IL-6 alters GLUT4 in adipocytes.....	98
Abstract	99
Introduction.....	100
Materials and Methods.....	102
Results.....	107
Discussion	125
CHAPTER 5 – Phenotypic conversation of C2D macrophage cells in brown and white adipose tissues.....	131
Abstract	132
Introduction.....	133
Materials and Methods.....	135
Results.....	141
Discussion	143
CHAPTER 6 – Future prospective.....	159
REFERENCE CITED	162

List of Figures

Figure 1 PI3K pathway involved in GLUT4 translocation.....	16
Figure 2 Localization of endogenous adiponectin in the Golgi/TGN.....	52
Figure 3 Adiponectin colocalizes with the vesicular stomatitis virus G protein	53
Figure 4 Secretion of adiponectin is inhibited by brefeldin A but not by cycloheximide.....	55
Figure 5 Colocalization of GGA proteins and endogenous adiponectin in adipocytes.....	57
Figure 6 Colocalization of GGA proteins and adiponectin.	59
Figure 7 Recombinant GGA1, but not GGA2 or GGA3, binds to adiponectin-containing vesicles.....	61
Figure 8 Mutants of GGA1 inhibits adiponectin secretion.....	62
Figure 9 Localization of adiponectin and leptin in 3T3L1 adipocytes.....	79
Figure 10 Adiponectin and leptin secretion are inhibited by BFA.	81
Figure 11 Secretion of adiponectin but not leptin is inhibited by endosomal inactivation.....	83
Figure 12 Adiponectin colocalizes with endosomal markers.	86
Figure 13 Expression of rab5 and rab11 mutants inhibit adiponectin secretion in 3T3L1 cells..	89
Figure 14 Secretion of leptin, but not adiponectin is inhibited by a mutant of PKD1.....	91
Figure 15 Detection of GLUT4 in 3T3L1 adipocytes.	108
Figure 16 Macrophages inhibit insulin-stimulated translocation of GLUT4 but not GLUT1....	110
Figure 17 3T3L1 adipocyte <i>GLUT4</i> transcription is inhibited by macrophages.	113
Figure 18 Secretion of TNF- α , IL-6 and IL-1 β in macrophage and 3T3L1 adipocytes co-cultures.	115
Figure 19 Effects of TNF- α , IL-6 and IL-1 β on insulin-stimulated GLUT4 translocation.....	116
Figure 20 Effects of TNF- α , IL-6 and IL-1 β on <i>GLUT4</i> gene transcription.	118
Figure 21 Effects of TNF- α , IL-6 and IL-1 β on GLUT4 protein expression.	119
Figure 22 TNF- α , IL-6 and IL-1 β affect Akt phosphorylation differently.	121
Figure 23 TNF- α , IL-6 and IL-1 β on 3T3L1 adipocyte differentiation.	122
Figure 24 Phenotype changes of C2D macrophage cells co-cultured with adipocytes or pre-adipocytes <i>in vitro</i>	142
Figure 25 Transcription of proinflammatory cytokine genes in C2D macrophage cells co-cultured with adipocytes or pre-adipocytes <i>in vitro</i>	144

Figure 26 Change in C2D macrophage cell morphology during co-cultured with adipocytes or pre-adipocytes <i>in vitro</i> and C2D macrophage cells infiltration into BAT or WAT <i>in vivo</i> into BAT or WAT <i>in vivo</i>	146
Figure 27 Phenotype changes in Peritoneal C2D macrophage cells isolated from WAT or BAT <i>in vivo</i> after <i>i.p.</i> adoptive transfer.....	149
Figure 28 Gene transcript modification in Peritoneal C2D macrophage cells infiltrated into WAT or BAT <i>in vivo</i> . . .	151

List of Tables

Table 1. Antibodies used for flow cytometry analysis (Chapter 5)	138
Table 2 Primers of RT-PCR(Chapter 5)	139
Table 3. Comparison of M1 and M2 macrophage markers in C2D macrophage cells after isolation from C57BL/6J mouse tissue.....	152

Acknowledgements

This dissertation could never have been completed without the help and support of a variety of individuals. I would like to thank Dr. Silvia Mora and Dr. Chapes, my major professors, for their insightful advising and guidance during my Ph.D study. They were always so patient and understanding. Whenever I had problems in my research, they were there to help.

I greatly appreciate Dr. Weiqun Wang, my outside chair of Ph.D committee and my master's advisor, for his continuous help and encouragement during my graduate study. I sincerely thank my committee members Dr. Gary Conrad and Dr. Dolores Takemoto for their invaluable advice and guidance. I would like to thank Dr. Anna Zolkiewska, for her reading and comments on my dissertation.

I would like to thank my colleagues in Dr.Chapes' and Dr.Mora's Labs. Without the help from Betsy Potts, Dr. Teresa Ortega, Cormac P. O'Reilly, Alison Fedrow, Shengzhi Wang, Anisha Gupte, Dr. Ke An and Whitney Mordica, the accomplishment of this dissertation would have been more difficult. I also thank Dr. Dan Boyle and Mrs. Tammy Koopman for their technique support with the confocal microscope and the flow cytometry.

I thank the Division of Biology for the financial support and the research training and the teaching experience. I am broadened in my experience for having attending various courses, seminars and meetings in the Division of Biology. I greatly appreciate the support of Dr. Brian S. Spooner and Dr. David Rintoul. Several fellow graduate students also provided support during the projects; I thank them all.

Above all, I thank my parents, Professor Ruihe Xie and Professor Qiuhua Gao; my brother, Dr. Yongzhe Xie and my husband, Ke Zhang, for their love and unwavering support.

CHAPTER 1

INTRODUCTION

1. Diabetes

Diabetes is a serious health problem all over the world. More than 171 million people have diabetes, and its prevalence is expected to reach 366 million by 2025 [1]. According to the National Estimates on Diabetes for 2005, there are 20.8 million children and adults or 7% of the population, who have diabetes. About 14.6 million have been diagnosed with diabetes; but 6.2 million people (or nearly one-third) are undiagnosed [2]. People with diabetes are at high risk of heart failure [3, 4], stroke [5, 6], retinopathy [7], chronic kidney disease [3, 8] and other associated disorders affecting the microvascular like diabetic foot [8-10].

1.1 Classification of diabetes mellitus

There are three major types of diabetes mellitus: Type 1 diabetes, Type 2 diabetes, and gestational diabetes.

1.1.1 Type 1 diabetes mellitus:

Type 1 diabetes mellitus (juvenile onset, T1DM) results from the body's failure to produce insulin. It results from combined genetic and environmental factors that affect the immune system and destroys the patient's insulin producing beta cells [11-13]. The lack of insulin leads to hyperglycemia and its devastating complications, including cardiovascular disease, blindness and kidney failure [12]. It is estimated that 5-10% of Americans who are diagnosed with diabetes have T1DM [12]. T1DM accounts for the majority of childhood diabetes. The American Diabetes Association (ADA) has proposed to classify diabetes with type 1A diabetes representing islet cell with the presence of autoantibodies mediating diabetes and type 1B representing a non-autoimmune associated form of type 1 diabetes [12, 14]. The best current marker for T1DM is the presence of three autoantibodies that are specific for glutamic acid decarboxylase (GAD65), insulin and insulinoma antigen-2 [14, 15]. Type 1A diabetes is

found most strongly associated with HLA DR and DQ loci in the class II region of the major histocompatibility complex [13]. Since the MHC-II region controls antigen presentation, T1DM is believed caused by antigen presentation to CD4⁺ cells, thymic selection and immune responsiveness [11, 15].

1.1.2 Type 2 diabetes mellitus

Type 2 diabetes (T2DM) results from insulin resistance combined with insulin deficiency. T2DM is found mostly in adults; however, the average age range of diabetics has been decreasing because of earlier screening. This epidemic has been associated with obesity and inactivity in children [16]. T2DM is now diagnosed in both adolescents and children. The mechanisms underlying T2DM are not fully understood, but it is believed to be a multi-factorial disorder. The more risk factors an individual has, the greater his/her likelihood of developing T2DM. Obesity is one of the high risk factors. Over 90% of persons with T2DM are overweight [16]. The Body Mass Index (BMI) is widely accepted as a prediction of T2DM. A BMI greater than 27 indicates a risk for developing type 2 diabetes. An apple-shaped figure of individuals who carry most of their weight in the trunk of their bodies is also considered a risk factor for T2DM [17]. Age increases the risk of T2DM. Rate of diabetes in those aged 65 and over (10.4%) is two times higher than the rate in those 35 to 64 (3.2%) [17]. A sedentary life style also increased the risk; however, regular physical activity improved blood glucose control in T2DM patients [17]. Other risk factors are family history of T2DM, history of gestational diabetes, ethnic ancestry, high blood pressure and high cholesterol or fats in blood [17].

1.1.3 Gestational diabetes mellitus

Gestational diabetes (GDM) occurs during pregnancy and affects about 12% of all pregnant women. There are approximately 135,000 cases in the United States each year, but the

symptoms resolve after pregnancy in about 90% of those women [18]. Women with a history of GDM have a higher risk of type II diabetes and higher frequency of reoccurrences of GDM in subsequent pregnancies [19]. The Australasian Carbohydrate Intolerance Study (ACHOIS) revealed that a quarter of the babies whose mothers had GDM without proper treatment, died and another 25% suffered with birth injury [20]. However, the hyperglycemia and hyperinsulinemia were corrected, the incidence of death and birth defects decreased to almost none [20]. The underlying mechanisms of GDM are not clear. However, a defect in pancreatic β cell function is consistently found in women with prior GDM [21]. Potential causes of inadequate β cell function are complex and are not fully understood. It may be related to the presence of autoantibodies specific for islet cells [21, 22], mutations in genes coding for some key proteins [23-25] like insulin promoter factor 1 [25-27] or hepatocyte nuclear factor 1 α [25, 28].

1.1.4 Other specific types of diabetes

Other diabetes, not classified into the above three categories are diagnosed as “other specific types of diabetes”. These syndromes can be related to genetic defects of β -cell function and insulin action, endocrinopathies, destruction of the pancreas by drugs or chemicals, infections or rare forms of immune-linked diabetes (*e.g.* Stiff-Person-syndrome)[2].

1.2 Diabetic complications

The burden of diabetes relates more to the complications associated with the disease than to its associated metabolic derangements. These include retinopathy, nephropathy, neuropathy and, most commonly, cardiovascular complications. Two of the most important risk factors for diabetic complications are hyperglycemia and elevated blood pressure caused by microvascular abnormalities [29, 30].

1.3 Insulin

Insulin is a key hormone in the body that regulates glucose and fatty acid metabolism. In mammals, insulin is synthesized in the pancreas within the β -cells of the islets of Langerhans. Insulin is composed of 51 amino acid residues and has a molecular weight of 5.8 kDa. The structure of insulin is highly conserved in mammals. Bovine insulin differs by 3 residues different from human insulin and by one residue different from porcine insulin [31]. Insulin is composed of two polypeptide chains, A and B. The integrity of the three native disulfides of insulin: CysA6-CysA11, CysA7-CysB7, CysA20-CysB19 are critical to insulin's biological activity [32]. Breakage or disarrangement of any of the three disulfide bonds leads to the loss of function of insulin.

Insulin binds to the insulin receptor to induce its biological function. The N-terminal α -helix of the insulin A-chain is a site with high affinity to the insulin receptor [33]. The second binding site is ValB12 and TyrB16 of the B-chain α -helix with the N-terminal of the α subunit of insulin receptor [34]. The binding of insulin to the insulin receptor triggers significant biochemical activity inside of the cell. These include: increased glycogen synthesis, increased fatty acid synthesis, decreased oxidation, decreased proteinolysis and lipolysis, decreased gluconeogenesis and it can induce DNA replication, gene transcription and protein synthesis [34].

In humans, skeletal muscle cells and adipocytes are the major cells involved in insulin-dependent glucose uptake. Binding of insulin to the insulin receptor in the skeletal muscle and adipocytes leads to activation of the AMP-activated protein kinase (AMPK) pathway that stimulates fatty acid β -oxidation and more importantly the activation of Phosphoinositide-3 kinase (PI3K) pathway that mobilizes glucose transporter proteins, such as GLUT4, to the plasma membrane [35-37].

1.4 Glucose transporter proteins

Glucose transporter proteins are integral proteins that transfer glucose across the plasma membrane into cells. The transporters are categorized into two distinct groups according to their structures and functions, the Na⁺-dependent glucose co-transporters (SGLT) [38] and the facilitative Na⁺-independent sugar transporters (GLUT family) [39, 40].

1.4.1 Sodium-dependent glucose transporters (SGLT)

SGLT transport glucose via a secondary active transport mechanism. Glucose transportation is coupled with the Na⁺ influx via a Na⁺-K⁺ ATPase pump that works against a concentration gradient [40]. This process occurs on the lumen of the small intestine and in the proximal tubules of kidneys [40]. There are three types of SGLT: SGLT1 and SGLT3 are found expressed in the lumen of the small intestine and SGLT2 is expressed in the proximal tubules of kidney [40].

1.4.2 Facilitative glucose transporters

The facilitative GLUT transporters transfer glucose by a diffusion gradient of glucose (and other sugars) across the plasma membranes [41]. GLUT1 was the first GLUT molecule to be isolated and this family now encompasses thirteen members [41]. All 13 members share a representing three-dimensional structural similarity. Their predicted structure has twelve transmembrane regions and both the N-terminal and the C-terminal are localized intracellularly [41].

1.4.2.1 Classification

Based on the sequence alignment of all GLUT members, they have been classified into three subclasses [41]. The class I facilitative transporters contain GLUT1–4. All four members

have been comprehensively studied in terms of structure, function and tissue distribution [41]. The class II family of facilitative transporters is composed of the fructose transporter (GLUT5), and also includes GLUT7, GLUT9, which has not yet been functionally characterized, and GLUT11 [40]. The class III group has five members: GLUT6, GLUT8, GLUT10, GLUT12 and HMIT [40].

1.4.2.2 Glucose uptake transporter 4 (GLUT4)

GLUT4 belongs to the class I facilitative transporters family [40]. It is expressed in heart, skeletal muscle and adipose tissue. During basal metabolism, GLUT4 cycles between the intracellular storage compartment and the plasma membrane. It has been estimated that more than 90% of the protein resides intracellularly [42-46]. Confocal microscopy demonstrated that GLUT4 localized at tubulo-vesicular structures in the perinuclear region and in distinct foci throughout the cytosol [43, 47]. GLUT4 has been partially localized in the Golgi compartment [48], the trans-Golgi network [48] and in the recycling endosome compartment (ERC) [43]. The non- ERC pool of GLUT4 is known as the GLUT4 storage vesicles (GSV). Details about GLUT4 storage and trafficking will be discussed later. GSV are quickly mobilized to the cell surface after insulin stimulation. The formation of GSV is dependent on the Golgi-localized γ -ear-containing Arf-binding protein (GGA) and sortilin [49-51]. Mutations in GGA blocked the formation of the GSV and inhibited insulin-stimulated glucose uptake in adipocytes [51].

GLUT4 mediates insulin induced glucose uptake into skeletal muscle, cardiac muscle and adipose tissue. There is a general agreement that insulin largely promotes GLUT4 exocytosis, and to a lesser extent, reduces GLUT4 endocytosis [44, 52]. It has been challenging to define the biochemical nature of the “specialized compartment or GLUT4 storage vesicle” (SC/GSV) upon insulin stimulation. The insulin-responsive aminopeptidase (IRAP) co-localized with GLUT4

and also moved to the cell surface with insulin stimulation [53]. Another protein associated with GLUT4 is vesicle-associated membrane protein 2 (VAMP2). It is a vesicular soluble *N*-ethylmaleimide-sensitive factor attachment protein receptor (v-SNARE) that is exclusively required for GLUT4 fusion with the membrane after the insulin-stimulation [48].

Defects in GLUT4 are closely associated with insulin resistance. Animal and human diabetic models exhibit reduced expression of GLUT4 in adipose tissue, but not in muscle [54]; however, in models where GLUT4 translocation is impaired upon insulin stimulation, it was impaired in both adipose tissue and skeletal muscle [55]. Male mice heterozygous for a GLUT4 mutation (GLUT4 +/-) exhibited a decrease in GLUT4 expression in adipose tissue and skeletal muscle. This reduction caused increased serum glucose and insulin, reduced muscle glucose uptake, hypertension, and diabetic histopathologies in the heart and liver similar to humans with non-insulin-dependent diabetes mellitus (NIDDM) in the absence of obesity [56-59]. Interestingly, adipose-specific GLUT4 is thought very important in regulating glucose homeostasis and it affects insulin sensitivity in other tissues. Overexpression of GLUT4 in fat not only normalized fasting hyperglycemia and glucose intolerance, but it also reversed the enhanced clearance of an oral lipid load in muscle specific GLUT4 knockout mice [60].

1.4.2. Insulin signaling in GLUT4 translocation

1.4.2.1 PI3K dependent pathway

Engagement of insulin with its receptor triggers a cascade of tyrosine phosphorylation events that ultimately promote the translocation of GLUT4-containing vesicles from the intracellular storage pool to the cell surface [32, 61]. The insulin-receptor is composed of two α and two β chains, which are linked by disulfide bonds. The α chains are entirely extracellular and bind to insulin. The linked β chains span the membrane. Binding of insulin to the α chains

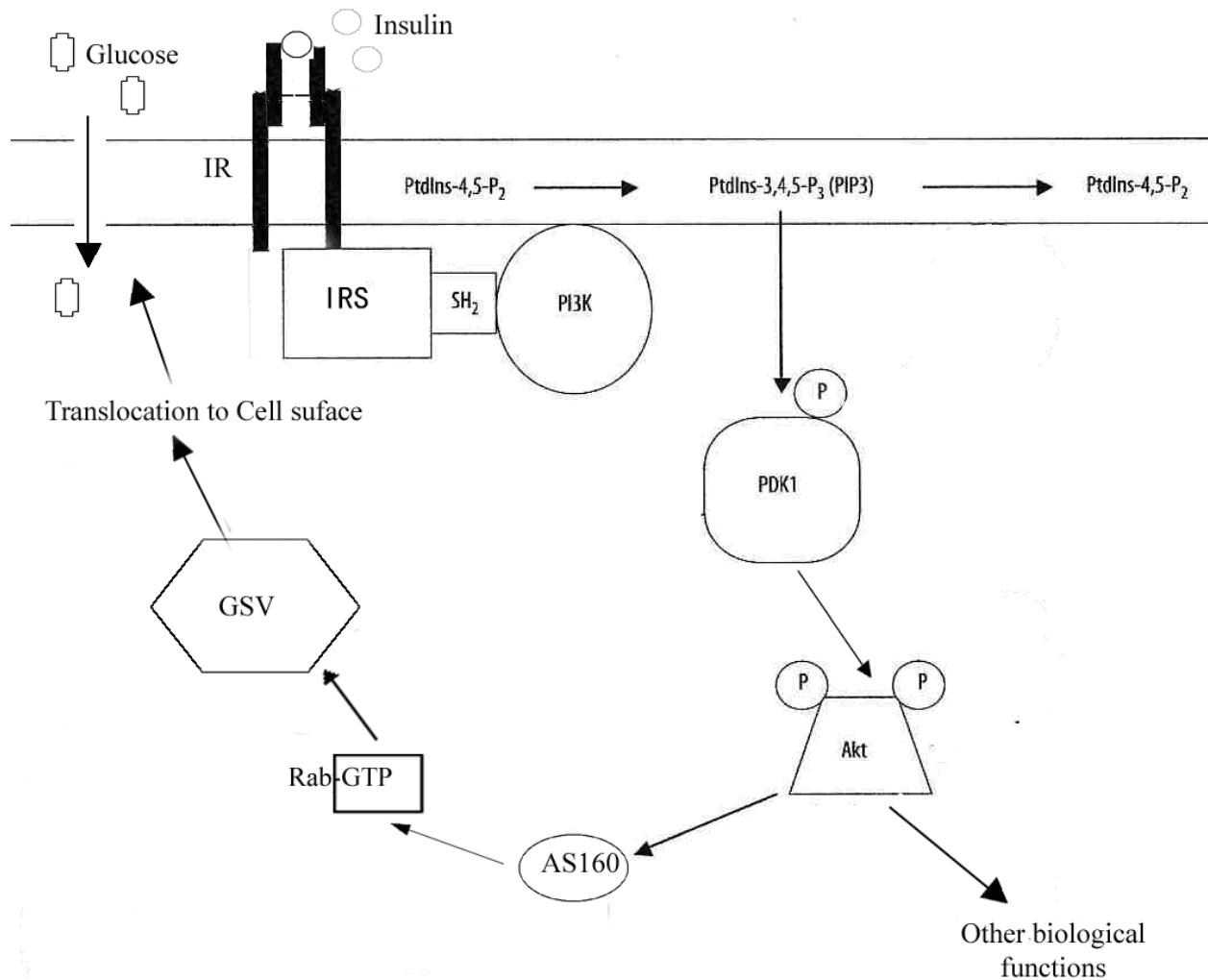


Figure 1. PI3K pathway involved in GLUT4 translocation. Insulin binding to insulin receptor triggers tyrosine phosphorylation of IRS. The SH₂ domain of IRS binds to and activates PI3K, which phosphorylates PI-4,5-P₂ and forms PI-3,4,5-P₃. PI-3,4,5-P₃ phosphorylates Akt at serine 437 and parallels the phosphorylation of PDK1. Akt is subsequently phosphorylate Thr308 and is released. Akt then phosphorylates its substrate, AS160 and the inhibitory of GLUT4 vesicles is released. GLUT4 is translocated to the plasma membrane and uptake glucose.

leads to autophosphorylation of tyrosine 972, and activates the intrinsic tyrosine kinase activity of the β subunits [32, 61].

GTP is dismissed. GLUT4 vesicles are thus able to translocate GLUT4 to the plasma membrane and uptake glucose.

Phosphorylation of the insulin receptor activates substrate proteins from the insulin receptor substrate family including IRS proteins (IRS-1,-2, 3,-4,-5 and -6), Gab-1, Shc, and others [32]. Insulin-dependent tyrosine phosphorylation of IRS-1/2 creates docking sites for downstream effector molecules including Class IA phosphatidylinositol 3-kinase (PI3K). This protein is composed of a p85 regulatory subunit and a p110 catalytic subunit. The p85 subunit binds to the Src homology 2 (SH2) domain of IRS, and activates the p110 catalytic domain. Activated PI-3K then phosphorylates PI-4,5-P₂ and forms PI-3,4,5-P₃, which is important to the translocation of GLUT4 [32]. Formation of PI-3,4,5-P₃ provides a docking site to Akt (Protein kinase B, PKB) via its pleckstrin homology (PH) domain and leads to the phosphorylation of serine 473 (ser 473). This phosphorylation parallels the phosphorylation of phosphoinositide-dependent-kinase-1 (PDK1), which promotes the interaction between Akt and PDK1. Thr308 subsequently is phosphorylated and Akt is then released [32].

There are three isoforms of Akt: Akt-1, -2 and -3 [62]. Bae et al. reported that Akt2/PKB was the major isoform involved in insulin-stimulated GLUT4 translocation [62, 63]. Akt2 binds with GLUT4-GSV during basal metabolism and the association increased with insulin stimulation in response to Akt2 phosphorylation [63].

AS160 is a substrate of Akt. AS160 is expressed in cultured adipocytes and murine skeletal muscle [48]. AS160 contains a GTPase activating domain (GAP) for Rab proteins, which also binds with insulin-stimulated GLUT4-GSV. Thus, AS160 might mediate the signal

between Akt and GLUT4-GSV trafficking. AS160 is also an inhibitor of basal GLUT4-GSV exocytosis [64, 65]. In the basal state, AS160 associates with GTPase Activating Protein (GAP), which binds Rabs and maintains them in an inactivated form [65]. AS160 also contains two phosphotyrosine-binding domains and multiple putative phosphorylation sites, including six phospho-Akt substrate (PAS) motifs, which targeted by Akt, AMPK, or other upstream kinases [66]. Upon insulin stimulation, AS160 is rapidly phosphorylated at PAS motifs [67] and dissociates from GLUT4 vesicles [64], thus accelerate the translocation of GLUT4. Goodyear's group studied the effects of wild type and mutant AS160 on basal and insulin- and contraction-stimulated glucose uptake in mouse skeletal muscle *in vivo*. They demonstrated that AS160 phosphorylation at PAS motifs was required for full insulin- and contraction-stimulated glucose uptake in mouse skeletal muscle and AS160 directly regulated insulin- and contraction-stimulated uptake in mouse skeletal muscle [68].

1.4.2.2 PI3K-independent pathway

A second pathway important to insulin stimulation is the Cbl /CAP dependent pathway [69, 70]. Mora's group found Cbl pathway components present in murine heart, adipose tissue, skeletal muscle, cultured L6 myotubes and 3T3L1 adipocytes [71].

Cbl and the adaptor protein CAP are recruited to the plasma membrane after the phosphorylation of APS (adaptor with pleckstrin homology (PH) and Src homology-2 (SH2) domains) on a tyrosine residue [61, 72]. Once phosphorylated by the receptor, Cbl-associated protein (CAP) binds to Cbl and targets Cbl to the lipid raft microdomains in the plasma membrane. Cbl/CAP recruit CrkII and the guanyl nucleotide exchange factor C3G to the lipid raft and provide a docking site to them. C3G then activates the small GTP binding protein TC10.

Activation of TC10 leads to cytoskeletal rearrangement, which is essential for the insulin-stimulated GLUT4 translocation [61, 72].

The importance of Cbl/CAP pathway in regulating GLUT4 translocation is controversial. Knock down of CAP; Cbl and CrkII by RNAi suggested that this pathway was not required for GLUT4 translocation [73]. Others, including the Mora lab, have indicated that Cbl pathway plays an important role in whole body glucose homeostasis through insulin action. Mora's group has reported that Cbl/CAP/TC10 pathway is activated in murine cardiac muscle and is impaired during obesity and insulin deficiency [71].

2. Adipocytes as endocrine cells

2.1 White adipose tissue (WAT) versus brown adipose tissue (BAT)

There are two different types of adipose tissue, white and brown. WAT and BAT (white and brown adipose tissue respectively) are normally localized in anatomically distinct areas in rodents [74]. The morphology of WAT and BAT adipocytes are very different. White adipocyte contains a scant ring of cytoplasm surrounding a single large lipid droplet, while brown adipocyte contains multiple lipid droplets of varying size and has high numbers of mitochondria packed with cristae [74].

WAT is an energy store organ as well as an endocrine organ [75, 76], which will be discussed next. BAT is commonly called 'baby fat' as it is present in babies and comprises up to 5% of body weight but diminishes with age and virtually disappears by adulthood [77]. Brown fat is of particular importance in neonates, small mammals in cold environments, and animals that hibernate, because it stores energy as heat [77]. Uncoupling protein 1 (UCP1) is the key protein that regulates thermogenic capacity of BAT, which can uncouple oxidative phosphorylation and utilize substrates to generate heat rather than ATP [78]. BAT is primarily

localized around the organs. Brown adipocytes are electrically coupled via gap junctions and highly vascularized with high blood flow rates for the requirement of the brain, spinal cord, heart, lungs and kidneys during cold stress [79].

Despite the distinct function between BAT and WAT, there are linkages between them. BAT is transformed into WAT during development, and WAT instead, can be turned into BAT in certain situation. Adenovirus-mediated expression of human PGC-1 alpha increased the expression of UCP1, respiratory chain proteins, and fatty acid oxidation enzymes in human subcutaneous white adipocytes. Therefore, these adipocytes acquired typical features of brown fat cells [80, 81]. In another study, after 14 days of hyperleptinemia induced by adenovirus, adipocytes became shrunken, fatless, and encased in a thick basement-membrane-like matrix. Gene expression of UCP-1 and -2 were increased and lipid-enzymes were down-regulated [82]. Long time treatment of β -carotene increased UCP-1 expression [83] and hypertrophy of WAT in a dose-dependent manner [84]. Thus, conversation of BAT from WAT has been regarded as a new stratagem for diabetes and obesity therapy.

There is evidence to show that BAT has an anti-obesity function. Hamann et al showed increased body weight and increased expression of TNF- α and decreased expression of GLUT4 in WAT of uncoupling protein-diphtheria toxin A chain (UCP-DTA) transgenic mice with decreased BAT and fed with high fat diet [85]. Mice lacking UCP1 are cold-sensitive, yet are neither obese nor prone to diet-induced obesity [86]. Moreover, dysfunction of BAT has been found in *ob/ob* (leptin-deficient) and *db/db* (leptin receptor-deficient) [87, 88].

2.2 Adipocyte secreted hormones

Adipocytes have been traditionally viewed as energy storage cells. More than 95% of cell body is composed of a storage form of triglycerides that can be released into the plasma

when needed. Adipocyte size ranges from 25 to 200 μm in diameter depending on the amount of lipid stored [89]. The major adipose tissue is called “white adipose tissue (WAT)”, which is composed of mostly adipocytes, surrounded by loose connective tissue macrophages, fibroblasts, adipocyte cell precursors, and various other cell types like endothelial cells, *etc* [76]. The largest WAT is found subcutaneously and around the viscera [74]. The rapid rise of insulin, glucose and lipids in the postprandial state stimulates the formation and storage of triglycerides in the liver and adipocytes. Conversely, a decrease in insulin concentration triggers glycogen breakdown and lipolysis via the action of glucagons, epinephrine, and glucocorticoids [90].

It is now clear that adipocytes serve not only as energy storage cells but also as endocrine cells, releasing many endocrine and paracrine factors [76]. Adipocytokines are those bioactive mediators secreted by adipose tissue composed of adipocytes and other cell types [89]. These include several highly activated molecules like adiponectin, leptin, visfatin, resistin and some cytokines like $\text{TNF-}\alpha$, IL-1, IL-6, and MCP-1.

2.2.1 Adiponectin

Adiponectin, also known as acrp30, adipoQ, GBP28 or ApM1, is a 247 amino acid protein [91]. Adiponectin belongs to the C1q family, which is characterized by a distinctive “globular domain” and a carboxyl terminus composed of collagen, “the stalk” [92]. The primary structure of adiponectin contains an N-terminal signal sequence, a variable domain, a collagen-like domain, and C-terminal globular domain. F1 mice from globular domain adiponectin (gAd) transgenic (Tg) mice crossed with leptin-deficient *ob/ob* mice showed amelioration of insulin resistance [93] and suggests that the globular domain is the active domain of adiponectin. Interestingly, the crystal structure of a homotrimeric fragment from adiponectin reveals an unexpected homology to the tumor necrosis factor (TNF) family [92], and suggested

shared impacts between TNF- α and adiponectin on inflammation, adaptive immunity, apoptosis and energy homeostasis.

Adiponectin circulates in the plasma in several different polymers, but not in monomeric form [94]. The multimers are formed through disulfide bonds at Cys-39 that binds the collagenous domains [94]. In human plasma and in culture medium, adiponectin can be found in a low molecular weight form composed of trimer or hexamers, or with a high molecular weight form made of a multimer larger than 300 kDa [95, 96]. Adiponectin concentration in human blood ranges from 5-10 mg/ml [97]. Low levels of total and high molecular weight but not trimeric or hexameric forms of adiponectin correlate with type 2 diabetes [98], metabolic syndrome and liver injury [99] and coronary artery disease (CAD) [94]. Prospective studies have shown that lower adiponectin levels are associated with a higher incidence and development of type 2 diabetes [100-102].

The factors that regulate the adiponectin levels are not completely understood. Females have higher concentrations of adiponectin and higher sensitivity to adiponectin than males, which suggests that female hormones are involved in its regulation [103, 104]. However, additional data are needed to test this hypothesis. Some dietary factors like soy protein and fish oil increase adiponectin levels, which partially explains why they improve insulin sensitivity [105, 106]. Restriction of methionine and carbohydrates also increases the level of adiponectin [107], whereas conjugated linoleic acid inhibits glucose metabolism, and leptin and adiponectin secretion in primary cultured rat adipocytes [108]. Therefore, there are many factors that can change the production of adiponectin.

The absence of adiponectin is closely related to insulin resistance, particularly when combined with a high-fat diet. Adiponectin KO mice exhibited severe diet-induced insulin

resistance with reduced IRS-1-associated P13-kinase activity in muscle [109]. Adiponectin administration to diabetic mice caused low blood glucose concentrations and ameliorated insulin resistance [93, 110, 111]. Scherer's group reported that a single injection of purified recombinant adiponectin into mice triggered a transient decrease in basal glucose levels by inhibiting both the expression of hepatic gluconeogenic enzymes and the rate of endogenous glucose production [111-113]. Lodish's group reported that acute treatment of mice with globular domain of Acrp30 increased fatty-acid oxidation in muscle and decreased plasma glucose in mice [114]. Therefore, alteration in mitochondrial function can impact the adiponectin-glucose balance. The thiazolidinedione class of antidiabetic drugs, which also have positive effects on cardiovascular diseases, increases the active form of adiponectin, resulting in increased insulin sensitivity [115]. These data are supported by data from adiponectin transgenic mice [116]. Globular adiponectin transgenic *ob/ob* mice have partial amelioration of insulin resistance, while adiponectin knockout mice showed mild insulin resistance [93].

Two adiponectin receptors (AdipoR1 and AdipoR2) have been reported. AdipoR1 was ubiquitously expressed and most abundantly expressed in skeletal muscle, whereas AdipoR2 was most abundantly expressed in mouse liver [117]. Suppression of AdipoR1/R2 expression by small-interfering RNA reduced the increase in fatty-acid oxidation by adiponectin [117]. Interestingly, AdipoR1^{-/-} mice showed increased adiposity associated with decreased glucose tolerance, while AdipoR2^{-/-} mice were lean, resistant to high-fat diet-induced obesity and had improved glucose tolerance. Thus, AdipoR1 and AdipoR2 are believed to be involved in energy metabolism but have opposing effects [118].

How adiponectin exerts its effect as an insulin sensitizer is still unclear. There are several hypotheses. Adiponectin increases the level of peroxisome proliferator-activated receptor

(PPAR)- γ , which caused a decreased triglyceride (TG) content in the liver and skeletal muscle [113, 119]. PPAR- γ agonist, rosiglitazone and TZD, both increased plasma levels of adiponectin [113, 119]. Thus, the effects of these drugs as insulin sensitizers could be attributable to the fact that they increase circulating adiponectin levels [113, 119]. Adiponectin stimulated phosphorylation and activation of AMPK in skeletal muscle and liver [120]. Therefore, it may also stimulate β -oxidation and glucose uptake. Adiponectin was also reported to increase glucose uptake via stimulating AMPK pathway in rat adipocytes [121].

Recently, Kubota et al reported that adiponectin enhances AMPK activity in the arcuate hypothalamus via its receptor AdipoR1 to stimulate food intake [122]. Huypens et al reported adiponectin induced an activation of AMPK in beta cells, which inhibited their biosynthesis of glucose-carbon to lipids [123].

Adiponectin may play a role in human innate immunity [76]. Matsuzawa's group reported that adiponectin suppressed bone marrow cell colony formation by colony-forming units (CFU)-granulocyte-macrophage, CFU-macrophage, and CFU-granulocyte precursor and inhibited mature macrophages function [124]. Treatment of cultured macrophages with adiponectin significantly inhibited their phagocytic activity and their lipopolysaccharide (LPS)-induced production of TNF- α [76]. Tilg's group reported that adiponectin induced the production of the anti-inflammatory mediators IL-10 and IL-1RA by primary human monocytes, monocyte-derived macrophages, and dendritic cells [125]. Adiponectin also inhibited LPS-stimulated IL-6 and TNF- α gene transcription [126, 127]. This is consistent with reports that adiponectin knockout mice had a higher level of TNF- α gene transcripts and a higher level of serum TNF- α [128]. Obviously, adiponectin is not only an important mediator in the regulation

of insulin resistance but also can suppress inflammation in vivo and cytokine release in cultured cells [76].

2.2.2 Leptin

Leptin is a 16 kDa polypeptide product of the *obese (ob)* gene. Like adiponectin, leptin is a major hormone secreted by adipocytes and it regulates a wide range of biological responses including energy homeostasis, neuroendocrine function, innate immunity and reproduction [129].

Leptin has a conserved homology among species and has a structural similarity to other proinflammatory cytokines such as IL-6 and IL-12 [129]. Leptin contains an intra-chain disulfide bond that appears to be necessary for its biological activity [130]. Leptin is mostly produced in adipose tissue although it has been detected in the gastric wall, vascular cells, placenta, ovary, skeletal muscle and liver [131]. Leptin expression is influenced by energy stores in fat [131]. Leptin levels increase within hours after a meal in rodents and after several days of overfeeding in humans [132]. Insulin stimulates leptin expression and secretion in primary adipocytes [133]. Other factors, such as dexamethasone [134], thyrotrophin (TSH) [135], TNF- α [136] and IL-6 [137] also regulate leptin release.

Leptin concentrations in the blood are in the range of several ng/ml, both as an active free form and as an inactive bound form which occurs by its association with plasma proteins and the leptin receptor isoform [131]. Leptin receptors (OB-R) are expressed in variety of tissues, which suggested that it has a wide range of actions. However, leptin receptor mutations cause early onset obesity in rodents [133]. This is consistent with measurements of high leptin concentration and low leptin receptor expression in most diabetic patients [89]. Human studies have discovered that leptin has pleiotropic effects in the human body. In children with protein-energy malnutrition, selective deficiencies of nutrients and poor general intake of food is associated with

low leptin levels [138, 139]. Children with leptin deficiency and massive obesity have a robust skeleton [139]. Clinically, providing leptin to girls with anorexia nervosa with leptin deficiency improves their immune system based on in vitro testing [139-141]. Low serum leptin and adiponectin levels are associated with premature intrauterine growth retardation in infants [142].

The primary physiological role of leptin is to communicate (CNS) the abundance of available energy stores to the central nervous system and brain and to restrain food intake [143]. The absence of leptin causes an increased appetite, increased food intake and extra energy storage in the form of fat. Indeed, administration of leptin to rodents decreased food intake and increased energy consumption, leading to weight loss [143]. However, leptin-induced weight loss was restricted to the fat and not lean tissue [143]. Leptin activated lipid oxidation, at least partially by inducing the expression of enzymes involved in lipid metabolism [143]. Leptin also stimulated apoptosis of adipocytes through activation of caspase-8 [144].

The ability of leptin to decrease body fat content suggests leptin is an anti-obesity hormone. However, high leptin levels have been found in obese and diabetic mice and humans [145], which is defined as “leptin resistance”. Sometimes it is combined with low-level expression of leptin receptors. Another mechanism is that leptin receptors become saturated as leptin levels rise, which leads to leptin resistance [139]. Therefore, disruption of leptin action is thought to play a role in development of diabetes. This hypothesis is supported by data showing that mutations of the *ob* gene cause early onset obesity and type II diabetes in mice and humans [143]. A frameshift/premature stop mutation, c.398delG (Delta133G mutation) caused a congenital leptin deficiency and led to severe early-onset obesity [146]. A homozygous frameshift mutation (delta133) in the human leptin (*ob*) gene was associated with undetectable serum leptin and extreme obesity [147].

Leptin binding to the leptin receptor leads to the formation of a Ob-R/JAK2 (Janus-activated kinase) complex that triggers phosphorylation [148]. JAK2 phosphorylation leads to activation of the PI3K and MAPK pathways that regulate apoptosis, energy homeostasis and gene transcription [149]. Leptin signaling occurs mainly through signal transducers and activators of transcription (STAT3). Phosphorylation of STAT3 triggers dimerization and translocation to the nucleus which leads to activation of gene transcription [148]. The targets include: genes of suppressors of the cytokine signaling family (SOCS3) [150]. Therefore, leptin regulates various signaling pathways and impacts gene transcription.

Leptin action also affects to the immune system. Leptin stimulates the proliferation of stem cells and regulates hematopoiesis [151]. It participates in innate immunity by promoting the maturation and survival of dendritic cells (DC) [152] and stimulates macrophage proliferation, phagocytosis, and production of proinflammatory cytokines [129]. Moreover, leptin plays a direct role in adaptive immunity by regulating the expression of Ob-R on both T and B cells and promoted the survival of T and B cells by suppressing Fas-mediated apoptosis [153]. Also, leptin has been shown to increase the production of IL-2 and IFN- γ by T lymphocytes [129].

Other roles of leptin include regulating fetal and brain development [129]. However, although leptin plays a wide range of roles, the major function of leptin is to regulate energy homeostasis.

2.2.3 Resistin

Resistin (resistance to insulin) is a member of a family of cysteine-rich C-terminal domain proteins called resistin-like molecules (RELM). Resistin is an approximately 12 kDa polypeptide containing a carboxy-terminal, disulfide-rich, β -sandwich domain and an amino-

terminal α -helical segment [89]. It is secreted as a disulfide-linked homodimer via disulfide bonds at cysteine residue (Cys26) [154].

Resistin is an insulin antagonist and it counterbalances the effects of adiponectin in the liver [155]. The physiological role of resistin in humans remains unclear. However in mice, its expression has been correlated to obesity [155]. Human resistin shares only 64% homology with murine resistin and lacks one of the isoforms found in mouse, which suggests a different physiological role in the two species [155]. In humans, in contrast to what happens in mice, resistin was produced at higher concentrations in cultured preadipocytes than in mature fat cells [156]. Furthermore, there is no consistent link between adipocyte expressed resistin or circulating resistin and adiposity or insulin resistance [156]. Thus, the function of resistin needs to be better understood.

In vitro and *in vivo* studies both showed murine resistin specifically expressed in adipose tissue were down regulated by thiazolidinedione [156]. However, the expression of resistin in humans was very low, even undetectable under certain conditions [154]. Recombinant resistin impaired insulin-stimulated glucose uptake in cultured adipocytes, whereas anti-resistin antibodies prevented this effect [156]. L6 myocytes treated with recombinant mouse resistin showed impaired glucose tolerance and insulin resistance [157]. These data suggest that resistin induces insulin resistance and that hyperresistinemia at least partially contributes to impaired insulin sensitivity in obese rodents. The role of resistin has also been studied in knockout mice. Loss of resistin in ob/ob mice improved glucose tolerance and insulin sensitivity by enhancing insulin-mediated glucose disposal in muscle and adipose tissue [158]. In contrast, in C57BL/6J mice with diet-induced obesity, resistin deficiency reduced hepatic glucose production and increased peripheral glucose uptake [158].

Although resistin was first identified as an “insulin resistant hormone”, more and more evidence indicates it also plays a role in the immune system. Proinflammatory cytokines such as TNF- α , IL-6 and LPS regulated resistin gene transcription in both 3T3L1 adipocytes and human peripheral blood mononuclear cells (PBMC) [159]. Resistin also regulated the expression of proinflammatory cytokines [154]. For example, resistin increased the expression of IL-6 and TNF- α by inducing translocation of NF- κ B [160]. Higher levels of resistin positively correlated with many inflammatory factors in persons with severe inflammation. Moreover, resistin was found to play a role in inflammation-related disease such as atherosclerosis, arthritis and Type 1 diabetes [154].

2.2.4 Visfatin

Visfatin, previously recognized as a pre-B cell colony-enhancing factor (PBEF), is expressed in bone marrow, liver and skeletal muscle. However, it is highly expressed in human visceral fat [161]. Both obese mice and people have higher concentrations of visfatin than lean individuals [162]. Visfatin mRNA was markedly higher in mature adipocytes than in preadipocytes, suggesting that lipid concentration affects its production [161] or it could be an adipocytes-specific factor expressed only when adipocytes are differentiated. This hypothesis is consistent with the observation that the amount of plasma visfatin strongly correlated with the amount of visceral fat as assessed by computer tomography [163].

There is still some debate about how visfatin and body fat are related. Some reported visfatin level was higher in obese people [164], while others failed to find differences between lean and obese people [165, 166]. There is also controversy about visfatin’s role in glucose metabolism and insulin resistance [167]. Moreover, except for one report [162], there do not appear to be differences in visfatin content between visceral and subcutaneous fat [167-169].

One time injection of visfatin reduced blood glucose, but insulin levels were not affected [161]. This suggests that visfatin plays a direct role in glucose uptake and glycolysis independent of insulin. The same effect was observed in other mouse models including lean mice, type II diabetic mice and obese mice [161]. Nishizawa's lab reported that visfatin mimicked insulin action in 3T3L1 adipocytes and L6 myocytes by stimulating glucose uptake [161]. They generated visfatin-deficient mice and found that plasma glucose was higher in visfatin^{-/+} heterozygote mice compared to knockout mice [161]. In addition, the knockout mice exhibited impaired glucose tolerance and insulin sensitivity [163]. Visfatin has been shown to induce adipogenesis [161]. Visfatin stimulated the differentiation of preadipocytes to mature fat cells, induced triglyceride accumulation, and accelerated triglyceride synthesis [161]. Visfatin binds to the same receptor of insulin, using a different epitope [161], which explains why it can parallel the action of insulin. It stimulated the phosphorylation of IRS-1/2, and activate both PI3K and Ras/MAPK [170, 171].

3. Role of macrophages and their interaction with adipocytes.

The growing understanding of adipose tissue macrophages in obese animals and individuals has revealed a strong interaction crosstalk between adipocytes and macrophages. Chapter 4 and 5 of this dissertation will address this interaction. Therefore, I will address the current understanding of this issue.

3.1 Insulin resistance: an inflammatory disease

Systemic chronic inflammation may have an important role in the pathogenesis of obesity-related diabetes [131]. In patients who are insulin resistant, there are high circulating levels of adiponectin, leptin, IL-6, CRP and TNF- α [172]. How these cytokines contribute to insulin resistance will be discussed later. The adipose tissue of patients with insulin

resistance has a large number of infiltrated macrophages [173]. These macrophages induce or exacerbate the amount of cytokine produced by the adipocytes [173]. Interestingly, adipocytes are a major source of TNF- α , IL6 and IL-1. One third of the IL-6 found in obese people with insulin resistance came from adipocytes [76].

3.2 Characteristics of Adipose tissue macrophages

Insulin resistance has been associated with chronic inflammation [131] and obesity is related to an elevated level of proinflammatory cytokines [149]. In particular, obesity is associated with significantly enhanced infiltration of macrophages into the adipose tissue [174].

The precise mechanisms causing inflammation into adipose tissue remains to be elucidated. Monocyte chemoattractant proteins such as (MCP-1, CCL-2) and its receptor and macrophage migration inhibitory factor (MIF) may play a role [174, 175]. The mRNA level of Monocyte chemotactic protein-1 (MCP-1) was higher in visceral adipose tissue in obese and diabetic patients compared to normal people [176]. Adipose tissue MCP-1 mRNA and the plasma MCP-1 concentrations were increased in genetically obese diabetic (*db/db*) mice and in WT mice with obesity induced by a high-fat diet compared to normal control mice [176]. Overexpression of MCP-1 in visceral adipose tissue resulted in insulin resistance, macrophage infiltration into adipose tissue, and increased hepatic triglyceride content [176].

Adipose tissue macrophages are the major source of TNF- α and MCP-1 in adipose tissue and they also expressed a very high level of IL-6 [177]. Clearly, adipocytes and macrophages share many characteristics. There is even some suggestion that adipocytes can be converted into expressing macrophage-like properties after *in vivo* adaptive transfer [178]. Both adipocytes and macrophages produce proinflammatory cytokines like TNF- α , IL-1 β and IL-6, whereas leptin and adiponectin released by adipocytes may have antiinflammatory effects as mentioned above.

Therefore, there must be cross-talk between the two cell types that result in the onset of type II diabetes.

There is a correlation between macrophage content in adipose tissue and insulin resistance [177]. However, resident macrophages in adipose tissue display a different phenotype compared to inflammatory macrophages. Macrophages are classified as either classically (M1) or alternatively (M2) activated macrophages [179, 180]. M1 macrophages are generated by IFN- γ alone or in combination of LPS, as well as by IL-12 or IL-18 [180] and are generally characterized by interleukin (IL)-12^{high}, IL-23^{high}, IL-10^{low} phenotype [181]. The M2 macrophages are generated through interaction with IL-4 and IL-13 and generally share an IL-12^{low}, IL-23^{low}, IL-10^{high} phenotype [179, 181]. M1 macrophages secrete proinflammatory cytokines, such as TNF- α , IL-6 and IL-1 β . M2 cells are characterized as anti-inflammatory macrophages during type I inflammatory responses and promote angiogenesis and wound healing [181]. Whereas inflammatory macrophages expressed high levels of proinflammatory cytokines, resident macrophages expressed high levels of Arginase-1, Ym-1 and Fizz-1 in inflammatory zone 1 (Fizz-1) [182], which are recognized as markers of “alternative macrophage” (M2 macrophages) [182, 183]. Resident macrophages in WAT have been found to display a M2 phenotype [182]. When M2 macrophages were inactivated in a macrophage-specific PPAR γ knockout mouse, the mice showed impaired glucose tolerance and insulin sensitivity when fed a high fat diet [182]. They also had significantly lower levels of oxidative phosphorylation gene expression in liver and muscle [182]. This affects energy metabolism and is one factor that leads to decreased insulin sensitivity. Odegaard et al suggested that M2 macrophages protect against the metabolic consequences of obesity; however, this hypothesis has yet to be tested.

3.3 Important cytokines involved in insulin resistance

3.3.1 TNF- α

TNF- α is a cytokine initially described as an endotoxin-induced factor that caused necrosis of tumors and was subsequently shown to be identical to cachexin, a factor secreted by macrophages *in vitro* [184]. TNF- α is now recognized as a multi-functional regulatory cytokine, involved in inflammation, apoptosis, cell survival, cytotoxicity, and insulin resistance.

TNF- α is a 26-kDa plasma membrane-bound protein that is cleaved into a 17-kDa biologically active protein [184]. There are two receptors for TNF- α , type I and type II that regulate different functions [184]. A death domain (DD) is important for TNF- α . This domain binds the TNF receptor 1-associated protein (TRADD), and at least three additional proteins, TRAF2, FADD, and RIP, are recruited [185] to activate downstream signaling. These signals regulate cell apoptosis or cell survival.

The association between TNF- α and insulin resistance was first discovered by Spiegelman's group [186]. Both mRNA and TNF- α protein were elevated in the adipose tissue of obese animals and humans [187]. Within adipose tissue, TNF- α was expressed mostly by adipocytes and stromovascular cells, although adipose tissue was composed of variety of cells types including immune cells [188]. Adipose tissue also expressed both types of TNF- α receptors [189].

Long term exposure of cultured cells or animals to TNF- α induced insulin resistance, characterized by hyperinsulinemia and an increased prevalence of obesity, hypertension, dyslipidemia and type 2 diabetes [184]. Furthermore it has been demonstrated that this is a direct effect of TNF- α because neutralization of TNF- α in 3T3L1 adipocytes increased insulin-

stimulated glucose uptake in these cells [190]. Moreover, the adoptive transfer of bone marrow cells from TNF^{+/+} into TNF- α KO mice reduced insulin resistance of the recipients [191].

Several hypotheses have been proposed to explain how TNF- α induces insulin resistance in adipocytes. For example, TNF- α inhibited insulin-stimulated IRS-1 phosphorylation. Thus, it might inhibit PI3K and inhibit a pathway that regulates glucose uptake [192]. In addition, TNF- α up regulates transcription of many preadipocyte genes and proinflammatory cytokines, such as IL-6 and MCP-1 [192]. These proteins were elevated in the plasma or adipose tissue of diabetic patients. TNF- α also inhibited adiponectin expression, which may impair insulin action [97]. Furthermore, TNF- α directly stimulated lipolysis, which caused an increase in plasma free fatty acids [97]. This also caused hepatic insulin resistance by inhibiting insulin suppression of glycogenolysis [193, 194].

3.3.2 IL-6

IL-6 is another cytokine that has long been recognized for its effects on the immune system [195]. It is associated with obesity and insulin resistance, too [196]. IL-6 belongs to the IL-6 family of cytokines, including IL-11, oncostatin M, leukemia inhibitory factor and other proteins, which commonly use gp130 (also known as IL-6R β or CD130) as part of their receptors [197]. IL-6 circulates in multiple glycosylated forms ranging from 22 to 27-kDa in size [75]. Several cell types, including most cells of the immune system, endothelial cells, skeletal and smooth muscle cells, adipocytes, islet β -cells, hepatocytes, microglial cells, and astrocytes, produce IL-6 [198]. Like TNF- α , adipose tissue is a major source of plasma IL-6 [199]. Adipocytes secrete 2 to 3 times more IL-6 than stromovascular cells [75].

IL-6 binds to a type I cytokine receptor complex containing a ligand-binding IL-6R α (gp120) and a signal-transducing component gp130 [197]. Upon formation of the IL-6/IL-

6Rβ/gp130 hexameric signaling complex, signals are passed either through Janus kinase (JAK)/signal transducers and activator of transcription (STAT) or the *Src* homology 2-containing tyrosine phosphatase (SHP-2)/extracellular signal-regulated kinase (ERK)/mitogen-activated protein kinase (MAPK) pathways or both [198]. IL-6 induces fever and the acute phase response, which is defined as the complex series of inflammatory reactions initiated in response to infection, physical trauma, or malignancy [200]. Therefore, enlarged adipose tissue has the potential to exacerbate both responses. IL-6 is made in responses to specific microbial molecules as pathogen associated molecular patterns (PAMPs). These PAMPs bind to Toll-like receptors, whose activation induces intracellular signaling cascades that give rise to inflammatory cytokine production [201, 202].

IL-6 is a strong inducer of the acute-phase response and is associated with a higher level of C-reactive protein (CRP) [203]. In proinflammatory insulin-resistant states, like obesity and type II diabetes, plasma IL-6 is found moderately increased [204]. The *in vivo* release of IL-6 from fat contributes more than one third of the basal circulating IL-6 and explains the positive correlation between serum levels of IL-6 and obesity [205]. Enhanced macrophages infiltration also accounts for the elevated IL-6 [204]. IL-6 decreases IRS-1 protein expression and insulin-stimulated tyrosine phosphorylation which reduces insulin-stimulated glucose transport in 3T3L1 adipocytes [206]. IL-6 suppresses insulin-induced lipogenesis and reduces expression of GLUT4 via repressed PKB/ERK pathway [207]. Furthermore, IL-6 decreased adiponectin gene expression and secretion in a dose- and time-dependent manner in 3T3L1 adipocytes [208]. All of these changes contribute to a glucose intolerant state.

In skeletal muscle, IL-6 is synthesized and released from skeletal muscle in large amounts during exercise [209]. Thus, it serves as an exercise signal involved in glucose

homeostasis by activation of AMP-activated protein kinase [199]. This regulation is exemplified by observations in the human hepatocarcinoma HepG2 cell line. In this cell line, IL-6 decreased SOCS3 transcription by inhibiting JAK/STAT activation, which caused inhibition of insulin receptor (IR) phosphorylation and insulin receptor substrate (IRS) phosphorylation [210]. Thus, increased glyconeogenesis and decreased gluconeogenesis decrease glycogen storage, a consequence of insulin resistance [211].

3.3.3 IL-1 β

IL-1 β is one of the major pro-inflammatory cytokines that is produced by monocytes, dendritic cells and macrophages [212]. The original member of the IL-1 family, includes IL-1 α , IL-1 β , IL-1 receptor antagonist (IL-1Ra) and six additional members including IL-18 and IL-1F7b [212, 213]. IL-1 β is 17 kDa but starts as a 31-kDa precursor protein. Mature IL-1 β is released from Pro-IL-1 β following cleavage by the interleukin-1 converting enzyme (ICE, caspase-1) [212]. The three-dimensional structure of IL-1 β is primarily barrel-shaped and composed of 12-14 β -strands [214].

There are three members of the IL-1 receptor gene family: IL-1RI, IL-1RII and IL-1sIIR [215]. IL-1 β has a higher affinity to IL-1RII than IL-1RI. IL-1RII contains a single transmembrane domain and the extracellular domain is found in the circulation as a soluble receptor (sR). Because IL-1sRII can bind to IL-1 β , it serves as a natural antagonist of IL-1 β [215].

IL-1 has wide ranging impacts gene transcription [212]. For example, IL-1 β affects molecules involved in inflammation, like IL-6, TNF- α , TNF- α receptor, IL-1R, and many chemokine proteins [212]. Signal transduction involves several pathways: 1) G-protein hydrolysis leads to the release of ceramide, which phosphorylates a p97 kinase and activates p38

MAPK [216]; 2) activation of phospholipase C (PLC) causes a hydrolysis of phosphatidylcholine (PC), phosphatidylethanolamine (PE) or phosphatidylserine (PS). These induce the release of diacylglycerol (DAG), the physiological substrate of protein kinase C (PKC). Phospholipid cleavage also phosphorylates protein kinase A, to activate the p38 MAPK pathway [217]. IL-1 β levels in the circulation of animals or humans correlate with the severity of some diseases; for example, tumor angiogenesis [218], age-related cognitive dysfunction [219] and arthritis [220].

The contribution of TNF- α and IL-6 to insulin resistance are better documented than those of IL-1 β . IL-1 β concentrations are higher in overweight and obese people [221]. Moreover, individuals with a higher combined levels of IL-1 β and IL-6 levels are at greater risk of developing type 2 diabetes than individuals with increased IL-6 alone [222]. Therefore, these are some suggestions that IL-1 β plays some role in obesity.

IL-1 and IL-1R regulate lipid metabolism *in vivo*. IL-1Ra^{-/-} mice gained less weight and accumulate less fat when they were fed a high-fat diet [223]. *In vitro*, recombinant murine interleukin 1 (rIL-1) inhibited lipoprotein lipase (LPL) activity in 3T3-L1 cells [224]. IL-1 β also inhibited adipocyte differentiation in long-term human bone marrow cultures [225]. Moreover, continuous treatment with IL-1 β decreased insulin receptor substrate (IRS-1) but not IRS-2 expression in both 3T3-L1 and human adipocytes [226].

3.4 Macrophage and adipocyte differentiation

It is now recognized that the stromal-vascular compartment of adipose tissue contains various precursors and stem cells, which give rise to multiple cell types [227]. Among the stromal cells, there are preadipocytes that differentiate into adipocytes [227]. Macrophage infiltration into the stroma of adipose tissue might inhibit adipogenesis [228]. Weisberg *et al.* [174] and Xu *et al.* [229] reported that inflammatory macrophages accumulated around small

adipocytes, and induced apoptosis. Little is known about the roles of macrophages in adipogenesis and obesity. Moreover, the reports on this topic are inconsistent. Nishimura et al., found two types of cell clusters that showed a macrophages phenotype [228]. CD34⁺ CD68⁺ cells were associated with the small differentiating adipocytes and CD34⁻ CD68⁺ macrophages were scattered in the stroma [228]. While the role of CD34⁻ CD68⁺ macrophages not clear, the CD34⁺ CD68⁺ cells appeared to accelerate angiogenesis and promote the differentiation of the preadipocytes [228].

Macrophages play a role in adipocyte differentiation by secreting proinflammatory cytokines. This hypothesis is supported by several observations that have been reviewed in detail above. However, two additional observations reinforce this key point. Somm et al reported decreased fat mass in IL-1Ra^{-/-} mice. This was a defect in adipogenesis and increased energy expenditure in those mice [230]. Hongan *et al.*, found that leukemia inhibitory factor (LIF) treatment had minimal effects on adipocyte differentiation, but did inhibit triacylglyceride (TAG) accumulation during adipogenesis [231]. Chapter 4 of this dissertation will address the importance of macrophages and cytokines on adipocytes.

4 Intracellular trafficking

Secreted proteins need to be transported outside of the cells after they are synthesized and processed in the endoplasmic reticulum (ER). The cellular biosynthetic-machinery allows cells to modify molecules it produces, to pass them through the Golgi complex, and to pack them into granules for exocytosis at the plasma membrane [232]. Vesicles continually bud from one membrane and fuse with another, the process by which cells acquire and secret. These processes are highly regulated and organized with specific proteins. Given the importance of the adipose tissue as a secretory organ, one of the main challenges is to discern the specific molecular

mechanisms that regulate and control protein trafficking. This has been one of the main areas of my doctoral work in chapter 2 and 3. Therefore I will provide some background information on this topic.

4.1 Transport from the ER through the Golgi apparatus

Newly synthesized proteins enter the ER by crossing the ER membrane from the cytosol. Some proteins carry a N-terminal signal sequence that is cleaved. Proteins are transported to the Golgi apparatus and from the Golgi apparatus to the cell surface or elsewhere. The golgi apparatus is a major site of carbohydrate synthesis, as well as a sorting organelle for the products of the ER [233]. Proteins that are sent to the Golgi apparatus are attached to the carbohydrates made in Golgi apparatus as oligosaccharide side chains [233]. These oligosaccharide chains are served as ‘tickets’ that direct specific proteins into vesicles going to the destination. A large number of plasma proteins are attached to a glycosylphosphatidylinositol (GPI) anchor to the C terminus. [233] Since these proteins are attached to the exterior of the plasma membrane only by GPI anchors, they can release soluble proteins in response to signals [233]. GPI anchors are also used to direct proteins into lipid rafts [233].

Proteins are first packaged into small COPII-coated transport vesicles. Some cargo proteins are actively recruited into such vesicles, where they become concentrated. Membrane proteins carries exit signals that recognize the COPII coat by complementary receptors that are packaged into budding COPII (coatamer protein II) -coat transport vesicles [234]. Recruitment of coat proteins from the cytosol to organelle membranes is mediated by ARF/Sal1 family of small GTPase in a GTP-dependent manner [235]. The vesicular tubular cluster, which is generated continually, mediates the transportation from ER to the Golgi apparatus and move along microtubules to carry proteins from the ER to the Golgi apparatus. The retrieval (or

retrograde) transport continues as the vesicular tubular clusters move to the Golgi apparatus [233]. Thus, those proteins participating in the ER budding reaction and the escaped proteins that are not properly folded and assembled are controlled and are returned to the ER to be reused. COPI is involved in the retrograde traffic from the Golgi to the ER and also functions in the endosomal compartment. COPII is involved in the anterograde traffic from the ER to the Golgi [233].

4.1.1 Arf proteins

Recently, the human Arf (ADP-ribosylation factor) family has been expanded to 21 members, with six Arf proteins and fifteen Arl (Arf-like protein) proteins [236]. Arf1, Arf 3-6 are found in human, while Arf2 has been lost in human [236]. These six molecules can be divided into three classes on the basis of their primary structure. Class I includes Arf1, Arf2 and Arf3; class II includes Arf4 and Arf5; class III includes Arf6 [236]. Arfs regulate the budding of vesicles in the endocytic and exocytic pathway by recruiting other adaptor proteins or coat Golgi membranes when bound to GTP or GTP γ S but not GDP [236]. Target proteins recruited by Arfs proteins include: COPI and II, AP-1, AP-3 and AP-4, GGA1-3 (Golgi-associated γ -adapting ear homology domain Arf-interacting protein1-3) and MINT1-3 (Munc18 interacting protein 1-3) [234].

Arf proteins cycle between their active-GTP-bound and inactive-GDP-bound forms. Hydrolysis of bound GTP is mediated by GTPase-activating proteins (GAPs), whereas guanine nucleotide-exchange factors (GEFs) exchange GDP to GTP [236]. The specific roles of different Arf are still poorly understood. However, Arf proteins 1, 3, 4, and 5 are predominantly cytosolic but could be recruited to a variety of intracellular, but not plasma membranes. Arf6 is uniquely localized to the plasma membranes, which suggested that Arf6 has unique functions [237] during

cell adhesion, migration, and cancer cell invasion [238] as well as during membrane trafficking [239]. The Arf6 GTPase cycle has been shown to regulate endosome membrane trafficking, regulated exocytosis, and actin remodeling at the cell surface [240]. Arf6 affects cell migration in epithelial cells by facilitating junction disassembling through its effect on endocytosis [241]. Therefore, the role of ARF6 at the cell surface parallels the role of ARF1 at the Golgi [242]. Two-hybrid assays of Arf-coat protein interaction showed little specificity and knocking down of a single Arf by RNAi has no effect on secretory traffic and endosome recycling [243, 244]. These data suggest that the function of Arf proteins is redundant. However, double knock down experiments show some specificity between Arfs. Arf1 and Arf3 are involved in the trafficking from ER to cis-Golgi [243, 244].

Arf1 regulates COPI, adaptor protein (AP)-1, AP-3, AP-4 and GGAs [245], and plays a role in the secretory pathway by budding transport vesicles. Arf-1-GTP and the COPI coatomer complex comprises the basic components of budded COPI-coated vesicles *in vitro* [246].

4.2 Transport from the *Trans* Golgi Network (TGN) to the cell exterior

When transport vesicles destined for the plasma membrane leave the TGN, the membrane proteins and the lipids in these vesicles provide new components for the plasma membrane, while the soluble proteins are secreted to the extracellular space. All cells use the constitutive secretory pathway to transport mature proteins to the outside of the cells. However, some specialized secretory cells have a regulated secretory pathway, in which soluble proteins are stored for later release [233].

Clathrin coats are the third well-characterized class of coated vesicles, which are involved in endocytosis and exocytosis, regulating traffic between TGN and endosomes. Clathrin coats contain clathrin and heterotrimeric adaptor protein (AP) complexes ([247]. There

are four types of APs in mammalian cells and only AP-1 and AP-2 have been widely studied. However, the unique intracellular localization of the four isotypes suggests their specialized function in different trafficking steps between TGN and plasma membrane [248]. At steady state, most AP-1 is localized to tubular, clathrin-coated structures on the TGN [249]. Recruitment of AP-1 to membranes is dependent on Arf. AP-1 mediates antegrade transport from the TGN to endosome and GGAs regulates the retrograde transport [248]. The AP-2 associates with the plasma membrane and mediates endocytosis [248]. The AP-3 is involved in protein trafficking to lysosomes, while little is known about AP-4 [250].

4.2.1 GGA proteins

GGAs was first identified by Boman et al in 2000 using a yeast two-hybrid screening of a human cDNA library with a Arf3-GTP as bait [251]. Until now, three isoforms of GGAs have been found in human: GGA1, GGA2 and GGA3; and two isoforms in yeast: Gga1p and Gga2p [250]. The molecular size of GGAs varies from 60-80 kDa. The GGAs have four functional domains: the N-terminal ~140-AA VHS domain, the GGA and Tom1 (GAT) domain, the hinge and the C-terminal ~160-AA γ -adaptin ear homology (GAE) domain [252].

The VHS domain recognizes the cytoplasmic domain of transmembrane proteins found in TGN[250]. It was shown that the acidic amino acid cluster-dileucine (ACLL) within the cytoplasmic domain of transmembrane protein is the site recognized by VHS of GGAs [250]. It has been found that the GGA binding proteins, CI-MPR, CD-MPR, sortilin and LRP3 all contained the ACLL similar site [250]. It is also interesting that the hinge of GGA1 and GGA3, but not GGA2 both contain a potential ACLL sequence and the phosphorylation of a serine in such sequence autoinhibits the interaction between VHS domain of GGA with the ACLL sequence of cargo proteins [253]. GGAs are recruited to the TGN via binding to activated (GTP-

bound) Arf proteins [252]. Treatment of brefeldin A (BFA), an inhibitor of guanine nucleotide exchange factors for Arfs, caused redistribution of GGAs from TGN to cytosol [254]. All human GGAs can interact with all forms of Arf [254]. However, it is unknown if specific isoforms of Arfs are involved in different isoforms of GGA. All of the GGAs contain a clathrin box, potential clathrin-binding sequence (consensus sequence, L (L/I)(D/E/N)(L/F)(D/E)) [255], through which GGAs on the TGN membrane recruit clathrin. The GAE domain shares several similar binding partners with the ear domain of γ -adaptin and functions on binding with accessory proteins [250].

Although it is well-established that GGA proteins regulate coat assembly and are involved in the trafficking between TGN and endosome, there are questions remaining about specialized proteins whose intracellular trafficking is regulated by GGA proteins.

4.2.2 Rab proteins

Rabs are a ubiquitously expressed family of small Ras-like GTPases [240]. There are more than 60 members in mammalian cells and 11 members in yeast [256]. Most of Rab proteins contain a C-terminal prenylation motif, a hypervariable domain and two switch regions [257]. The C-terminal prenylation motif is important for membrane insertion [258]. Pfeffer *et al.* found that modification of the two cysteines to a single cysteines on Rab5a and Rab27a led to improper insertion of those into the ER and Golgi instead of into early endosomes and melanosomes, respectively [259]. The hypervariable domain is a flexible domain that changes conformation upon the exchange of GDP and GTP bound forms [257]. The hypervariable domain is thought to contain the targeting signal for Rab protein [260]. However, a recent study found that replacing the hypervariable domain of Rab5a with that of Rab1a, Rab2a, Rab7 and Rab27a had no effect on its function and localization on early endosome [261].

Rab GTPase cycles between their GTP-bound and GDP-bound states. Like Arf proteins, this switch is regulated by GEF and GAPs [262]. Rab proteins also recycle between membrane bound and cytosolic forms, which is coupled to their nucleotide load. Membrane insertion requires the modification of two carboxyl-terminal cysteines with isoprenyl lipid moieties [258]. Ras-GDP binds to the GDP dissociation inhibitor (GDI), masking the isoprenyl anchor and thus maintains the Ras-GDP localization in the cytosol [258]. Once dissociation from the GDI by GDI displacement factor (GDF) [263], Rab proteins can exchange GDP to GTP form under the control of GEF [258]. The active Rab-GTP is able to insert into the target membrane.

Rab effectors are important to help establishment of the membrane domain marked by specific Rab proteins. For example, mannose 6-phosphate receptors (MPRs) are involved in sorting during vesicle formation and Rab9 on the late endosome is required for the recycling of MPRs [264]. Early endosome antigen 1 (EEA1) and Rabaptin5 bind to Rab5 in endosome-endosome fusion [265].

Rabs are versatile catalysts. They participate in receptor cargo collection; enabling motor proteins to interact with membranes and interact with effectors to mediate the accurate docking and fusion of transport vesicles with their targets [266]. Rab proteins are involved in the endocytic and exocytic pathway by recruiting sets of effectors to distinct regions [257]. These effectors mediate endosomal functions including endosome membrane fusion, packaging of cargo into vesicles [266]. Rab proteins localize to specific intracellular compartments consistent with their function in distinct vesicular transport process. Rab1 localizes in the intermediate compartment of the cis-Golgi network and regulate ER to Golgi transport [267]. Rab4 and Rab5 are involved in the early endosome and regulate clathrin-coated-vesicle-mediated transport [268]. Rab11 is in the recycling endosome and mediates the recycling of membrane proteins to

the plasma membrane [268]. Rab 9 and Rab7 are segregated in late endosomes [266, 269]. Distinct intracellular localization and functions in intracellular trafficking have been established for other Rab members.

4.3 Constitutively vs regulated secretory pathway in adipocytes

It is known that adipocytes secrete over 300 proteins that affect numerous cell biological and metabolic pathways. However, little is known about which pathways are used to transport these proteins outside of the cell. Adipocytes have two transport pathways: constitutively and regulated secretory pathways [270]. To compare these two pathways, I will summarize the intracellular trafficking of GLUT4 as an example of the regulated secretory pathway and the intracellular trafficking of leptin as an example of the constitutive secretory pathway.

4.3.1 Regulated secretory pathway in adipocytes: intracellular trafficking of GLUT4

GLUT4 continuously recycles between the plasma membrane and intracellular storage compartment [48]. GLUT4 is found in many organelles, including the plasma membrane, sorting endosomes, recycling endosomes, the TGN and small vesicles that mediate the transport of GLUT4 between these compartments [48]. At basal state, almost no GLUT4 stays on the plasma membrane. However, within 15 minutes after insulin stimulation, about 95% of GLUT4 is transported to the plasma membrane [69, 271, 272]. How insulin affects GLUT4 exocytosis is still not clear.

Colocalization study by confocal microscopy showed 40% to 50% of GLUT4 was colocalized with a transferrin receptor (TfnR)-positive endosomal compartment, while 50 to 60% is in a second, TfnR-negative compartment [273]. Endosomal ablation showed that only 30-40% of the GLUT4 was in the endosomes under basal conditions [274]. It is GLUT4 in the TfnR-negative compartment that is rapidly mobilized after insulin stimulation [43]. The insulin-

responsive aminopeptidase (IRAP), identified as a receptor for angiotension IV [275], was shown to be colocalized with GLUT4 and transported to the plasma membrane upon insulin stimulation in parallel with GLUT4 [276]. In fibroblasts, most GLUT4 and IRAP are colocalized with TfR in endosomes [277] away from the insulin-regulatable storage compartment, which explains why the insulin-mediated redistribution of Glut4 effect is relatively small in these cells.

Other GLUT4 pools responsive to insulin stimulation are TGN-originating small vesicles. Recent evidence indicates that GLUT4 recycles between the TGN and endosomes [278]. GLUT4 localized to adaptor-protein-1 (AP-1) positive, clathrin-coated, vesicles around the TGN in adipocytes [279]. These vesicles also contained syntaxin 6 and syntaxin 16 [48], which confirms that they bud off from the TGN.

A more insulin responsive GLUT4 storage compartment, GLUT4 storage vesicles (GSVs), has been identified, as the TGN pool and the endosomal pool of GLUT4 is less insulin-sensitive. These vesicles are relatively small (around 50 nm) and do not contain TfR [48], however, they contain IRAP [53] and the v-SNARE, vesicle-associated membrane protein (VAMP2), which forms a complex with t-SNAREs on the plasma membranes in muscle and adipocytes [280]. GGAs, found in the GSVs, plays a role in the sorting of GLUT4 from the TGN to the GSVs [127]. It is also suggested that GGAs binds to the ubiquitinated cargos and regulate the degradation of IRAP and GLUT4 [281].

A comprehensive model of GLUT4 transportation can be divided into six steps. The biogenesis of GSVs [282], transport of GSVs along microtubules and corticle actin [141], tethering [283], docking [280] and fusion with the plasma membrane [284], and endocytosis.

The insulin signaling pathways that lead to the translocation of GLUT4 has been identified as the PI3K pathway [285]. Activation of PI3K occurs through PI3K-dependent kinase and its downstream target Akt/PKB, which has been reviewed earlier. Recently, a Rab GTPase activating protein (RabGAP), Akt-substrate of 160 kDa (AS160) has been identified to function during insulin-stimulated GLUT4 translocation. AS160, as a RabGAP, may regulate the Rab activity that occurs in the GLUT4 transport [286]. The unstimulated AS160 maintains a RabGDP form that prevents GLUT4 translocation [286]. Akt phosphorylates AS160 at four separate sites. Activated AS160 catalyses 14-3-3 binding and facilitates the activation of Rab proteins [287]. Recently, Rab 2A, Rab 11, Rab 14 and Rab 10 have been identified in the insulin-stimulated GSVs mobilization [288]. Despite the intense study of GLUT4 intracellular transport, our understanding of the regulation of this pathway, especially by macrophages, remains incomplete.

4.3.2 The continuous secretory pathway in adipocytes: intracellular trafficking of leptin

Insulin stimulates leptin secretion. A two-hour incubation of rat adipocytes with insulin did not affect the transcription of leptin, but the secretion of leptin increased two fold [134]. Dexamethasone, however, stimulated both *ob* gene transcription and leptin secretion by 2-4 fold in the same cells within 2-hour after insulin stimulation [134]. Treatment of adipocytes with the PI3K inhibitor LY294002 and MAPK kinase inhibitor PD98059 for two hours showed no effect on *ob* gene transcription or the basal secretion of leptin. However, leptin secretion stimulated by both insulin and dexamethasone was significantly decreased [134]. These data suggested that insulin stimulated leptin secretion is regulated through both PI3K and MAPK pathways.

To analyse the leptin pool, Bradley et al did subcellular fractionation on rat adipocytes. They identified two internal membrane fractions, the low density microsomes (LDM) and the

high density microsomes (HDM). ER-specific proteins, translocon-associated protein- α (TRAP- α) and calnexin localized in the HDM and leptin primarily associated with the HDM [289]. Consistent with these data, Roh *et al.*, identified the major leptin-containing membrane compartment as an ER- rich compartment in rat adipocytes using sucrose gradient centrifugation and confocal microscopy techniques [290].

Barr *et al.* reported insulin stimulated leptin exocytosis from an ER-rich compartment without any observable accumulation in secretory vesicles [289]. As leptin is not glycosylated, it is rapidly transport to the Golgi once synthesized in the ER [289]. The absence of leptin in the Golgi-rich LDM also confirmed this point. However, an intact Golgi is also required for the secretion of leptin. Bradley *et al.* showed that brefeldin A treatment inhibited secretion of leptin in both basal and insulin-stimulated conditions [289]. A temperature of 20 °C is able to recruit proteins that exit from ER into the Golgi compartment. Incubation of rat adipocytes at 20 °C for 1.5 hours induced a redistribution of leptin from the ER-rich HDM to Golgi-rich LDM [134]. These data suggest that leptin is transported through the Golgi apparatus and trans-Golgi network.

The hypothesis that leptin secretion is primarily through a constitutive secretory pathway is widely accepted by most of the researchers. However, the specific mechanisms regulating the insulin-stimulated leptin secretion are poorly understood. Chapter 3 of my dissertation sheds light into the mechanism regulating adiponectin and leptin trafficking in adipocytes.

CHAPTER 2

INTRACELLULAR TRAFFICKING AND SECRETION OF ADIPONECTIN IS DEPENDENT ON GGA-COATED VESICLES

ABSTRACT

Adiponectin (Acrp30) is an insulin-sensitizing hormone produced and secreted exclusively by adipose tissue. Confocal fluorescent microscopy demonstrated the colocalization of adiponectin with the Golgi membrane markers p115, β -COP, and the trans-Golgi network marker, syntaxin 6. Treatment of cells with brefeldin A redistributed adiponectin to the endoplasmic reticulum where it colocalized with the chaperone protein BIP and inhibited secretion of adiponectin demonstrating a requirement for a functional Golgi apparatus for adiponectin release. Confocal fluorescent microscopy also demonstrated a colocalization of endogenous adiponectin with that of expressed GGA1myc (Golgi-localizing γ -adaptin ear homology ARF-binding protein) but with no significant overlap between adiponectin and the GGA2myc or GGA3myc isoforms. Consistent with confocal fluorescent microscopy, transmission electron microscopy demonstrated the colocalization of GGA1 with adiponectin. Although GGA1 did not directly interact with the adiponectin protein, the adiponectin enriched membrane compartments of adipocyte were precipitated by aGST-GGA1cargo binding domain (VHS) fusion protein but not with a GST-GGA2 VHS or GST-GGA3 VHS fusion proteins. Moreover, co-expression of adiponectin with a GGA1 dominant-interfering mutant (GGA1-VHS GAT domain) resulted in a marked inhibition of adiponectin secretion in both 3T3L1 adipocytes and HEK293 cells, whereas no inhibition was detected with the truncated mutants GGA2-VHSGAT or GGA3-VHSGAT. Moreover, co-expression of wild type GGA1 with adiponectin enhanced secretion of adiponectin. Interestingly, leptin secretion was unaffected by neither the wild type form or GGA1 mutant. Taken together these data demonstrate that the trafficking of adiponectin through its secretory pathway is dependent on GGACoated vesicles.

INTRODUCTION

Over the past several years many studies have documented that in addition to being a fat storage depot, adipocytes are a *bona fide* endocrine tissue that secrete several hormones that control insulin sensitivity and energy balance [90, 270, 291]. In particular, adiponectin, also called adipocyte complement-related protein of 30 kDa (Acrp30), adipoQ, GBP28, and apM1, was originally isolated as a highly induced gene following adipocyte differentiation [292]. This hormone is secreted exclusively by adipocytes [292-295] and functions *in vivo* as an insulin sensitizer [111, 114, 296], reducing glucose production by the liver [112] and enhancing fatty acid oxidation in skeletal muscle [114] through the activation of two distinct receptor isoforms [117]. These receptors mediate increased AMP-dependent kinase activation [121, 297, 298] and peroxisome proliferating activated receptor- γ ligand activity [93].

Adiponectin serum levels inversely correlate with insulin resistance in both in animals and humans [299-303] in contrast to that observed for other adipokines such as tumor necrosis factor- α and resistin [222, 304-306]. Type 2 diabetic patients also display reduced levels of adiponectin [307-310]. Moreover, injection of purified adiponectin decreases glucose levels in *ob/ob*, non-obese diabetic, or streptozotocin-induced diabetic mice [91].

Adiponectin is initially synthesized as pre-hormone with a classical signal sequence that is cotranslationally removed as the protein translocates into the lumen of the endoplasmic reticulum [311]. The secreted protein consists of an amino-terminal collagen domain that shares significant homology to collagen VIII and X [4, 6], a carboxylterminal globular domain that is homologous to the complement factor C1q [92], and the hibernation-regulated serum proteins, *hib20*, *hib25*, and *hib27* [293]. The three-dimensional structure determined by x-ray analysis also revealed that adiponectin shares significant homology to tumor necrosis factor- α , another

adipocyte-secreted hormone that is implicated in the induction of insulin resistance [92]. However, in serum adiponectin circulates as two forms, a lower molecular weight trimer-dimer and a higher oligomeric molecular weight complex. Recent studies have demonstrated that disulfide bond formation through Cys-39 is essential for the assembly of the higher oligomeric complexes [95].

The GGA2 proteins (for Golgi localizing γ -adaptin ear homology domain ARF-binding protein) are a family of ubiquitously expressed monomeric clathrin adaptors that mediate sorting at the trans-Golgi network (TGN) of specific cargo in an Arf-dependent manner. There are three different isoforms of GGA proteins termed GGA1, GGA2, and GGA3. These proteins have a modular structure consisting of an NH₂-terminal VHS (Vps27, Hrs, STAM) domain, and Arf-binding GAT (GGA and TOM1) domain, a clathrin binding hinge region, and a COOH-terminal γ -adaptin “ear” (GAE) domain. The VHS domain binds acidic cluster-dileucine sorting signals present in the cytosolic domain of transmembrane vesicle proteins [312, 313] such as the mannose 6-phosphate receptor [254], sortilin [314], and β -secretase [315]. The GAT domain binds to activated ADP-ribosylating factors [316-319], whereas the hinge region recruits clathrin [316]. The GAE region has been shown to interact with accessory proteins including rabaptin-5 [320, 321], enthoprotin [322], γ -synergin [323], and with ubiquitin [324].

In the present study, we demonstrate that adiponectin in the steady state is predominantly localized in a peri-nuclear compartment indistinguishable from the Golgi apparatus/TGN. Consistent with the morphological observations, secretion of adiponectin is severely inhibited by treatment of cells with brefeldin A (BFA). Furthermore a dominant interfering mutant of the GGA1 protein (GGA1VHSGAT domain) was able to block both traffic of the GLUT4 glucose transporter to its insulin-sensitive intracellular compartment and secretion of adiponectin but did

not affect leptin secretion. In addition, confocal and transmission electron microscopy studies showed colocalization of adiponectin with the GGA1 isoform. These data suggest that adiponectin (but not leptin) secretion is dependent on GGA proteins and suggest that GGA adaptors participate in the regulation of selective adipokine trafficking in adipocytes.

EXPERIMENTAL PROCEDURES

Materials

Brefeldin A and cycloheximide were obtained from Sigma. Brefeldin A was prepared as a 5 mg/ml stock in methanol and used at a final concentration of 5 µg/ml. Cycloheximide was prepared as a 10 mg/ml stock and used at a final concentration of 10 µg/ml. Adiponectin antibody was obtained as described previously (5). Antibodies for syntaxin 6, p115, and BIP were from BD Biosciences. Antibody for vesicular stomatitis virus-G (VSV-G) protein was obtained from Acurate Biochemicals. Anti-myc and anti-GGA1 antibodies were from Santa Cruz Biotechnology. Biotin-conjugated anti-myc antibody was from Sigma. Antibody anti-GFP was from Roche Applied Science, Dulbecco's modified Eagle's medium (DMEM), Opti-MEM I, fetal bovine serum, calf serum, and trypsin were from Invitrogen. Lipofectamine 2000 was obtained from invitrogen. Radioimmunoassay kit for adiponectin was obtained from Linco Research (St. Charles, MO). ELISA kits for adiponectin and leptin were purchased from R&D Systems. The GGA1, GGA2, and GGA3 wild type constructs and eGFP-VHS-GAT domain were obtained from Dr. J. Bonifacino (National Institutes of Health). A plasmid encoding for the VSV-G protein wild type protein was a gift from Dr. M. McNiven (Mayo Clinic and Graduate School, Rochester, MN).

Generation of DNA Constructs

The GST-GGA1 VHS-GAT, GSTGGA2 VHS-GAT, and GST-GGA3 VHS-GAT constructs were generated by PCR amplification of the VHS-GAT domains of the wild type forms of GGA1– 3, followed by ligation into the GST-expressing vector pGEX4T (Amersham Biosciences).

Cell Culture and Transient Transfection

3T3L1 cells were obtained from the American Type Tissue Culture repository. Cells were cultured in DMEM supplemented with 25 mM glucose, 10% calf serum at 37 °C with 8% CO₂. The cells were differentiated into adipocytes with 1 µg/ml insulin, 1 µM dexamethasone, and 0.5 mM isobutyl-1-methylxanthine as described previously [325]. Differentiated adipocytes were electroporated at 950 microfarads and 0.15 V, using a Gene Pulse II electroporator from Bio-Rad. Following electroporation cells were plated on collagen IV-treated coverslips and allowed to recover in DMEM supplemented with 10% Serum. HEK293 cells were cultured in minimal essentialmedium containing 10% of FBS and penicillin/streptomycin at 37 °C with 5% CO₂. Cells were plated in 24-well plates and transfected using Lipofectamine 2000 (Invitrogen) following the manufacturer's instructions.

Immunofluorescence and Image Analysis

Transfected and intact adipocytes were washed in phosphate buffered saline (PBS) and treated for 15 min with a solution containing 4% paraformaldehyde, 0.2% Triton X-100, and 0.4% bovine serum albumin (BSA). Cells were then incubated in blocking buffer containing 5% donkey serum (Sigma) and 1% BSA for 1 h at room temperature. Primary and secondary antibodies, as indicated in the figure legends to Figs. 1, 2, 4, and 7, were used at 1:100 dilutions in blocking buffer. The cells were washed three times with PBS and mounted on glass slides with Vectashield (Vector Laboratories) and were imaged using a Zeiss LSM 510 META confocal microscope. Images were then imported to Adobe Photoshop (Adobe Systems, Inc.) for processing.

Temperature Block

After electroporation 3T3L1 adipocytes were placed overnight in DMEM containing 10% fetal bovine serum at either 16 or 19°C. Following an overnight incubation cells were fixed and permeabilized as indicated above and processed for immunofluorescence.

Pull-down Assay and Western Blot Analysis

For the pull-down assay, whole cell extracts were prepared in HES buffer: 30 mM HEPES, pH 7.4, 1 mM EDTA, 250 mM sucrose) supplemented with 1 mM phenylmethylsulfonyl fluoride, 10 µg/ml aprotinin, 1 µg/ml leupeptin, and 1 µg/ml pepstatin. Cells were then homogenized in a Dounce homogenizer (five times) and lysates centrifuged to 37,000 rpm for 10 min at 4 °C. Equal volumes of the supernatant were taken (1 mg of protein) and incubated with glutathione beads (GST or GST-GGA1VHS GAT) for 2 h at 4°C. Samples were centrifuged briefly (13,000 rpm for 1 min), and the beads were washed three times with PBS. Pelleted samples were eluted in 2 X loading sample buffer. Samples were boiled for 5 min and loaded onto a SDS-PAGE. Samples transferred to a nitrocellulose membrane and immunoblotted with an antibody specific for adiponectin.

Radioimmunoassays and ELISA

Fully differentiated cells were trypsinized for 10 min and replated at equal densities into 12 well multidishes and were allowed to recover overnight in DMEM containing 10% FBS. Following an overnight incubation the medium was changed to DMEM without serum supplementation, and at different time intervals an aliquot of medium was collected for radioimmunoassay following the manufacturer's instructions (Linco Research). Similarly, ELISA assays were performed on aliquots of medium taken 24-30 h following transfection. Prior to radioimmunoassay/ELISA floating cells were removed by centrifugation at 500 g for 5 min

and the supernatant used for the radioimmunoassay/ELISA quantification. In parallel an aliquot of the whole cell lysate was also quantified.

Transmission Electron Microscopy

HEK293 cells were collected by trypsinization (5 min) followed by inactivation of trypsin with 10% FBS medium. Cells were then centrifuged and washed twice with PBS. Pelleted cells were fixed in 2% paraformaldehyde, 0.2% glutaraldehyde for 24 h at 4°C. Cells were dehydrated in ascending alcohol series (50-100%) 15 min each and infiltrated in LR White resin overnight. Samples were then cured at 50°C for 48 h, sectioned, and mounted on nickel grids. Following aldehyde quenching with 50 mM glycine, for 30 min, samples were incubated in a blocking solution containing 5% donkey serum and 1% BSA for 1 h at room temperature. Immunolabeling with specific primary antibodies at 1:100 was done overnight at 4°C. Samples were washed three times with PBS and secondary antibodies (goat anti-rabbit IgG 25-nm gold and goat anti-mouse IgG 10-nm gold) were added at 1:50 for 2 h at room temperature. Samples were washed in PBS and water and visualized in a FEI CM100 microscope.

Statistical Analysis

One-way ANOVA was performed using SAS statistical software.

RESULTS

Intracellular Localization of Adiponectin in 3T3L1 Adipocytes

To characterize the intracellular localization of adiponectin, we examined the distribution of adiponectin with several intracellular markers. The endogenous adiponectin protein (Figure 2, *a*, *d*, and *g*) was primarily localized in the peri-nuclear compartment as well as some scattered vesicle staining throughout the cytoplasm. The peri-nuclear distribution overlapped with Golgi markers p115 (Figure 2, *a-c*), syntaxin 5 (Figure 2, *d-f*), and β -COP (data not shown) and the TGN marker syntaxin 6 (Figure 2, *g-i*).

We further confirmed the Golgi localization of adiponectin by using reduced temperature to block secretory protein trafficking. VSV-G protein is a membrane protein in the constitutive secretory pathway that accumulates in the endoplasmic reticulum at 16°C and in the Golgi complex at 19°C [326]. Incubation of cells at 16°C immediately following transfection resulted in a diffuse intracellular labeling of VSV-G protein, consistent with the endoplasmic reticulum distribution in these cells (Figure 3A, *panel a*). At 19°C, VSV-G protein displayed a predominant peri-nuclear distribution consistent with Golgi localization (Figure 3, *panel b*). To ensure that the temperature block did not damage the cells and thereby resulted in an aberrant accumulation in the Golgi, following incubation at 19°C the cells were shifted to 37°C for 1 h (Figure 3A, *panel c*). Under these conditions, the VSV-G protein was fully capable of exiting the Golgi and traffic to the plasma membrane. In parallel, at 19°C, VSV-G protein colocalized with endogenous adiponectin (Figure 3B, *panels d-f*).

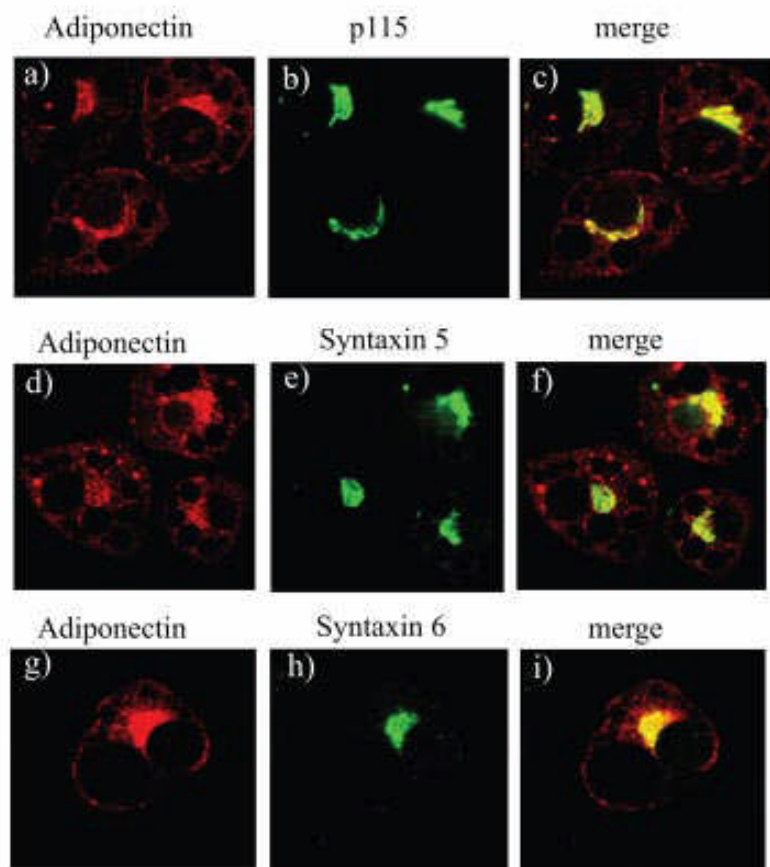


FIGURE 2. Localization of endogenous adiponectin in the Golgi/TGN. Fully differentiated adipocytes were fixed, permeabilized, and immunostained with a specific polyclonal antibody specific for adiponectin (*panels a, d, and g*) or with the cis-Golgi markers p115 (*panel b*) and syntaxin 5 (*panel e*), or with the trans-Golgi network marker syntaxin 6 (*panel h*). The merged images are shown in the *right panels*. The *yellow color* in the merged images (*panels c, f, and i*) indicates colocalization. Images were obtained using a Zeiss 510 META confocal microscope.

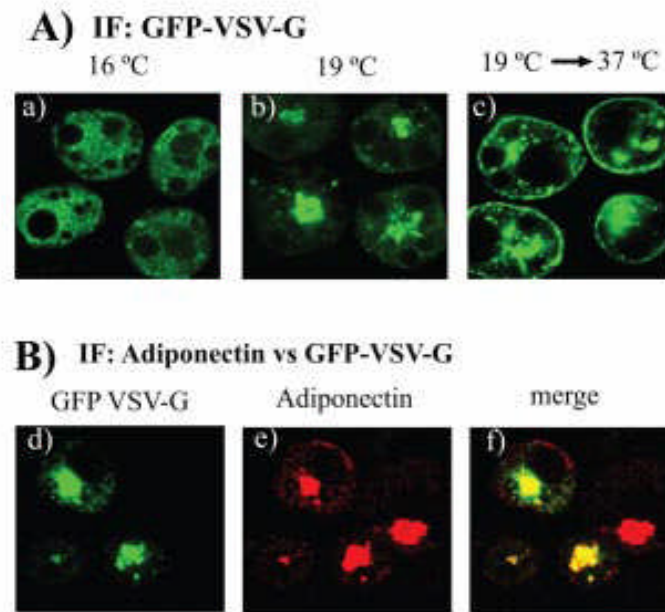


FIGURE 3. Adiponectin colocalizes with the vesicular stomatitis virus G protein. *A*, temperature block of the VSV-G protein. Fully differentiated adipocytes were electroporated with a construct coding for the vesicular stomatitis virus protein. After electroporation cells were incubated overnight at 16°C (*panel a*), overnight at 19°C (*panel b*), or incubated overnight at 19°C and then placed at 37°C for 1 h prior to analysis (*panel c*). Following these incubations cells were fixed permeabilized, and immunostained with an antibody specific for VSV-G protein obtained from Acurate Biochemicals, Inc., as described under “Experimental Procedures.” Images were obtained using a Zeiss 510 META confocal microscope. *B*, colocalization of endogenous adiponectin and VSV-G protein. Fully differentiated adipocytes were electroporated with a construct coding for the vesicular stomatitis virus G protein. After electroporation cells were incubated overnight at 19°C. The next day, cells were fixed, permeabilized, and immunostained with an antibody specific for VSV-G protein (*panel d*) or with an antibody specific for adiponectin (*panel e*) as described under “Experimental Procedures.” *Panel d* shows GFP VSV-G protein. The *yellow color* in the merged image (*panel f*) indicates colocalization. Images were obtained using a Zeiss 510 META confocal microscope. *IF*, immunofluorescence.

BFA is a fungal metabolite that inhibits guanylnucleotide exchange factors that act on class I Arf GTP-binding proteins [327]. This inhibition results in a block of anterograde Golgi trafficking and thereby causes the collapse of the Golgi stacks back into the endoplasmic reticulum [328, 329]. We next determined the effect of BFA on adiponectin secretion by radioimmunoassay (Figure 3A). In control cells, there was a constitutive secretion of adiponectin into the medium that was relatively linear over the time course examined (Figure 4A). Treatment with BFA completely blocked the release of adiponectin, whereas the protein synthesis inhibitor, cycloheximide, had no effect (Figure 4A). Identical results were obtained when the incubation medium was assayed by immunoblotting (Data not shown). Furthermore, cycloheximide treatment for 2 h did not alter the distribution of intracellular endogenous adiponectin in 3T3L1 adipocytes, which remained associated with the Golgi markers (Figure 4B). As a control for cycloheximide action, HEK293 cells were transfected with a vector coding for a green fluorescent protein. Immediately following transfection a subset of cells were treated with cycloheximide. Imaging of these cells revealed no reporter gene expression in the cells treated with the drug (Figure 4C).

Adiponectin Colocalizes with GGA Isoforms

Since adiponectin was localized in the Golgi/TGN region at steady state in 3T3L1 adipocytes we postulated that adaptor proteins at the TGN could regulate adiponectin secretion in adipocytes. GGA proteins are molecular adaptors that mediate sorting at the TGN of specific cargo vesicles and recruit clathrin in an Arf-dependent manner. Recent reports have documented that GGA adaptors facilitate transport of the glucose transporter GLUT4 to the insulin-sensitive compartment in adipocytes (53, 54). To investigate whether GGA coat adaptors are involved in

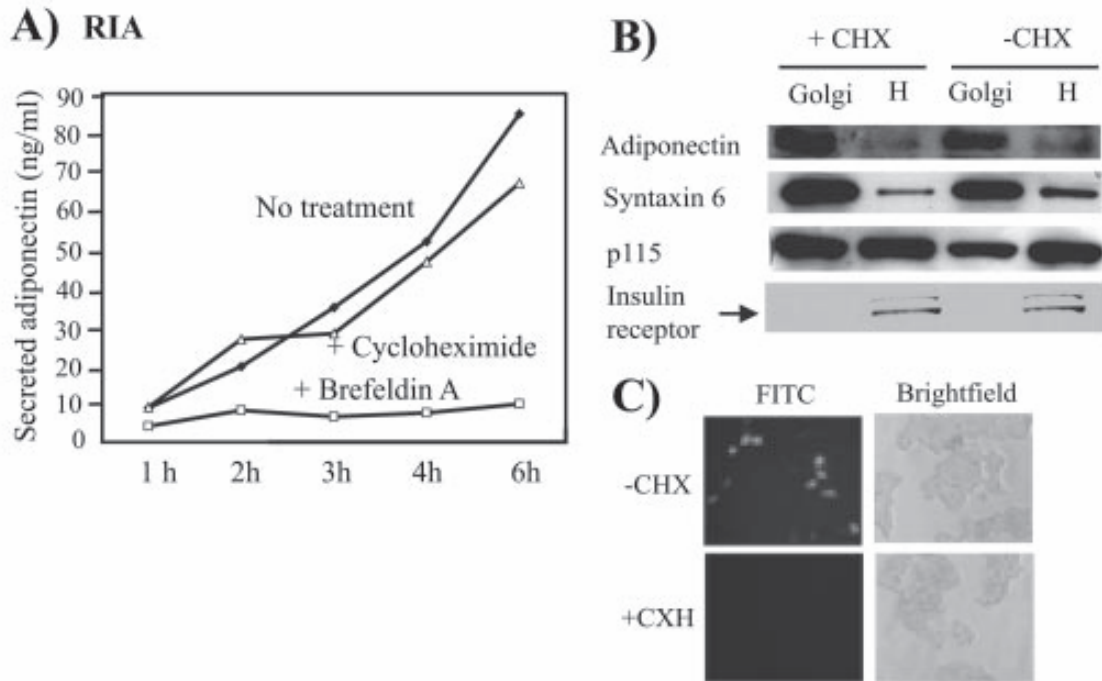
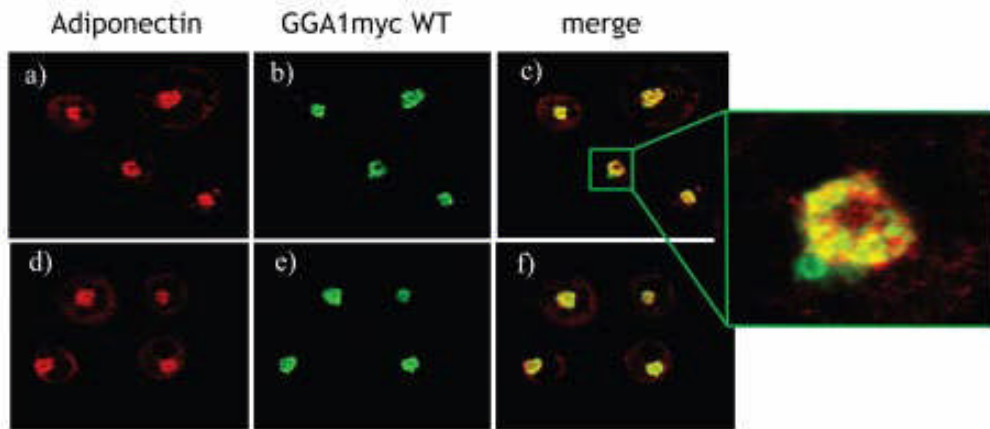


FIGURE 4. Secretion of adiponectin is inhibited by brefeldin A but not by cycloheximide. *A*, time course of adiponectin secretion. Fully differentiated adipocytes were replated in 12-well dishes with the same cell density and allowed to recover in DMEM with 10% FBS. 24 h later, medium was changed to DMEM without serum, in the absence of drug (*No treatment*), in the presence of 5 μ g/ml brefeldin A, (*+Brefeldin A*), or in the presence of 10 μ g/ml cycloheximide (*+Cycloheximide*). A small aliquot of medium was taken at the indicated times, spun for 5 min at 3000 rpm, and the supernatant collected to determine the amount of adiponectin by radioimmunoassay (*RIA*). *B*, Golgi preparation of 3T3L1 adipocytes. Differentiated adipocytes were left untreated or treated with 10 μ g/ml cycloheximide (*CHX*) for 2h at 37 °C. Following this time, cells were fractionated and the Golgi membranes purified as described under “Experimental Procedures.” Equal amounts of the total lysate or the purified Golgi fraction were loaded onto a SDS-PAGE and immunoblotted with the indicated specific antibodies. A representative blot of three independent experiments is shown. *H*, homogenate. *C*, cycloheximide inhibits the expression of the green fluorescent reporter gene ARF-1 GFP. HEK293 cells were transfected with a construct coding for a GFP-tagged ARF-1 protein. Immediately after transfection cycloheximide (*+CHX*) was added to group of cells, whereas a group of cells were left untreated (*+CHX*). Following the treatment with the drug, images of cells were taken on a NIKON TE2000 microscope on a fluorescein isothiocyanate (*FITC*) or brightfield setting.

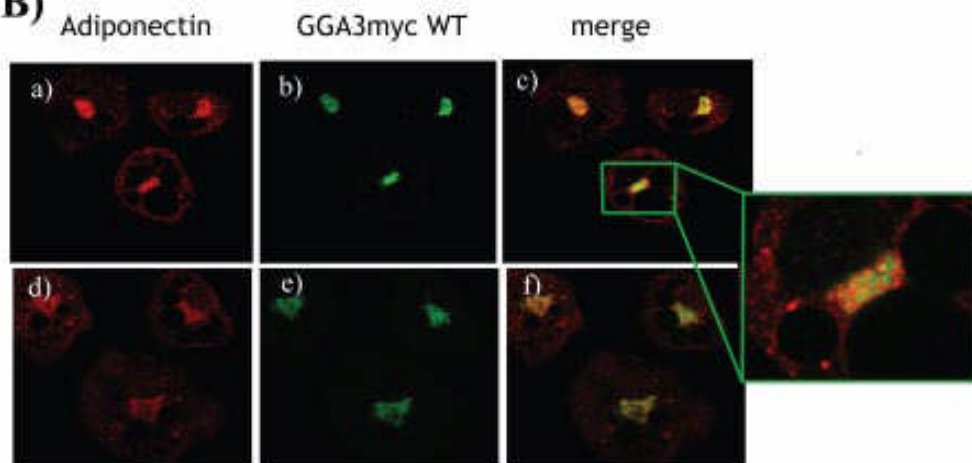
adiponectin secretion, we first examined the colocalization of the GGA isoforms with endogenous adiponectin by confocal microscopy imaging. This was performed in adipocytes that expressed the wild type forms of GGA1myc, GGA2myc, or GGA3myc. Double staining was performed as indicated under “Experimental Procedures” using a myc antibody and an antibody specific for adiponectin (Figure 5, A-C). As shown in Figure 5A, *panel b*, expressed GGA1myc displayed a perinuclear localization that substantially overlapped with that of endogenous adiponectin (Figure 5A, *panel c*). Similar distributions were observed for GGA2myc (Figure 5B, *panel b*) and GGA3myc (Figure 5C, *panel c*) isoforms. Interestingly, insulin treatment of the cells for 30 min had no significant effect on the distribution of neither adiponectin nor the expressed GGA isoforms (Figure 5A, *panel f* and Figure 5B, *panel f*). Overall, these results demonstrate that GGA proteins broadly colocalized with endogenous adiponectin and suggest that GGA adaptors may be involved in the trafficking of adiponectin from Golgi/TGN compartments.

To further confirm these studies, we next examined the localization of endogenous adiponectin and endogenous GGA1 in isolated mouse adipocytes and the localization of expressed adiponectin and GGA1-VHS-eGFP in HEK293 cells by transmission electron microscopy (Figure 6). In isolated fat tissue, immunogold labeling of adiponectin (10-nm gold) and GGA1 (25-nm gold) indicated that these proteins were in close proximity (Figure 6, A and B). Similar results were obtained in HEK293 cells expressing adiponectin (25-nm gold particles) and GGA1-VHS (10-nm gold particles), where both proteins were primarily confined to the perinuclear region (Figure 6, C and D). Although we were unable to preserve a high degree of membrane morphology, higher magnification clearly demonstrated that the GGA1 positive gold particles were colocalized with the adiponectin-positive gold particles (Figure 6, B and D).

A)



B)



C)

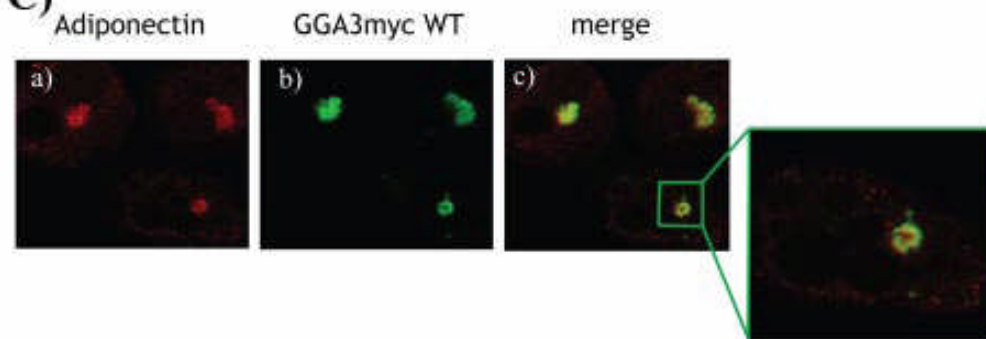


FIGURE 5. Colocalization of GGA proteins and endogenous adiponectin

inadipocytes. Fully differentiated adipocytes were electroporated with a construct coding for the wild type form of GGA1 myc (A), GGA2myc (B), or GGA3myc (C). Following an overnight incubation to allow for protein expression, cells were fixed, permeabilized, and stained as indicated under “Experimental Procedures” with an antibody specific for adiponectin (*panels a and d*) and an antibody for myc (*panels b and c*). When indicated a subset of cells was treated with 100 nM insulin for 30 min prior to fixation. Confocal imaging was performed in a Zeiss 510 META confocal microscope. The *yellow color* in the merged images (*panels c and f*) indicates colocalization. Shown are representative cells of three independent experiments.

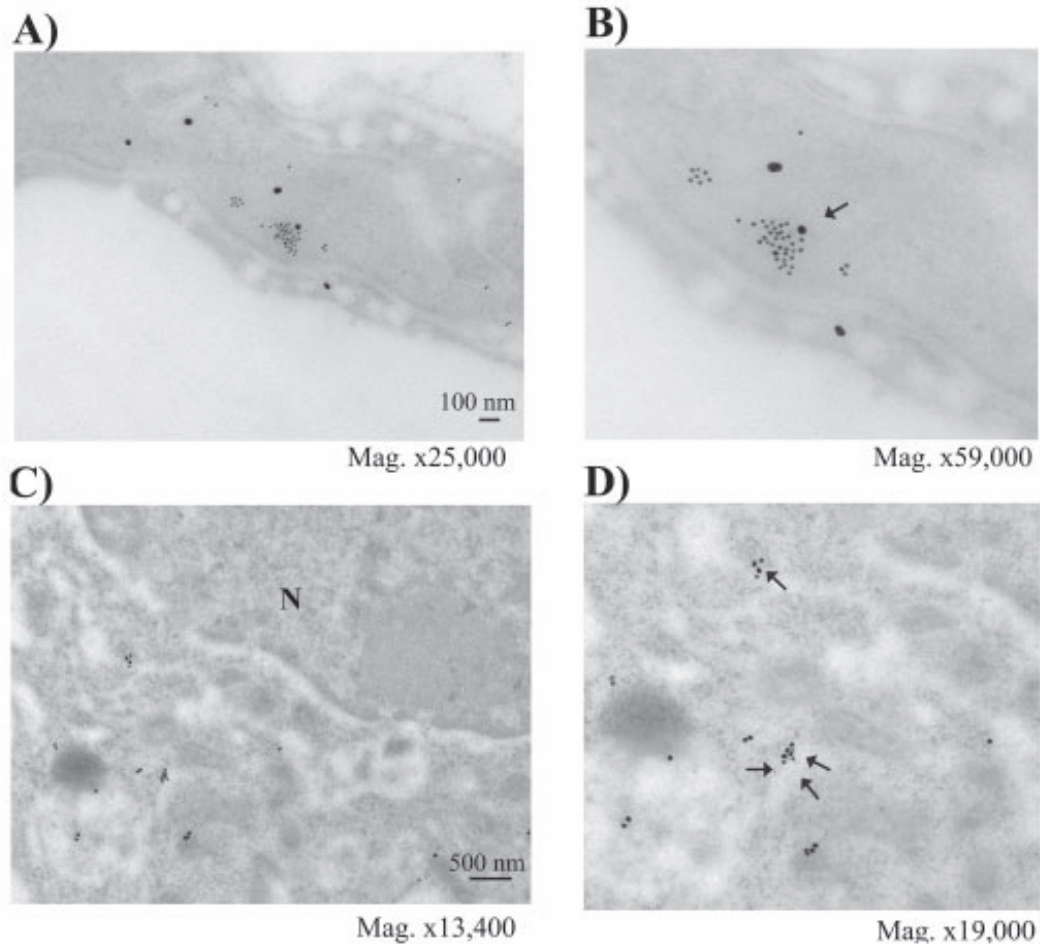


FIGURE 6. Colocalization of GGA proteins and adiponectin. *A* and *B*, isolated mice adipocytes were fixed and processed for electron microscopy as indicated under “Experimental Procedures.” Immunolabeling was performed with an antibody against adiponectin and antibody against GGA1 (Santa Cruz Biotechnology). Secondary antibodies were: goat anti rabbit IgG 10-nm gold for adiponectin and donkey anti-goat IgG 25-nm gold for GGA1. Samples were visualized in a FEI CM100 transmission electron microscope. The *arrows* indicate colocalization of the two proteins. *C* and *D*, HEK293 cells were cultured and cotransfected with a vector expressing adiponectin-myc and either the GGA1 VHS-GFP. 24 h following transfection cells were processed for transmission electron microscopy as described under “Experimental Procedures.” Immunolabeling was performed with an antibody against adiponectin and antibody against GFP (Roche Applied Science). Secondary antibodies were: goat anti rabbit IgG 25-nm gold for adiponectin and goat anti-mouse IgG 10-nm gold for GFP. Samples were visualized in a FEI CM100 transmission electron microscope. The *arrows* indicate colocalization of the two proteins.

Unfortunately, the lack of suitable GGA2- and GGA3-specific antibodies prevented us from examining the colocalization of these proteins with endogenous adiponectin in electron microscopy studies. To further characterize the interaction between adiponectin-containing vesicles and the different GGA isoforms, we designed biochemical and functional assays, which are detailed below.

To investigate whether recombinant GGA proteins could bind to adiponectin-containing vesicles *in vitro*, we next generated constructs expressing the cargo binding domain (VHS) and Arf binding domain (GAT) of either GGA1, GGA2, or GGA3 proteins fused in frame to GST (GST-GGA1VHSGAT, GST-GGA2VHSGAT, or GST-GGA3VHSGAT) and performed *in vitro* pull down assays. Adiponectin vesicles from adipocyte lysates could be effectively precipitated with recombinant GST GGA1-VHSGAT immobilized to glutathione-Sepharose beads (Figure 6A, lane 2, but not with GST alone (Figure 7A, lane 1). This was specific for the GGA1 VHS-GAT domain as neither the GGA2 nor GGA3 VHS-GAT domains were capable of precipitating adiponectin-containing compartments (Figure 7A, lanes 3 and 4). Precipitation of adiponectin by recombinant GST-GGA1VHSGAT occurred in the absence of detergent (Figure 7B, lane 2), but there was no precipitation of adiponectin in the presence of detergent (Figure 7B, lane 4). Although the amount of adiponectin precipitated by GST GGA1-VHS was relatively small compared with the total amount of adiponectin present (Figure 7, A and B, lane 2), these data demonstrated that GGA1 could interact with adiponectin-containing compartments but not directly with adiponectin itself.

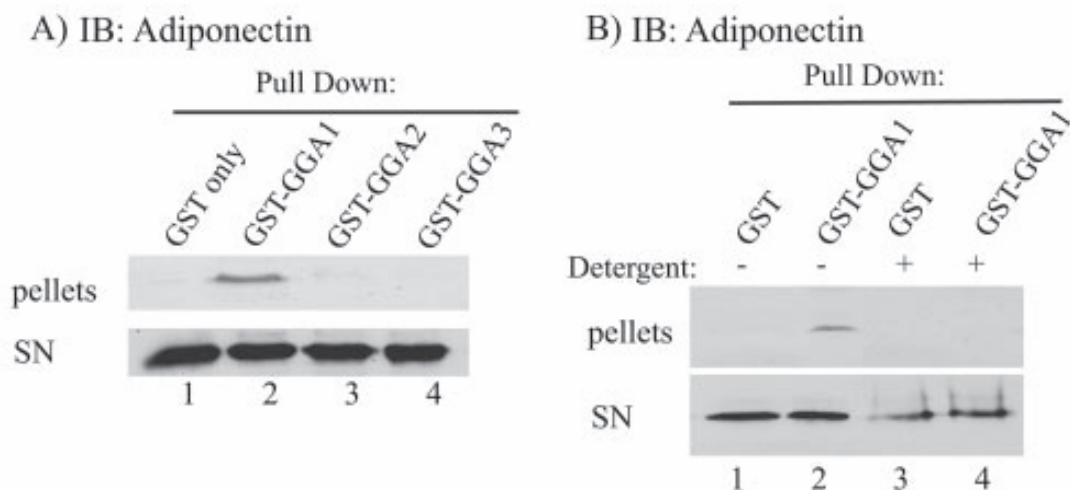


FIGURE 7. Recombinant GGA1, but not GGA2 or GGA3, binds to adiponectin-containing vesicles. *A*, a GST alone or a GST fusion protein with the VHS-GAT domain of either GGA1, GGA2, or GGA3 was produced in bacteria, purified, and bound to glutathione beads as indicated under “Experimental Procedures.” Whole cell lysates obtained from fully differentiated 3T3L1 adipocytes were incubated with either the GST or GSTGGA1/2/3-VHS-GAT fusion proteins for 2 h at 4°C. Following this incubation the bound material (*pellets*) and the non-bound material (*SN*) were separated by brief centrifugation, the pellets washed, and the samples loaded onto an SDS-PAGE for immunoblotting with a specific antibody against adiponectin. A representative blot of five independent experiments is shown. *B*, whole cell lysates obtained from fully differentiated 3T3L1 adipocytes were incubated with either GST or GST-GGA1VHS-GAT fusion protein for 2 h at 4°C in the absence of detergent (*lanes 1 and 2*) or in the presence of 1% Triton X-100 (*lanes 3 and 4*). Following this incubation the bound material (*pellets*) and the non-bound material (*SN*) were separated by brief centrifugation, the pellets washed, and the samples loaded onto an SDS-PAGE for immunoblotting with a specific antibody against adiponectin. A representative blot of three independent experiments is shown.

FIGURE 8. *A*, the VHS domain of GGA1 act as a dominant negative inhibiting Glut4 translocation in response to insulin. Fully differentiated adipocytes were co-electroporated with a construct coding for the myc tag Glut4 glucose transporter and the empty vector pcDNA3.1 (*panels a* and *f*) or the vector coding for the glucose transporter Glut4myc and a construct expressing the VHS and GAT domains of GGA1 fused to eGFP (*panels b, c, g, and h*) or the vector encoding for the glucose transporter glut4 fused to eGFP (Glut4eGFP) and a construct coding for the wild type form of GGA1 (GGA1myc) (*panels d, e, i, and j*). Following electroporation cells were allowed to recover for 24 h and incubated in DMEM without serum or for 2 h at 37 °C. A subset of cells was then stimulated with 100 nM insulin for 30 min at 37 °C. Following these incubations cells were fixed, permeabilized, and immunostained with an antibody specific against the myc epitope (*panels a, b, e, f, g, and j*). Images were obtained using a Zeiss 510 confocal microscope. *B*, the VHS domain of GGA1 inhibits adiponectin secretion in 3T3L1 adipocytes. Differentiated 3T3L1 adipocytes were cultured and co-electroporated with a vector expressing adiponectin-myc, a vector expressing adiponectin-myc and the wild type GGA1 construct, or the adiponectin-myc vector and a construct coding for the corresponding dominant-interfering mutant (VHS-GAT domains) of each GGA protein (GGA1-VHS, GGA2-VHS, GGA3-VHS). 24–36 h following transfection medium and whole cell lysates were obtained, and an aliquot was quantified by ELISA as described under “Experimental Procedures.” *C*, the VHS domain of GGA1 inhibits adiponectin secretion but not leptin secretion in 293 cells. 293 cells were cotransfected with a vector expressing adiponectin-myc and either an empty vector, a irrelevant protein (the glucose transporter GLUT1), a construct coding for GGA1 wild type (GGA1 WT), or a vector coding vector for the corresponding dominant-interfering mutant (VHS-GAT domains) of each GGA protein (GGA1-VHS, GGA2-VHS, GGA3-VHS). An independent set of cells was transfected with a construct expressing full-length of leptin and either an empty vector or a construct coding for GGA1 wild type or the dominant-interfering mutant of GGA1 mutant, which contains only the VHS-GAT domain. 24–36 h following transfection medium and whole cell lysates were obtained and an aliquot quantified by ELISA as described under “Experimental Procedures.” Secreted adiponectin (expressed as percent of total adiponectin expressed) ± S.E. is represented from three independent experiments. Expression of GGA proteins was confirmed by Western blot analysis (data not shown). A one-way ANOVA was utilized to determine significance. The adipokine_empty vector control was utilized as a reference. Significance (*asterisk*) was considered if $p < 0.01$. *D*, adiponectin-myc localizes to a perinuclear compartment in 3T3L1 adipocytes. Adipocytes were transfected with a construct coding for myc-tagged adiponectin (adiponectin-myc) and a construct coding for the GFP-labeled ADP-ribosylating factor-1 protein (ARF-1 GFP). Cells were allowed to recover and the next day were fixed, permeabilized, and immunostained with an antibody for anti-myc (*panel a*) and a secondary antibody conjugated to Texas Red. *Panel b* shows ARF-1 GFP. Images were obtained using a Zeiss 510 META confocal microscope. *Panel c* shows the merged image.

A Dominant-interfering Mutant of GGA1 Blocks Adiponectin Secretion

We next investigated whether GGA proteins are involved in the cargo selection of adiponectin-containing vesicles in 3T3L1 adipocytes. Expression of GLUT4 in adipocytes resulted in the typical perinuclear localization of this protein and insulin-stimulated the translocation of GLUT4 to the plasma membrane (Figure 8A, *panels a* and *f*). Co-expression of the dominant-interfering GGA1 mutants (VHS domain) had no apparent effect on GLUT4 localization but markedly inhibited the insulin-stimulated translocation of the newly synthesized GLUT4 protein (Figure 8A, *panels b, c, g, and h*). As a control, co-expression of the full-length GGA1 protein had no significant effect on the basal or insulin-stimulated translocation of GLUT4 (Figure 8A, *panels d, e, i, and j*). These data are consistent with previous data demonstrating that the expression of a dominant-interfering GGA1 mutant inhibits the insulin-stimulated translocation of the newly synthesized GLUT4 protein [50].

To assess the functional effect of the GGA1 VHS domain on adiponectin secretion, 3T3L1 adipocytes (Figure 8B) or HEK293 cells (Figure 8C, *open bars*) were cotransfected with a construct expressing a myc-tagged adiponectin protein and various control and GGA mutants. The expressed adiponectin-myc protein displayed perinuclear localization (Figure 8D, *panel a*) that overlapped with that of the Golgi localized GFP-tagged ADP-ribosylating factor (ARF-1 GFP) (Figure 8D, *panels b* and *c*). Expression of the full-length GGA1 protein had no significant effect on adiponectin-myc secretion in 3T3L1 adipocytes (Figure 8B), whereas a small reproducible enhancement of adiponectin secretion was observed in HEK293 cells compared with cells transfected with adiponectin alone or cells transfected with adiponectin and an irrelevant protein, GLUT1 (Figure 8C). In contrast, expression of the GGA1VHSGAT domain inhibited adiponectin secretion in both cell types. The inhibitory action of GGA1VHSGAT was

specific, as the VHSAT domains of GGA2 and GGA3 were without affect (Figure 8, *B* and *C*). Moreover, the GGA1VHSAT domain had no significant effect on the secretion of leptin (Figure 8*C*, *filled bars*). Taken together, these data support a model in which adiponectin secretion is specifically dependent upon GGA1 function.

DISCUSSION

Adiponectin increases energy expenditure and decreases circulating glucose and fatty acid levels without a reduction in food uptake [91, 111, 114, 297]. Based upon the central role that adiponectin plays in the control of metabolism, energy homeostasis, and insulin sensitivity, we elected to study the secretory membrane trafficking pathways that are responsible for the release of this adipokine from adipocytes. Confocal microscopy studies in 3T3L1 adipocytes showed that adiponectin was mostly distributed to the perinuclear region; with some punctuate staining throughout the cytoplasm. The adiponectin perinuclear distribution stained positive for markers of the Golgi/TGN, such as p115 and syntaxin 6, whereas no colocalization was detected with endosomal markers or endoplasmic reticulum markers (data not shown). In addition, temperature blocks at 19 °C showed colocalization of endogenous adiponectin with the VSV-G protein, which at this temperature is trapped specifically in the TGN. Thus, our data support the hypothesis that a substantial amount of adiponectin in the steady state is located in the Golgi/TGN. Another study had previously reported that adiponectin containing transport vesicles partially overlap with the endoplasmic reticulum marker GRP94 [330]. Although we do not know the basis for these differences, consistent with adiponectin transport through the Golgi complex, brefeldin A completely blocked adiponectin secretion, indicating that a functional Golgi apparatus is required for adiponectin secretion.

It is well established that traffic through the Golgi requires the recruitment of coat proteins on Golgi membranes, through a process regulated by members of the ADP-ribosylation factors (Arf) family of small GTP-binding proteins (39, 42, 58). These factors recruit adaptor molecules that in turn recruit clathrin to the nascent vesicles. To examine what other elements are required for the trafficking of adiponectin containing vesicles, we examined the role of the

coat adaptor GGA proteins. Recently it has been reported that these proteins mediate the sorting of GLUT4-containing vesicles into the insulin-responsive storage compartment in 3T3L1 adipocytes (53, 54).

To examine whether this interaction between GGA and adiponectin occurs *in vivo*, we transfected fully differentiated adipocytes with GGA1myc, GGA2myc, or GGA3myc constructs and analyzed by confocal microscopy whether endogenous adiponectin colocalized with these GGA proteins. Our results showed that expressed GGA proteins exhibited a substantial degree of colocalization with that of endogenous adiponectin in differentiated 3T3L1 cells. Transmission electron microscopy studies also confirmed localization of GGA1 adaptor proteins with adiponectin in mouse adipocytes.

Structural analysis of GGA proteins has showed differences in the VHS domains of GGA1 and GGA2, with GGA2 having a more flexible and unwound $\alpha 6$ helix end [331], and this can contribute to the recognition of distinct cargo vesicles. While evidence exists that insulin enhances secretion of adiponectin (5, 56), we did not observe any change in the degree of colocalization between GGA and adiponectin following the treatment of cells with insulin. This would suggest that the pool of adiponectin under investigation here is constitutively secreted. Alternatively, insulin may act through a distal (post-TGN) target compartment. Further studies are needed to determine the site of insulin action that results in enhanced adiponectin secretion in adipocytes.

Nevertheless, using GGA precipitation assays, we observed an interaction of the GGA1 VHSGAT domain with adiponectin-containing transport compartments. This binding was specific, since no separation was achieved using the GST portion only or GST fusions with the other GGA isoforms. Importantly, GGA1 did not directly interact with the GGA1 protein but

indirectly associated with the adiponectin-containing transport compartments. This is consistent with the known topology of the GGA proteins (cytosolic) and adiponectin (intraluminal) and further indicates that the adiponectin transport vesicles also contain a specific GGA1 target protein necessary for appropriate cargo selection. At present, the identity of this protein is unknown, and further work is needed to determine which additional proteins participate in the GGAc coating of adiponectin vesicles.

In addition to the ability of GGA1 to associate with adiponectin-containing compartments, expression of the dominant-interfering GGA1 mutant that contains the vesicle-binding domain VHS-GAT inhibited adiponectin secretion. This again was specific for GGA1, as the same domains in GGA2 and GGA3 were without affect. GGA1 function was also specific for adiponectin secretion as another adipokine, leptin, was not affected by expression of the dominant-interfering GGA1 mutant. Interestingly, we also found that expression of fulllength wild type GGA1 protein enhanced adiponectin release in HEK293 cells but not in differentiated 3T3L1 adipocytes, which suggests that the amount of GGA1 protein in HEK293 cells may be rate-limiting for adiponectin secretion in these cells.

In summary, our microscopy biochemical and functional data strongly suggest that GGAc coat adaptors regulate selective cargo formation at the TGN of adipocytes. While intracellular traffic and secretion of adiponectin are mediated by GGA1-coated vesicles, leptin secretion is independent of GGA adaptors. Further studies will now be needed to determine whether GGA-mediated adiponectin secretion is a direct plasma membrane secretory pathway, independent of the recycling endosome system, and to identify other protein components that participate in the generation of adiponectin-containing vesicles.

CHAPTER 3

**ADIPONECTIN AND LEPTIN ARE SECRETED THROUGH
DISTINCT TRAFFICKING PATHWAYS IN ADIPOCYTES.**

ABSTRACT

Adiponectin and leptin are two adipokines secreted by white adipose tissue that regulate insulin sensitivity. Previously we reported that adiponectin but not leptin release depends on GGA-coated vesicle formation, suggesting that leptin and adiponectin may follow different secretory routes. Here we have examined the intracellular trafficking pathways that lead to the secretion of these two hormones. While adiponectin and leptin displayed distinct localization in the steady-state, treatment of adipocytes with brefeldin A inhibited both adiponectin and leptin secretion to a similar level, indicating a common requirement for class III ADP-ribosylating factors and an intact Golgi apparatus. Adiponectin secretion was significantly reduced by endosomal inactivation in both 3T3L1 and rat isolated adipocytes, whereas this treatment had no effect on leptin secretion. Importantly, endosomal inactivation completely abolished the insulin stimulatory effect on adiponectin release in rat adipocytes. Confocal microscopy studies revealed colocalization of adiponectin with endogenous rab11 a marker for the recycling endosome, and with expressed rab5-GFP mutant (rab5Q75L) a marker for the early endosome compartment. Colocalization of adiponectin and rab5Q75L was increased in endosome inactivated cells. Consistent with these findings adiponectin secretion was reduced in cells expressing mutants of Rab11 and Rab5 proteins. In contrast, expression of an inactive (kinase dead) mutant of Protein Kinase D1 moderately, but significantly inhibited leptin secretion without altering adiponectin secretion. Taken together, these results suggest that leptin and adiponectin secretion involve distinct intracellular compartments and that endosomal compartments are required for adiponectin but not for leptin secretion.

INTRODUCTION

Adiponectin and leptin are two hormones secreted by white adipose tissue that regulate insulin sensitivity and energy balance [270, 332, 333]. Adiponectin, functions *in vivo* as an insulin sensitizer [111, 114, 296, 303], reducing glucose production by the liver [112] and enhancing fatty acid oxidation in skeletal muscle [114]. Leptin acts in the hypothalamus to regulate food intake and energy expenditure (reviewed in [334-336]) and also activates fatty acid oxidation in skeletal muscle through the stimulation of the enzyme AMP-dependent kinase (AMPK) [337].

Serum levels of leptin correlate with adipose cell mass and BMI [338-341]. Leptin levels are also increased by feeding and decreased by fasting. Leptin synthesis and secretion is stimulated by insulin [133, 134, 289, 342], glucocorticoids [134, 343-345], glycolytic substrates and amino acids [346, 347] and inhibited by β -adrenergic agonists [348-350]. Insulin is thought to increase both transcription of the leptin gene and secretion [134]. Like leptin, adiponectin secretion is stimulated by insulin [351, 352] and reduced in the fasting state. However, in contrast to leptin, adiponectin serum levels are negatively correlated with obesity and fat cell size [340], and peroxisome proliferative activated receptor (PPAR) gamma agonists increase adiponectin production and secretion [113, 353, 354]. Adiponectin is known to be secreted in different oligomeric forms [95, 355], with the highest oligomeric form being the most biologically active [95, 355].

While substantial information exists on the physiological effects of leptin and adiponectin, the precise intracellular compartmentalization and trafficking pathways leading to the secretion of these two hormones and the molecular components that mediate the traffic of these adipokines are still poorly understood. Our previous observations [356] and the work by

others [293] support the hypothesis that adiponectin is secreted following synthesis at the endoplasmic reticulum, and processing in the Golgi/trans-Golgi network. We have recently reported that at the trans-Golgi network, formation and exit of adiponectin-containing vesicles is dependent on the formation of Golgi localizing γ -ear adaptor 1 (GGA1) coated vesicles, while the secretion of leptin is independent of GGA1 coat formation [347]. These results suggested that these two hormones may be located in distinct intracellular compartments and may follow distinct trafficking pathways. Indeed, the intracellular compartmentalization of leptin in adipocytes has remained controversial. While several studies [289, 347] have reported that in rat adipocytes a substantial amount of leptin is localized in the endoplasmic reticulum in the steady state, other studies suggest that the majority of leptin is accumulated in distinct small intracellular vesicle compartments [357]. Recent fluorescence microscopy studies provided evidence that a portion of leptin is localized in the endoplasmic reticulum, Golgi apparatus and also in small intracellular vesicular vesicles [347].

In the present study, we aimed to elucidate the intracellular compartmentalization and trafficking pathways of these two hormones in 3T3L1 and isolated rat adipocytes. We report here that adiponectin and leptin have distinct intracellular localization in their steady state and adiponectin but not leptin release occurs via endosomal compartments in both 3T3L1 and isolated rat adipocytes. Moreover, insulin-mediated stimulation of adiponectin release is completely blocked by endosomal inactivation in isolated rat adipocytes suggesting that insulin acts at the level of endosomes to enhance adiponectin release. Further, we found that expression of a kinase dead mutant of the enzyme protein kinase D1 selectively inhibits leptin but not adiponectin release. Taken together, these data support the hypothesis that these two proteins take divergent trafficking pathways at the trans-Golgi network, and thus, while adiponectin

release is dependent on intact recycling and early endosome compartments, leptin secretion is independent of the endosomal system.

MATERIALS AND METHODS

Materials and antibodies.

Brefeldin A, DAB, BSA and were obtained from Sigma (St. Louis, MO). Anti-myc antibody (Clone 9E11) was obtained from Santa Cruz Biotechnology, anti-HA antibody was obtained from Sigma, anti-rab5 and anti-rab 11 were acquired from BD Biosciences, anti-adiponectin antibody was a gift from Dr. P. Scherer (Albert Einstein, NY), and anti-transferrin receptor was obtained from Zymed. Transferrin-HRP was acquired from Accurate Chemical & Scientific Corp. Dulbecco's Modified Eagle Media, Opti-Minimum Essential Media, Fetal Bovine Serum, Calf Serum and Trypsin were purchased from Invitrogen. Collagenase type I was obtained from Worthington pharmaceuticals.

Generation of DNA constructs.

The construct encoding for human adiponectin was generated by RT-PCR and subcloned in the pcDNA3 vector (Invitrogen) incorporating a myc tag at the C-terminus. The clone coding for the mouse leptin was subcloned into the pcDNA 3 vector (Invitrogen) and an HA (Haemagglutinin tag) was added in frame in the C-terminus. Identity and positioning of the clone was confirmed by sequencing. The plasmid encoding for GFP tagged syntaxin 6 protein was a gift from Dr. J. Pessin (SUNY, Stonybrook). Plasmids encoding the GFP tagged wild type or K618N mutant of the protein kinase D1 were provided by Dr. V. Malhotra (UCSD). Plasmids encoding the GFP-rab5 wild type, Q79L and S34N mutants were provided by Dr. B. Ceresa (University of Oklahoma). Plasmids encoding the GFP-rab11 Q70L and S25N mutants were provided by Dr. M. McCaffrey (University College Cork).

Animals and adipocyte isolation.

Sprague-Dawley rats (160-200g) were obtained from Charles River. Animals were housed in a 12 hr light/dark cycle and fed *ad libitum*. Animals were euthanized by carbon dioxide asphyxiation and the epididymal adipose pads were quickly removed. Isolation of adipocytes was performed as previously described [358]. The experimental protocol was examined and approved by the Kansas State University Institutional Committee for the Use of animals.

Cell culture and transient transfection.

3T3L1 adipocytes was transfected as previously reported [356].

Pull-down Assay and Western Blot Analysis.

Pull-down Assay and Western Blot Analysis was performed as described [356].

Immunofluorescence and image analysis.

Cells were washed in phosphate buffered saline (PBS) and were fixed, permeabilized and immunostained as described [356].

Inactivation of the endosomal compartments.

Endosomal ablation of 3T3-L1 cells was performed as described previously [359]. Endosomal ablation of isolated rat adipocytes was performed with a minor modification. Briefly, after isolation adipocytes were incubated in Krebs-ringer solution for 1.5 h at 37°C. Cells were then incubated in Krebs-ringer solution containing Tfn-HRP (20 µg/ml) for 1.5 h at 37°C. Cells were then washed three times with isotonic citrate buffer (150 mM NaCl, 200 mM Sodium Citrate, pH= 5.0) for 10 minutes each time and once with Krebs-ringer solution. Krebs-ringer solution containing 200µg/ml DAB and 0.04% H₂O₂, pH=7.2, was then added to the cells. Following a 60 min. incubation at 37°C in the dark, the reaction was stopped by washing with

warm Krebs-Ringer containing 0.5% BSA. Cells were then incubated in Krebs-Ringer for 2 hours. When indicated insulin was added at a final concentration of 20 nM.

Sucrose gradient centrifugation of adipocytes.

Cells were lysed in ice-cold HES buffer (0.25M glucose, 20 mM HEPES, pH 7.4, 1 mM EDTA and 150 mM NaCl) containing protease inhibitors: 1 mM phenylmethylsulfonyl fluoride, 10 µg/ml aprotinin, 1 µg/ml leupeptin, and 1 µg/ml pepstatin. Cells were homogenized with 5 strokes on a glass Dounce homogenizer. Homogenates were centrifuged at 2,095 x g for 15 min. and the supernatants were collected and loaded onto a discontinuous sucrose gradient containing: 1.5M, 1.3M, 1.1M, 1.0M, 0.9M, 0.8M, 0.7M, 0.6M and 0.5M sucrose in HES. Samples were then centrifuged at 75,000 x g for 24h at 4°C and 0.5 ml fractions recovered from the top of the tube. Equal volumes of each fraction were separated by SDS-PAGE and transferred to nitrocellulose filters for immunoblotting.

Determination of adipokine secretion by ELISA.

ELISA kits specific for adiponectin or leptin were obtained from R&D Systems (Minnesota). Prior to the ELISA, floating cells were removed by a brief centrifugation at 500 x g for 5 min and an aliquot of the supernatant was used for the quantification. In parallel, an aliquot of the whole cell lysate was also quantified. Adipokine secretion was calculated as a percentage of total adipokine content as follows: adipokine in the media/ total adipokine (= media + lysate) x 100. To detect adiponectin-myc a modified sandwich ELISA protocol was used with an anti-human adiponectin antibody (DY1065 from R&D Systems at a final concentration of 2µg/ml) and an antibody anti-myc conjugated to biotin (Sigma, Cat. n°: B7554) as a capture antibody.

Statistical Analysis.

A one way ANOVA was performed using SAS statistical software. Statistical significance was considered if $p < 0.05$.

RESULTS

Adiponectin and leptin secretion require an intact Golgi apparatus.

Our previous findings demonstrated the requirement of the formation of GGA1-coated vesicles at the trans-Golgi network for adiponectin release but not for leptin release [356]. This suggested that the intracellular trafficking pathways for the secretion of these hormones may be different. To test this hypothesis we determined by confocal fluorescence microscopy the steady-state intracellular compartmentalization of these two hormones in adipocytes. Differentiated 3T3L1 cells were electroporated with either a myc-tagged adiponectin or HA-tagged leptin constructs to allow for the detection of these proteins using the tag specific antibodies. This was especially important for leptin, since in our hands, the endogenous expression in 3T3L1 cells is very low. After expression of these proteins, cells were fixed permeabilized and immunostained with anti-tag and antibodies against well known intracellular markers. We found that while adiponectin-myc was localized in the perinuclear region [356] and significantly colocalized with syntaxin 6 (Fig9A panels a-c), leptin displayed no colocalization with syntaxin 6 (Figure 9B panels a-c). Leptin distribution overlapped with the endoplasmic reticulum marker BIP (Fig 9B, panels d-f) whereas the majority of adiponectin-myc was not colocalized with this marker (Figure 9A, panels d-f).

Despite having substantially different steady-state localization, it is possible that both hormones traffic through the same secretory pathway. To examine whether a functional Golgi apparatus is required for leptin secretion, fully differentiated 3T3L1 adipocytes expressing leptin-HA were either left untreated or treated with the fungal metabolite brefeldin A (BFA) for 2 hrs. Since BFA inhibits guanidyl nucleotide exchange factors that act on ARF-GTP binding proteins in the Golgi [327], this inhibition causes a block in the anterograde

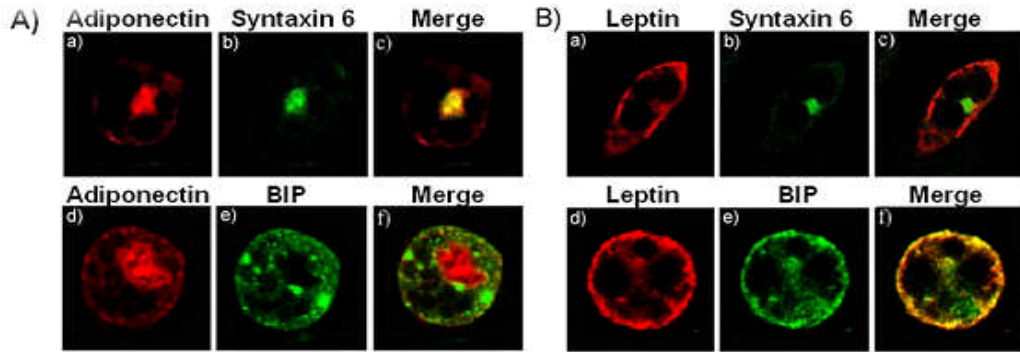


Figure 9. Localization of adiponectin and leptin in 3T3L1 adipocytes. Fully differentiated adipocytes were electroporated with a construct coding for either adiponectin-myc (panel A) or leptin-HA (panel B). Cells were then fixed, permeabilized, and immunostained with a specific antibody anti-myc and a secondary antibody conjugated to Texas red (A, *panels a and d*), or a primary anti-HA antibody and a secondary Texas red-conjugated antibody (B, *panels a and d*) or with an antibody specific for the trans-Golgi network marker syntaxin 6 (A and B, *panel b*), the ER marker BIP (A and B, *panel e*). The merged images are shown in the *right panels*. The *yellow color* in the merged images (A and B, *panels c and f*) indicate colocalization. Images were obtained with a Zeiss 510 META confocal microscope.

Golgi trafficking and thereby causes the collapse of the Golgi stacks back into the endoplasmic reticulum [328, 360]. Following treatment, the amount of secreted leptin-HA (or adiponectin as control) in the conditioned media was measured by ELISA. As shown in Figure 10A, Brefeldin A significantly inhibited the secretion of both adiponectin and leptin-HA to $53.0 \pm 6.4\%$ and $65.0 \pm 6.6\%$, respectively, in 3T3L1 adipocytes. Similar results were obtained in isolated rat adipocytes treated *in vitro* with BFA (Fig 10.B), where an inhibition of $61.0 \pm 3.5\%$ and $64.0 \pm 8.4\%$ was seen for endogenous adiponectin and leptin respectively. These findings demonstrate that blockage of class I ADP-ribosylating factors (ARFs) in the secretory pathway significantly inhibits secretion of both hormones and suggest that both leptin and adiponectin traffic through the Golgi and trans-Golgi network.

Adiponectin but not leptin secretion requires intact endosomes.

We have previously reported that adiponectin release requires the function of GGA1 adaptor proteins [356]. Since GGA proteins have been reported to direct traffic of selective cargo from the trans-Golgi network to the endosomes [361], we hypothesized that adiponectin secretion may occur via the endosomal system. To test this hypothesis, fully differentiated 3T3L1 adipocytes and rat isolated adipocytes were subjected to the endosomal inactivation procedure described by Livingstone et al. [359]. As a control, a subset of cells were incubated in the presence of HRP-conjugated transferrin (Tfn-HRP) but without the substrate DAB. Following the endosome inactivation procedure, both the control and endosome inactivated cells were lysed and fractionated to equilibrium in a sucrose gradient ultracentrifugation as described in the methods section. The fractions were separated by SDS-PAGE transferred to a nitrocellulose membrane and immunoblotted with the endosomal markers: transferrin receptor, rab5 (an early endosome marker) and rab 11 (a recycling endosome). As

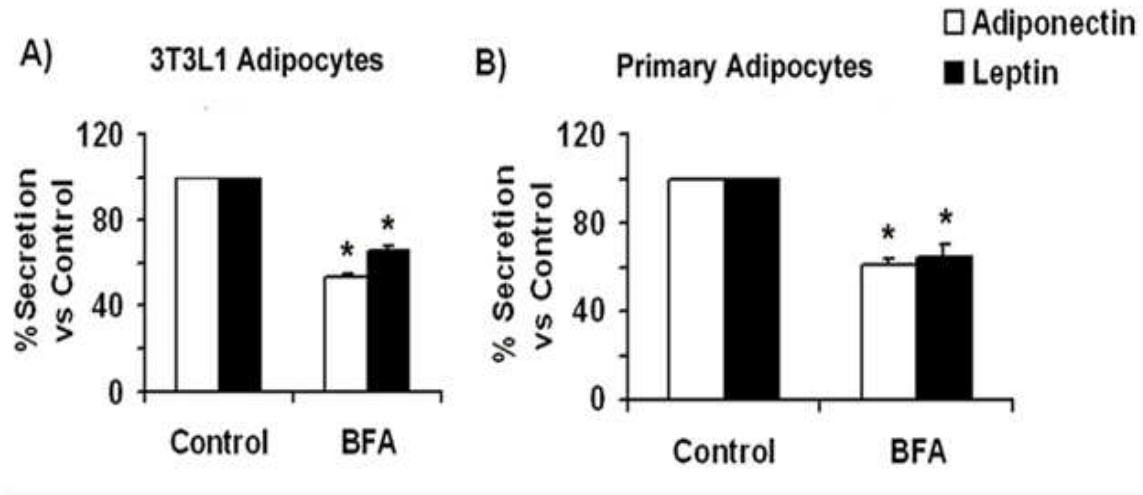
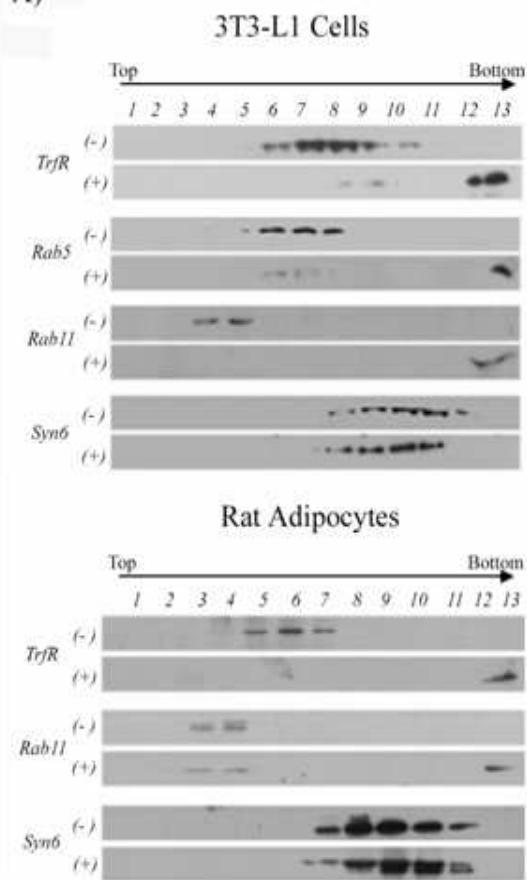


Figure 10. Adiponectin and leptin secretion are inhibited by BFA. **A)** *Secretion in 3T3L1 adipocytes.* Adiponectin secretion (white bars): Fully differentiated 3T3L1 adipocytes were trypsinized and replated in 12-well dishes to distribute the same number of cells per dish. Two hours later the medium was changed to DMEM without serum in the absence (control) or presence of 5 $\mu\text{g/ml}$ BFA. Cells were incubated for additional 4hrs, and an aliquot of media and cell lysate were then taken for adiponectin content quantification by ELISA as indicated in the methods section. Leptin secretion (black bars): Fully differentiated adipocytes were electroporated with a construct coding for leptin-HA and replated in 12-well dishes. 18 h following the electroporation the media was changed to DMEM without BFA, or to DMEM supplemented with 5 $\mu\text{g/ml}$ BFA. Four hours later, media and whole cell lysates were obtained and an aliquot quantified by ELISA as described in the methods section. **B)** *Secretion in isolated rat adipocytes:* Isolated rat adipocytes were obtained as described in the methods section. Equal volumes of packed cells were distributed in separate tubes and incubated in Krebs-Ringer buffer in the absence or presence of 5 $\mu\text{g/ml}$ BFA for 2 hours. A small aliquot of medium was taken to independently determine the amount of adiponectin and leptin by ELISA. Cell lysates were prepared and an aliquot quantitated for the amount of each adipokine by ELISA. The amount of secreted adipokine (expressed as % of total adipokine content) was calculated as described in the methods section and compared to the value obtained for control adipocytes (no BFA treated). The graphs represent the percentage of adiponectin or leptin secreted vs. control adipocytes (-BFA) \pm S.E. obtained from three independent experiments, each performed in triplicate. Differences were considered significantly different when $p < 0.001$ and is indicated by an asterisk.

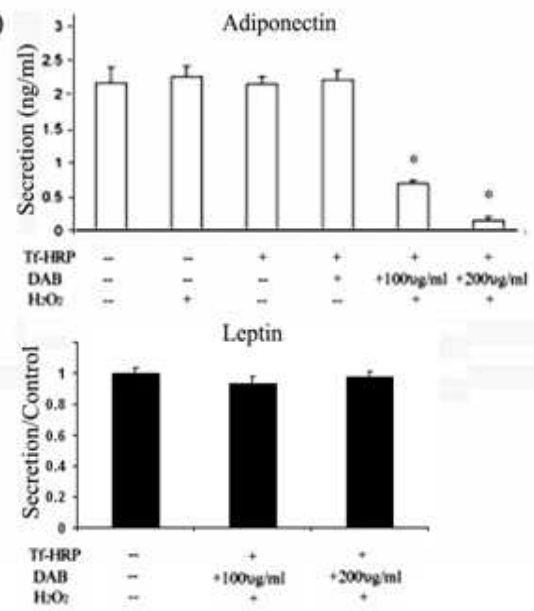
shown in Figure 11A, in control cells where the DAB was omitted, transferrin receptor, rab 5 and rab 11, were revealed in light to medium sucrose density fractions. Under conditions where cells were incubated in the presence of the HRP substrates DAB and H₂O₂, endosomal inactivation was made evident by the presence of these proteins in the heaviest fractions (pelleted material). For 3T3L1 cells (Fig 11A, top panel) a nearly complete endosomal inactivation was observed. To confirm that the endosome inactivation procedure did not affect other non-endosome compartments, samples were immunoblotted with an antibody for the trans-Golgi network marker syntaxin 6. The localization of syntaxin 6 was unchanged after the endosomal inactivation. In addition, the endosomal inactivation procedure did not alter the overall cell morphology or affect the intracellular steady-state localization of adiponectin-myc and leptin-HA in these cells (data not shown). These results were reproduced in rat isolated adipocytes (Figure 11A lower panel).

We next determined whether adiponectin and leptin secretion are affected by endosome inactivation in 3T3L1 adipocytes. As shown in Figure 11B (top panel) endosomal ablation significantly reduced the amount of adiponectin secreted. This effect was DAB dose dependent (Figure 11B, top panel). In contrast, leptin HA secretion in was not affected (Figure 11B, lower panel). To determine whether endosomes are important for adiponectin or leptin secretion in rat-isolated adipocytes and to investigate whether insulin-stimulated release of these hormones is dependent on the endosomal system, the same experiments were performed in isolated rat adipocytes. Cells were incubated with transferrin-HRP and either vehicle or DAB. Following the ablation, a subset of cells were either left untreated or were treated with 20 nM of insulin and were incubated for 2 hrs. Aliquots of media were then taken and quantitated by ELISA for

A)



B)



C)

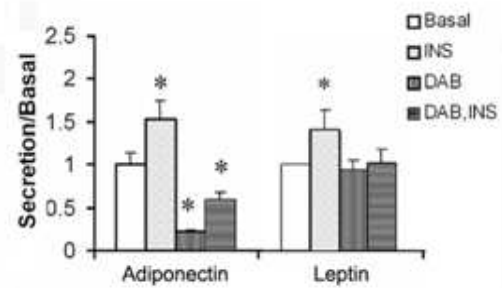


Figure 11. Secretion of adiponectin but not leptin is inhibited by endosomal inactivation. A) Distribution of membranes containing transferrin receptor, rab5, rab11 and syntaxin 6 (syn6) in control cells (-) or cells subjected to endosomal inactivation (+). Fully differentiated 3T3L1 cells (top panel) or rat isolated adipocytes (bottom panel) were subjected to the endosomal inactivation procedure as described in the methods section. As a control, a subset of cells was subjected to the same procedure without the substrates DAB and H₂O₂. Total internal membranes were prepared and separated on a discontinuous sucrose gradient as described in the methods section. Fractions of 0.5 ml were collected from the top of the tube. For each fraction, an aliquot of 50 µl was separated by SDS/PAGE, transferred to a nitrocellulose filter and immunoblotted with specific antibodies to detect transferrin receptor, rab5, rab11 and syntaxin 6 as indicated. Fraction 13 was the pellet at the bottom of the gradient. **B)** Secretion of adiponectin (top) and leptin (bottom) in 3T3L1 cells is inhibited by endosomal inactivation. Cells were subjected to the endosome inactivation technique as described in the methods section using different dosages of DAB as indicated. As a control, a subset of cells were either left untreated or treated with H₂O₂ only, DAB only, or transferrin-HRP only. After endosomal inactivation, cells were incubated in serum free DMEM for 4 hours at 37°C. At that time an aliquot of media was harvested and whole cell lysates prepared and an aliquot of each was quantitated by ELISA for the presence of adiponectin. The graphs display the amount of secreted adiponectin ± S.E. obtained from three independent experiments, each experiment was performed in triplicate. Differences were considered significantly different when $p < 0.05$ and is indicated with an asterisk. **C)** Secretion of adiponectin but not leptin in isolated rat adipocytes is inhibited by endosomal inactivation. Isolated epididymal rat adipocyte cells were obtained by collagenase digestion as described in the methods section. An equal volume of packed cells were incubated in Krebs-Ringer buffer containing transferrin-HRP. A subset of cells were then treated with DAB and H₂O₂ as described in the methods section to inactivate the endosomal compartments. A subgroup of adipocytes was further incubated in the absence or presence of 20 nM insulin at 37°C for 1, 2 hrs. After this time, the conditioned media and a cell lysate were obtained and quantitated with adiponectin or leptin specific ELISA kits. The results shown are the secretion percentage values respective to the secretion measured in control cells (no endosomal inactivation) without insulin and are the mean ± S.E., representing data from three independent experiments and each experiment was performed in triplicate. Differences were considered significantly different when $p < 0.05$ and is indicated with an asterisk.

adiponectin or leptin. As shown in Figure 11C, insulin stimulated adiponectin release by 1.5 fold (+INS group) whereas endosomal inactivation (+DAB) significantly inhibited adiponectin secretion. Interestingly, insulin-mediated activation of adiponectin release was completely abolished by endosomal inactivation (Fig 11C, +DAB+INS group). These results suggest that insulin stimulates adiponectin release by increasing membrane traffic through the endosomal system. Insulin caused a small but significant increase of leptin secretion (Fig 11C, +INS group) but in contrast to adiponectin, leptin secretion was not affected by endosomal inactivation (Figure 11C, +DAB group). Further, insulin-mediated increase in leptin secretion was not affected by endosomal ablation (Figure 11C, +DAB+INS group).

Recycling and early endosomes are involved in adiponectin secretion

We next identified which endosomal compartments participate in adiponectin trafficking. We analyzed by confocal fluorescence microscopy the localization of adiponectin-myc and of endogenous rab11 and rab 5 proteins or expressed GFP-tagged wild type and constitutively active/inactive mutants of rab5. We found that adiponectin-myc partially colocalized with the endogenous rab 5 (data not shown) or with expressed wild type GFP-rab5 (Fig 12A, panels a-c). Adiponectin-myc could be detected in enlarged early endosomes generated by the expression of the constitutively active form of rab5 (rab5Q79L) (Figure 12A, panels d-f). Increased colocalization of adiponectin-myc with GFP-Rab Q79L was observed in cells subjected to the endosomal inactivation (Fig 12B, panels d-f) compared to cells with functional endosomes (Figure 12B, panels a-c). We also found significant colocalization between adiponectin-myc and endogenous rab11 (Fig 12A, panels g-i).

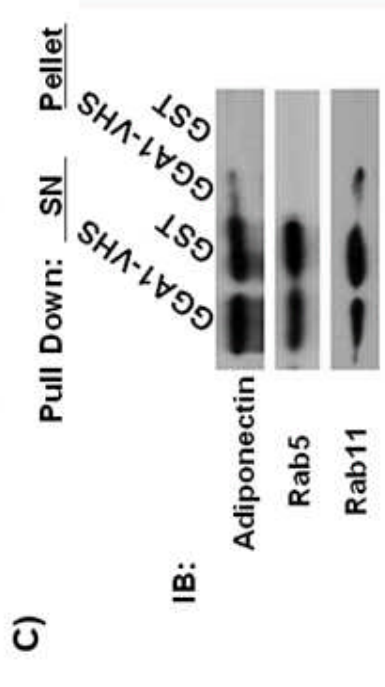
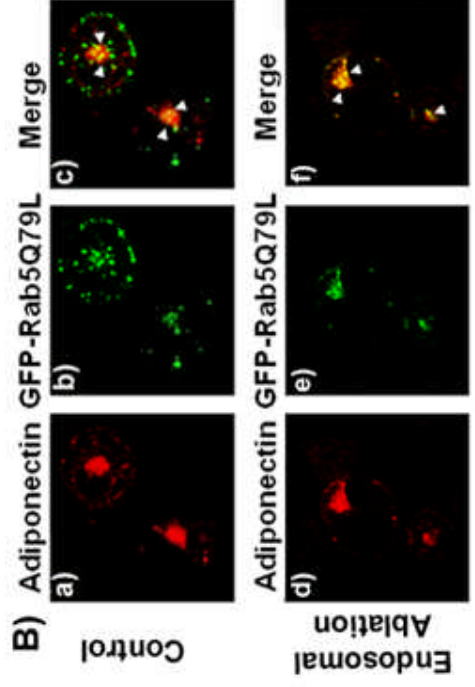
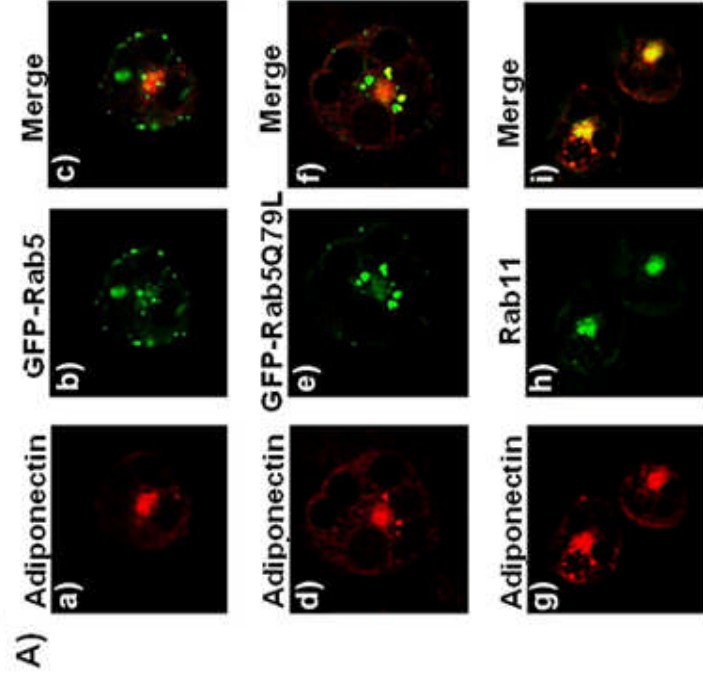


Figure 12. Adiponectin colocalizes with endosomal markers. **A)** Fully differentiated adipocytes were coelectroporated with a construct coding for adiponectin-myc and either a construct coding for a GFP- tagged wild type rab5 (*panels a-c*), or constitutive active mutant of rab5 (Rab5Q79L) (*panel d-f*). Cells were then fixed, permeabilized, and immunostained with a specific antibody for myc and a secondary antibody conjugated to Texas red (*panels a, d and g*), or for endogenous Rab11 and a secondary antibody conjugated to Alexa-488 (*panel h*). The merged images are shown in the *right panels (c-i)*. Images were obtained using a Zeiss 510 META confocal microscope. **B)** A fraction of adiponectin-myc is retained in the early endosome compartment after endosomal inactivation. Fully differentiated adipocytes expressing adiponectin-myc and the GFP-tagged rab5 Q75L protein were subjected to the endosomal inactivation. Upper panels (a to c) show the control group without DAB, lower panels (d-f) show the endosome inactivated cells. Cells were then fixed, permeabilized, and immunostained with a specific antibody for myc and a secondary antibody conjugated to Texas red (*panels a, and d*). The merged images are shown in the *right panels (c-f)*. Images were obtained using a Zeiss 510 META confocal microscope. **C)** Recombinant GST- GGA1 protein precipitates vesicles containing adiponectin and rab 11. Pull down assays were performed with recombinant GST or GST-GGA1VHS recombinant protein as described in the methods section. The pelleted samples and supernatants (SN) were separated by SDS-PAGE transferred to a nitrocellulose membrane and immunoblotted with an antibody specific for adiponectin, rab5 or rab11. A representative blot of five independent experiments is shown.

These results suggested that the recycling and early endosome compartments may form part of the secretory pathway for adiponectin in adipocytes. To confirm these results, we conducted biochemical and functional studies in 3T3L1 adipocytes. We have previously reported that a fraction of intracellular vesicles containing adiponectin can be precipitated with recombinant GGA1 protein fused to GST [356]. We conducted pull down assays of 3T3L1 intracellular membranes using either GST or GST-GGA1 recombinant proteins immobilized to glutathione-sepharose beads as we have described [356]. The pelleted samples were washed in PBS, separated by SDS-PAGE, transferred to a nitrocellulose membrane and immunoblotted with specific antibodies to detect endogenous adiponectin, rab5 and rab 11. The results displayed in Figure 12C, show that a substantial amount of rab11 was readily detected selectively in the precipitates containing adiponectin and the GST-GGA1 but not in the pellets of samples incubated with control GST recombinant protein. This result is consistent with the amount of colocalization between adiponectin-myc and rab11 detected in the immunofluorescence studies. However, we were unable to detect endogenous rab 5 in the GGA1 precipitates of the pull down assay (Figure 12B). The absence of rab5 in the precipitates could also originate from low sensitivity of the assay, since only a fraction of adiponectin-containing vesicles precipitated with GGA1. To complement these results, we performed functional studies to determine whether the expression of mutant rab 5 or rab11 proteins could affect the amount of secreted adiponectin in 3T3L1 adipocytes. As a control, we measured the secretion of leptin in the conditioned medium of these cells. The results expressed as a percentage of adiponectin or leptin secreted vs. total adipokine present in the cell was compared to that obtained in cells expressing either adipokine or an empty vector. As shown in Fig 13A the over expression of either rab11 mutant moderately (~25%) but significantly inhibited the secretion of adiponectin without affecting leptin release.

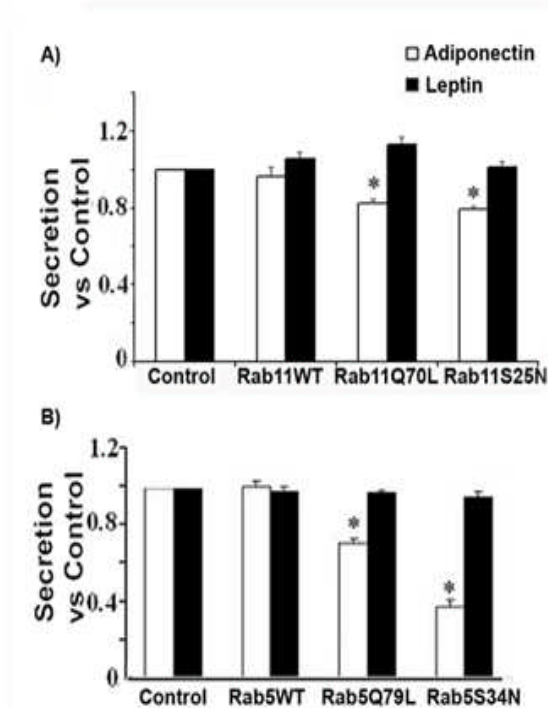


Figure 13. Expression of rab5 and rab11 mutants inhibit adiponectin secretion in 3T3L1 cells. Fully differentiated 3T3L1 cells were electroporated with a construct expressing adiponectin-myc (white bars) or leptin-HA (black bars) and either an empty vector, wild type or constitutive active and inactive mutants of rab 11 (Panel A) or rab5 (Panel B). Following expression of the proteins, media and whole cell lysates were harvested and an aliquot of each were quantified by ELISA as described in the methods section. The amount of secretion is shown as the ratio to the secretion obtained in control adipocytes expressing each adipokine and the empty vector \pm S.E. The graph represents data from three independent experiments and 18 independent observations. Differences were considered significantly different when $p < 0.05$ and is indicated with an asterisk. Expression of adiponectin-myc, leptin-HA and rab proteins were confirmed by western blot analysis (data not shown). For this ELISA we utilized an adiponectin capture and detection antibodies, respectively, as described before [356].

A greater inhibition of adiponectin (~30% with rab5Q75L, ~64% with rab5S34N) was observed in cells expressing mutants of rab5. As expected, no change in leptin secretion was observed with either rab11 or rab5 mutants (Figure 13). Taken together, these results support the hypothesis that both the recycling and early endosome compartments participate in the secretion of adiponectin.

Leptin but not adiponectin traffic uses protein kinase D1.

Our results are consistent with the hypothesis that adiponectin and leptin take divergent trafficking pathways en route to the plasma membrane. Recent evidence in the literature suggests that the serine/threonine Protein Kinase D1, regulates fission at the trans-Golgi network of transport vesicles that deliver cargo to the plasma membrane [362, 363]. We hypothesized that if leptin secretion occurs directly from the TGN to the plasma membrane, its secretion would be inhibited by mechanisms that block activation of this enzyme. To test this hypothesis, we expressed a wild-type form of a GFP-tagged PKD1 or a GFP-kinase-dead mutant incorporating the substitution K618N in 3T3L1 adipocytes. This mutation renders the protein catalytically inactive but allows it to function as a dominant interfering mutant blocking the activation of the endogenous PKD1 [362, 364]. The localization of PKD1 proteins in the Golgi/TGN compartment was confirmed by confocal fluorescent microscopy and compared to the localization of adiponectin-myc. The results shown in Figure 14A demonstrate that GFP-PKD1 and GFP-PKD1-K618N localize in a perinuclear compartment (Figure 14A, panels b and e) and in close proximity to adiponectin-myc (Figure 14A, panels c and f). These results are consistent with the TGN localization of the expressed GFP-PKD1 proteins. We then determined whether expression of these PDK1 constructs would alter the secretion of co-expressed adiponectin-myc

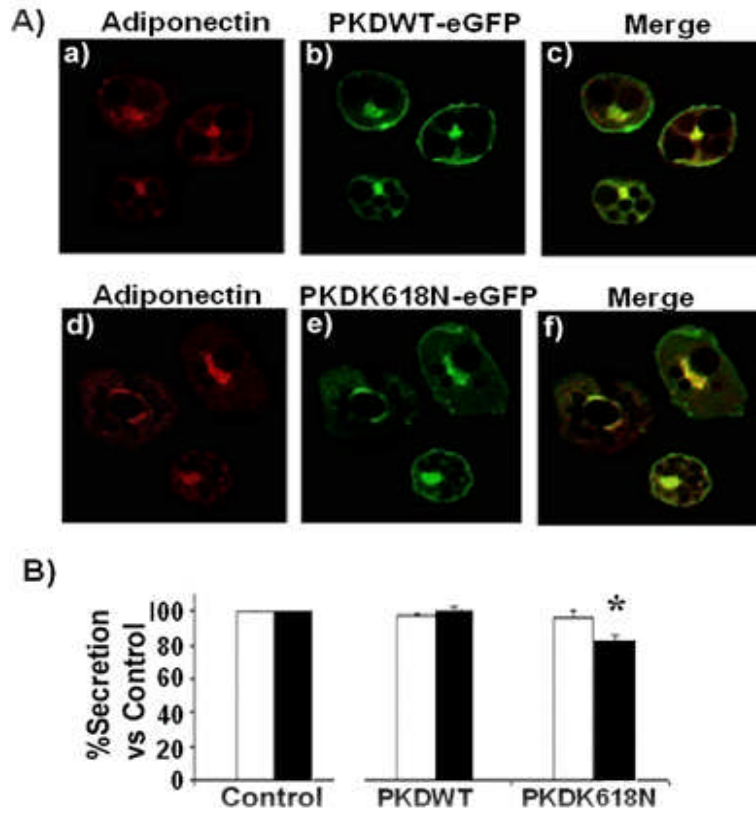


Figure 14. Secretion of leptin, but not adiponectin is inhibited by a mutant of PKD1. **A)** Colocalization of adiponectin and PKD1. Fully differentiated adipocytes were co-electroporated with a construct coding for adiponectin-myc and either a construct coding for a GFP-tagged wild type PKD (*panels a-c*), or a construct coding for the PKD1 dominant interfering mutant PKD1-K618N (*panel d-f*). Cells were then fixed, permeabilized and immunostained with a specific antibody anti-myc and a secondary antibody conjugated to Texas red (*panels a and d*). The merged images are shown in the right panels. Images were obtained using a Zeiss 510 META confocal microscope. **B)** A PKD1 mutant inhibits leptin but not adiponectin secretion in 3T3L1 cells. Cells were co-electroporated with a vector expressing adiponectin-myc or leptin-HA and either an empty vector, a construct coding for PKD1 wild type or a construct coding for the mutant PKD1-K618N. Following expression of the proteins, the conditioned media and whole cell lysates were obtained and an aliquot was taken for the adipokine quantification by ELISA as described in the methods section. The secreted adipokine was calculated in each group as a percentage of total adipokine content and compared to the secretion obtained in the control group expressing adipokine plus the empty vector. The graph shows adipokine secretion vs. control \pm S.E, representing data from three independent experiments, each experiment performed in triplicate. Differences were considered significantly different when $p < 0.05$ and is indicated with an asterisk. Adiponectin: White bars. Leptin: black bars.

or leptin-HA. While we did not detect any change in the secretion of adiponectin-myc by expressing either in the amount of secreted leptin-HA in cells selectively expressing the PKD1 mutant (Figure14B, black bars).

DISCUSSION

In addition to its important role as a lipid storage depot, adipocytes play a key role in the control of energy balance and insulin sensitivity through the secretion of various hormones. Several studies have documented that secretion of these proteins occurs by both constitutive and regulated mechanisms. For example, it is well documented that insulin stimulates the secretion of leptin [289], adiponectin [330], and adipisin [365, 366]. The specific intracellular compartmentalization and trafficking of these hormones is poorly understood. In this report, we examined and compared the intracellular secretory pathways of two critical adipocyte hormones, adiponectin and leptin.

Biochemical and fluorescence microscopy studies have previously demonstrated that neither leptin [290] nor adiponectin [330] localize intracellularly with the well-studied intracellular compartment containing the insulin-responsive glucose transporter Glut4. Furthermore, the precise intracellular steady-state distribution of leptin in adipocytes has remained somewhat controversial. While initial studies [289] had reported that a substantial amount of leptin is found in the cortical endoplasmic reticulum of rat isolated adipocytes, other biochemical studies [357] had found that the distribution of leptin-containing vesicles separated by equilibrium sucrose density centrifugation was not consistent with that of the localization of endoplasmic reticulum markers. To reconcile these differences and to investigate the intracellular trafficking pathways required for leptin secretion in adipocytes, we first compared the intracellular steady-state distribution of expressed leptin-HA with that of another adipokine, adiponectin-myc in 3T3L1 adipocytes. Here we report that these hormones have distinct steady state localizations, whereas adiponectin is localized within the TGN overlapping with the marker syntaxin6, leptin is predominantly localized in close proximity of the endoplasmic reticulum

marker BIP. Thus our results support those found by Barr et.al. [289] in rat adipocytes, and confirm that in the steady-state the majority of adiponectin and leptin are located in distinct intracellular compartments.

Despite displaying a distinct intracellular localization, treatment with brefeldin A, inhibited the secretion of both adipokines in either cultured adipocytes or rat isolated adipose cells (by 58% and 35% in 3T3L1 and 39% and 36% in rat adipocytes for adiponectin and leptin secretion respectively). This finding suggests that both adiponectin and leptin traffic via Golgi/TGN. Interestingly however, in both cell types, BFA did not completely inhibit the secretion of these adipokines, indicating that the short term release of these hormones occurs partially through a BFA insensitive mechanism, and most probably, a post-TGN compartment which we hypothesize could represent the site for regulated secretion.

GGA adaptor proteins are important for the formation of adiponectin-containing vesicles at the TGN of adipocytes [356]. Since GGA proteins participate in the TGN to endosome traffic, we hypothesized that adiponectin secretion but not leptin secretion would involve the endosomal compartment(s). To test this hypothesis, we conducted biochemical experiments to selectively inactivate the endosomes of 3T3L1 adipocytes following the procedure first described by Livingstone et al., 1996 [359]. We also adapted this technique to isolated rat adipocytes. To our knowledge this is the first time that this technique has been applied to these cells. With this technique we achieved a complete inactivation of the endosomal compartments in 3T3L1 cells and a substantial (60%) inactivation of the endosomes in isolated rat adipocytes. Several reasons could account for this difference. First, transferrin-HRP internalization may be slower or less efficient than in 3T3L1 cells or alternatively, rat adipocytes may contain a larger endosomal compartment than 3T3L1 adipocytes which may require higher amounts of Tfn-HRP and DAB

to achieve a complete inactivation. Attempts to increase the time of capture of transferrin-HRP or DAB and H₂O₂ substrate concentrations did not result in an increase in endosome inactivation in these cells. Furthermore, higher concentrations of H₂O₂ resulted in decreased viability of adipocytes (not shown). Nevertheless, our findings in rat isolated adipocytes corroborated the results obtained in the cell line 3T3L1. Endosomal inactivation profoundly reduced the amount of adiponectin secreted while leptin release remained unaffected, indicating that adiponectin but not leptin secretion requires functional endosomes.

To identify the endosomal compartments involved in adiponectin secretion we used confocal immunofluorescence and secretion studies in 3T3L1 adipocytes expressing adiponectin-myc and GFP-tagged wild type and/or constitutively active/inactive mutants of the endosomal markers rab11 and rab5. Immunofluorescence studies revealed adiponectin-myc distributed in close proximity to the endogenous rab 11 and rab5 proteins. In addition, rab11 was detected in precipitated adiponectin-containing vesicles. Furthermore, over expression of a constitutively active or inactive forms of either rab11 or the rab5 proteins, modestly but significantly, inhibited adiponectin-myc release in 3T3L1 cells without affecting leptin release. Taken together, these findings strongly suggest that intact endosomal compartments are required for adiponectin but not leptin secretion. In agreement with these results, Gould's group recently reported that a mutant of rab11 (rab11S25N) inhibited both basal and insulin-stimulated adiponectin secretion in 3T3L1 cells [367]. In line with this, our results in rat adipocytes strongly support the idea that insulin-stimulation of adiponectin release may be mediated via insulin-mediated activation of the endosomal membrane recycling. Similarly to adiponectin, adipisin, a serine protease released by adipocytes is also released via TGN to endosome traffic [366]. While the acute effects of insulin on leptin secretion have been reported to act at the level of secretion [134], our data support a

model where insulin may increase secretion of adiponectin and leptin in different ways. It remains to be established whether a similar or distinct insulin intracellular signaling cascades are utilized to control secretion of each adipokine.

To further identify molecular regulators for leptin secretion we tested whether leptin secretion is dependent on Protein Kinase D1 activity, and enzyme that regulates the formation of TGN-derived vesicles en route to the plasma membrane [363, 368]. Over expression of a dominant interfering mutant PKD1 K618N exhibited a moderate but significant decrease in leptin release. This suggests the possibility that PKD1 may be involved in regulating at least partially, the trafficking of leptin-containing vesicles. Further experiments are required to test whether the PKD1 activity is required for the insulin-stimulated effect on leptin secretion.

Taken together, our results demonstrate that adiponectin and leptin are secreted through distinct intracellular trafficking pathways and suggest that adipocytes rely on different avenues for the constitutive and regulated secretion of these adipokines.

FOOTNOTES

Abbreviations: ARF: ADP-ribosylating factor; BFA: Brefeldin A; BSA: Bovine Serum Albumin; DAB: 3,3'-Diaminobenzidine; GGA1: Golgi localizing γ -adaptin ear homology domain ARF binding protein; GST: Glutathione-S-transferase; HRP: Horse-Radish Peroxidase; PDK1: protein kinase D1; PPAR: Peroxisome Proliferator-Activated receptor- γ agonist; Tfn: Transferrin; HRP: Horse radish peroxidase; TGN: Trans-Golgi network.

CHAPTER 4

MACROPHAGE-DERIVED IL-6 ALTERS GLUT4 IN ADIPOCYTES

ABSTRACT

Adipose tissue was originally classified as an energy reservoir where excess energy was stored in the form of triacylglycerols. It is now clear that it also secretes leptin and adiponectin, along with IL-6, TNF- α and many other cytokines, and insulin resistance is associated with macrophage infiltration. We tested the hypothesis that macrophages affect insulin resistance by disrupting insulin-stimulated glucose transport and adipocyte differentiation. To test this hypothesis, we co-cultured 3T3L1 adipocytes with C2D macrophage cells or primary peritoneal mouse macrophages. We found that peritoneal macrophages significantly decreased insulin-stimulated GLUT4 but not constitutive GLUT1 translocation to the plasma membrane, regardless of whether the 3T3L1 cells were directly in contact with macrophages or were co-cultured in transwell plates. The cytokines, TNF- α , IL-6 and IL-1 β all inhibited GLUT4 translocation and transcription. However, only IL-6 was inhibitory at concentrations found in macrophage-adipocyte co-cultures. IL-6 and TNF- α but not IL-1 β , inhibited Akt phosphorylation within 15 minutes of insulin stimulation. However, only IL-6 was inhibitory 30 minutes after stimulation. Lastly, we found that adipocyte differentiation was inhibited by macrophages or by recombinant TNF- α , IL-6 and IL-1 β , with IL-6 having the most impact. These data support the hypothesis that macrophages induce insulin resistance by inhibiting glucose transport in adipocytes and by inhibiting their differentiation by secretion of proinflammatory cytokines with IL-6 being the most effective.

INTRODUCTION

Insulin resistance is characterized as an impairment of glucose utilization and insulin sensitivity. There is increasing evidence of a relationship between inflammation and the development of insulin resistance. One hypothesis is that inflammation causes “metabolic syndrome”, which is defined as a combination of symptoms associated with insulin resistance and known to precede the onset of type 2 diabetes [190, 369].

Insulin resistance not only accompanies chronic inflammation but also abnormal mediator secretion [370]. Adipose tissue is now appreciated as an endocrine organ that secretes hormones and cytokines including TNF- α , IL-1 β and IL-6 [371]. The cytokines are associated with increased number of adipose tissue macrophages in obese and diabetic patients [174, 229]. Direct or indirect interactions between adipose tissue macrophages and adipocytes may impair insulin action, affect key protein expression or activate inflammatory pathways. For example, increased levels of TNF- α , IL-6, C-reactive protein (CRP) and monocyte chemoattractant protein-1 (MCP-1; CCL-2) are elevated in obese and diabetic people [175, 372, 373]. In the obese mouse (*ob/ob*), the absence of the TNF- α improved insulin sensitivity and glucose homeostasis [191]. The adoptive transfer of bone marrow cells from TNF^{+/+} mice into TNF- α knock-out mice reduced insulin sensitivity of the recipients [374]. Therefore, it is clear that TNF- α has an impact on insulin sensitivity. However, it is not clear if TNF- α is the only cytokine that is required to induce insulin resistance. IL-6 is overexpressed in adipose tissue of obese and diabetes patients [375]. It reduced the adiponectin concentrations in human adipose tissue and reduced transcription of insulin receptor substrate-1 (IRS-1) and glucose transporter 4 (GLUT-4) in 3T3L1 cells [207, 372, 376]. IL-1 β has also been reported to be higher in

overweight and obese individuals. It reduced insulin receptor substrate (IRS) expression in differentiated 3T3L1 adipocytes [377]. Moreover, individuals with a combined increase in IL-1 β and IL-6 levels were at greater risk of developing type 2 diabetes than individuals with increased IL-6 alone [222].

Collectively, these data demonstrate that TNF- α , IL1 β and IL-6 play a critical role in the onset of obesity-related insulin resistance. However, both macrophages and adipocytes produce proinflammatory cytokines. Given that these cytokines synergize and regulate each other, there are many unanswered questions about what happens during the adipocyte-macrophage interaction and how insulin resistance is induced.

We hypothesized that macrophages would affect glucose uptake and the signaling that occurs in response to insulin. To test this hypothesis, we co-cultured macrophages and differentiated adipocytes and examined the impact of the interaction on adipocytes.

MATERIALS AND METHODS

Antibodies and recombinant cytokines.

Mouse recombinant TNF- α , IL-1 β and IL-6 were purchased from R&D systems (Minneapolis, MN). Rabbit anti-mouse GLUT4 Polyclonal antibody (Cat. ab654-250) was obtained from Abcam (Cambridge, MA). Rabbit anti-mouse GLUT1 Polyclonal antibody (Cat. CBL242) was obtained from BD Biosciences (San Jose, CA). Rabbit anti-Akt polyclonal antibody (Cat.9272) and rabbit anti-phospho Akt (serine 473, Cat. 9271S) were obtained from Cell Signaling (Beverly, MA). Allophycocyanin (APC)-conjugated goat anti-rabbit IgG (Cat. sc-3846) was purchased from Santa Cruz Biotechnology (Santa Cruz, CA). For ELISA, anti-TNF- α antibody (capture, Cat.551225), biotinylated anti- TNF- α antibody (detection, Cat.554415), anti-IL6 antibody (capture, Cat.554400) and biotinylated anti-IL6 antibody (detection, Cat.554402) were obtained from BD Biosciences (San Jose, CA, Cat.); anti-IL1 β antibody (capture, Cat.MAB401) and biotinylated anti-IL-1 β antibody (detection, Cat. BAF401) were obtained from R&D systems (Minneapolis, MN).

Cell culture.

3T3L1 adipocytes were obtained from the American Type Culture Collection (Manassas, VA). Adipocytes were cultured and differentiated as described previously [356].

The C2D macrophage cell line was created by our group and was cultured in DMEM₁₀ as described previously [378]. The BHK cells were purchased from the ATCC and were cultured in DMEM₁₀ at 37 °C with 8% CO₂.

Peritoneal macrophages were obtained from C57BL/6J mice by peritoneal lavage 4 days after intraperitoneal injection of 1.5 ml of 4% thioglycollate. Macrophages were incubated in ammonium chloride lysis buffer (0.15M NH₄Cl, 10mM KHCO₃, 0.1mM Na₂EDTA, pH=7.3) for

5 minutes on ice to lyse contaminating red blood cells. Cells were washed three times with PBS. Indirect co-culture was performed by incubating peritoneal macrophages (1×10^6 cells) or C2D macrophages (1×10^5 cells) in 0.4 μm cell culture inserts from BD Bioscience and placing them in 6-well plates containing 3T3L1 adipocytes differentiated at day 8 (1×10^6 cells) for 4 days. Direct co-cultured was performed by directly adding peritoneal macrophages (1×10^6 cells) or C2D macrophage cells (1×10^5 cells) into the 6-well plates containing undifferentiated 3T3L1 adipocytes (1×10^6 cells). Fewer C2D macrophage cells were added because they continue to proliferate ($T_{1/2} \approx 24$ hrs) [378], while peritoneal macrophages do not.

Transfection of BHK and 3T3L1 cells.

GFP tagged GLUT1 and GLUT4 constructs were a gift from Dr. J. E. Pessin (SUNY Stonybrook) and were used as previously described [379]. The eGFP-N1 empty vector plasmid was from Clontech. Plasmids were transiently transfected into BHK cells by Transfectamine 2000 from Invitrogen (Invitrogen, Carlsbad CA) according to the manufacturer's protocol. Briefly, BHK cells grown in a 12-well plate were washed with Opti-MEM (Invitrogen) when cells were about 80% confluent. Plasmid DNA was resuspended at a concentration of 3 μg per 50 μl opti-MEM and lipofectamine was resuspended at a concentration of 5 μg per 50 μl in Opti-MEM. Plasmid DNA and lipofectamine were then mixed and incubated at room temperature for 20 minutes in DMEM₁₀. One hundred μl of the reaction mixture were added to cells in the 24-mm wells of the 12-well plates. BHK cells were incubated for 24 hours at 37°C. Transfection efficiency was determined by counting positive cells among 100 randomly selected cells using a fluorescent microscope 24 hours after transfection. Only BHK cells with transfection efficiency above 50% were used in our experiments. 3T3L1 adipocytes were transfected by electroporation as described before [356].

Immunofluorescence and Image Analysis.

Transfected and intact adipocytes were washed in phosphate buffered saline (PBS), fixed, permeabilized and immunostained as described previously [356]. The cells were imaged using a Zeiss LSM 510 META confocal microscope. Images were then imported to Adobe Photoshop (Adobe Systems, Inc.) for processing.

One-step RT-PCR analysis.

Total RNA was extracted from cells by Trizma Reagent from Sigma-Aldich according to the manufacturer's protocol with some modification. One-step RT-PCR was performed by using Access RT-PCR Core Reagents from Promega (Madison, WI) according to the manufacturer's protocol. Primers were designed using Primer3 software (<http://frodo.wi.mit.edu/>) using sequence data from NCBI sequence database. Primer sequences (forward/reverse) used were as follows: β -actin (Gene bank ID: NM_007393) 5'-tcctgtggcatccacgaaact-3'/ 5'-gaagcatttgcggtggacgat-3'; GLUT4 (Gene bank ID: AB008453) 5'-caacagctctcaggcatcaa-3'/ 5'-ctcaaagaaggccacaaagc-3'; IL-1 β (Gene bank ID: NM_008361) 5'-caggcaggcagatcactca-3'/ 5'-aggccacaggtattttgtcg-3'; IL-6 (Gene bank ID: NM_031168) 5'-ttcctctctgcaagagact-3'/ 5'-tgtatctctctgaaggact-3'; TNF- α (Gene bank ID: NM_013693) 5'-gggatgagaagttcccaaag-3'/ 5'-ctccagctggaagactcctcccag-3'; adiponectin (Gene bank ID: NM_009605) 5'-gttgcaagctctctgttcc-3'/5'-tctccaggagtgccatctct-3'; GLUT1 (Gene bank ID: D10229) 5'-gctgtgcttatgggtctctc-3'/ 5'-agaggccacaagtctgcatt-3'. The RT -PCR products were visualized under UV light by the FluorChemTM 8800 Advanced Imaging System (Alpha Innotech, San Leandro, CA). The relative density of the target band was normalized to the β -actin loading control and then expressed as a percentage of the controls.

Flow cytometry analysis.

For the analysis of cell surface GLUT4 and GLUT1, cells were immediately fixed in 2% paraformaldehyde at 37°C for 15 minutes. After twice washing with PBS, cells were blocked with goat serum for 0.5 hour and were then treated with rabbit anti-mouse GLUT4 or GLUT1 antibodies for 1 hour at room temperature. After two washes with PBS, cells were stained with APC-conjugated goat anti-rabbit IgG for 0.5 hour. Cells were resuspended in PBS and assessed by flow cytometry after washing with PBS twice.

For the analysis of the intracellular molecules, cells were first fixed in 2% paraformaldehyde for 20 minutes at 37°C. Cells were then permeabilized by incubating the cells in 90% ice-cold methanol for 30 minutes. The cells were washed twice in PBS and were blocked and probed with antibody as described above. Samples were analyzed using a FACS Caliber analytical flow cytometer (Becton Dickinson, San Jose, CA). 5,000-10,000 events measured for each sample. Data analysis was performed with Winlist software (Verity Software House, Topsham, ME).

Enzyme-Linked ImmunoSorbent Assay (ELISA).

TNF- α , IL-1 β and IL-6 in cell culture supernatants were measured by ELISA [380]. Briefly, the ELISA plates were coated with capture antibodies overnight at room temperature. After 1 hour blocking, samples were added to each well and incubated at room temperature for 2 hours. After three washes with PBS completed with 0.5% Tween-20 (PBST), biotin-conjugated detection antibodies were added and incubated at room temperature for 2 hours. HRP-streptavidin was then added and incubated in room temperature for 30 minutes. After three washes, substrate was added to the wells. Within 30 minutes, the reaction was stopped by 1N H₂SO₄ and absorbance was assessed using a BioRad microplate reader Model 680 (Bio-Rad Laboratory, Inc., Hercules, CA) at 450 nm.

Assessment of 3T3L1 adipocytes differentiation.

3T3L1 fibroblasts were induced to differentiate for 4 days as described [356]. On day four, peritoneal macrophages or cytokines were added for 4 days. On day 8, adipocytes were fixed with 2% paraformaldehyde at 4 °C for 15 minutes. The cells were washed twice with PBS and were stained with Sudan IV saturated 70% isopropanol for 15 minutes. Cells were then washed twice with 50% isopropanol. Cells were mounted on microscope slides using several drops of glycerol and were viewed on a light microscope and photographed. To measure the differentiation based on the amount of lipid present in the cells, absorbance was read at 500 nm using a Packard SpectraCount spectrophotometer (Packard Instrument Company, Meriden, CT).

Statistical analysis

Data were analyzed by ANOVA. Sets with statistically significant F score were analyzed for group-to-group variation using the least significant difference method (Fisher's LSD). Differences were considered significantly different when $p < 0.05$.

RESULTS

Macrophage induced insulin resistance in 3T3L1 adipocytes.

To examine the impact of macrophages on insulin sensitivity of 3T3L1 adipocytes, we first tested the hypothesis that cell-cell contact was required between macrophages and adipocytes to affect the insulin responsiveness of 3T3L1 adipocytes. To test the hypothesis, we examined the translocation of insulin-responsive GLUT4 from intracellular compartments to the plasma membrane. This is a key process necessary for insulin-stimulated glucose uptake [381]. We evaluated whether the GLUT4 specific antibody for western blots would detect membrane-located GLUT4 proteins in the plasma membrane. We expressed GLUT4-GFP in differentiated 3T3L1 cells. As described in the methods, we fixed cells with or without 0.2% Triton X-100. We then probed the cells for GLUT4 protein with the rabbit anti-mouse GLUT4 antibody followed by goat anti-rabbit IgG conjugated with Texas red. Permeabilized, unstimulated adipocytes showed colocalization of GLUT4-GFP expressed intracellularly with endogenous GLUT4 (Figure 15i), while nonpermeabilized cells expressed only GLUT4-GFP (Figure 15a). Insulin-stimulated cells expressed GLUT4-GFP both intracellularly and on the plasma membrane (Figure 15d). However, we only detected GLUT4 on the plasma membrane with anti-GLUT4 antibodies in nonpermeabilized cells (Figure 15e). In contrast, we detected GLUT4 intracellularly and on the plasma membrane in permeabilized cells with the antibody probe (Figure 15k).

Since the anti-GLUT4 antibody could detect both intracellular and plasma membrane expressed GLUT4, we used it to determine if macrophages affect GLUT4 trafficking. In our first experiment, we overexpressed GLUT4 in BHK cells. We cultured transfected BHK cells with C2D macrophage cells for two days and we assessed GLUT4 translocation with the antibody

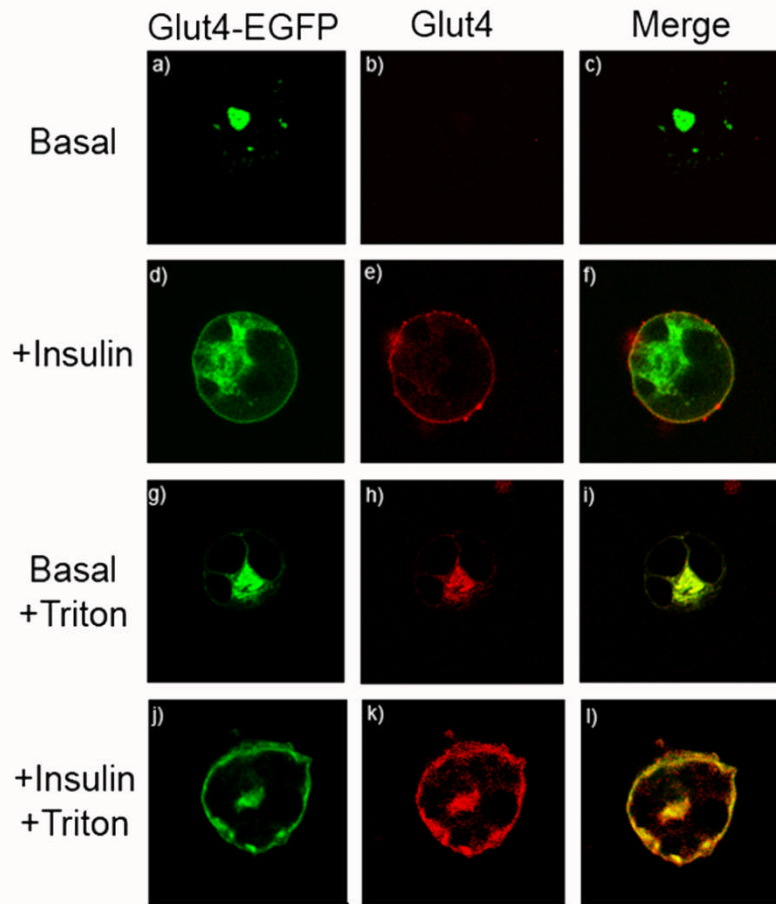


Figure 15. Detection of GLUT4 in 3T3L1 adipocytes. *GLUT4*-GFP was expressed in 3T3L1 adipocytes (Panels a, d, g, j). Eighteen hours later, cells were incubated in serum-free medium for 2 hours, then stimulated with (panels d, c, f, j, k, l) or without (panels a, b, c, g, h, i) insulin, permeabilized (panels g-l), fixed (panels a-f) and immuno-stained (panels b, e, h, k) as described in the Materials and Methods.

probe in cells positive for GLUT4-GFP described in our flow cytometry methods. In the absence of insulin, BHK cells co-cultured with C2D macrophage cells expressed significantly less membrane GLUT4 compared to BHK cells grown without C2D macrophage cells (Figure 16A). With insulin stimulation, there was significantly more ($p < 0.05$) translocation of GLUT4 from intracellular storage compartments to the plasma membrane in the population of GLUT4-GFP transfected BHK cells cultured alone than co-cultured with C2D macrophage cells (Figure 16A, compare open bars, L to R, 1 & 3 and 2 & 4). However, membrane expressed GLUT4 levels were much lower in cells cultured with C2D macrophage cells (Figure 16A, left 2 open bars). In contrast, BHK cells transfected with the GFP-vector only, had no change in plasma membrane GLUT4 expression (Figure 16A dark bars). We also examined the impact of C2D macrophage cells on endogenous GLUT4 trafficking in differentiated 3T3L1 adipocytes to determine whether macrophages would disrupt glucose trafficking. We co-cultured C2D macrophage cells with 3T3L1 adipocytes for 4 days by culturing them together so that they were in contact with one another or by culturing them apart in transwell plates. In the absence of insulin, co-culture had no impact on basal membrane GLUT4 expression (Figure 16B, open bars). However, there was significantly less ($p < 0.05$) membrane GLUT4 in 3T3L1 adipocytes directly co-cultured with C2D macrophage cells compared to control 3T3L1 adipocytes after insulin stimulation (Figure 16B). An alternative analysis shows that the increase in insulin-stimulated translocation of GLUT4 compared to basal translocation was 2.3 fold more in adipocytes incubated alone. These ratios were lower for adipocytes incubated with C2D macrophage cells, 1.6 and 1.5 in transwell or direct co-culture, respectively (Figure 16B). C2D macrophage cells have an immature phenotype and secrete small amounts of IL-6 and no TNF- α or IL-1 β *in vitro* [20]. Therefore; if a combination of cytokines was necessary to alter GLUT4 metabolism, they may not be the most

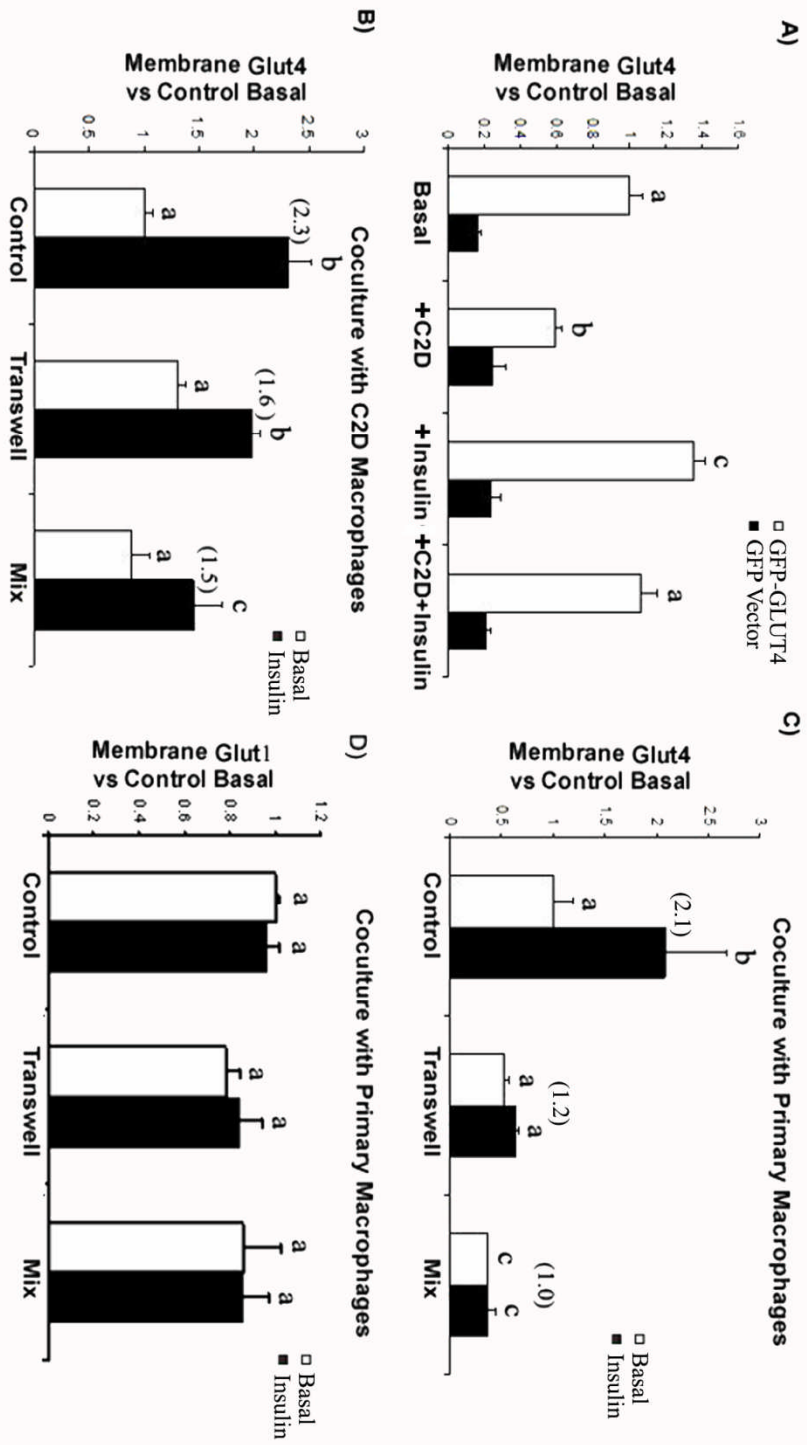


Figure 16. Macrophages inhibit insulin-stimulated translocation of GLUT4 but not GLUT1. Cells were cultured in serum-free DMEM for 2 hours and then were stimulated with insulin (100 nM) for 20 minutes. Cells were quickly dislodged from plates, fixed and immunostained for flow cytometry as described in Materials and Methods. A) BHK cells were transfected with GLUT4-GFP or GFP-N1 vector incubated with or without C2D macrophage cells. B) 3T3L1 adipocytes were co-cultured with C2D macrophage cells directly or in transwell plates for 4 days. The fold increase of plasma membrane GLUT4 upon insulin stimulation is shown in the parentheses. C & D) 3T3L1 adipocytes were co-cultured with peritoneal macrophages directly or in transwell plates for 4 days and assessed for plasma membrane expression of GLUT4 or GLUT1. The fold increase of plasma membrane GLUT4 upon insulin stimulation is shown in the parentheses. The data are presented as mean \pm SEM (n= 3-6 independent replicates per treatment). Different letters indicate a significant difference. A p value of < 0.05 was considered significant.

effective macrophages. To test this hypothesis, we co-cultured thioglycollate-elicited peritoneal macrophages with 3T3L1 adipocytes for 4 days together in direct contact or separated in transwell plates. The basal level of GLUT4 expressed on the adipocyte cell surface was greatly decreased by macrophages in both culture orientations (Figure 16C). Moreover, insulin-stimulated GLUT4 translocation was totally blocked in both experimental groups with the insulin-stimulated increase over basal level, 1.2 and 1.0 fold for transwell and co-culture, respectively (Figure 16C). We also measured the GLUT1 protein translocation in adipocytes in direct or in-direct co-cultures with peritoneal macrophages and we observed no change in GLUT1 trafficking in response to macrophages (Figure 16D).

To determine if changes in GLUT4 translocation were associated with decreased transcription, we used RT-PCR to measure the mRNA levels of *ACDC* (adiponectin), *GLUT 4* and *GLUT1* in 3T3L1 cells cultured alone, directly co-cultured with peritoneal macrophages or cultured in transwells. We added macrophages into the transwells at day 0, day 4 or day 8 after inducing differentiation and co-cultured them for 4 days after which RNA was isolated. We observed increased transcript levels of all three genes, *GLUT4*, *GLUT1* and *ACDC*, in adipocytes as they differentiated. The *GLUT4* gene transcript level in adipocytes was lower after 4 days of culture with peritoneal macrophages throughout all the differentiation process in transwell plates (Figure 17A and 17D). However, the impact was most pronounced on cells during days 4-8 and days 8-12 ($p < 0.05$) of differentiation. We did not see any differences in *ACDC* (Figure 3A and 3B) and *GLUT1* (Figure 17A and 17C) transcript levels between adipocytes alone or adipocytes with macrophages. Therefore, the impact of macrophages was specifically on insulin-stimulated glucose metabolism.

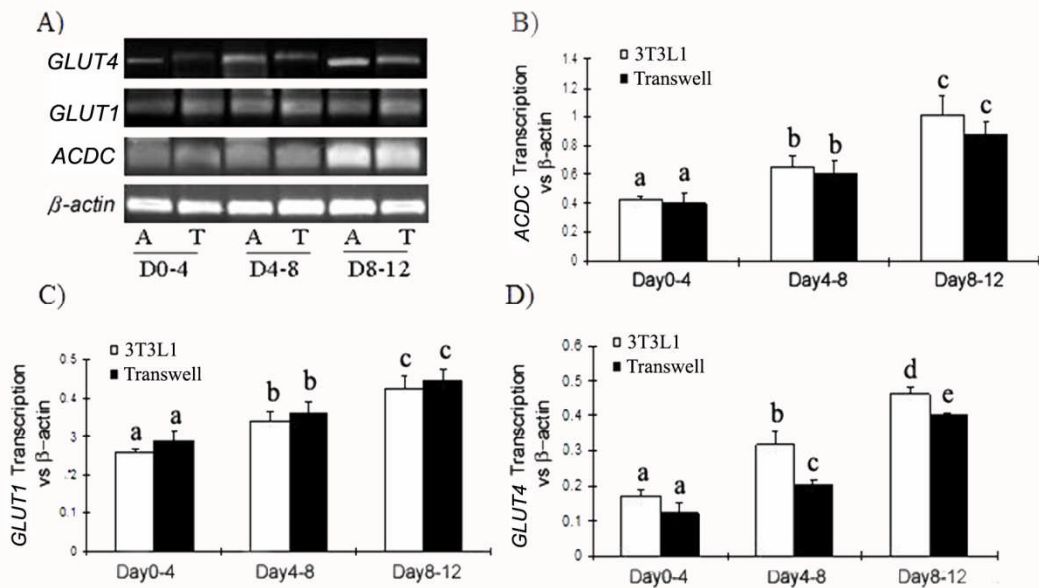


Figure 17. 3T3L1 adipocyte *GLUT4* transcription is inhibited by macrophages. 3T3L1 adipocytes were cultured in the bottom of transwell plates and peritoneal macrophages were cultured in the top chamber for 4 days as described in Materials and Methods. Total RNA of 3T3L1 adipocytes was extracted and mRNA levels were analyzed by RT-PCR. Ratio of gene: β -actin transcript was determined using densitometry. A) RT-PCR result of *ACDC*, *GLUT1*, *GLUT4* and β -actin. A, adipocytes only, T, adipocytes co-cultured with macrophages by transwell B) *ACDC* normalized to β -actin. C) *GLUT1* normalized to β -actin. D) *GLUT4* normalized to β -actin. The data are presented as mean \pm SEM (n= 3 independent replicates per treatment). Different letters indicate a significant difference. A p value of < 0.05 was considered significant.

Cytokine secretion in 3T3L1 adipocytes and peritoneal macrophage co-cultures.

Since GLUT4 translocation was inhibited in transwell cultures with macrophages, it suggested that cytokines played a role in the adipocyte-macrophage interaction [222, 369]. We assessed an array of cytokines for changes during macrophage-adipocyte co-culture including: IFN- γ , IL-1 α , IL-2, IL-4, IL-5, IL-10, IL-17, and GM-CSF (data not shown). However, only IL-1 β , TNF- α and IL-6 were altered in the co-cultures by the presence of macrophages. Therefore, we examined the TNF- α , IL-1 β and IL-6 concentrations in supernatant from macrophage and/or adipocyte cultures by ELISA. Both macrophages and 3T3L1 adipocytes secreted TNF- α , IL-1 β and IL-6 (Figure 18). For this reason, we compared the cytokines in supernatants from co-cultures to the sum of the secretion (SUM) by 3T3L1 cells and macrophages when they were cultured alone. We found the concentrations of IL-1 β (Figure 18C) and TNF- α (Figure 18A) were significantly lower in both direct and in-direct (transwell) co-cultures. However, there was a difference between the amount of IL-6 detected in direct co-culture and transwell cultures. Whereas IL-6 was significantly lower compared to SUM in transwell cultures, it was significantly higher when macrophages and adipocytes were cultured directly together (Figure 18B).

Cytokine inhibition of insulin-stimulated GLUT4 translocation.

Transwell co-culture of macrophages and adipocytes greatly inhibited GLUT4 translocation to the adipocyte plasma membrane. Since the inhibition was independent of cell-cell contact and TNF- α , IL-6 and IL-1 β were present in the co-cultures, we hypothesized that GLUT4 trafficking would be affected by the proinflammatory cytokines. To test this hypothesis, we treated fully differentiated 3T3L1 adipocytes with TNF- α , IL-1 β or IL-6 for 48 hours and measured the plasma membrane translocation of GLUT4 by flow cytometry. We first tested the

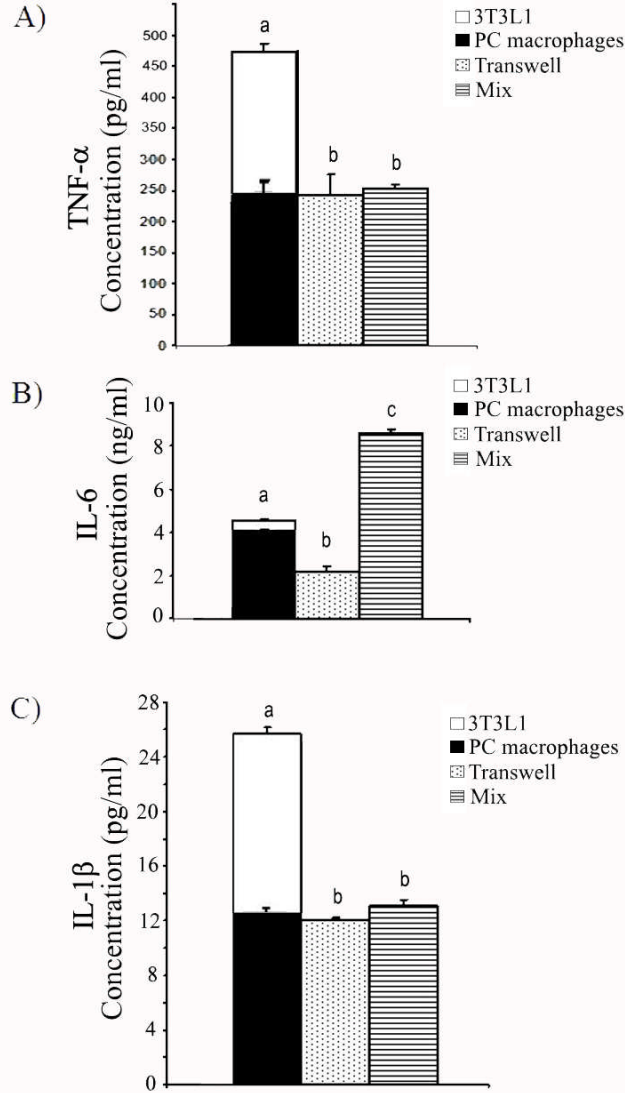


Figure 18. Secretion of TNF- α , IL-6 and IL-1 β in macrophage and 3T3L1 adipocytes cocultures. 3T3L1 adipocytes and peritoneal macrophages were incubated alone or were directly mixed together or in transwell plates for 4 days (from day 8 to 12 in adipocyte differentiation). Supernatants were collected and cytokine concentrations were determined by ELISA. A) TNF- α ; B) IL-6 ; C) IL-1 β . The data are presented as mean \pm SEM (n= 3-6 independent replicates per treatment). Different letters indicate a significant difference. A p value of < 0.05 was considered significant.

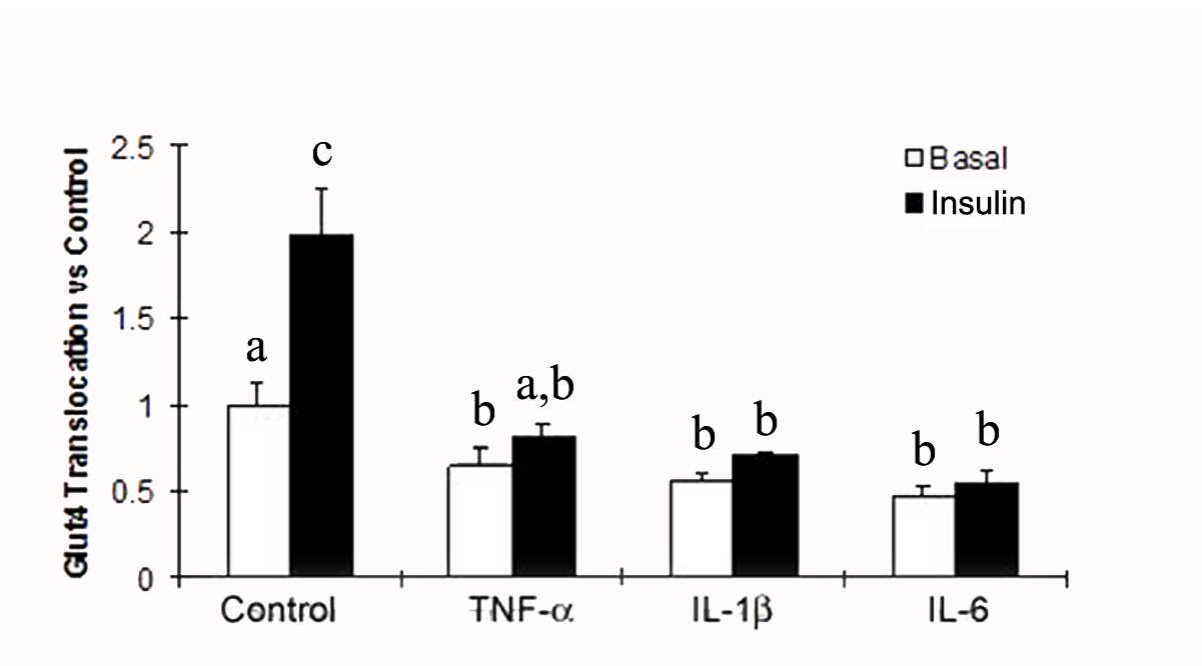


Figure 19. Effects of TNF- α , IL-6 and IL-1 β on insulin-stimulated GLUT4 translocation. Fully differentiated adipocytes were incubated in recombinant mouse TNF- α (2 ng/ml), IL-6 (10 ng/ml) or IL-1 β (20 ng/ml) for 2 days. Cells were serum starved for 2 hours and then were treated with insulin (100 nM) for 20 minutes. Cells were fixed and analyzed by flow cytometry as described in the Materials and Methods. The data are presented as mean \pm SEM (n= 3-6 independent replicates per treatment). Different letters identify a significant difference between control and treatments. A p value of < 0.05 was considered significant.

effects of TNF- α (300 pg/ml) , IL-1 β (20 pg/ml) and IL-6 (2 ng/ml) in the concentration ranges of what we detected in supernatants of transwell co-culture during our experiments. Interestingly, no significant decrease of insulin-stimulated GLUT4 translocation occurred with any of those treatments (Data not shown). There also was no effect when we mixed the three cytokines together at those concentrations (data not shown). It is possible that cytokine concentrations measured did not reflect the amount of cytokine that was consumed and/or degraded during the co-culture process. Therefore, we treated 3T3L1 adipocytes with higher concentrations of TNF- α (2 ng/ml), IL-1 β (20 ng/ml) or IL-6 (10 ng/ml) for 48 hours. Under these conditions, the number of GLUT4 molecules translocated to the plasma membrane with or without insulin stimulation was reduced with all three cytokines treatments (Figure 19).

TNF- α , IL-1 β and IL-6 decrease GLUT4 transcription and expression.

Since high concentrations of TNF- α , IL-1 β or IL-6 inhibited GLUT4 translocation to the adipocyte plasma membrane, we examined the effects of TNF- α , IL-1 β and IL-6 on GLUT4 gene transcription. We treated fully differentiated adipocytes with TNF- α (2 ng/ml), IL-1 β (20 ng/ml) or IL-6 (10 ng/ml) for 48 hours and subsequently measured the *ACDC*, *GLUT1* and *GLUT4* mRNA levels by semi-quantitative RT-PCR. We showed TNF- α , but neither IL-1 β nor IL-6, significantly decreased adiponectin transcript levels (Figure 20A and 20B). No cytokine affected *GLUT1* gene transcripts (Figure 20A and 20C). However, *GLUT4* transcript levels were reduced by TNF- α and IL-6, but not IL-1 β (Figure 20A and 20D). We assessed the action of TNF- α , IL-1 β and IL-6 on GLUT4 protein expression using flow cytometry to measure the total GLUT4 protein in 3T3L1 adipocytes. Treatment of adipocytes with TNF- α , IL-1 β or IL-6 all significantly decreased total GLUT4 protein level (Figure 21A), but not GLUT1 proteins (Figure 21B).

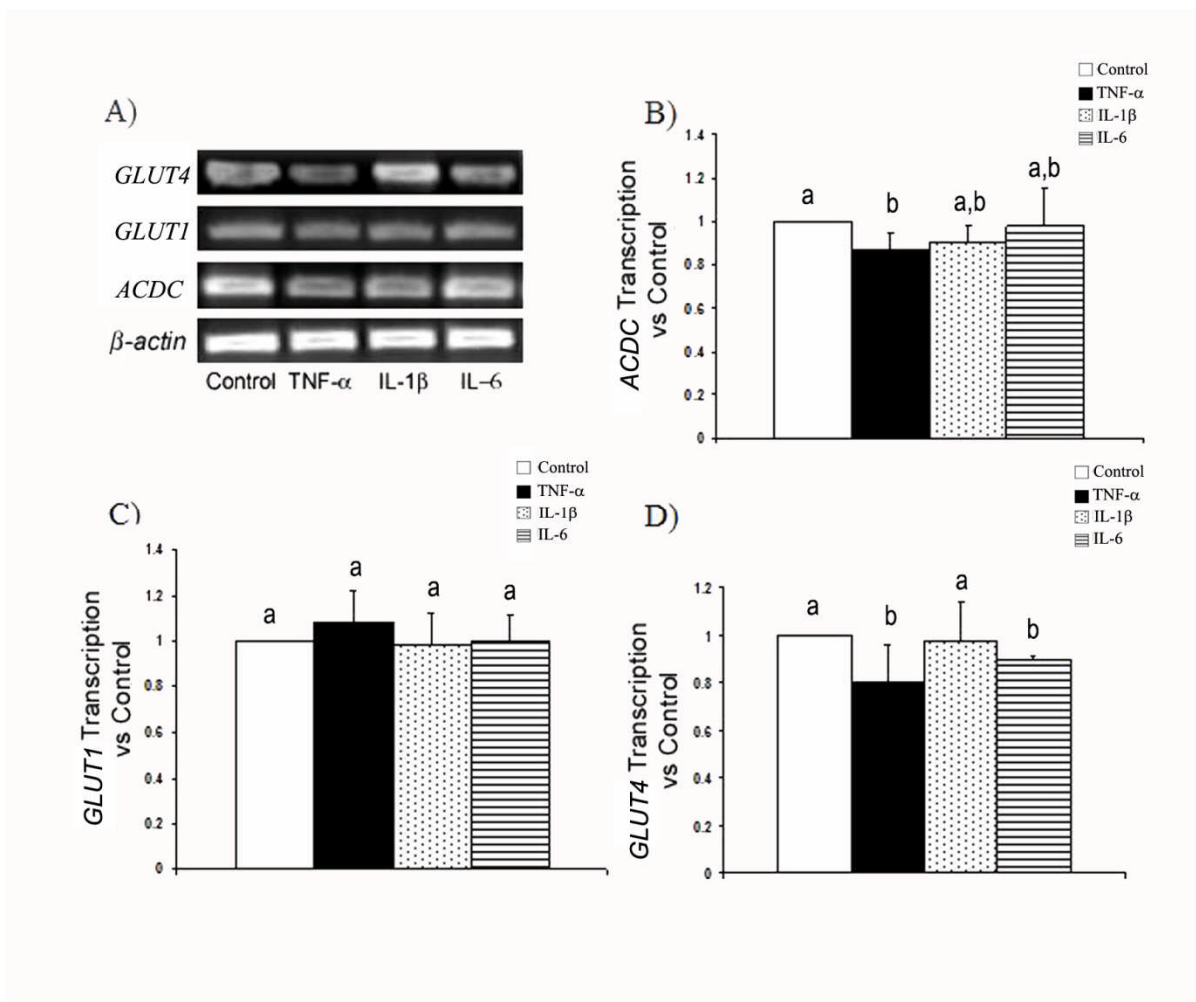


Figure 20. Effects of TNF- α , IL-6 and IL-1 β on *GLUT4* gene transcription. Fully differentiated 3T3L1 adipocytes were incubated in recombinant mouse TNF- α (2 ng/ml), IL-6 (10 ng/ml) or IL-1 β (20 ng/ml) for 2 days. Total RNA was extracted and transcript levels were analyzed by RT-PCR. Ratio of gene: β -actin expression was determined by densitometry. A) RT-PCR result of *ACDC*, *GLUT4*, *GLUT1* and β -actin. B) *ACDC* normalized to β -actin. C) *GLUT1* normalized to β -actin. D) *GLUT4* normalized to β -actin. The data are presented as mean \pm SEM (n= 3 independent replicates per treatment). Different letters indicate a significant difference. A p value of < 0.05 was considered significant.

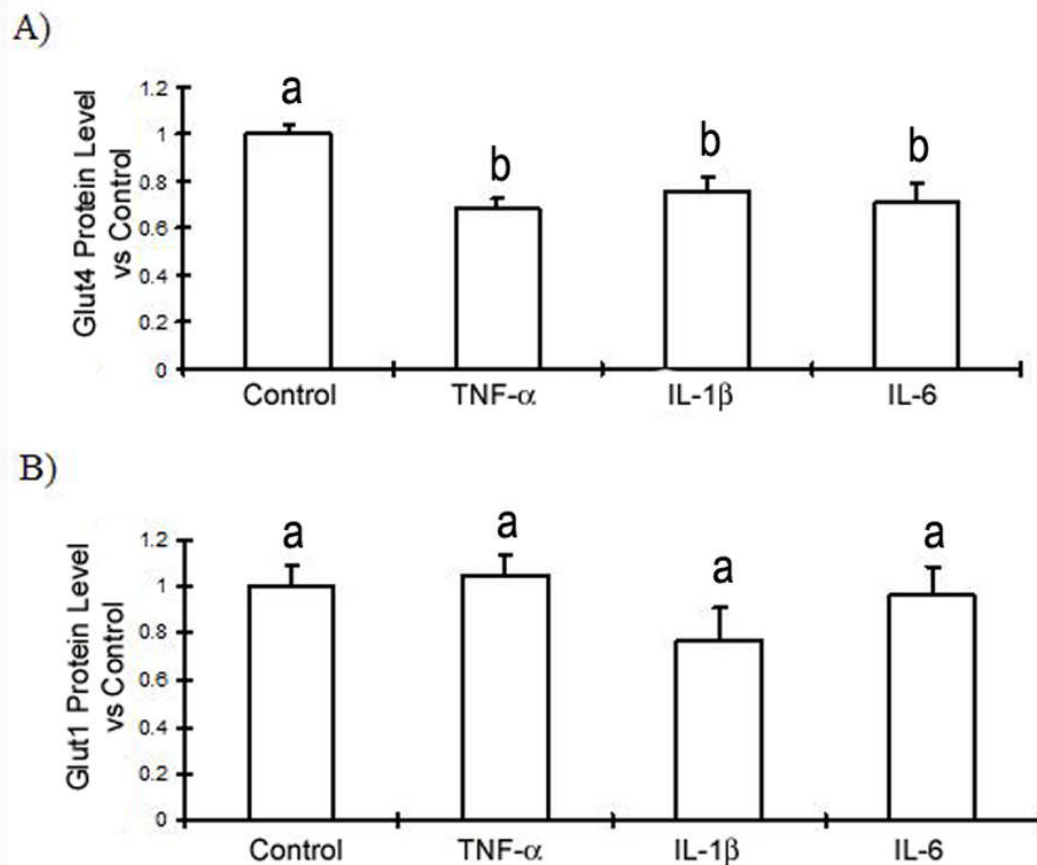


Figure 21. Effects of TNF- α , IL-6 and IL-1 β on GLUT4 protein expression. Fully differentiated adipocytes were incubated in recombinant mouse TNF- α (2 ng/ml) , IL-6 (10ng/ml) or IL-1 β (20 ng/ml) for 2 days. Cells were fixed and immuno-stained for GLUT1 and GLUT4 expression using flow cytometry as described in Materials and Methods. The data are presented as mean \pm SEM (n= 3-6 independent replicates per treatment). Different letters indicate a significant difference. A p value of < 0.05 was considered significant.

TNF- α , IL-6, and IL-1 β affect Akt phosphorylation differently.

GLUT4 translocation is triggered by insulin because PI3K activation leads to phosphorylation of the Akt protein within 15 minutes after insulin treatment [47]. Therefore, we evaluated the impact of TNF- α , IL-1 β and IL-6 on Akt phosphorylation using flow cytometry. Total cellular Akt protein levels were not altered by any of the treatments (Figure 22A). However, when we measured the phosphorylation of p473-Akt at 0, 5, 10, 15 and 30 minutes after insulin stimulation, we observed peak phosphorylation at 15 minutes and by 30 minutes phosphorylation was diminishing (Figure 22B). The time-dependent phosphorylation pattern of adipocytes treated with IL-1 β was the same as the control (Figure 22B). In contrast, Akt phosphorylation remained at baseline levels for 30 minutes observation in adipocytes treated with IL-6 (Figure 22B) with almost 100% inhibition. However, TNF- α did not completely block insulin signaling. It delayed the phosphorylation of Akt for approximately 10 minutes.

To confirm that IL-6 and TNF- α inhibited the phosphorylation of Akt 15 minutes after insulin stimulation; we treated cells with different concentrations of IL-6 or TNF- α for 48 hours. We then stimulated the cells with insulin and measured phosphorylated Akt after 15 minutes. There was a dose dependent inhibition of Akt phosphorylation by IL-6 or TNF- α (Figure 22C).

TNF- α , IL-6 and IL-1 β inhibit 3T3L1 differentiation.

We observed that *GLUT4* transcription increased as 3T3L1 adipocytes became more differentiated (Figure 3). Co-culturing 3T3L1 with peritoneal macrophages led to significant inhibition of GLUT4 translocation (Figure 19). It was reported that macrophage infiltration inhibited adipocyte differentiation [382]. Therefore, the impact macrophages have on GLUT4

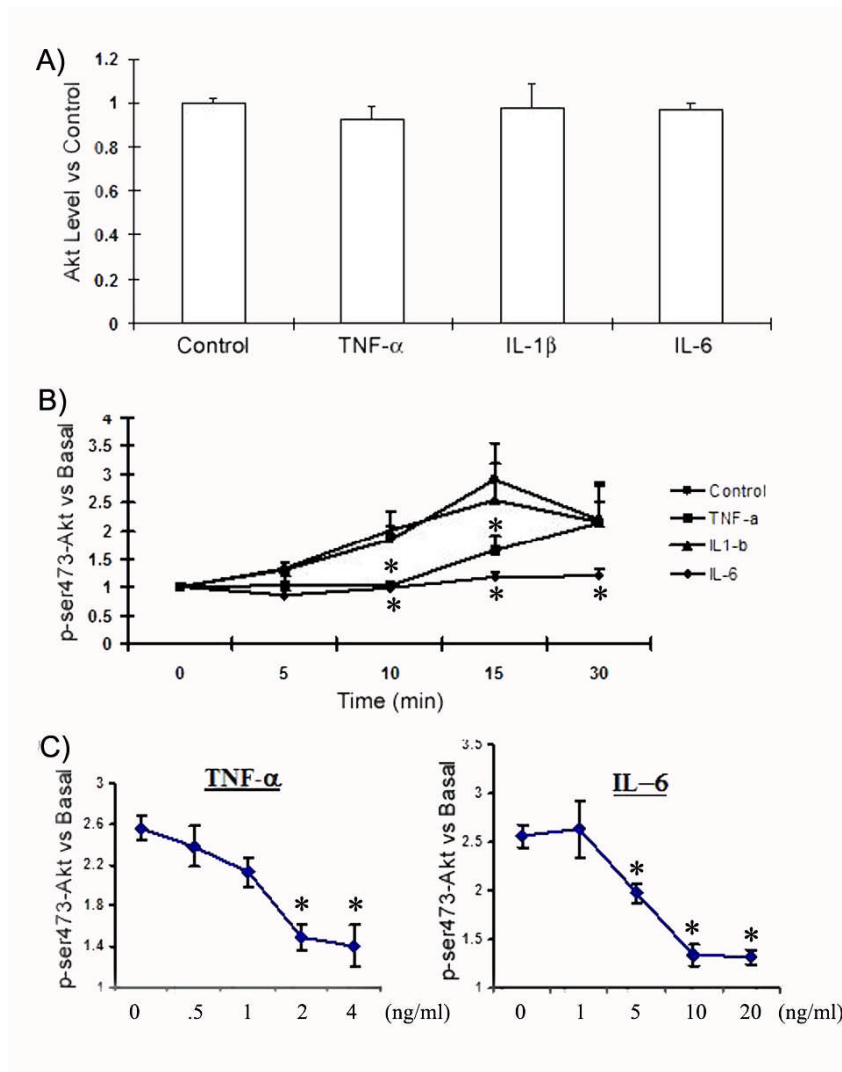


Figure 22. TNF- α , IL-6 and IL-1 β affect Akt phosphorylation differently. Fully differentiated adipocytes were incubated with recombinant mouse TNF- α , IL-6 or IL-1 β for 2 days. Cells were serum starved for 2 hours, stimulated with insulin (100nM) for 20 minutes, fixed and assessed for Akt and p-Akt by flow cytometry as described in Materials and Methods. A) Total Akt protein levels were detected after treatment with cytokines. Normalized to control set to 1. B) p-Akt was detected at 0, 5, 10, 15 or 30 minutes after insulin stimulation. C) Fully differentiated adipocytes were incubated in DMEM₁₀ containing TNF- α , IL-6 or IL-1 β for 2 days. p-Akt was detected at 15 minutes after insulin stimulation. The data are presented as mean \pm SEM (n= 3-6 independent replicates per treatment). An asterisk identifies a significant difference between control (no cytokines treatment) and treatments each time point. A p value of < 0.05 was considered significant.

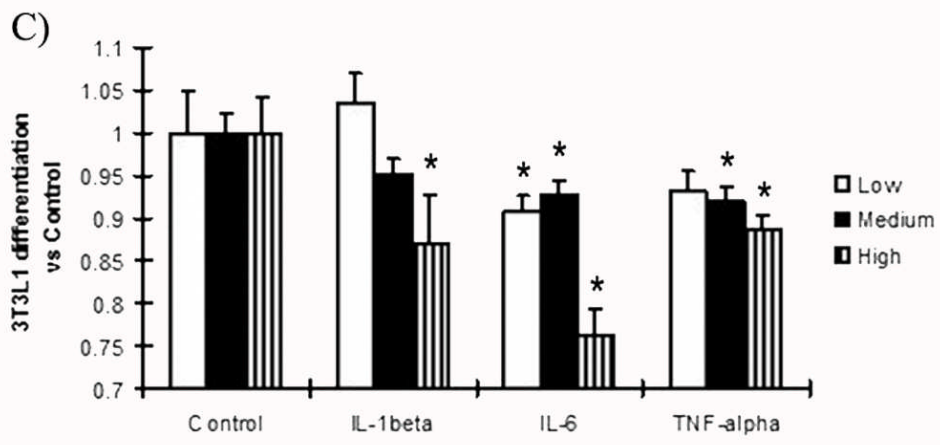
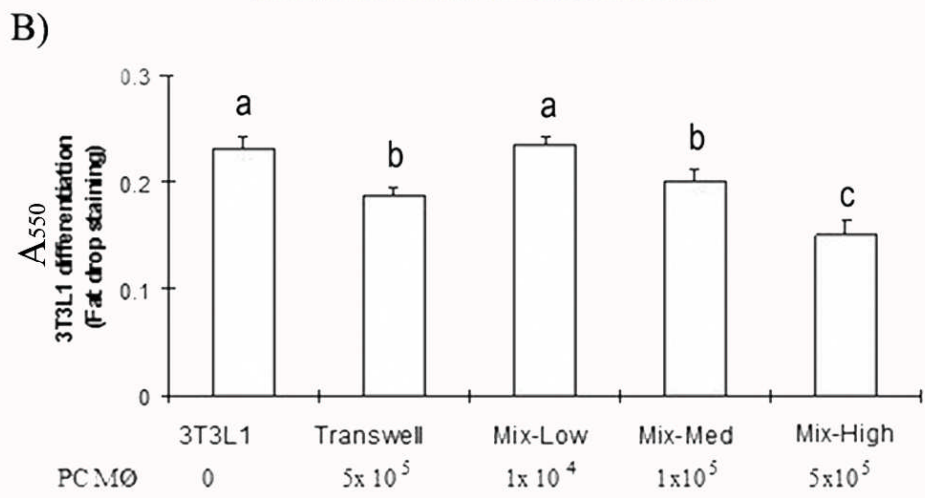
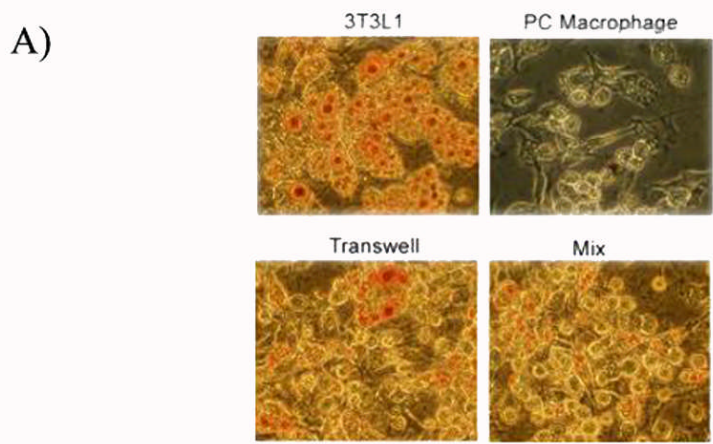


Figure 23. TNF- α , IL-6 and IL-1 β on 3T3L1 adipocyte differentiation. 3T3L1 cells were differentiated for 4 days with peritoneal macrophages in direct co-culture or in transwells. Cells were fixed and stained with Sudan IV dye as described in Materials and Methods. A) Cells were imaged at 200X magnification on a light microscope B) Lipid concentration was determined by measuring absorbance at 550 nm. Different letters indicate a significant difference. C) 3T3L1 cells were differentiated for 4 days and treated with TNF- α , IL-6 or IL-1 β for additional 4 days. (For TNF- α , *high*: 2 ng/ml, *medium*: 1 ng/ml, *low*: 0.5 ng/ml; for IL1- β , *high*: 20 ng/ml, *medium*: 10 ng/ml, *low*: 1 ng/ml; for IL-6, *high*: 10 ng/ml, *medium*: 5 ng/ml, *low*: 2 ng/ml). At day 8, cells were fixed and stained by Sudan IV as described in Materials and Methods. Differentiation was determined by measuring absorbance at 550 nm. The data are presented as mean \pm SEM (n= 3-6 independent replicates per treatment). An asterisk identifies a significant difference between control and treatments of each time point. A p value of < 0.05 was considered significant.

trafficking and Akt phosphorylation would be compounded if macrophages also inhibited adipocyte differentiation. To test this possibility, we assessed adipocyte differentiation using Sudan IV staining to detect increasing intracellular lipid as adipocytes differentiated. We observed less Sudan IV staining in 3T3L1 cells co-cultured with peritoneal macrophages compared to controls regardless of whether the macrophages and adipocytes were separated in transwells or were mixed together (Figure 23A). We found a macrophage number-dependent inhibition of 3T3L1 adipocyte differentiation (Figure 23B). We also assessed the effects of TNF- α , IL-6 and IL-1 β on 3T3L1 differentiation. Adipocytes were incubated with varying concentrations of cytokines ranging from 0.5-2 ng/ml of TNF- α , 1–20 ng/ml of IL1- β and 1-10 ng/ml of IL-6 for 4 days and were then assessed for differentiation using Sudan red. Ten ng/ml of IL-6 had the most pronounced inhibition on differentiation, causing a 24% decrease in lipid accumulation. Lower concentrations of IL-6 had a more modest inhibitory effect. Only 20 ng/ml of IL-1 β was significantly inhibitory, reducing lipid accumulation on average of 17% ($p < 0.05$). Two concentrations of TNF- α were inhibitory ($p < 0.05$), but they only inhibited differentiation at most by 10% (2 ng/ml). These data support the hypothesis that TNF- α , IL-6 and IL-1 β affect glucose transport by partially inhibiting 3T3L1 adipocyte differentiation.

DISCUSSION

According to the World Health Organization, more than 1 billion adults are overweight or clinically obese worldwide [383]. Obesity is now known as an inflammatory disease with pathologies similar to type 2 diabetes [384]. It is also associated with increased risk of diabetes mellitus and decreased glucose sensitivity [369]. We studied how macrophages affect adipocyte GLUT4 in this investigation and provide the most comprehensive analysis of this process to date.

We demonstrated that macrophages inhibited insulin-stimulated GLUT4 translocation in adipocytes by a contact-independent process. This is consistent with data showing that macrophage-conditioned medium blocked insulin-stimulated GLUT4-eGFP translocation and that TNF- α decreased 3T3L1 adipocyte GLUT4 protein levels [190]. The inhibition of GLUT4 could be partially due to decreased transcription since we found lower *GLUT4* transcript levels in 3T3L1 adipocytes in adipocyte-macrophages transwell co-cultures (Figure 17D). Unlike Lumeng et al, we have found a significant inhibition of GLUT4 translocation both in the basal state (ie. No insulin) and upon insulin stimulation. Part of the discrepancy may be because they over-expressed GLUT4 in 3T3L1 cells, which may have affected the natural regulation of the protein.

We found that C2D macrophage cells did not inhibit GLUT4 translocation as effectively as peritoneal macrophages. C2D macrophage cells maintained *in vitro* have an immature macrophage phenotype, expressing Ly-6C [26], a marker for monocytes and immature macrophages and do not make TNF- α and IL-1 β [162]. It appears their effectiveness is limited to the impact of their secretion of IL-6. Leumeng *et al.* also found that unstimulated macrophage medium did not inhibit GLUT4 translocation [190]. Therefore, these data are consistent with the

hypothesis that macrophages induce insulin resistance by secreting proinflammatory cytokines and that contact is not necessary (Figure 16).

Although peritoneal macrophages effectively inhibited GLUT4 translocation, they did not inhibit GLUT1 transport. Moreover, we did not observe any changes in GLUT1 protein level when adipocytes were incubated with proinflammatory cytokines. This contrasts observations where adipocyte basal glucose uptake was increased by macrophages [190]. GLUT1 regulates basal glucose metabolism and it is constitutively localized at the plasma membrane [385]. Therefore, macrophages only inhibit insulin-regulated glucose uptake which requires active mobilization of the molecule [44].

The inhibition of GLUT4 trafficking by macrophage cytokines and observations that macrophages secrete TNF- α in response to adipocytes exemplifies the paracrine interaction between the two cell types [386]. Lumeng *et al.* reported moderate but significantly enhanced TNF secretion in macrophage-adipocyte co-cultures compared to what was secreted by macrophages alone [190]. Adipocytes also secrete TNF- α , IL-6 and IL-1 β . Therefore, conclusions based on macrophage secretion alone may not be valid. Indeed, except for IL-6 when macrophages and adipocytes were directly co-cultured, the amount of secreted proinflammatory cytokines was significantly less than the sum of what macrophages and adipocytes made on their own (Figure 18). Our data suggest that the cytokines were metabolized, downregulated or were degraded. Transcription of TNF- α and IL-1 β are regulated through NF- κ B pathway [387]. Therefore, it is not surprising that they paralleled each other. It is possible that cytokine concentrations were lower in co-cultures because adipocytes secreted adiponectin, which suppressed TNF- α and IL-6 production [127]. However, the concentration of adiponectin detected in our co-cultures was much lower than the reported *in vitro* inhibitory

concentration (1.2 mg/ml vs. 30 mg/ml). Therefore, it is unlikely that it inhibited those cytokines. Since we also did not find decreased macrophage TNF- α , IL-6 and IL-1 β transcription when adipocytes and macrophages were co-cultured (Data not shown), the proinflammatory cytokines were most likely consumed or degraded. Moreover, except for IL-6 we cannot conclude that macrophages secreted more of these cytokines in response to the adipocytes.

Although TNF- α , IL-6 and IL-1 β contributed to insulin resistance by inhibiting the expression of the GLUT4 receptor on 3T3L1 adipocytes (Figure 19), the cellular mechanisms involved are still being defined. One mechanism may be that cytokines directly inhibit protein synthesis [190]. Stephen and Pekela found that as little as 5nM of TNF- α was able to inhibit *GLUT4* and *C/EBP* transcription [388] and altered the mRNA half life [389], which could lead to the protein decrease. However, Niu *et al.* have suggested that GLUT4 transport is independent of its activation in the plasma membrane and proinflammatory cytokines inhibit p38 MAPK from activating the molecule at the plasma membrane [390]. Alternatively, TNF- α activates sphingomyelinase. This enzyme releases ceramide, inhibits the GLUT4 promoter [391], depresses *GLUT4* transcription [389], and which could ultimately affect glucose transport. Another mechanism involves protein kinase B (also called Akt). Medina *et al.* reported that a 6 hr TNF- α treatment caused Akt degradation in adipocytes [192]. Together with our demonstration that TNF- α and IL-6 decreased GLUT4 translocation and inhibited phosphorylation of Akt suggests that Akt signal transduction is important to GLUT4 synthesis and transcription directly or through other critical signaling molecules like PI3-kinase. Indeed, Sun *et al.* demonstrated that the expression of silent mating type information regulation 2 homolog 1 (SIRT1) reversed insulin resistance and the absence of SIRT1 in muscle cells

inhibited Akt phosphorylation [392]. Interestingly, treatment of adipocytes with TNF- α reduced *ACDC* transcription and may partially explain how TNF- α induced insulin resistance [97]. Our data also support that argument. Lastly, TNF- α induces the secretion of other cytokines by adipocytes including IL-6, macrophage chemotactic protein-1 (MCP-1; CCL2), and even TNF- α [393] which can alter GLUT4 trafficking. Therefore, it appears that the development of insulin resistance may be exacerbated by increased macrophage activation by the production of multiple cytokines, some of which come from adipocytes themselves impacting multiple signaling mechanisms.

Although our data are consistent with observations that IL-6 can promote insulin resistance [206, 207], it contrasts the observation that IL-6 enhances glucose transport in 3T3L1 adipocytes [376]. Carey *et al.* showed treatment of IL-6 for 120 minutes increased fatty acid oxidation, basal and insulin-stimulated glucose uptake, and translocation of GLUT4 to the plasma membrane in L6 myotubes [287]. Their observation along with ours suggests that short treatments of IL-6 have opposite effects from longer treatments (2 days). Alternatively, the concentrations of IL-6 may be critical to the outcome. Additional side-by-side comparisons will be necessary to resolve this discrepancy. Nevertheless, we found that Akt phosphorylation was effectively inhibited by IL-6. Since Akt signaling is critical to GLUT4 translocation to the plasma membrane [394], our observations are internally consistent and are supported by observations that IL-6 inhibits IRS-1 expression which is also important for Akt phosphorylation and signaling [207].

IL-1 β also inhibited insulin-induced GLUT4 translocation. However, whereas TNF- α and IL-6 treatments were effective at cytokine concentrations in ranges close to those found in macrophage-adipocyte co-cultures (*e.g.* IL-6, 8 ng/ml detected compared to 10 ng/ml that was

needed to activate; TNF- α , 250 pg/ml detected compared to 2 ng/ml that was needed to activate), we had to use extremely high concentrations (20 ng/ml needed to activate compared to 10 pg/ml in co-cultures) of recombinant IL-1 β to see an effect. Jager *et al.* [226] also found that 20 ng/ml of IL-1 β inhibited insulin-stimulated GLUT4 but not GLUT1 translocation in adipocytes. Therefore, it is clear that high concentrations of IL-1 β can be inhibitory. These data are also consistent with observations that treating adipocytes for a long time, *e.g.* 6-10 days, inhibit signal transduction important to glucose transport (IRS-1, Akt and Erk 1 / 2) in both human and mouse adipocytes [377]. Interestingly, although we saw that high concentrations of IL-1 β could affect GLUT4 translocation, we did not see an effect on Akt phosphorylation. Therefore, IL-1 β may inhibit insulin-stimulated glucose transport by nonspecific mechanisms compared to either TNF α or IL-6, which inhibited Akt phosphorylation (Figure 22B). Therefore, IL-1 β may function most effectively because it synergizes with IL-6 and TNF α not because it works by itself.

Macrophages not only inhibited GLUT4, they also inhibited the differentiation of adipocytes by secreting IL-1 β , IL-6 and TNF- α (Figure 23). It is now recognized that the stromal-vascular compartment of adipose tissue contains various precursor and stem cells, which populate different cell lineages *in vivo* and *in vitro* [227]. Among the stromal cells, there are preadipocytes that differentiate into adipocytes [227]. Weisberg *et al.* [174] and Xu *et al.* [229] reported that inflammatory macrophages accumulated around small adipocytes, possibly to promote cell apoptosis. Constant *et al.* reported that macrophage-conditioned medium inhibited the differentiation of 3T3L1 and human abdominal preadipocytes [395]. IL-1 β and TNF- α inhibited adipogenesis directly [396, 397]. Therefore, we have confirmed those data. This inhibition probably was caused by suppression of PPAR- γ and NF- κ B [398]. However, we did not test that hypothesis directly.

In summary, our data suggest that macrophages induce insulin resistance in adipocytes by secreting a proinflammatory cocktail that inhibits insulin action, disrupts glucose uptake, and inhibits adipocyte differentiation. Whereas others have suggested that TNF- α plays a leading role in this process [190, 396], our data suggest that IL-6 is the most potent of the individual proinflammatory cytokines. C2D macrophage cells only make IL-6 *in vitro* but could still inhibit GLUT4 translocation (Figure 16). IL-6 was the only cytokine to be increased in macrophage-adipocyte co-cultures (Figure 18) and to completely inhibit Akt phosphorylation (Figure 22). It also had the most significant impact on adipocyte differentiation (Figure 23). This isn't to say that IL-1 β and TNF- α don't affect adipocytes. Indeed, all these proinflammatory cytokines impaired adipocyte function in ways that contributed to the development of insulin resistance. We suggest that IL-1 β and TNF- α acted in synergy with IL-6. Thus, insulin resistance will be difficult to regulate because of the multifactorial impact and complex nature of the adipocyte-macrophage interaction.

CHAPTER 5

**PHENOTYPIC CONVERSION OF C2D MACROPHAGE
CELLS IN
BROWN AND WHITE ADIPOSE TISSUE**

ABSTRACT

Macrophage populations exhibit a wide range of functional phenotypes depending on environmental stimuli. C2D macrophage cells reside early in the macrophage lineage *in vitro*, but differentiate to a more mature pro-inflammatory phenotype after adoptive transfer to and isolation from the peritoneal cavity. These C2D macrophage cells expressed higher transcript levels of pro-inflammatory cytokine genes after co-culture with 3T3L1 adipocytes *in vitro* for 2 days. After intraperitoneal injection, C2D macrophage cells migrated into both white adipose tissue (WAT) and brown adipose tissue (BAT). C2D macrophage cells isolated from WAT expressed high level of Ly-6C, CD11b, Mac-2 and F4/80, while C2D macrophage cells isolated from BAT expressed very low levels of those molecules. Although TNF- α , IL-6 and IL-1 β , and *Fizz-1* transcript levels significantly increased in C2D macrophage cells isolated from WAT compared to C2D macrophage cells *in vitro*, only the transcript levels of IL-1 β and *Fizz-1* were elevated in C2D macrophage cells isolated from BAT. These data suggest that C2D macrophage cells exhibit distinct functions and phenotypes in BAT and WAT and that the phenotype switch occurs in less than 2 days.

INTRODUCTION

Macrophages are present in every tissue in the body. Macrophages contribute significantly to innate defense against microorganisms and the responsiveness of the adaptive immune system because of their heterogeneous capabilities. Heterogeneity can be generated through differentiation-related mechanisms, activation by foreign bodies by endogenous stimuli [399, 400]. After monocytes/macrophage migration into a tissue the environment significantly influences the function of macrophages such that macrophages residing in different tissues display distinct functional patterns [401, 402]. White adipose tissue (WAT) and brown adipose tissue (BAT) have distinct physiological functions. WAT is an energy storage organ as well as an endocrine organ [75, 76]. In contrast, BAT functions as an energy-dissipating organ through adaptive-thermogenesis [403]. Adipocytes of WAT contain a single large lipid droplet, while adipocytes of BAT have multiple lipid droplets of varying size and contain many mitochondria packed with cristae [74]. While WAT is distributed into multiple subcutaneous and visceral deposits [404], BAT is primarily localized around bodily organs [405]. BAT is highly vascularized for high blood flow to meet the requirements of the brain, spinal cord, heart, lungs and kidneys during cold stress [79].

In the last few years, there has been increased study on the role of macrophages in WAT. Proinflammatory cytokines such as TNF- α , IL-6 and IL-1 β are thought to contribute to insulin resistance induction and are closely related to increased immigration of inflammatory macrophages in obese and diabetes patients [76, 131, 206, 226, 406, 407]. In contrast, resident macrophages, activated under the control of PPAR- γ in white adipose tissue, enhance insulin sensitivity in adipocytes, and have an alternative macrophage phenotype [182]. Despite of increased study of macrophages in WAT, the macrophages in BAT are poorly understood.

Macrophages express polarized functional properties during inflammation and many of these activities appear to be antagonistic: proinflammatory versus anti-inflammatory, immunogenic versus tolerogenic, and tissue-destruction versus tissue-angiogenesis [402].

Based on these properties, macrophages are classified as either classically (M1) or alternatively (M2) activated macrophages [179]. M1 macrophages express proinflammatory cytokines, such as TNF- α , IL-6 and IL-1 β . M2 cells are characterized as anti-inflammatory macrophages during type I inflammatory responses to promote angiogenesis and wound healing [408]. To study M2 macrophages, Ghassabeh *et al* have defined M2 macrophages by their expression of *Fizz1* (Found in inflammatory zone 1; reistin like alpha), Arginase-1 and YM-1 (also called T-lymphocyte-derived eosinophil chemotactic factor (ECF-L) of M2 [409].

In a previous study, we have found that macrophages induced insulin resistance in adipocytes by altering GLUT4 gene transcription, GLUT4 protein expression and translocation and inhibited preadipocytes differentiation. Our working hypothesis is that there is a synergistic interaction between adipocytes and macrophages. Given that macrophages adapt to microenvironmental signals and little is known about BAT-macrophage interactions, we assessed the immediate impact of BAT and WAT on macrophages with a special emphasis on the immediate response of macrophages when they enter WAT and BAT *in vivo*.

MATERIALS AND METHODS

Mouse strains.

C57BL/6J (B6, MHCII^{+/+}, Tlr4^{Lps-n}) mice were originally obtained from the Jackson Laboratory (Bar Harbor, ME). All mice were bred in the rodent facility of the Division of Biology at Kansas State University. All animal experiments were approved by the Institutional Animal Care and Use Committee.

Antibodies and Reagents.

Antibodies and corresponding isotypes are listed on table 1. Collagense (Type II), insulin from bovine pancreas, 3-Isobutyl-1-methylxanthine (IBMX), and dexamethasone were obtained from Sigma-Aldrich Co. (St. Louis, MO). Carboxyfluorescein diacetate, succinimidyl ester was purchased from Molecular probes (CFDA-SE, Molecular Probes, Eugene, OR)

Cell lines and cell culture.

The C2D macrophage cell line was created as described by our group [378]. These cells were derived from C2D murine bone marrow and selected in the presence of CSF-1. These cells have the MHCII^{-/-} and Tlr4^{Lps-n} genotype and are histocompatible with mice of the H-2^b haplotype. C2D cells were grown in Dulbecco's Modified Eagle's Medium with 4% serum (DMEM₄) supplemented with 0.3% Glutamax and 10% Opti-MEM in 150-mm tissue culture plates.

3T3L1 adipocytes were obtained from the American Type Culture Collection (Manassas, VA). Adipocytes were cultured and differentiated as described previously [356]. Briefly, 3T3L1 cell differentiation was induced by culturing cells in DMEM with 10 % calf serum (DMEM₁₀) containing 1 μM dexamethasone, 1.7 μM insulin and 0.5 mM IBMX for 4 days. On the fourth day, the 3T3L1 cells were cultured in DMEM₁₀ with 1.7 μM insulin. On day 8, 3T3L1 cells were

maintained in DMEM₁₀. Preadipocytes without differentiation and adipocytes differentiated for 6-8 days were used in the experiments.

3T3L1 cells (1×10^6 cells) were directly co-cultured with 1×10^5 C2D cells grown exclusively *in vitro* or 1×10^6 cells adoptive transferred C2D macrophage cells reisolated from the peritoneal cavity.

Adoptive transfer of labeled cells.

C2D cells were suspended in sterile, pre-warmed (37°C) Phosphate Buffered Saline (PBS; 137 mM NaCl, 10 mM Phosphate, 2.7 mM KCl, pH 7.4) at a concentration of 1.5×10^6 cells per ml, further stained with CFDA-SE according to the manufacturer's protocol. Briefly, C2D cells were incubated with 22 μ M of CFDA-SE solution at 37 °C for 15 minutes. After centrifugation at 370 x g for 10 minutes, cell pellets were suspended in pre-warmed PBS and incubated in 37°C for an additional 20 minutes. Cells were then washed twice in PBS, and suspended at a concentration of 3×10^7 cells/ml in PBS. One and one-half ml of the cell suspension of CFDA-SE labeled C2D or normal C2D cells was injected intraperitoneally (*i.p.*) per mouse.

Peritoneal cells extraction and fat tissues isolation

C2D macrophage cells were obtained from C57BL/6J mice by peritoneal lavage 36 hours after intraperitoneal injection of 4×10^7 of C2D macrophage cells labeled with CFDA-SE. The peritoneal exudates were incubated in ammonium chloride lysis buffer (0.15M NH₄Cl, 10mM KHCO₃, 0.1mM Na₂EDTA, pH=7.3) for 5 minutes on ice to burst red blood cells. One-half of the cells were treated with 1 mg/ml collagenase type II at 37°C with shaking (60 rpm) for 40 minutes. Control or collagenase treated cells were washed three times with PBS and 3×10^6 cells were plated into 15 cm cell culture plates and incubated in DMEM₄ for 16 hours.

Isolation of adipocytes and CFDA-SE labeled C2D macrophage cells was performed as previously described [357, 410]. Adipocytes were isolated from B6 mice epididymal fat pads and perispleen adipose tissues by collagenase digestion [411]. The fat pads were minced in pre-warmed (37°C) Krebs-Ringer phosphate (KRP) buffer (12.5 mM HEPES, 120 mM NaCl, 6 mM KCl, 1.2 mM MgSO₄, 1 mM CaCl₂, 0.6 mM Na₂HPO₄, 0.4 mM Na₂PO₄, 2.5 mM D-glucose, and 2 % bovine serum albumin, pH 7.4) and incubated with Type II collagenase (1mg/ml) for 40 min at 37°C with constant shaking at 60 rpm. Cells were centrifuged at 370 x g for 1 minute. The adipocytes isolated from epididymal fat pads were separated into 2 major fractions. The floating upper layer was primarily white adipocytes and the pelleted fraction was a mixture of stromal-vascular fraction (SVF) cells containing macrophages. Both cell fractions were collected and washed twice with KRP buffer. The adipocytes isolated from perispleen adipose were collected from the cell pellets and washed twice with KRP buffer.

A mixture of white adipocytes (upper layer) and SVF cells was co-incubated at 37°C in DMEM₁₀, pH 7.4, for 16 hours at a concentration of 1 x 10⁵ cells/ml in the 15-cm culture plate. The adipocytes remained dispersed in the medium and the SVF cells attached to the 15-cm culture plate. Brown adipocytes from perispleen adipose tissue (3 x 10⁶) were cultured at 37°C in DMEM₁₀ in a 15 cm culture plate for 16 hours.

Flow cytometry analysis.

C2D macrophage cells isolated from peritoneal cavity, WAT and BAT were detached with 0.02% EDTA and resuspended in DMEM₄. Cells were transferred to wells of 96-well, round-bottom plates and they were blocked with PBS-goat serum (50%-50%; 50 µl) at 4 °C for 0.5 hour. Subsequently, macrophage cell surface proteins were marked by direct or indirect labeling. Antibodies and isotypes concentrations are shown in Table 1. For direct labeling,

Table 1. Antibodies used for flow cytometry analysis

	Conjugate	Type	Company	Cat #
CD11c (Integrin α M, Mac-1 α)	APC	DA	eBioscience	17-0114-82
IgG	APC	ISO	eBioscience	17-4888-82
F4/80	APC	DA	eBioscience	17-4801-82
IgG2a	APC	ISO	eBioscience	17-4321-81
CD11b	APC	DA	eBioscience	17-0112-82
IgG2b	APC	ISO	eBioscience	17-4031-82
Mac 2 (galectin-3)	ALEXA Fluor 647	DA	eBioscience	51-5301-82
IgG2a	ALEXA Fluor 647	ISO	eBioscience	51-4321-80
c-fms-(CD115)	Biotin	PA	eBioscience	13-1152-82
IgG2a	Biotin	ISO	eBioscience	13-4321-82
Streptavidin	APC	SA	eBioscience	17-4317-82
Ly-6C (ER-MP20)	Biotin	PA	BD Pharmingen	557359
IgM	Biotin	ISO	BD Pharmingen	559941
Streptavidin	APC	SA	eBioscience	17-4317-82
APC: Allophycocyanin DA: Direct antibody, PA: Primary antibody, SA: Secondary antibody, and ISO: Isotype eBioscience Inc, San Diego, CA BD Pharmingen, San Jose, CA				

blocked cells were incubated with the specific antibody or isotype diluted in Hank's Buffered Salt Solution (HBSS; 0.137 M NaCl, 5.4 mM KCl, 0.25 mM Na₂HPO₄, 0.44 mM KH₂PO₄, 1.3 mM CaCl₂, 1.0 mM MgSO₄, 4.2 mM NaHCO₃) for 1 hour in the dark at 4°C. After two washes with HBSS, cells were fixed in 1% formalin. For indirect labeling, blocked cells were incubated for 1 hour with primary antibody or isotype antibody diluted in HBSS for a total volume of 50 μ l. Incubation continued in the dark for 1 hour at 4°C. Thereafter, cells were washed twice with HBSS. Secondary antibodies diluted in HBSS for a 50 μ l final volume were added to the cells and incubation proceeded for 40 min in the dark at 4°C. Cells were washed twice with HBSS and

they were fixed in 1% formalin. Labeled cell surface proteins were assessed by flow cytometry. Only CFDA-SE-positive cells were scored for the presence of absence of the selected markers.

FACS analysis

Cells from peritoneal lavages, BAT and SVF cells from WAT were sorted by FACS analysis as described previously [410]. Cell sorting was based on C2D macrophage cell CFDA-SE fluorescence, with the lowest 10 % of the positive cells not selected. Briefly, cell sorting was performed with a FACSVantage SE cell sorter (Becton Dickson, Rockville, MD) using specimen optimization and calibration techniques according to the manufacturer's recommendations. Cells were sorted at a rate of 15,000 cells per second and approximately 1×10^6 positive cells per group were collected on ice for RT-PCR analysis.

One-step RT-PCR analysis.

Total RNA was extracted from cells by Tri-Reagent (Molecular Research Center Inc) according to the manufacturer's protocol with some modification. One-step RT-PCR was

Table 2. Primers for RT-PCR

		Forward (5' to 3')	Reverse (5' to 3')
<i>TNF-α</i>	NM_013693	gggatgagaagtcccaaatg	ctccagctggaagactcctcccag
<i>IL-6</i>	NM_031168	Ttctctctgcaagagact	tgtatctctctgaaggact
<i>IL-1β</i>	NM_008361	caggcaggcagtatcactca	aggccacaggtattttgtcg
<i>Arg-1</i>	NM_007482	acctggcctttgtgatgtccta	aaggtctcttccatcaccttgcca
<i>Ym-1</i>	M94584	ttccaaggctgctactcacttcca	agaccacggcacctcctaaattgt
<i>Fizz-1</i>	NM_023881	tccagctgatgggtcccagtgaata	aagctgggttctccaccttcat
<i>β-actin</i>	NM_007393	tcctgtggcatccacgaaact	gaagcatttgcggtggacgat

performed using the Access RT-PCR Core Reagents from Promega according to the manufacturer's protocol. Primers were designed using Primer3 software

(<http://frodo.wi.mit.edu/>) using sequence data from NCBI sequence database. Primer sequences (forward/reverse) are shown in Table 2. The RT-PCR products were visualized under UV light by the use of a FluorChemTM 8800 Advanced Imaging System (Alpha Innotech, San Leandro, CA). The relative density of the target band was normalized to the β -actin loading control and then expressed as a percentage of the controls.

Immunofluorescence and Image Analysis.

Epididymal fat pads and perispleen adipose tissue were washed in Krebs-Ringer phosphate (KRP) buffer. Fat tissue was fixed, dehydrated, embedded and processed to slice. The cells were imaged using a Zeiss LSM 510 META confocal microscope. Images were then imported to Adobe Photoshop (Adobe Systems, Inc.) for processing.

Statistical analysis

Data were analyzed by ANOVA. Sets with statistically significant F score were analyzed for group-to-group variation using the least significant difference method (Fisher's LSD). Differences were considered significantly different when $p < 0.05$.

RESULTS

Phenotype modification of peritoneal C2D macrophage cells co-cultured with 3T3L1 adipocytes *in vitro*

To examine the impact of adipocytes on macrophages, we evaluated the phenotypic alteration of macrophages or C2D macrophage cells co-cultured with pre-adipocytes or adipocytes. We measured the expression of cell surface makers, Ly-6C, Mac-2 and CD11b using flow cytometry (Figure 24). C2D macrophage cells express Mac-2 and Ly-6C, but no CD11b, indicative of an immature macrophage phenotype [410]. These cells are excellent measures of changes in macrophage phenotype because they are well defined *in vitro* and provide a common starting point from which to gauge change in response to adipocytes *in vitro* and *in vivo*. We observed no change in any of the three cell surface markers on C2D macrophage cells co-cultured with pre-adipocytes (Figure 24A) compared to C2D macrophage cells cultured alone. However, we observed significant ($p < 0.05$) decrease of Ly-6C on C2D macrophage cells co-cultured with adipocytes (Figure 24A).

The peritoneal cavity microenvironment induces significant change in C2D macrophage cells changing them into cells having a functional, pro-inflammatory phenotype [410, 412], which is accompanied by an increase in CD11b. We hypothesized that contact with adipocytes would cause C2D macrophage cells isolated from peritoneal cavity after adoptive transfer to alter their phenotypes. To test this hypothesis, we co-cultured peritoneal C2D macrophage cells with adipocytes or pre-adipocytes and measured the expression of macrophage markers. Adipocytes induced significantly more Mac-2 expression on C2D macrophage isolated from peritoneal cavity compared to C2D macrophage cells incubated *in vitro* alone or with pre-adipocytes (Figure 1B). We observed a small but significant decrease of CD11b and Mac-2 in macrophages

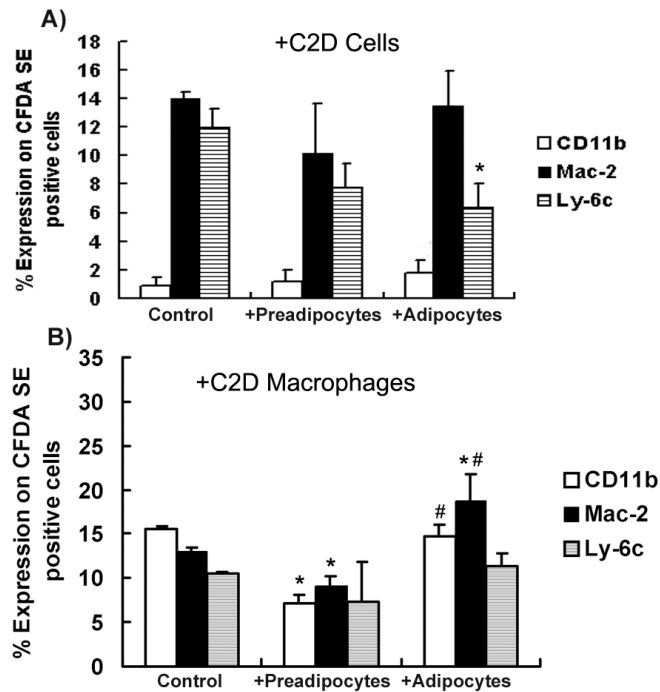


Figure 24. Phenotype changes of C2D macrophage cells co-cultured with adipocytes or pre-adipocytes *in vitro*. C2D macrophage cells were labeled with CFDA-SE or C2D macrophage cells labeled with CFDA-SE and isolated from peritoneal cavity were cultured alone or co-cultured with 3T3L1 adipocytes or pre-adipocytes as described in the methods and materials. The cell mixture was dispersed with 0.025% EDTA and was resuspended in HBSS buffer. Cells were immunostained for flow cytometry as described in Materials and Methods. A) C2D macrophage cells grown *in vitro* were cultured alone, co-cultured with adipocytes or with pre-adipocytes. B) C2D macrophage cells isolated from the peritoneal cavity were cultured alone, co-cultured with adipocytes or with pre-adipocytes. The data present mean \pm SEM (n= 3 independent replicates per treatment). An asterisk (“*”) identifies a significant difference of macrophages between control C2D macrophage cells incubated alone and treatments for each surface marker. A pound (“#”) identifies significant difference of macrophages between co-culture with pre-adipocytes and co-culture with adipocytes. A p value of < 0.05 was considered significant.

co-cultured with pre-adipocytes (Figure 24B). These data confirm that adipocytes alter the C2D macrophage cell phenotype.

Gene transcript modification in peritoneal C2D macrophage cells co-cultured with 3T3L1 adipocytes *in vitro*

The increased expression of Mac-2 on C2D macrophage cells co-cultured with adipocytes suggested that the cells were more differentiated [412, 413]. Therefore, we hypothesized that the change would affect their cytokine profile. To test this hypothesis, C2D macrophage cells labeled with CFDA-SE were purified by fluorescence-activated cell sorting after being cultured with adipocytes or pre-adipocytes for two days. Cytokine gene transcripts were detected by RT-PCR (Figure 25). C2D macrophage cells cultured alone *in vitro* express no *TNF- α* , and expressed very low levels of *IL-1 β* and low levels of *IL-6* transcripts (Figure 25). In co-culture with adipocytes, C2D macrophage cells had higher levels of *IL-6* (Figure 25A, lane C+A and Figure 25B), but no alteration in *TNF- α* (Figure 25A, lane C+A and Figure 25C) or *IL-1 β* (Figure 25A, lane C+A and Figure 25D). No change was found in cytokine transcription when C2D macrophage cells were co-cultured with pre-adipocytes (Figure 25A, lane C+P).

We hypothesized that peritoneal cavity-isolated C2D macrophage cells would be more responsive to adipocytes. Therefore, we co-cultured peritoneal C2D macrophage cells with 3T3L1 adipocytes or pre-adipocytes and measured cytokine gene transcript levels. There were significantly enhanced levels of *TNF- α* , *IL-1 β* and *IL-6* (Figure 25A, lane M), in these C2D macrophage cells. We detected a significant increase in *IL-6* and *TNF- α* transcript level by C2D macrophage cells co-cultured with adipocytes (Figure 2A, lane M+A, Figure 25B and 25C), but not in C2D macrophage cells co-cultured with pre-adipocytes (Figure 25A, lane M+P). We did not find any change in the expression *IL-1 β* in C2D macrophage cells co-cultured with either

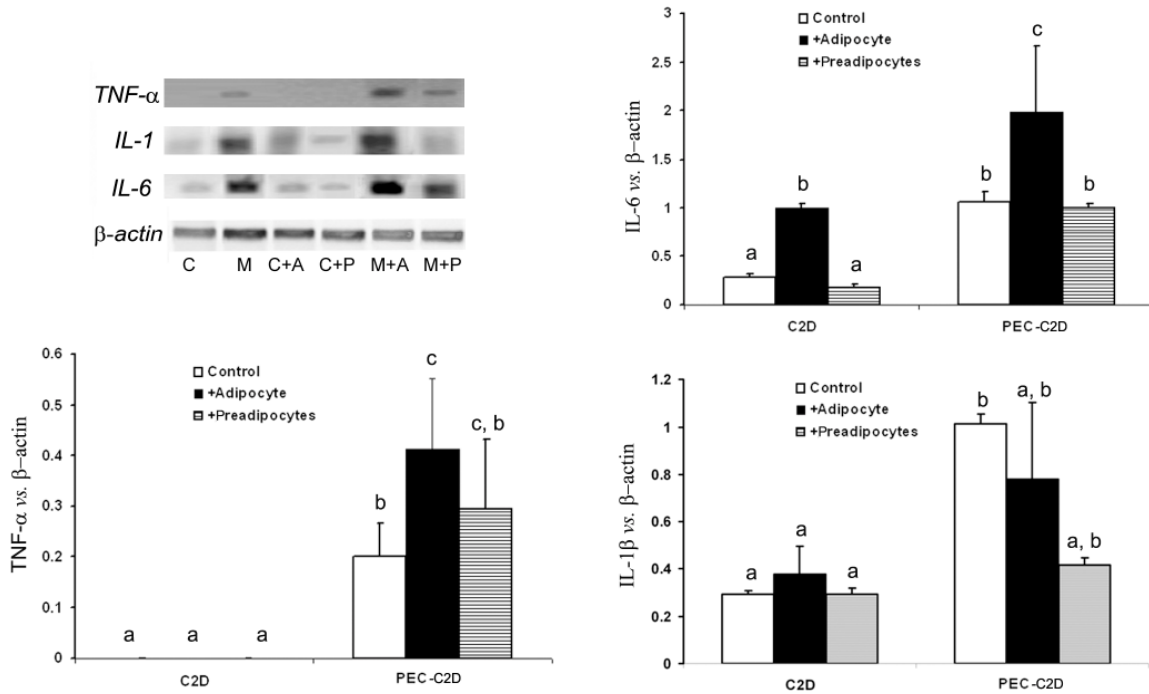


Figure 25. Transcription of proinflammatory cytokine genes in C2D macrophage cells co-cultured with adipocytes or pre-adipocytes *in vitro*. C2D macrophage cells were labeled with CFDA-SE or C2D macrophage cells labeled with CFDA-SE and isolated from peritoneal cavity were cultured alone or co-cultured with 3T3L1 adipocytes or pre-adipocytes as described in the methods and materials. Cell mixtures were dispersed with 0.025% EDTA and were resuspended in HBSS buffer. CFDA positive C2D cells were sorted by FACS as described in methods. Gene transcripts were measured by semi-quantitative RT-PCR as described in methods. A) C, C2D macrophage cells; M, C2D macrophage cells isolated from peritoneal cavity; C+A, C2D macrophage cells sorted from co-cultures with 3T3L1 adipocytes; C+P, C2D macrophage cells sorted from co-cultures with 3T3L1 pre-adipocytes; M+A, C2D macrophage cells isolated from peritoneal cavity were sorted from co-cultures with 3T3L1 adipocytes; M+P, C2D macrophage cells isolated from peritoneal cavity were sorted from co-cultures with 3T3L1 pre-adipocytes. B) *IL-6* normalized to *β -actin*. C) *TNF- α* normalized to *β -actin*. D) *IL-1 β* normalized to *β -actin*. The data are presented as mean \pm SEM (n= 3-4 independent replicates per treatment). Different letters indicate a significant difference. A p value of < 0.05 was considered significant.

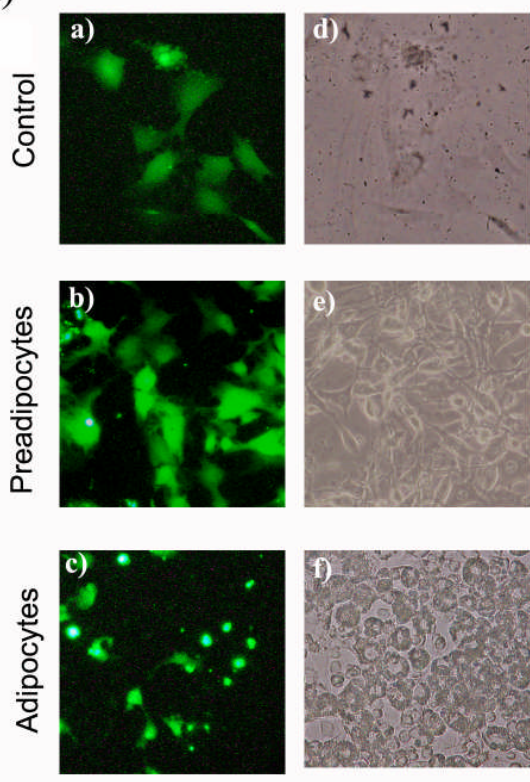
adipocytes (Figure 25A, lane M+A and Figure 25D) or pre-adipocytes (Figure 25A, lane M+P and Figure 25D).

Morphological changes of modification of C2D macrophage cells in response to adipocytes *in vitro* and *in vivo*

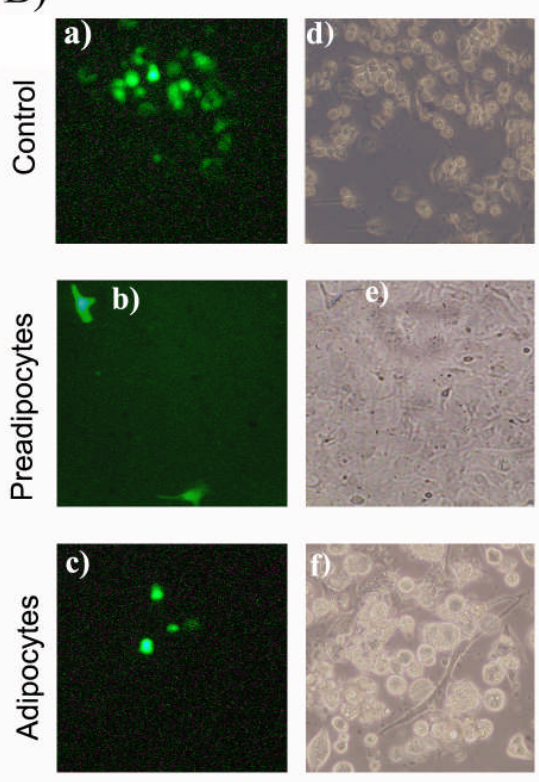
Since we observed a phenotype difference in C2D macrophage cells co-cultured with adipocytes we assessed if there were concurrent changes in cell morphology. Peritoneal cavity-isolated C2D macrophage cells are round after cell isolation (Figure 26B, panel a and d), compared to their larger stretched morphology when grown *in vitro* (Figure 26A, panel a and d). When those C2D macrophages were cultured with preadipocytes, the cells stretched out (Figure 26A and 26B, panels b and e). In contrast, when *in vitro* grown or peritoneal cavity-isolated C2D macrophage cells were co-cultured with adipocytes, we found that the cells maintained a mostly, smaller, round morphology (Figure 26A and 26B, panels e and f), suggesting that 3T3L1 adipocytes inhibit normal adherence and stretching by the C2D macrophage cells.

The morphological and functional differences between BAT and WAT have been widely noted, although they both belong to adipose tissue [74]. Macrophages isolated from WAT have been characterized as a classically activated macrophages [131, 229]. Macrophages from BAT are not well understood. We previously found that C2D macrophage cells stained with CFDA-SE could be isolated from perinodal WAT [410]. Therefore, we assessed C2D macrophage cell migration into WAT and BAT, with more cells being identified in WAT (Figure 26C, panels a and c).

A)



B)



C)

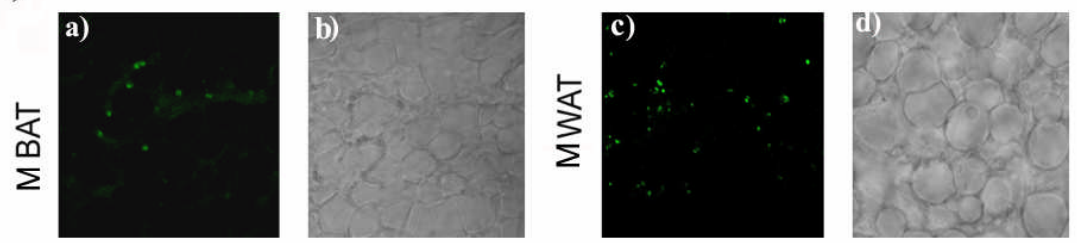


Figure 26. Change in C2D macrophage cell morphology during co-cultured with adipocytes or pre-adipocytes *in vitro* and C2D macrophage cells infiltration into BAT or WAT *in vivo*. A and B) C2D macrophage cells were labeled with CFDA-SE or C2D macrophage cells labeled with CFDA-SE and isolated from peritoneal cavity were cultured alone or co-cultured with 3T3L1 adipocytes or pre-adipocytes as described in the methods and materials. Panels a, b and c; CFDA-labeled C2D macrophage cells viewed on the fluorescent microscope (Magnification x 200). Panels d, e and f are phase contrast images of cells in a, b and c. C) WAT and BAT were collected from mice adoptive transferred with C2D macrophage cells labeled with CFDA-SE two days after adoptive transfer. WAT and BAT were processed to slice as described in Materials and Methods. Panels a and c images from the confocal microscop (x 100). Panels b and d are phase contrast images of the same fields.

Phenotype of C2D macrophage cells 36 hours after trafficking into WAT and BAT

The identification of C2D macrophage cells in both WAT and BAT provided a unique opportunity to determine the impact of these distinct adipose tissues on recently immigrating macrophages. We hypothesized that macrophages develop different phenotypic heterogeneity in response to different environmental stimuli from WAT or BAT. We previously demonstrated that C2D macrophage cells acquired proinflammatory phenotypes when adoptively transferred into the peritoneal cavity [410, 412]. The isolation of C2D macrophage cells from BAT and WAT required collagenase digestion of tissue to recover the CFDA-SE labeled cells. We found about a 70% loss of all cell surface markers (Ly-6C, Mac-2, CD11b and F4/80) with collagenase treatment (data not shown). Therefore, in order to phenotype the recovered C2D macrophage cells from BAT and WAT, we allowed the cells to recover *in vitro* at 37°C in DMEM₁₀. Recovery of cell surface molecules occurred within 16 hours of culture. Therefore, we cultured macrophages isolated from the peritoneal cavity, BAT and WAT in DMEM₁₀ for 16 hours at 37°C and treated with antibodies specific for Ly-6C, Mac-2, CD11b and F4/80. We observed a high expression of Ly-6C (33% expression) on WAT isolated CFDA-SE labeled C2D macrophage cells, while there was almost no expression of Ly-6C (0.4%) on BAT isolated CFDA-SE labeled C2D macrophage cells (Figure 27A, white bar). A moderately but significantly higher level of Mac-2 was found in WAT CFDA-SE labeled macrophage cells compared to BAT labeled CFDA-SE macrophage cells (Figure 27A, black bar). We observed over 30% expression of F4/80 on WAT isolated CFDA-SE labeled macrophage cells, but almost no expression on C2D macrophage cells from BAT (Figure 27A, striped bar). Surface CD11b expression was also significantly higher on C2D macrophage cells isolated from WAT compared to those isolated from BAT (Figure 27A, dotted bar).

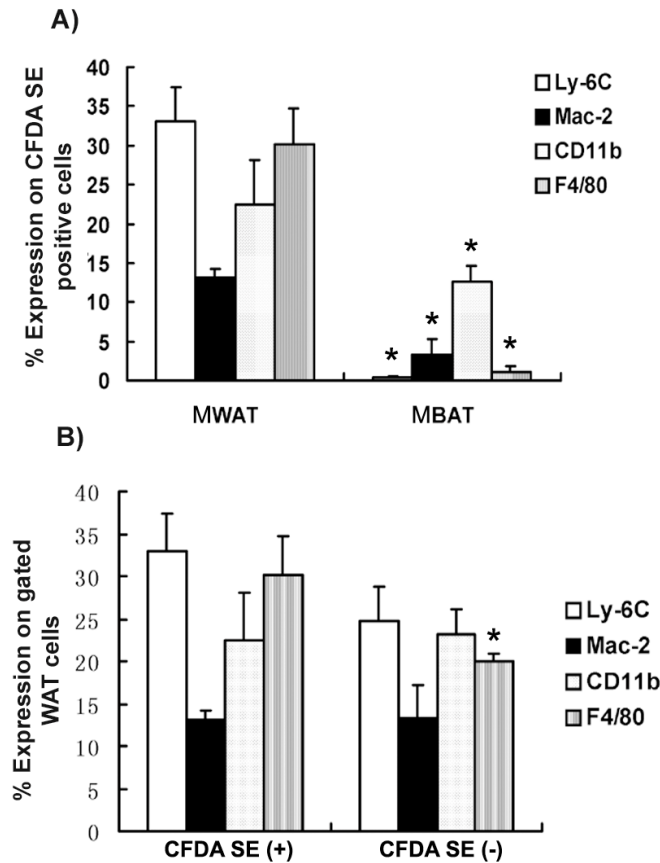


Figure 27. Phenotype changes in Peritoneal C2D macrophage cells isolated from WAT or BAT *in vivo* after *i.p.* adoptive transfer. WAT and BAT were collected from mice adoptively transferred with C2D macrophage cells labeled with CFDA-SE two days after *i.p.* injection of cells. C2D macrophage cells were isolated from BAT and WAT by collagenase treatment as described in Materials and Methods. Cells were re-plated on dishes and incubated in DMEM₁₀ at 37°C for 16 hours to allow cell surface molecule regenerated. Cells were dispersed and immunostained for detecting Ly-6C, Mac-2, CD11b and F4/80 by flow cytometry as described in Materials and Methods. A) Surface markers expression was assessed on CFDA-SE-positive cells isolated from BAT or WAT-SVF. B) Surface markers expression was assessed on CFDA-SE-positive cells, panel A, or CFDA-SE-negative cells, panel B, in SVF isolated from WAT. The data are presented as mean ± SEM (n= 3-6 independent replicates per treatment). An asterisk (“*”) identifies a significant difference between macrophages different treatment groups for each surface marker. A p value of < 0.05 was considered significant.

Odegaard *et al.* reported that resident macrophages in WAT displayed an alternatively activated phenotype [182]. We hypothesized that recently immigrating C2D macrophage cells would also adopt an M2-phenotype in the WAT. We found significantly more F4/80 on recent recently immigrated C2D macrophage cells compared to resident macrophages (Figure 27B, striped bar). However, there were no differences in Ly-6C, Mac-2 and CD11b between immigrating C2D macrophage cells and resident cells, however (Figure 27B).

Functional modification of C2D macrophage cells migrating into WAT and BAT

Since CFDA-SE labeled C2D macrophage cells had higher expression of several machineries of mature macrophages, we hypothesized that the cells would also have different cytokine profiles. To test this hypothesis, we used fluorescence-activated cell sorting of CFDA-SE labeled C2D macrophage cells isolated from peritoneal cavity, WAT and BAT 36 hours after adoptive transfer the cells into mice. We assessed the transcript levels of *TNF- α* , *IL-6*, *IL-1 β* , *Arg-1*, *Ym-1* and *Fizz-1* using semi-quantitative RT-PCR to determine if the macrophages exhibited an M1 or M2 profiles (Figure 28, Table 3). There were significantly increased *TNF- α* transcript levels in C2D macrophage cells isolated from peritoneal cavity and WAT (Figure 28A and Figure 28B), with 42 fold increase in C2D macrophage cells isolated from peritoneal cavity and 107 fold increase in C2D macrophage cells isolated from WAT compared to C2D macrophage cells maintained *in vitro* (Table 3). In contrast, there was little *TNF- α* expression in C2D macrophage cells sorted from BAT. *IL-6* transcript levels also increased 2 fold in C2D macrophage cells isolated from peritoneal cavity and by 10 fold in C2D macrophage cells isolated from WAT, while decreasing in cells isolated from BAT (Figure 28A and 28B, Table 3). We observed significantly higher level of *IL-1 β* transcript levels in C2D macrophage cells isolated from the peritoneal and WAT compared to those isolated from BAT, although transcript

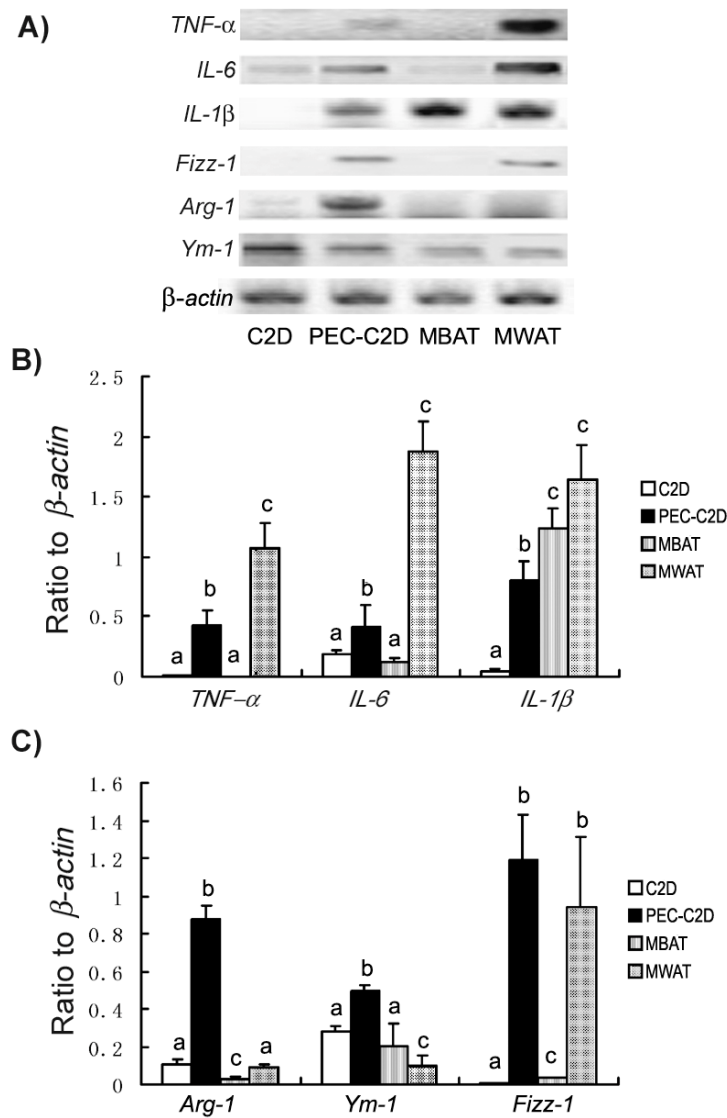


Figure 28. Gene transcript modification in Peritoneal C2D macrophage cells infiltrated into WAT or BAT *in vivo*. WAT and BAT were collected from mice adoptively transferred with C2D macrophage cells labeled with CFDA-SE two days after *i.p.* injection of cells. C2D macrophage cells were isolated from BAT and WAT by collagenase treatment as described in Materials and Methods. C2D macrophage cells isolated from WAT or BAT were sorted by FACS as described in methods. Gene transcripts were measured by one-step RT-PCR as described in methods. A) RT-PCR result of *TNF-α*, *IL-6*, *IL-1β*, *Arg-1*, *Ym-1* and *Fizz-1* B) gene transcript levels of *TNF-α*, *IL-6* and *IL-1β* normalized to β -actin; C) gene transcript levels of *Arg-1*, *Ym-1* and *Fizz-1* normalized to β -actin. C2D, C2D macrophage cells *in vitro*; PEC-C2D, C2D macrophage cells isolated from peritoneal cavity; MBAT, C2D macrophage cells isolated from BAT; MWAT, C2D macrophage cells isolated from WAT. The data are presented as mean \pm SEM (n= 3-4 independent replicates per treatment). Different letters indicate a significant difference. A p value of < 0.05 was considered significant.

Table 3. Comparison of M1 and M2 macrophage markers in C2D macrophage cells after isolation from C57BL/6J mouse tissue

Fold increase in gene transcripts compare to C2D macrophage cells grown <i>in vitro</i>			
Transcript	PEC ⁵	MBAT ⁵	MWAT ⁵
<i>TNF-α</i> ⁴	42 ± 12 ^{1,2}	1 ± 0	108 ± 20
<i>IL-6</i>	2 ± 0	1 ± 0	10 ± 1
<i>IL-1β</i>	20 ± 4	31 ± 4	41 ± 7
<i>Arg-1</i>	8 ± 1	<1 ± 0 ³	1 ± 0
<i>Ym-1</i>	2 ± 0	1 ± 0	<1 ± 0
<i>Fizz-1</i> ⁴	119 ± 24	3 ± 0	94 ± 38

1. Fold increase calculated as (transcript of genes *in vivo*/β-actin) ÷ (transcript of gene *in vitro*/β-actin).
2. Number represents mean ± SEM of 2-3 independent samples of 3 mice pooled per sample.
3. Transcript upregulated <1 fold in independent replicated are expressed in the fashion to reflect a decrease in transcription compared to C2D macrophage cells cultured *in vitro*.
4. The absence of transcript *in vitro* is expressed as 0.01 for calculations of fold increase for this analysis.
5. PEC: C2D macrophage cells isolated from peritoneal cavity; MBAT: C2D macrophage cells isolated from BAT; C2D macrophage cells isolated from WAT

levels were increased in C2D macrophage cells in all three microenvironments compared to C2D macrophage cells maintained *in vitro*.

Since we observed distinct proinflammatory cytokine expression profiles by C2D macrophage cells isolated from WAT and BAT, we hypothesized that C2D macrophage cells isolated from BAT would display an alternative activated (M2) phenotype. To test this hypothesis, we measured the gene transcript levels of *Arg-1*, *Ym-1* and *Fizz-1* using semi-quantitative RT-PCR. There was significantly increased expression of all three gene transcripts

in C2D macrophage cells isolated from the peritoneal cavity (Figure 28C, black bars). C2D macrophage cells isolated from BAT had significantly lower transcript levels compared to C2D macrophage cells from the peritoneal cavity. *Arg-1* and *Ym-1* were also lower in C2D macrophage cells isolated from WAT compared to those isolated from the peritoneal cavity. However, *Fizz-1* transcript levels were significantly elevated compared to C2D macrophage cells maintained *in vitro* or isolated from BAT.

DISCUSSION

Macrophages are remarkable for their ubiquitous distribution and their capability to display a wide range of functions and phenotypes dependent on their microenvironments [399, 414, 415]. We used the C2D macrophage cell line [378] to explore adipose tissue microenvironments. In previous work, C2D macrophage cells switched their phenotype from a primarily Th2 profile when grown *in vitro* to a Th1 profile after *in vivo* intraperitoneal culture [410]. In the current study, we discovered additional cellular changes as the C2D macrophage cells migrated from the peritoneum into white and brown adipose tissue.

Brown and white adipocytes have distinct morphologies and functions [416]. White adipocytes store energy and brown adipocytes dissipate energy through their numerous mitochondria [416]. Although several studies have reported the functional phenotype of macrophages immigrating into WAT [417-419], little is known about macrophages in BAT. Our unique model system allowed us to trace the *in vivo* migration of C2D macrophage cells into adipose tissue and to recover them to define the changes induced by these two distinct sites. This system is also unique because it allowed us to monitor the “before” *in vivo* phenotype to the “after” *in vivo* phenotype using cells that were derived from the same defined population that has not been under the prolonged influence of the recipient host. Therefore, we are confident that the changes in the macrophages were due to their immediate exposure to the BAT or WAT environments as opposed to the cumulative exposures encountered by host resident macrophages over a period of time.

C2D macrophage cells isolated from BAT expressed very little Ly-6C, Mac-2, CD11b and F4/80 compared to C2D macrophage cells isolated from the peritoneal cavity [412] or from WAT. This phenotypic difference accompanied the expression of low transcript numbers for *IL-*

6, *TNF α* and *Fizz-1* in C2D macrophage cells isolated from the BAT. These mRNA levels were high in C2D macrophage cells sorted from the peritoneum or the WAT (Figure 28). Odegaard *et al.* demonstrated that resident macrophages in WAT expressed an M2 phenotype with elevated *Arg-1* and *Ym-1* [182]. In contrast, inflammatory macrophages detected in WAT had M1 phenotypes in obese and diabetic states [131, 149, 229]. Therefore, the C2D macrophage cells in WAT better resemble macrophages bearing an M1 phenotype. In contrast, BAT suppressed the development or maintenance of a proinflammatory macrophage phenotype without inducing what is considered an anti-inflammatory (M2) phenotype. *Fizz-1*, also known as resistin-like molecule alpha, was also up-regulated in Th2 environments [420]. This also supports the hypothesis that that WAT, but not BAT, is a proinflammatory environment whereas BAT is not. It is possible that longer exposure of the C2D macrophage cells to BAT is necessary for the upregulation of *Arg-1* and *Ym-1*. Alternatively, macrophages in BAT may acquire a unique phenotype not defined by classic M1 and M2 markers. Studies isolating C2D macrophage cells from BAT after longer periods of time will be necessary to answer this question.

Chronic excessive caloric intake leads to macrophage infiltration [76, 421]. Those macrophages contributed to the elevated level of proinflammatory cytokines in those chronic conditions [131, 149, 173, 183, 229, 422]. However, those studies were performed on people or animals that were obese [174] or were in diabetic states [229] and do not provide clues about the contribution of normal adipocytes to macrophage change *in vivo*. We provide direct evidence that macrophage changes in WAT, or lack of changes, in BAT, occur in response to normal adipocytes *in vivo*.

Adipocytes are derived from multipotent mesenchymal stem cells that pass through two phases of adipogenesis as they mature into adipocytes [416]. The first phase involves the

transition of stem cells to pre-adipocytes and the second phase involves the conversion from pre-adipocytes into adipocytes [416]. Previous studies have found that co-culture of macrophages with pre-adipocytes inhibited adipocytes differentiation [382]. However, the impact of this interaction on macrophages is not well understood. We found that C2D macrophage cells downregulated many mature macrophage markers when co-cultured with pre-adipocytes *in vitro*. Therefore, not only is adipogenesis inhibited by the presence of macrophages [382], macrophages are also affected by the interaction. C2D macrophage cell *IL-6* gene transcription and protein secretion were increased by co-culture with adipocytes (Figure 25). This is consistent with our previous report that *IL-6* inhibited 3T3L1 adipocyte differentiation at concentrations generated during their co-culture. Although these data suggest that the initiation of the macrophage changes begins even before the lipid accumulation in the adipocytes, there were still important differences in the macrophage responses to preadipocytes and adipocytes. Whereas preadipocytes allowed C2D macrophage cells to spread, regardless of their source (Figure 26), adipocytes inhibited macrophage spreading. Increased spreading is associated with macrophage differentiation [423], therefore, this may reflect selective differentiation into proinflammatory phenotype. Indeed, macrophages differentiated in substrates that cause similar phenotypes are capable of secreting both *TNF- α* and *IL-6* [424].

The C2D macrophage cells isolated from the peritoneum expressed a relatively differentiated macrophage phenotype [413, 425] when co-cultured with adipocytes *in vitro* (Figure 25A and 25B). This was similar to the phenotype of the C2D macrophage cells isolated from the WAT. Both macrophage populations demonstrated the same expression patterns of CD11b, Mac-2 and F4/80 as mature resident macrophages (Figure 27B). Therefore, C2D macrophage cells rapidly adapted the same phenotype as resident adipose macrophages. It also

validates that the C2D macrophage cells are serving as reliable indicators of the tissue environment.

In summary, the WAT microenvironment alters the capabilities of C2D macrophage cells, causing them to express primarily a functional pro-inflammatory phenotype. However, the BAT environment keeps C2D macrophage cells quiescent. To our knowledge, this is the first study to directly compare the macrophages response to different adipose tissues in the absence of complicating chronic diseases or altered genetic states. The evidence that infiltrating macrophages display a pro-inflammatory phenotype even in normal mice suggests that the “inflammatory fire” [426] begins relatively quickly in permissive environments. WAT appears to be one of those environments however, BAT does not. Determining the properties of BAT that make it refractory may give us clues on how to extinguish the inflammatory fire.

CHAPTER 6

FUTURE PROSPECTIVE

My studies have demonstrated that adiponectin and leptin are secreted through distinct intracellular trafficking pathways. Adiponectin, in the steady state, is localized in *trans* Golgi Network (TGN). Adiponectin exits from TGN, dependent on GGA1- coated vesicles. Adiponectin trafficking also requires Rab11 and Rab5 proteins, thus implicating endosome compartments are required. In contrast, trafficking of leptin to the plasma membrane does not require endosomal compartments, although leptin also passes through the TGN. Leptin secretion occurs through a constitutively pathway dependent on PKD1.

Future studies will need to identify other protein and components that participate in the generation and trafficking of adiponectin and leptin-containing vesicles. For example, our preliminary data showed overexpression of constitutively active forms of Arf1, Arf3 or Arf5 all inhibited adiponectin secretion. However, Arf proteins seem to have overlapping functions [243, 244]. Thus, double interfering or triple knock down of Arf proteins will need to determine specific isoforms in adiponectin trafficking. Also, recent studies have shown that replacing the hypervariable domain of Rab5a with that of Rab1a, Rab2a, Rab7 and Rab27a had no effect on its function and localization on early endosome [261]. These kinds of experiments indicate other Rab proteins might also participates in the secretion of adiponectin. Bose *et al.* reported v-SNARE Vti1a regulated adiponectin secretion [427]. Which t-SNARE proteins are required for adiponectin secretion and in which steps they are involved during trafficking and secretion also need further clarification. Potential t-SNARE proteins can be screened by yeast two hybrid studies and their functions can be explored. For leptin, it will be important to determine if the PKD1 dependent constitutively secretory pathway is the only secretory route. Actually, the knock down of PKD1 only inhibited leptin secretion by 15%, which suggests other protein or pathway may also exist. Indeed, the intracellular compartmentalization of leptin in adipocytes

has remained controversial [357]. Although our study demonstrated that leptin mostly localized in the ER, there is some questions on whether leptin distributes in other small intracellular vesiculars. Furthermore, the mechanisms by which insulin stimulates adiponectin or leptin secretion are still poorly understood.

Obesity and diabetes are now regarded as inflammatory diseases. Understanding the interaction between macrophages and adipocytes will help define the underlying mechanisms leading to the onset of those diseases. I demonstrated that macrophages induced insulin resistance in 3T3L1 adipocytes by secreting TNF- α , IL-1 β and IL-6. IL-6 might be most important cytokine during the induction of insulin resistance by altering GLUT4. I also studied the action of adipocytes on macrophages. I demonstrated that C2D macrophage cells increased their IL-6 transcript levels co-culture with adipocytes *in vitro*. *In vivo*, C2D macrophage cells infiltrated into WAT display primarily functional pro-inflammatory phenotypes, however, BAT environment keeps C2D macrophage cells quiescent.

Future study will need to test the interaction of macrophages and adipocytes *in vivo*. Those studies will require a focus on the role of IL-6 in the onset of diabetes *in vivo*. Charriere *et al.* showed that preadipocytes have the potential to be efficiently and rapidly converted into mature macrophages in a macrophage environment [178]. The cytokine profile of that macrophage population and whether this population is involved in causing diabetes is still unknown. Moreover, whether the secretion of hormones like adiponectin, leptin, resistin, *etc.*, by adipocytes is altered in the presence of these macrophage cells also needs to be studied. Studies are proposed to explore C2D macrophage cells infiltrated into WAT after adoptive transfer in diabetic mice or mice on a high fat diet and it will also lead to insights on how that tissue changes the functional phenotype of these macrophages as the chronic disease progress. These

studies will shed light on the cellular and molecular basis of obesity and diabetes as an inflammatory disease and whether macrophages are the cause or the effect of the disease.

References

1. Rathmann, W., Giani, G. (2004) Global prevalence of diabetes: estimates for the year 2000 and projections for 2030. *Diabetes Care* **27**, 2568-9; author reply 2569.
2. Diamant, A.L., Babey, S.H., Hastert, T.A., Brown, E.R. (2007) Diabetes: the growing epidemic. *Policy Brief UCLA Cent Health Policy Res*, 1-12.
3. Gilbert, R.E., Connelly, K., Kelly, D.J., Pollock, C.A., Krum, H. (2006) Heart failure and nephropathy: catastrophic and interrelated complications of diabetes. *Clin J Am Soc Nephrol* **1**, 193-208.
4. Pinder, M.C., Duan, Z., Goodwin, J.S., Hortobagyi, G.N., Giordano, S.H. (2007) Congestive heart failure in older women treated with adjuvant anthracycline chemotherapy for breast cancer. *J Clin Oncol* **25**, 3808-15.
5. Hughes, M., Lip, G.Y. (2007) Risk factors for anticoagulation-related bleeding complications in patients with atrial fibrillation: a systematic review. *Qjm*.
6. Air, E.L., Kissela, B.M. (2007) Diabetes, the Metabolic Syndrome and Ischemic Stroke: Epidemiology and Possible Mechanisms. *Diabetes Care*.
7. Rema, M., Pradeepa, R. (2007) Diabetic retinopathy: an Indian perspective. *Indian J Med Res* **125**, 297-310.
8. Williams, M.E. (2006) Coronary revascularization in diabetic chronic kidney disease/end-stage renal disease: a nephrologist's perspective. *Clin J Am Soc Nephrol* **1**, 209-20.
9. Leung, P.C. (2007) Diabetic foot ulcers--a comprehensive review. *Surgeon* **5**, 219-31.
10. Henderson, E.A. (2007) Role of diabetic microvascular disease in the development of foot wounds. *J Wound Care* **16**, 275-8.

11. Kim, M.S., Polychronakos, C. (2005) Immunogenetics of type 1 diabetes. *Horm Res* **64**, 180-8.
12. Dejkhamron, P., Menon, R.K., Sperling, M.A. (2007) Childhood diabetes mellitus: recent advances & future prospects. *Indian J Med Res* **125**, 231-50.
13. Pugliese, A. (2005) The insulin gene in type 1 diabetes. *IUBMB Life* **57**, 463-8.
14. Eisenbarth, G.S. (2007) Update in type 1 diabetes. *J Clin Endocrinol Metab* **92**, 2403-7.
15. Nazaimoon, W.M., Azmi, K.N., Rasat, R., Ismail, I.S., Singaraveloo, M., Mohamad, W.B., Letchuman, R., Sheriff, I.H., Faridah, I., Khalid, B.A. (2000) Autoimmune markers in young Malaysian patients with type 1 diabetes mellitus. *Med J Malaysia* **55**, 318-23.
16. Adler, A. (2002) Obesity and target organ damage: diabetes. *Int J Obes Relat Metab Disord* **26 Suppl 4**, S11-4.
17. Wallace, C. (2002) Primary prevention of type 2 diabetes. *Tenn Med* **95**, 471-2.
18. Kjos, S.L., Buchanan, T.A., Greenspoon, J.S., Montoro, M., Bernstein, G.S., Mestman, J.H. (1990) Gestational diabetes mellitus: the prevalence of glucose intolerance and diabetes mellitus in the first two months post partum. *Am J Obstet Gynecol* **163**, 93-8.
19. Kim, C., Berger, D.K., Chamany, S. (2007) Recurrence of gestational diabetes mellitus: a systematic review. *Diabetes Care* **30**, 1314-9.
20. Phillips, P.J., Jeffries, B. (2006) Gestational diabetes--worth finding and actively treating. *Aust Fam Physician* **35**, 701-3.
21. Ryan, E.A., Imes, S., Liu, D., McManus, R., Finegood, D.T., Polonsky, K.S., Sturis, J. (1995) Defects in insulin secretion and action in women with a history of gestational diabetes. *Diabetes* **44**, 506-12.

22. Weng, J., Ekelund, M., Lehto, M., Li, H., Ekberg, G., Frid, A., Aberg, A., Groop, L.C., Berntorp, K. (2002) Screening for MODY mutations, GAD antibodies, and type 1 diabetes--associated HLA genotypes in women with gestational diabetes mellitus. *Diabetes Care* **25**, 68-71.
23. Kousta, E., Ellard, S., Allen, L.I., Saker, P.J., Huxtable, S.J., Hattersley, A.T., McCarthy, M.I. (2001) Glucokinase mutations in a phenotypically selected multiethnic group of women with a history of gestational diabetes. *Diabet Med* **18**, 683-4.
24. Ellard, S., Beards, F., Allen, L.I., Shepherd, M., Ballantyne, E., Harvey, R., Hattersley, A.T. (2000) A high prevalence of glucokinase mutations in gestational diabetic subjects selected by clinical criteria. *Diabetologia* **43**, 250-3.
25. Guazzini, B., Gaffi, D., Mainieri, D., Multari, G., Cordera, R., Bertolini, S., Pozza, G., Meschi, F., Barbetti, F. (1998) Three novel missense mutations in the glucokinase gene (G80S; E221K; G227C) in Italian subjects with maturity-onset diabetes of the young (MODY). Mutations in brief no. 162. Online. *Hum Mutat* **12**, 136.
26. Landmann, E., Geller, F., Schilling, J., Rudloff, S., Foeller-Gaudier, E., Gortner, L. (2006) Absence of the wild-type allele (192 base pairs) of a polymorphism in the promoter region of the IGF-I gene but not a polymorphism in the insulin gene variable number of tandem repeat locus is associated with accelerated weight gain in infancy. *Pediatrics* **118**, 2374-9.
27. Gragnoli, C., Stanojevic, V., Gorini, A., Von Preussenthal, G.M., Thomas, M.K., Habener, J.F. (2005) IPF-1/MODY4 gene missense mutation in an Italian family with type 2 and gestational diabetes. *Metabolism* **54**, 983-8.
28. Kolatsi-Joannou, M., Bingham, C., Ellard, S., Bulman, M.P., Allen, L.I., Hattersley, A.T., Woolf, A.S. (2001) Hepatocyte nuclear factor-1beta: a new kindred with renal cysts and diabetes and gene expression in normal human development. *J Am Soc Nephrol* **12**, 2175-80.
29. Pasquier, F., Boulogne, A., Leys, D., Fontaine, P. (2006) Diabetes mellitus and dementia. *Diabetes Metab* **32**, 403-14.

30. Chyun, D.A., Young, L.H. (2006) Diabetes mellitus and cardiovascular disease. *Nurs Clin North Am* **41**, 681-95, viii-ix.
31. Conlon, J.M., Trauth, S.E., Sever, D.M. (1997) Purification and structural characterization of insulin from the lesser siren, *Siren intermedia* (Amphibia: Caudata). *Gen Comp Endocrinol* **106**, 295-300.
32. Mayer, J.P., Zhang, F., Dimarchi, R.D. (2007) Insulin structure and function. *Biopolymers* **88**, 687-713.
33. Wan, Z., Xu, B., Huang, K., Chu, Y.C., Li, B., Nakagawa, S.H., Qu, Y., Hu, S.Q., Katsoyannis, P.G., Weiss, M.A. (2004) Enhancing the activity of insulin at the receptor interface: crystal structure and photo-cross-linking of A8 analogues. *Biochemistry* **43**, 16119-33.
34. Huang, K., Xu, B., Hu, S.Q., Chu, Y.C., Hua, Q.X., Qu, Y., Li, B., Wang, S., Wang, R.Y., Nakagawa, S.H., Theede, A.M., Whittaker, J., De Meyts, P., Katsoyannis, P.G., Weiss, M.A. (2004) How insulin binds: the B-chain alpha-helix contacts the L1 beta-helix of the insulin receptor. *J Mol Biol* **341**, 529-50.
35. Hribal, M.L., Oriente, F., Accili, D. (2002) Mouse models of insulin resistance. *Am J Physiol Endocrinol Metab* **282**, E977-81.
36. Farese, R.V., Sajan, M.P., Standaert, M.L. (2005) Insulin-sensitive protein kinases (atypical protein kinase C and protein kinase B/Akt): actions and defects in obesity and type II diabetes. *Exp Biol Med (Maywood)* **230**, 593-605.
37. Hue, L., Rider, M.H. (2007) The AMP-activated protein kinase: more than an energy sensor. *Essays Biochem* **43**, 121-38.
38. Wright, E.M. (2001) Renal Na⁽⁺⁾-glucose cotransporters. *Am J Physiol Renal Physiol* **280**, F10-8.
39. Chandrasena, G., Giltay, R., Patil, S.D., Bakken, A., Unadkat, J.D. (1997) Functional expression of human intestinal Na⁺-dependent and Na⁺-independent nucleoside transporters in *Xenopus laevis* oocytes. *Biochem Pharmacol* **53**, 1909-18.

40. Wood, I.S., Trayhurn, P. (2003) Glucose transporters (GLUT and SGLT): expanded families of sugar transport proteins. *Br J Nutr* **89**, 3-9.
41. Joost, H.G., Thorens, B. (2001) The extended GLUT-family of sugar/polyol transport facilitators: nomenclature, sequence characteristics, and potential function of its novel members (review). *Mol Membr Biol* **18**, 247-56.
42. Rea, S., James, D.E. (1997) Moving GLUT4: the biogenesis and trafficking of GLUT4 storage vesicles. *Diabetes* **46**, 1667-77.
43. Malide, D., Ramm, G., Cushman, S.W., Slot, J.W. (2000) Immunoelectron microscopic evidence that GLUT4 translocation explains the stimulation of glucose transport in isolated rat white adipose cells. *J Cell Sci* **113 Pt 23**, 4203-10.
44. Holman, G.D., Lo Leggio, L., Cushman, S.W. (1994) Insulin-stimulated GLUT4 glucose transporter recycling. A problem in membrane protein subcellular trafficking through multiple pools. *J Biol Chem* **269**, 17516-24.
45. Cushman, S.W., Goodyear, L.J., Pilch, P.F., Ralston, E., Galbo, H., Ploug, T., Kristiansen, S., Klip, A. (1998) Molecular mechanisms involved in GLUT4 translocation in muscle during insulin and contraction stimulation. *Adv Exp Med Biol* **441**, 63-71.
46. Malide, D., Dwyer, N.K., Blanchette-Mackie, E.J., Cushman, S.W. (1997) Immunocytochemical evidence that GLUT4 resides in a specialized translocation post-endosomal VAMP2-positive compartment in rat adipose cells in the absence of insulin. *J Histochem Cytochem* **45**, 1083-96.
47. Dugani, C.B., Klip, A. (2005) Glucose transporter 4: cycling, compartments and controversies. *EMBO Rep* **6**, 1137-42.
48. Bryant, N.J., Govers, R., James, D.E. (2002) Regulated transport of the glucose transporter GLUT4. *Nat Rev Mol Cell Biol* **3**, 267-77.
49. Hou, J.C., Pessin, J.E. (2007) Ins (endocytosis) and outs (exocytosis) of GLUT4 trafficking. *Curr Opin Cell Biol* **19**, 466-73.

50. Watson, R.T., Khan, A.H., Furukawa, M., Hou, J.C., Li, L., Kanzaki, M., Okada, S., Kandrор, K.V., Pessin, J.E. (2004) Entry of newly synthesized GLUT4 into the insulin-responsive storage compartment is GGA dependent. *Embo J* **23**, 2059-70.
51. Li, L.V., Kandrор, K.V. (2005) Golgi-localized, gamma-ear-containing, Arf-binding protein adaptors mediate insulin-responsive trafficking of glucose transporter 4 in 3T3-L1 adipocytes. *Mol Endocrinol* **19**, 2145-53.
52. Rudich, A., Klip, A. (2003) Push/pull mechanisms of GLUT4 traffic in muscle cells. *Acta Physiol Scand* **178**, 297-308.
53. Keller, S.R. (2003) The insulin-regulated aminopeptidase: a companion and regulator of GLUT4. *Front Biosci* **8**, s410-20.
54. Astrup, A., Finer, N. (2000) Redefining type 2 diabetes: 'diabesity' or 'obesity dependent diabetes mellitus'? *Obes Rev* **1**, 57-9.
55. Miura, T., Suzuki, W., Ishihara, E., Arai, I., Ishida, H., Seino, Y., Tanigawa, K. (2001) Impairment of insulin-stimulated GLUT4 translocation in skeletal muscle and adipose tissue in the Tsumura Suzuki obese diabetic mouse: a new genetic animal model of type 2 diabetes. *Eur J Endocrinol* **145**, 785-90.
56. Dutour, A. (1996) Knockout mice lacking GLUT4 glucose transporters. *Eur J Endocrinol* **134**, 421-2.
57. Stenbit, A.E., Tsao, T.S., Li, J., Burcelin, R., Geenen, D.L., Factor, S.M., Houseknecht, K., Katz, E.B., Charron, M.J. (1997) GLUT4 heterozygous knockout mice develop muscle insulin resistance and diabetes. *Nat Med* **3**, 1096-101.
58. Lamothe, B., Baudry, A., Desbois, P., Lamotte, L., Bucchini, D., De Meyts, P., Joshi, R.L. (1998) Genetic engineering in mice: impact on insulin signalling and action. *Biochem J* **335** (Pt 2), 193-204.
59. Oh, W., Abu-Elheiga, L., Kordari, P., Gu, Z., Shaikenov, T., Chirala, S.S., Wakil, S.J. (2005) Glucose and fat metabolism in adipose tissue of acetyl-CoA carboxylase 2 knockout mice. *Proc Natl Acad Sci U S A* **102**, 1384-9.

60. Carvalho, E., Kotani, K., Peroni, O.D., Kahn, B.B. (2005) Adipose-specific overexpression of GLUT4 reverses insulin resistance and diabetes in mice lacking GLUT4 selectively in muscle. *Am J Physiol Endocrinol Metab* **289**, E551-61.
61. McCarthy, A.M., Elmendorf, J.S. (2007) GLUT4's itinerary in health & disease. *Indian J Med Res* **125**, 373-88.
62. Bae, S.S., Cho, H., Mu, J., Birnbaum, M.J. (2003) Isoform-specific regulation of insulin-dependent glucose uptake by Akt/protein kinase B. *J Biol Chem* **278**, 49530-6.
63. Calera, M.R., Martinez, C., Liu, H., Jack, A.K., Birnbaum, M.J., Pilch, P.F. (1998) Insulin increases the association of Akt-2 with Glut4-containing vesicles. *J Biol Chem* **273**, 7201-4.
64. Larance, M., Ramm, G., Stockli, J., van Dam, E.M., Winata, S., Wasinger, V., Simpson, F., Graham, M., Junutula, J.R., Guilhaus, M., James, D.E. (2005) Characterization of the role of the Rab GTPase-activating protein AS160 in insulin-regulated GLUT4 trafficking. *J Biol Chem* **280**, 37803-13.
65. Eguez, L., Lee, A., Chavez, J.A., Miinea, C.P., Kane, S., Lienhard, G.E., McGraw, T.E. (2005) Full intracellular retention of GLUT4 requires AS160 Rab GTPase activating protein. *Cell Metab* **2**, 263-72.
66. Kramer, H.F., Witczak, C.A., Fujii, N., Jessen, N., Taylor, E.B., Arnolds, D.E., Sakamoto, K., Hirshman, M.F., Goodyear, L.J. (2006) Distinct signals regulate AS160 phosphorylation in response to insulin, AICAR, and contraction in mouse skeletal muscle. *Diabetes* **55**, 2067-76.
67. Kane, S., Sano, H., Liu, S.C., Asara, J.M., Lane, W.S., Garner, C.C., Lienhard, G.E. (2002) A method to identify serine kinase substrates. Akt phosphorylates a novel adipocyte protein with a Rab GTPase-activating protein (GAP) domain. *J Biol Chem* **277**, 22115-8.
68. Kramer, H.F., Witczak, C.A., Taylor, E.B., Fujii, N., Hirshman, M.F., Goodyear, L.J. (2006) AS160 regulates insulin- and contraction-stimulated glucose uptake in mouse skeletal muscle. *J Biol Chem* **281**, 31478-85.

69. Chiang, S.H., Baumann, C.A., Kanzaki, M., Thurmond, D.C., Watson, R.T., Neudauer, C.L., Macara, I.G., Pessin, J.E., Saltiel, A.R. (2001) Insulin-stimulated GLUT4 translocation requires the CAP-dependent activation of TC10. *Nature* **410**, 944-8.
70. Ribon, V., Saltiel, A.R. (1997) Insulin stimulates tyrosine phosphorylation of the proto-oncogene product of c-Cbl in 3T3-L1 adipocytes. *Biochem J* **324** (Pt 3), 839-45.
71. Gupte, A., Mora, S. (2006) Activation of the Cbl insulin signaling pathway in cardiac muscle; dysregulation in obesity and diabetes. *Biochem Biophys Res Commun* **342**, 751-7.
72. Chiang, S.H., Chang, L., Saltiel, A.R. (2006) TC10 and insulin-stimulated glucose transport. *Methods Enzymol* **406**, 701-14.
73. Mitra, P., Zheng, X., Czech, M.P. (2004) RNAi-based analysis of CAP, Cbl, and CrkII function in the regulation of GLUT4 by insulin. *J Biol Chem* **279**, 37431-5.
74. Klaus, S. (1997) Functional differentiation of white and brown adipocytes. *Bioessays* **19**, 215-23.
75. Fain, J.N., Madan, A.K., Hiler, M.L., Cheema, P., Bahouth, S.W. (2004) Comparison of the release of adipokines by adipose tissue, adipose tissue matrix, and adipocytes from visceral and subcutaneous abdominal adipose tissues of obese humans. *Endocrinology* **145**, 2273-82.
76. Fantuzzi, G. (2005) Adipose tissue, adipokines, and inflammation. *J Allergy Clin Immunol* **115**, 911-9; quiz 920.
77. Klaus, S., Ely, M., Encke, D., Heldmaier, G. (1995) Functional assessment of white and brown adipocyte development and energy metabolism in cell culture. Dissociation of terminal differentiation and thermogenesis in brown adipocytes. *J Cell Sci* **108** (Pt 10), 3171-80.
78. Klingenspor, M. (2003) Cold-induced recruitment of brown adipose tissue thermogenesis. *Exp Physiol* **88**, 141-8.

79. Nedergaard, J., Bengtsson, T., Cannon, B. (2007) Unexpected evidence for active brown adipose tissue in adult humans. *Am J Physiol Endocrinol Metab* **293**, E444-52.
80. Tiraby, C., Langin, D. (2003) Conversion from white to brown adipocytes: a strategy for the control of fat mass? *Trends Endocrinol Metab* **14**, 439-41.
81. Tiraby, C., Tavernier, G., Lefort, C., Larrouy, D., Bouillaud, F., Ricquier, D., Langin, D. (2003) Acquirement of brown fat cell features by human white adipocytes. *J Biol Chem* **278**, 33370-6.
82. Orci, L., Cook, W.S., Ravazzola, M., Wang, M.Y., Park, B.H., Montesano, R., Unger, R.H. (2004) Rapid transformation of white adipocytes into fat-oxidizing machines. *Proc Natl Acad Sci U S A* **101**, 2058-63.
83. Serra, F., Bonet, M.L., Puigserver, P., Oliver, J., Palou, A. (1999) Stimulation of uncoupling protein 1 expression in brown adipocytes by naturally occurring carotenoids. *Int J Obes Relat Metab Disord* **23**, 650-5.
84. Murano, I., Morroni, M., Zingaretti, M.C., Oliver, P., Sanchez, J., Fuster, A., Pico, C., Palou, A., Cinti, S. (2005) Morphology of ferret subcutaneous adipose tissue after 6-month daily supplementation with oral beta-carotene. *Biochim Biophys Acta* **1740**, 305-12.
85. Hamann, A., Flier, J.S., Lowell, B.B. (1996) Decreased brown fat markedly enhances susceptibility to diet-induced obesity, diabetes, and hyperlipidemia. *Endocrinology* **137**, 21-9.
86. Enerback, S., Jacobsson, A., Simpson, E.M., Guerra, C., Yamashita, H., Harper, M.E., Kozak, L.P. (1997) Mice lacking mitochondrial uncoupling protein are cold-sensitive but not obese. *Nature* **387**, 90-4.
87. Shi, T., Wang, F., Stieren, E., Tong, Q. (2005) SIRT3, a mitochondrial sirtuin deacetylase, regulates mitochondrial function and thermogenesis in brown adipocytes. *J Biol Chem* **280**, 13560-7.

88. Kang, S., Bajnok, L., Longo, K.A., Petersen, R.K., Hansen, J.B., Kristiansen, K., MacDougald, O.A. (2005) Effects of Wnt signaling on brown adipocyte differentiation and metabolism mediated by PGC-1alpha. *Mol Cell Biol* **25**, 1272-82.
89. Trujillo, M.E., Scherer, P.E. (2006) Adipose tissue-derived factors: impact on health and disease. *Endocr Rev* **27**, 762-78.
90. Guerre-Millo, M. (2002) Adipose tissue hormones. *J Endocrinol Invest* **25**, 855-61.
91. Berg, A.H., Combs, T.P., Scherer, P.E. (2002) ACRP30/adiponectin: an adipokine regulating glucose and lipid metabolism. *Trends Endocrinol Metab* **13**, 84-9.
92. Shapiro, L., Scherer, P.E. (1998) The crystal structure of a complement-1q family protein suggests an evolutionary link to tumor necrosis factor. *Curr Biol* **8**, 335-8.
93. Yamauchi, T., Kamon, J., Waki, H., Imai, Y., Shimozawa, N., Hioki, K., Uchida, S., Ito, Y., Takakuwa, K., Matsui, J., Takata, M., Eto, K., Terauchi, Y., Komeda, K., Tsunoda, M., Murakami, K., Ohnishi, Y., Naitoh, T., Yamamura, K., Ueyama, Y., Froguel, P., Kimura, S., Nagai, R., Kadowaki, T. (2003) Globular adiponectin protected ob/ob mice from diabetes and ApoE-deficient mice from atherosclerosis. *J Biol Chem* **278**, 2461-8.
94. Inoue, T., Kotooka, N., Morooka, T., Komoda, H., Uchida, T., Aso, Y., Inukai, T., Okuno, T., Node, K. (2007) High molecular weight adiponectin as a predictor of long-term clinical outcome in patients with coronary artery disease. *Am J Cardiol* **100**, 569-74.
95. Pajvani, U.B., Du, X., Combs, T.P., Berg, A.H., Rajala, M.W., Schulthess, T., Engel, J., Brownlee, M., Scherer, P.E. (2003) Structure-function studies of the adipocyte-secreted hormone Acrp30/adiponectin. Implications for metabolic regulation and bioactivity. *J Biol Chem* **278**, 9073-85.
96. Lara-Castro, C., Luo, N., Wallace, P., Klein, R.L., Garvey, W.T. (2006) Adiponectin multimeric complexes and the metabolic syndrome trait cluster. *Diabetes* **55**, 249-59.
97. Kern, P.A., Di Gregorio, G.B., Lu, T., Rassouli, N., Ranganathan, G. (2003) Adiponectin expression from human adipose tissue: relation to obesity, insulin resistance, and tumor necrosis factor-alpha expression. *Diabetes* **52**, 1779-85.

98. Nakashima, R., Kamei, N., Yamane, K., Nakanishi, S., Nakashima, A., Kohno, N. (2006) Decreased total and high molecular weight adiponectin are independent risk factors for the development of type 2 diabetes in Japanese-Americans. *J Clin Endocrinol Metab* **91**, 3873-7.
99. Liu, Y., Retnakaran, R., Hanley, A., Tungtrongchit, R., Shaw, C., Sweeney, G. (2007) Total and High molecular weight (HMW) but not trimeric or hexameric forms of adiponectin correlate with markers of the metabolic syndrome and liver injury in Thai subjects. *J Clin Endocrinol Metab*.
100. Yatagai, T., Nagasaka, S., Taniguchi, A., Fukushima, M., Nakamura, T., Kuroe, A., Nakai, Y., Ishibashi, S. (2003) Hypoadiponectinemia is associated with visceral fat accumulation and insulin resistance in Japanese men with type 2 diabetes mellitus. *Metabolism* **52**, 1274-8.
101. Lindsay, R.S., Funahashi, T., Hanson, R.L., Matsuzawa, Y., Tanaka, S., Tataranni, P.A., Knowler, W.C., Krakoff, J. (2002) Adiponectin and development of type 2 diabetes in the Pima Indian population. *Lancet* **360**, 57-8.
102. Krakoff, J., Funahashi, T., Stehouwer, C.D., Schalkwijk, C.G., Tanaka, S., Matsuzawa, Y., Kobes, S., Tataranni, P.A., Hanson, R.L., Knowler, W.C., Lindsay, R.S. (2003) Inflammatory markers, adiponectin, and risk of type 2 diabetes in the Pima Indian. *Diabetes Care* **26**, 1745-51.
103. Combs, T.P., Berg, A.H., Rajala, M.W., Klebanov, S., Iyengar, P., Jimenez-Chillaron, J.C., Patti, M.E., Klein, S.L., Weinstein, R.S., Scherer, P.E. (2003) Sexual differentiation, pregnancy, calorie restriction, and aging affect the adipocyte-specific secretory protein adiponectin. *Diabetes* **52**, 268-76.
104. Seftel, A.D. (2005) Testosterone selectively reduces the high molecular weight form of adiponectin by inhibiting its secretion from adipocytes. *J Urol* **174**, 1045-6.
105. Nagasawa, A., Fukui, K., Funahashi, T., Maeda, N., Shimomura, I., Kihara, S., Waki, M., Takamatsu, K., Matsuzawa, Y. (2002) Effects of soy protein diet on the expression of adipose genes and plasma adiponectin. *Horm Metab Res* **34**, 635-9.

106. Itoh, M., Suganami, T., Satoh, N., Tanimoto-Koyama, K., Yuan, X., Tanaka, M., Kawano, H., Yano, T., Aoe, S., Takeya, M., Shimatsu, A., Kuzuya, H., Kamei, Y., Ogawa, Y. (2007) Increased adiponectin secretion by highly purified eicosapentaenoic acid in rodent models of obesity and human obese subjects. *Arterioscler Thromb Vasc Biol* **27**, 1918-25.
107. Malloy, V.L., Krajcik, R.A., Bailey, S.J., Hristopoulos, G., Plummer, J.D., Orentreich, N. (2006) Methionine restriction decreases visceral fat mass and preserves insulin action in aging male Fischer 344 rats independent of energy restriction. *Aging Cell* **5**, 305-14.
108. Perez-Matute, P., Marti, A., Martinez, J.A., Fernandez-Otero, M.P., Stanhope, K.L., Havel, P.J., Moreno-Aliaga, M.J. (2007) Conjugated linoleic acid inhibits glucose metabolism, leptin and adiponectin secretion in primary cultured rat adipocytes. *Mol Cell Endocrinol* **268**, 50-8.
109. Maeda, N., Funahashi, T. (2004) [Adiponectin knockout mice]. *Nippon Rinsho* **62**, 1067-76.
110. Xu, A., Yin, S., Wong, L., Chan, K.W., Lam, K.S. (2004) Adiponectin ameliorates dyslipidemia induced by the human immunodeficiency virus protease inhibitor ritonavir in mice. *Endocrinology* **145**, 487-94.
111. Berg, A.H., Combs, T.P., Du, X., Brownlee, M., Scherer, P.E. (2001) The adipocyte-secreted protein Acrp30 enhances hepatic insulin action. *Nat Med* **7**, 947-53.
112. Combs, T.P., Berg, A.H., Obici, S., Scherer, P.E., Rossetti, L. (2001) Endogenous glucose production is inhibited by the adipose-derived protein Acrp30. *J Clin Invest* **108**, 1875-81.
113. Combs, T.P., Wagner, J.A., Berger, J., Doebber, T., Wang, W.J., Zhang, B.B., Tanen, M., Berg, A.H., O'Rahilly, S., Savage, D.B., Chatterjee, K., Weiss, S., Larson, P.J., Gottesdiener, K.M., Gertz, B.J., Charron, M.J., Scherer, P.E., Moller, D.E. (2002) Induction of adipocyte complement-related protein of 30 kilodaltons by PPARgamma agonists: a potential mechanism of insulin sensitization. *Endocrinology* **143**, 998-1007.
114. Fruebis, J., Tsao, T.S., Javorschi, S., Ebbets-Reed, D., Erickson, M.R., Yen, F.T., Bihain, B.E., Lodish, H.F. (2001) Proteolytic cleavage product of 30-kDa adipocyte complement-

- related protein increases fatty acid oxidation in muscle and causes weight loss in mice. *Proc Natl Acad Sci U S A* **98**, 2005-10.
115. Tonelli, J., Li, W., Kishore, P., Pajvani, U.B., Kwon, E., Weaver, C., Scherer, P.E., Hawkins, M. (2004) Mechanisms of early insulin-sensitizing effects of thiazolidinediones in type 2 diabetes. *Diabetes* **53**, 1621-9.
 116. Otabe, S., Yuan, X., Fukutani, T., Wada, N., Hashinaga, T., Nakayama, H., Hirota, N., Kojima, M., Yamada, K. (2007) Overexpression of human adiponectin in transgenic mice results in suppression of fat accumulation and prevention of premature death by high-calorie diet. *Am J Physiol Endocrinol Metab* **293**, E210-8.
 117. Yamauchi, T., Kamon, J., Ito, Y., Tsuchida, A., Yokomizo, T., Kita, S., Sugiyama, T., Miyagishi, M., Hara, K., Tsunoda, M., Murakami, K., Ohteki, T., Uchida, S., Takekawa, S., Waki, H., Tsuno, N.H., Shibata, Y., Terauchi, Y., Froguel, P., Tobe, K., Koyasu, S., Taira, K., Kitamura, T., Shimizu, T., Nagai, R., Kadowaki, T. (2003) Cloning of adiponectin receptors that mediate antidiabetic metabolic effects. *Nature* **423**, 762-9.
 118. Bjursell, M., Ahnmark, A., Bohlooly, Y.M., William-Olsson, L., Rhedin, M., Peng, X.R., Ploj, K., Gerdin, A.K., Arnerup, G., Elmgren, A., Berg, A.L., Oscarsson, J., Linden, D. (2007) Opposing effects of adiponectin receptors 1 and 2 on energy metabolism. *Diabetes* **56**, 583-93.
 119. Sharabi, Y., Oron-Herman, M., Kamari, Y., Avni, I., Peleg, E., Shabtay, Z., Grossman, E., Shamiss, A. (2007) Effect of PPAR-gamma agonist on adiponectin levels in the metabolic syndrome: lessons from the high fructose fed rat model. *Am J Hypertens* **20**, 206-10.
 120. Viollet, B., Foretz, M., Guigas, B., Horman, S., Dentin, R., Bertrand, L., Hue, L., Andreelli, F. (2006) Activation of AMP-activated protein kinase in the liver: a new strategy for the management of metabolic hepatic disorders. *J Physiol* **574**, 41-53.
 121. Wu, X., Motoshima, H., Mahadev, K., Stalker, T.J., Scalia, R., Goldstein, B.J. (2003) Involvement of AMP-activated protein kinase in glucose uptake stimulated by the globular domain of adiponectin in primary rat adipocytes. *Diabetes* **52**, 1355-63.

122. Kubota, N., Yano, W., Kubota, T., Yamauchi, T., Itoh, S., Kumagai, H., Kozono, H., Takamoto, I., Okamoto, S., Shiuchi, T., Suzuki, R., Satoh, H., Tsuchida, A., Moroi, M., Sugi, K., Noda, T., Ebinuma, H., Ueta, Y., Kondo, T., Araki, E., Ezaki, O., Nagai, R., Tobe, K., Terauchi, Y., Ueki, K., Minokoshi, Y., Kadowaki, T. (2007) Adiponectin stimulates AMP-activated protein kinase in the hypothalamus and increases food intake. *Cell Metab* **6**, 55-68.
123. Huypens, P., Moens, K., Heimberg, H., Ling, Z., Pipeleers, D., Van de Casteele, M. (2005) Adiponectin-mediated stimulation of AMP-activated protein kinase (AMPK) in pancreatic beta cells. *Life Sci* **77**, 1273-82.
124. Yokota, T., Oritani, K., Takahashi, I., Ishikawa, J., Matsuyama, A., Ouchi, N., Kihara, S., Funahashi, T., Tenner, A.J., Tomiyama, Y., Matsuzawa, Y. (2000) Adiponectin, a new member of the family of soluble defense collagens, negatively regulates the growth of myelomonocytic progenitors and the functions of macrophages. *Blood* **96**, 1723-32.
125. Wolf, A.M., Wolf, D., Rumpold, H., Enrich, B., Tilg, H. (2004) Adiponectin induces the anti-inflammatory cytokines IL-10 and IL-1RA in human leukocytes. *Biochem Biophys Res Commun* **323**, 630-5.
126. Nishida, M., Moriyama, T., Ishii, K., Takashima, S., Yoshizaki, K., Sugita, Y., Yamauchi-Takahara, K. (2007) Effects of IL-6, adiponectin, CRP and metabolic syndrome on subclinical atherosclerosis. *Clin Chim Acta* **384**, 99-104.
127. Ajuwon, K.M., Spurlock, M.E. (2005) Adiponectin inhibits LPS-induced NF-kappaB activation and IL-6 production and increases PPARgamma2 expression in adipocytes. *Am J Physiol Regul Integr Comp Physiol* **288**, R1220-5.
128. Maeda, N., Shimomura, I., Kishida, K., Nishizawa, H., Matsuda, M., Nagaretani, H., Furuyama, N., Kondo, H., Takahashi, M., Arita, Y., Komuro, R., Ouchi, N., Kihara, S., Tochino, Y., Okutomi, K., Horie, M., Takeda, S., Aoyama, T., Funahashi, T., Matsuzawa, Y. (2002) Diet-induced insulin resistance in mice lacking adiponectin/ACRP30. *Nat Med* **8**, 731-7.
129. Lam, Q.L., Lu, L. (2007) Role of leptin in immunity. *Cell Mol Immunol* **4**, 1-13.

130. Grasso, P., Leinung, M.C., Ingher, S.P., Lee, D.W. (1997) In vivo effects of leptin-related synthetic peptides on body weight and food intake in female ob/ob mice: localization of leptin activity to domains between amino acid residues 106-140. *Endocrinology* **138**, 1413-8.
131. Guzik, T.J., Mangalat, D., Korbut, R. (2006) Adipocytokines - novel link between inflammation and vascular function? *J Physiol Pharmacol* **57**, 505-28.
132. Kolaczynski, J.W., Considine, R.V., Ohannesian, J., Marco, C., Opentanova, I., Nyce, M.R., Myint, M., Caro, J.F. (1996) Responses of leptin to short-term fasting and refeeding in humans: a link with ketogenesis but not ketones themselves. *Diabetes* **45**, 1511-5.
133. Saladin, R., De Vos, P., Guerre-Millo, M., Leturque, A., Girard, J., Staels, B., Auwerx, J. (1995) Transient increase in obese gene expression after food intake or insulin administration. *Nature* **377**, 527-9.
134. Bradley, R.L., Cheatham, B. (1999) Regulation of ob gene expression and leptin secretion by insulin and dexamethasone in rat adipocytes. *Diabetes* **48**, 272-8.
135. Menendez, C., Baldelli, R., Camina, J.P., Escudero, B., Peino, R., Dieguez, C., Casanueva, F.F. (2003) TSH stimulates leptin secretion by a direct effect on adipocytes. *J Endocrinol* **176**, 7-12.
136. Trujillo, M.E., Lee, M.J., Sullivan, S., Feng, J., Schneider, S.H., Greenberg, A.S., Fried, S.K. (2006) Tumor necrosis factor alpha and glucocorticoid synergistically increase leptin production in human adipose tissue: role for p38 mitogen-activated protein kinase. *J Clin Endocrinol Metab* **91**, 1484-90.
137. Trujillo, M.E., Sullivan, S., Harten, I., Schneider, S.H., Greenberg, A.S., Fried, S.K. (2004) Interleukin-6 regulates human adipose tissue lipid metabolism and leptin production in vitro. *J Clin Endocrinol Metab* **89**, 5577-82.
138. Buyukgebiz, B., Ozturk, Y., Yilmaz, S., Arslan, N. (2003) Serum leptin concentrations in children with mild-to-moderate protein-energy malnutrition. *Pediatr Int* **45**, 550-4.

139. O'Rahilly, S. (2002) Leptin: defining its role in humans by the clinical study of genetic disorders. *Nutr Rev* **60**, S30-4; discussion S68-84, 85-7.
140. Oswiecimska, J., Ziora, K., Geisler, G., Broll-Waska, K. (2005) Prospective evaluation of leptin and neuropeptide Y (NPY) serum levels in girls with anorexia nervosa. *Neuro Endocrinol Lett* **26**, 301-4.
141. Holtkamp, K., Hebebrand, J., Mika, C., Grzella, I., Heer, M., Heussen, N., Herpertz-Dahlmann, B. (2003) The effect of therapeutically induced weight gain on plasma leptin levels in patients with anorexia nervosa. *J Psychiatr Res* **37**, 165-9.
142. Coelho, R., Wells, J., Symth, J., Semple, R., O'Rahilly, S., Eaton, S., Hussain, K. (2007) Severe hypoinsulinaemic hypoglycaemia in a premature infant associated with poor weight gain and reduced adipose tissue. *Horm Res* **68**, 91-8.
143. Ahima, R.S., Flier, J.S. (2000) Leptin. *Annu Rev Physiol* **62**, 413-37.
144. Pajvani, U.B., Trujillo, M.E., Combs, T.P., Iyengar, P., Jelicks, L., Roth, K.A., Kitsis, R.N., Scherer, P.E. (2005) Fat apoptosis through targeted activation of caspase 8: a new mouse model of inducible and reversible lipoatrophy. *Nat Med* **11**, 797-803.
145. Munzberg, H., Bjornholm, M., Bates, S.H., Myers, M.G., Jr. (2005) Leptin receptor action and mechanisms of leptin resistance. *Cell Mol Life Sci* **62**, 642-52.
146. Gibson, W.T., Farooqi, I.S., Moreau, M., DePaoli, A.M., Lawrence, E., O'Rahilly, S., Trussell, R.A. (2004) Congenital leptin deficiency due to homozygosity for the Delta133G mutation: report of another case and evaluation of response to four years of leptin therapy. *J Clin Endocrinol Metab* **89**, 4821-6.
147. Rau, H., Reaves, B.J., O'Rahilly, S., Whitehead, J.P. (1999) Truncated human leptin (delta133) associated with extreme obesity undergoes proteasomal degradation after defective intracellular transport. *Endocrinology* **140**, 1718-23.
148. Banks, A.S., Davis, S.M., Bates, S.H., Myers, M.G., Jr. (2000) Activation of downstream signals by the long form of the leptin receptor. *J Biol Chem* **275**, 14563-72.

149. Black, P.H. (2006) The inflammatory consequences of psychologic stress: relationship to insulin resistance, obesity, atherosclerosis and diabetes mellitus, type II. *Med Hypotheses* **67**, 879-91.
150. Seron, K., Corset, L., Vasseur, F., Boutin, P., Gomez-Ambrosi, J., Salvador, J., Fruhbeck, G., Froguel, P. (2006) Distinct impaired regulation of SOCS3 and long and short isoforms of the leptin receptor in visceral and subcutaneous fat of lean and obese women. *Biochem Biophys Res Commun* **348**, 1232-8.
151. Bennett, B.D., Solar, G.P., Yuan, J.Q., Mathias, J., Thomas, G.R., Matthews, W. (1996) A role for leptin and its cognate receptor in hematopoiesis. *Curr Biol* **6**, 1170-80.
152. Mattioli, B., Straface, E., Quaranta, M.G., Giordani, L., Viora, M. (2005) Leptin promotes differentiation and survival of human dendritic cells and licenses them for Th1 priming. *J Immunol* **174**, 6820-8.
153. Sirotkin, A.V., Mlyncek, M., Makarevich, A.V., Florkovicova, I., Hetenyi, L. (2007) Leptin affects proliferation-, apoptosis- and protein kinase A-related peptides in human ovarian granulosa cells. *Physiol Res*.
154. Pang, S.S., Le, Y.Y. (2006) Role of resistin in inflammation and inflammation-related diseases. *Cell Mol Immunol* **3**, 29-34.
155. Meier, U., Gressner, A.M. (2004) Endocrine regulation of energy metabolism: review of pathobiochemical and clinical chemical aspects of leptin, ghrelin, adiponectin, and resistin. *Clin Chem* **50**, 1511-25.
156. Steppan, C.M., Bailey, S.T., Bhat, S., Brown, E.J., Banerjee, R.R., Wright, C.M., Patel, H.R., Ahima, R.S., Lazar, M.A. (2001) The hormone resistin links obesity to diabetes. *Nature* **409**, 307-12.
157. Moon, B., Kwan, J.J., Duddy, N., Sweeney, G., Begum, N. (2003) Resistin inhibits glucose uptake in L6 cells independently of changes in insulin signaling and GLUT4 translocation. *Am J Physiol Endocrinol Metab* **285**, E106-15.

158. Qi, Y., Nie, Z., Lee, Y.S., Singhal, N.S., Scherer, P.E., Lazar, M.A., Ahima, R.S. (2006) Loss of resistin improves glucose homeostasis in leptin deficiency. *Diabetes* **55**, 3083-90.
159. Kaser, S., Kaser, A., Sandhofer, A., Ebenbichler, C.F., Tilg, H., Patsch, J.R. (2003) Resistin messenger-RNA expression is increased by proinflammatory cytokines in vitro. *Biochem Biophys Res Commun* **309**, 286-90.
160. Bokarewa, M., Nagaev, I., Dahlberg, L., Smith, U., Tarkowski, A. (2005) Resistin, an adipokine with potent proinflammatory properties. *J Immunol* **174**, 5789-95.
161. Beltowski, J. (2006) Apelin and visfatin: unique "beneficial" adipokines upregulated in obesity? *Med Sci Monit* **12**, RA112-9.
162. Hug, C., Lodish, H.F. (2005) Medicine. Visfatin: a new adipokine. *Science* **307**, 366-7.
163. Fukuhara, A., Matsuda, M., Nishizawa, M., Segawa, K., Tanaka, M., Kishimoto, K., Matsuki, Y., Murakami, M., Ichisaka, T., Murakami, H., Watanabe, E., Takagi, T., Akiyoshi, M., Ohtsubo, T., Kihara, S., Yamashita, S., Makishima, M., Funahashi, T., Yamanaka, S., Hiramatsu, R., Matsuzawa, Y., Shimomura, I. (2005) Visfatin: a protein secreted by visceral fat that mimics the effects of insulin. *Science* **307**, 426-30.
164. Ingelsson, E., Larson, M.G., Fox, C.S., Yin, X., Wang, T.J., Lipinska, I., Pou, K.M., Hoffmann, U., Benjamin, E.J., Keaney, J.F., Jr., Vasan, R.S. (2007) Clinical correlates of circulating visfatin levels in a community-based sample. *Diabetes Care* **30**, 1278-80.
165. Chen, M.P., Chung, F.M., Chang, D.M., Tsai, J.C., Huang, H.F., Shin, S.J., Lee, Y.J. (2006) Elevated plasma level of visfatin/pre-B cell colony-enhancing factor in patients with type 2 diabetes mellitus. *J Clin Endocrinol Metab* **91**, 295-9.
166. Axelsson, J., Witasp, A., Carrero, J.J., Qureshi, A.R., Suliman, M.E., Heimbürger, O., Barany, P., Lindholm, B., Alvestrand, A., Schalling, M., Nordfors, L., Stenvinkel, P. (2007) Circulating levels of visfatin/pre-B-cell colony-enhancing factor 1 in relation to genotype, GFR, body composition, and survival in patients with CKD. *Am J Kidney Dis* **49**, 237-44.

167. Pagano, C., Pilon, C., Olivieri, M., Mason, P., Fabris, R., Serra, R., Milan, G., Rossato, M., Federspil, G., Vettor, R. (2006) Reduced plasma visfatin/pre-B cell colony-enhancing factor in obesity is not related to insulin resistance in humans. *J Clin Endocrinol Metab* **91**, 3165-70.
168. Varma, V., Yao-Borengasser, A., Rasouli, N., Bodles, A.M., Phanavanh, B., Lee, M.J., Starks, T., Kern, L.M., Spencer, H.J., 3rd, McGehee, R.E., Jr., Fried, S.K., Kern, P.A. (2007) Human visfatin expression: relationship to insulin sensitivity, intramyocellular lipids, and inflammation. *J Clin Endocrinol Metab* **92**, 666-72.
169. Berndt, J., Kloting, N., Kralisch, S., Kovacs, P., Fasshauer, M., Schon, M.R., Stumvoll, M., Bluher, M. (2005) Plasma visfatin concentrations and fat depot-specific mRNA expression in humans. *Diabetes* **54**, 2911-6.
170. Moschen, A.R., Kaser, A., Enrich, B., Mosheimer, B., Theurl, M., Niederegger, H., Tilg, H. (2007) Visfatin, an adipocytokine with proinflammatory and immunomodulating properties. *J Immunol* **178**, 1748-58.
171. Dominici, F.P., Argentino, D.P., Munoz, M.C., Miquet, J.G., Sotelo, A.I., Turyn, D. (2005) Influence of the crosstalk between growth hormone and insulin signalling on the modulation of insulin sensitivity. *Growth Horm IGF Res* **15**, 324-36.
172. Hotamisligil, G.S., Shargill, N.S., Spiegelman, B.M. (1993) Adipose expression of tumor necrosis factor- α : direct role in obesity-linked insulin resistance. *Science* **259**, 87-91.
173. Tilg, H., Moschen, A.R. (2006) Adipocytokines: mediators linking adipose tissue, inflammation and immunity. *Nat Rev Immunol* **6**, 772-83.
174. Weisberg, S.P., McCann, D., Desai, M., Rosenbaum, M., Leibel, R.L., Ferrante, A.W., Jr. (2003) Obesity is associated with macrophage accumulation in adipose tissue. *J Clin Invest* **112**, 1796-808.
175. Chacon, M.R., Fernandez-Real, J.M., Richart, C., Megia, A., Gomez, J.M., Miranda, M., Caubet, E., Pastor, R., Masdevall, C., Vilarrasa, N., Ricard, W., Vendrell, J. (2007) Monocyte chemoattractant protein-1 in obesity and type 2 diabetes. Insulin sensitivity study. *Obesity (Silver Spring)* **15**, 664-72.

176. Kanda, H., Tateya, S., Tamori, Y., Kotani, K., Hiasa, K., Kitazawa, R., Kitazawa, S., Miyachi, H., Maeda, S., Egashira, K., Kasuga, M. (2006) MCP-1 contributes to macrophage infiltration into adipose tissue, insulin resistance, and hepatic steatosis in obesity. *J Clin Invest* **116**, 1494-505.
177. Sharma, A.M., Staels, B. (2007) Review: Peroxisome proliferator-activated receptor gamma and adipose tissue--understanding obesity-related changes in regulation of lipid and glucose metabolism. *J Clin Endocrinol Metab* **92**, 386-95.
178. Charriere, G., Cousin, B., Arnaud, E., Andre, M., Bacou, F., Penicaud, L., Casteilla, L. (2003) Preadipocyte conversion to macrophage. Evidence of plasticity. *J Biol Chem* **278**, 9850-5.
179. Gordon, S. (2003) Alternative activation of macrophages. *Nat Rev Immunol* **3**, 23-35.
180. Mantovani, A., Sica, A., Locati, M. (2007) New vistas on macrophage differentiation and activation. *Eur J Immunol* **37**, 14-6.
181. Mantovani, A., Sica, A., Sozzani, S., Allavena, P., Vecchi, A., Locati, M. (2004) The chemokine system in diverse forms of macrophage activation and polarization. *Trends Immunol* **25**, 677-86.
182. Odegaard, J.I., Ricardo-Gonzalez, R.R., Goforth, M.H., Morel, C.R., Subramanian, V., Mukundan, L., Eagle, A.R., Vats, D., Brombacher, F., Ferrante, A.W., Chawla, A. (2007) Macrophage-specific PPARgamma controls alternative activation and improves insulin resistance. *Nature* **447**, 1116-20.
183. Lumeng, C.N., Bodzin, J.L., Saltiel, A.R. (2007) Obesity induces a phenotypic switch in adipose tissue macrophage polarization. *J Clin Invest* **117**, 175-84.
184. Ruan, H., Lodish, H.F. (2003) Insulin resistance in adipose tissue: direct and indirect effects of tumor necrosis factor-alpha. *Cytokine Growth Factor Rev* **14**, 447-55.
185. Wallach, D., Boldin, M., Varfolomeev, E., Beyaert, R., Vandenabeele, P., Fiers, W. (1997) Cell death induction by receptors of the TNF family: towards a molecular understanding. *FEBS Lett* **410**, 96-106.

186. Hofmann, C., Lorenz, K., Braithwaite, S.S., Colca, J.R., Palazuk, B.J., Hotamisligil, G.S., Spiegelman, B.M. (1994) Altered gene expression for tumor necrosis factor-alpha and its receptors during drug and dietary modulation of insulin resistance. *Endocrinology* **134**, 264-70.
187. Habecker, B.A., Martin, J.M., Nathanson, N.M. (1993) Isolation and characterization of a novel cDNA which identifies both neural-specific and ubiquitously expressed GS alpha mRNAs. *J Neurochem* **61**, 712-7.
188. Tracey, K.J., Cerami, A. (1993) Tumor necrosis factor: an updated review of its biology. *Crit Care Med* **21**, S415-22.
189. Fain, J.N., Bahouth, S.W., Madan, A.K. (2004) TNFalpha release by the nonfat cells of human adipose tissue. *Int J Obes Relat Metab Disord* **28**, 616-22.
190. Lumeng, C.N., Deyoung, S.M., Saltiel, A.R. (2007) Macrophages block insulin action in adipocytes by altering expression of signaling and glucose transport proteins. *Am J Physiol Endocrinol Metab* **292**, E166-74.
191. Uysal, K.T., Wiesbrock, S.M., Marino, M.W., Hotamisligil, G.S. (1997) Protection from obesity-induced insulin resistance in mice lacking TNF-alpha function. *Nature* **389**, 610-4.
192. Medina, E.A., Afsari, R.R., Ravid, T., Castillo, S.S., Erickson, K.L., Goldkorn, T. (2005) Tumor necrosis factor- α decreases Akt protein levels in 3T3-L1 adipocytes via the caspase-dependent ubiquitination of Akt. *Endocrinology* **146**, 2726-35.
193. Boden, G. (2003) Effects of free fatty acids (FFA) on glucose metabolism: significance for insulin resistance and type 2 diabetes. *Exp Clin Endocrinol Diabetes* **111**, 121-4.
194. Boden, G., Cheung, P., Stein, T.P., Kresge, K., Mozzoli, M. (2002) FFA cause hepatic insulin resistance by inhibiting insulin suppression of glycogenolysis. *Am J Physiol Endocrinol Metab* **283**, E12-9.
195. Kishimoto, T. (1989) The biology of interleukin-6. *Blood* **74**, 1-10.

196. Hamid, Y.H., Urhammer, S.A., Jensen, D.P., Glumer, C., Borch-Johnsen, K., Jorgensen, T., Hansen, T., Pedersen, O. (2004) Variation in the interleukin-6 receptor gene associates with type 2 diabetes in Danish whites. *Diabetes* **53**, 3342-5.
197. Simpson, R.J., Hammacher, A., Smith, D.K., Matthews, J.M., Ward, L.D. (1997) Interleukin-6: structure-function relationships. *Protein Sci* **6**, 929-55.
198. Kamimura, D., Ishihara, K., Hirano, T. (2003) IL-6 signal transduction and its physiological roles: the signal orchestration model. *Rev Physiol Biochem Pharmacol* **149**, 1-38.
199. Ruderman, N.B., Keller, C., Richard, A.M., Saha, A.K., Luo, Z., Xiang, X., Giralt, M., Ritov, V.B., Menshikova, E.V., Kelley, D.E., Hidalgo, J., Pedersen, B.K., Kelly, M. (2006) Interleukin-6 regulation of AMP-activated protein kinase. Potential role in the systemic response to exercise and prevention of the metabolic syndrome. *Diabetes* **55 Suppl 2**, S48-54.
200. Kushner, I., Ganapathi, M., Schultz, D. (1989) The acute phase response is mediated by heterogeneous mechanisms. *Ann N Y Acad Sci* **557**, 19-29; discussion 29-30.
201. Kikkert, R., Bulder, I., de Groot, E.R., Aarden, L.A., Finkelman, M.A. (2007) Potentiation of Toll-like receptor-induced cytokine production by (1->3)-beta-D-glucans: implications for the monocyte activation test. *J Endotoxin Res* **13**, 140-9.
202. Chalifour, A., Jeannin, P., Gauchat, J.F., Blaecke, A., Malissard, M., N'Guyen, T., Thieblemont, N., Delneste, Y. (2004) Direct bacterial protein PAMP recognition by human NK cells involves TLRs and triggers alpha-defensin production. *Blood* **104**, 1778-83.
203. Mortensen, R.F. (2001) C-reactive protein, inflammation, and innate immunity. *Immunol Res* **24**, 163-76.
204. Hung, Y.J., Hsieh, C.H., Chen, Y.J., Pei, D., Kuo, S.W., Shen, D.C., Sheu, W.H., Chen, Y.C. (2007) Insulin sensitivity, proinflammatory markers and adiponectin in young males with different subtypes of depressive disorder. *Clin Endocrinol (Oxf)*.

205. Mohamed-Ali, V., Goodrick, S., Rawesh, A., Katz, D.R., Miles, J.M., Yudkin, J.S., Klein, S., Coppel, S.W. (1997) Subcutaneous adipose tissue releases interleukin-6, but not tumor necrosis factor-alpha, in vivo. *J Clin Endocrinol Metab* **82**, 4196-200.
206. Rotter, V., Nagaev, I., Smith, U. (2003) Interleukin-6 (IL-6) induces insulin resistance in 3T3-L1 adipocytes and is, like IL-8 and tumor necrosis factor-alpha, overexpressed in human fat cells from insulin-resistant subjects. *J Biol Chem* **278**, 45777-84.
207. Lagathu, C., Bastard, J.P., Auclair, M., Maachi, M., Capeau, J., Caron, M. (2003) Chronic interleukin-6 (IL-6) treatment increased IL-6 secretion and induced insulin resistance in adipocyte: prevention by rosiglitazone. *Biochem Biophys Res Commun* **311**, 372-9.
208. Fasshauer, M., Kralisch, S., Klier, M., Lossner, U., Bluher, M., Klein, J., Paschke, R. (2003) Adiponectin gene expression and secretion is inhibited by interleukin-6 in 3T3-L1 adipocytes. *Biochem Biophys Res Commun* **301**, 1045-50.
209. Pedersen, B.K., Steensberg, A., Fischer, C., Keller, C., Keller, P., Plomgaard, P., Wolsk-Petersen, E., Febbraio, M. (2004) The metabolic role of IL-6 produced during exercise: is IL-6 an exercise factor? *Proc Nutr Soc* **63**, 263-7.
210. Senn, J.J., Klover, P.J., Nowak, I.A., Zimmers, T.A., Koniaris, L.G., Furlanetto, R.W., Mooney, R.A. (2003) Suppressor of cytokine signaling-3 (SOCS-3), a potential mediator of interleukin-6-dependent insulin resistance in hepatocytes. *J Biol Chem* **278**, 13740-6.
211. Kristiansen, O.P., Mandrup-Poulsen, T. (2005) Interleukin-6 and diabetes: the good, the bad, or the indifferent? *Diabetes* **54 Suppl 2**, S114-24.
212. Dinarello, C.A. (1994) The interleukin-1 family: 10 years of discovery. *Faseb J* **8**, 1314-25.
213. Dunn, E., Sims, J.E., Nicklin, M.J., O'Neill, L.A. (2001) Annotating genes with potential roles in the immune system: six new members of the IL-1 family. *Trends Immunol* **22**, 533-6.

214. Vigers, G.P., Caffes, P., Evans, R.J., Thompson, R.C., Eisenberg, S.P., Brandhuber, B.J. (1994) X-ray structure of interleukin-1 receptor antagonist at 2.0-Å resolution. *J Biol Chem* **269**, 12874-9.
215. Symons, J.A., Eastgate, J.A., Duff, G.W. (1991) Purification and characterization of a novel soluble receptor for interleukin 1. *J Exp Med* **174**, 1251-4.
216. Welsh, N. (1996) Interleukin-1 beta-induced ceramide and diacylglycerol generation may lead to activation of the c-Jun NH₂-terminal kinase and the transcription factor ATF2 in the insulin-producing cell line RINm5F. *J Biol Chem* **271**, 8307-12.
217. Fernandez, M.C., Marucha, P.T., Rojas, I.G., Walters, J.D. (2000) The role of protein kinase C and calcium in induction of human polymorphonuclear leukocyte IL-1 beta gene expression by GM-CSF. *Cytokine* **12**, 445-9.
218. Voronov, E., Carmi, Y., Apte, R.N. (2007) Role of IL-1-mediated inflammation in tumor angiogenesis. *Adv Exp Med Biol* **601**, 265-70.
219. Gemma, C., Bickford, P.C. (2007) Interleukin-1beta and caspase-1: players in the regulation of age-related cognitive dysfunction. *Rev Neurosci* **18**, 137-48.
220. Nandakumar, K.S., Holmdahl, R. (2006) Antibody-induced arthritis: disease mechanisms and genes involved at the effector phase of arthritis. *Arthritis Res Ther* **8**, 223.
221. Trayhurn, P., Wood, I.S. (2005) Signalling role of adipose tissue: adipokines and inflammation in obesity. *Biochem Soc Trans* **33**, 1078-81.
222. Spranger, J., Kroke, A., Mohlig, M., Hoffmann, K., Bergmann, M.M., Ristow, M., Boeing, H., Pfeiffer, A.F. (2003) Inflammatory cytokines and the risk to develop type 2 diabetes: results of the prospective population-based European Prospective Investigation into Cancer and Nutrition (EPIC)-Potsdam Study. *Diabetes* **52**, 812-7.
223. Matsuki, T., Horai, R., Sudo, K., Iwakura, Y. (2003) IL-1 plays an important role in lipid metabolism by regulating insulin levels under physiological conditions. *J Exp Med* **198**, 877-88.

224. Beutler, B.A., Cerami, A. (1985) Recombinant interleukin 1 suppresses lipoprotein lipase activity in 3T3-L1 cells. *J Immunol* **135**, 3969-71.
225. Delikat, S., Harris, R.J., Galvani, D.W. (1993) IL-1 beta inhibits adipocyte formation in human long-term bone marrow culture. *Exp Hematol* **21**, 31-7.
226. Jager, J., Gremeaux, T., Cormont, M., Le Marchand-Brustel, Y., Tanti, J.F. (2007) Interleukin-1beta-induced insulin resistance in adipocytes through down-regulation of insulin receptor substrate-1 expression. *Endocrinology* **148**, 241-51.
227. Ailhaud, G. (2006) Adipose tissue as a secretory organ: from adipogenesis to the metabolic syndrome. *C R Biol* **329**, 570-7; discussion 653-5.
228. Nishimura, S., Manabe, I., Nagasaki, M., Hosoya, Y., Yamashita, H., Fujita, H., Ohsugi, M., Tobe, K., Kadowaki, T., Nagai, R., Sugiura, S. (2007) Adipogenesis in obesity requires close interplay between differentiating adipocytes, stromal cells, and blood vessels. *Diabetes* **56**, 1517-26.
229. Xu, H., Barnes, G.T., Yang, Q., Tan, G., Yang, D., Chou, C.J., Sole, J., Nichols, A., Ross, J.S., Tartaglia, L.A., Chen, H. (2003) Chronic inflammation in fat plays a crucial role in the development of obesity-related insulin resistance. *J Clin Invest* **112**, 1821-30.
230. Somm, E., Henrichot, E., Pernin, A., Juge-Aubry, C.E., Muzzin, P., Dayer, J.M., Nicklin, M.J., Meier, C.A. (2005) Decreased fat mass in interleukin-1 receptor antagonist-deficient mice: impact on adipogenesis, food intake, and energy expenditure. *Diabetes* **54**, 3503-9.
231. Hogan, J.C., Stephens, J.M. (2005) Effects of leukemia inhibitory factor on 3T3-L1 adipocytes. *J Endocrinol* **185**, 485-96.
232. Mellman, I., Warren, G. (2000) The road taken: past and future foundations of membrane traffic. *Cell* **100**, 99-112.
233. Alberts, B., Johnson, A., Lewis, J., Raff, M., Roberts, K., Walter, P. (2002) *Molecular biology of the cell*. Garland science, New York.

234. Duden, R. (2003) ER-to-Golgi transport: COP I and COP II function (Review). *Mol Membr Biol* **20**, 197-207.
235. Barlowe, C. (2003) Signals for COPII-dependent export from the ER: what's the ticket out? *Trends Cell Biol* **13**, 295-300.
236. Kahn, R.A., Gilman, A.G. (1986) The protein cofactor necessary for ADP-ribosylation of Gs by cholera toxin is itself a GTP binding protein. *J Biol Chem* **261**, 7906-11.
237. Cavenagh, M.M., Whitney, J.A., Carroll, K., Zhang, C., Boman, A.L., Rosenwald, A.G., Mellman, I., Kahn, R.A. (1996) Intracellular distribution of Arf proteins in mammalian cells. Arf6 is uniquely localized to the plasma membrane. *J Biol Chem* **271**, 21767-74.
238. Sabe, H. (2003) Requirement for Arf6 in cell adhesion, migration, and cancer cell invasion. *J Biochem (Tokyo)* **134**, 485-9.
239. Donaldson, J.G. (2003) Multiple roles for Arf6: sorting, structuring, and signaling at the plasma membrane. *J Biol Chem* **278**, 41573-6.
240. Chavrier, P., Goud, B. (1999) The role of ARF and Rab GTPases in membrane transport. *Curr Opin Cell Biol* **11**, 466-75.
241. Palacios, F., Price, L., Schweitzer, J., Collard, J.G., D'Souza-Schorey, C. (2001) An essential role for ARF6-regulated membrane traffic in adherens junction turnover and epithelial cell migration. *Embo J* **20**, 4973-86.
242. D'Souza-Schorey, C., Chavrier, P. (2006) ARF proteins: roles in membrane traffic and beyond. *Nat Rev Mol Cell Biol* **7**, 347-58.
243. Volpicelli-Daley, L.A., Li, Y., Zhang, C.J., Kahn, R.A. (2005) Isoform-selective effects of the depletion of ADP-ribosylation factors 1-5 on membrane traffic. *Mol Biol Cell* **16**, 4495-508.

244. Kahn, R.A., Volpicelli-Daley, L., Bowzard, B., Shrivastava-Ranjan, P., Li, Y., Zhou, C., Cunningham, L. (2005) Arf family GTPases: roles in membrane traffic and microtubule dynamics. *Biochem Soc Trans* **33**, 1269-72.
245. Robinson, M.S. (2004) Adaptable adaptors for coated vesicles. *Trends Cell Biol* **14**, 167-74.
246. Spang, A., Matsuoka, K., Hamamoto, S., Schekman, R., Orci, L. (1998) Coatamer, Arf1p, and nucleotide are required to bud coat protein complex I-coated vesicles from large synthetic liposomes. *Proc Natl Acad Sci U S A* **95**, 11199-204.
247. Robinson, M.S., Bonifacino, J.S. (2001) Adaptor-related proteins. *Curr Opin Cell Biol* **13**, 444-53.
248. Hinners, I., Tooze, S.A. (2003) Changing directions: clathrin-mediated transport between the Golgi and endosomes. *J Cell Sci* **116**, 763-71.
249. Tooze, S.A. (1998) Biogenesis of secretory granules in the trans-Golgi network of neuroendocrine and endocrine cells. *Biochim Biophys Acta* **1404**, 231-44.
250. Nakayama, K., Wakatsuki, S. (2003) The structure and function of GGAs, the traffic controllers at the TGN sorting crossroads. *Cell Struct Funct* **28**, 431-42.
251. Boman, A.L., Zhang, C., Zhu, X., Kahn, R.A. (2000) A family of ADP-ribosylation factor effectors that can alter membrane transport through the trans-Golgi. *Mol Biol Cell* **11**, 1241-55.
252. Lohi, O., Poussu, A., Mao, Y., Quioco, F., Lehto, V.P. (2002) VHS domain -- a longshoreman of vesicle lines. *FEBS Lett* **513**, 19-23.
253. Doray, B., Bruns, K., Ghosh, P., Kornfeld, S.A. (2002) Autoinhibition of the ligand-binding site of GGA1/3 VHS domains by an internal acidic cluster-dileucine motif. *Proc Natl Acad Sci U S A* **99**, 8072-7.

254. Puertollano, R., Aguilar, R.C., Gorshkova, I., Crouch, R.J., Bonifacino, J.S. (2001) Sorting of mannose 6-phosphate receptors mediated by the GGAs. *Science* **292**, 1712-6.
255. Dell'Angelica, E.C., Payne, G.S. (2001) Intracellular cycling of lysosomal enzyme receptors: cytoplasmic tails' tales. *Cell* **106**, 395-8.
256. Schultz, J., Doerks, T., Ponting, C.P., Copley, R.R., Bork, P. (2000) More than 1,000 putative new human signalling proteins revealed by EST data mining. *Nat Genet* **25**, 201-4.
257. Ali, B.R., Seabra, M.C. (2005) Targeting of Rab GTPases to cellular membranes. *Biochem Soc Trans* **33**, 652-6.
258. Kinsella, B.T., Maltese, W.A. (1992) rab GTP-binding proteins with three different carboxyl-terminal cysteine motifs are modified in vivo by 20-carbon isoprenoids. *J Biol Chem* **267**, 3940-5.
259. Pfeffer, S., Aivazian, D. (2004) Targeting Rab GTPases to distinct membrane compartments. *Nat Rev Mol Cell Biol* **5**, 886-96.
260. Ullrich, O., Stenmark, H., Alexandrov, K., Huber, L.A., Kaibuchi, K., Sasaki, T., Takai, Y., Zerial, M. (1993) Rab GDP dissociation inhibitor as a general regulator for the membrane association of rab proteins. *J Biol Chem* **268**, 18143-50.
261. Ali, B.R., Wasmeier, C., Lamoreux, L., Strom, M., Seabra, M.C. (2004) Multiple regions contribute to membrane targeting of Rab GTPases. *J Cell Sci* **117**, 6401-12.
262. Segev, N. (2001) Cell biology. A TIP about Rabs. *Science* **292**, 1313-4.
263. Dirac-Svejstrup, A.B., Sumizawa, T., Pfeffer, S.R. (1997) Identification of a GDI displacement factor that releases endosomal Rab GTPases from Rab-GDI. *Embo J* **16**, 465-72.

264. Lombardi, D., Soldati, T., Riederer, M.A., Goda, Y., Zerial, M., Pfeffer, S.R. (1993) Rab9 functions in transport between late endosomes and the trans Golgi network. *Embo J* **12**, 677-82.
265. Grosshans, B.L., Ortiz, D., Novick, P. (2006) Rabs and their effectors: achieving specificity in membrane traffic. *Proc Natl Acad Sci U S A* **103**, 11821-7.
266. Pfeffer, S. (2005) A model for Rab GTPase localization. *Biochem Soc Trans* **33**, 627-30.
267. Nuoffer, C., Davidson, H.W., Matteson, J., Meinkoth, J., Balch, W.E. (1994) A GDP-bound of rab1 inhibits protein export from the endoplasmic reticulum and transport between Golgi compartments. *J Cell Biol* **125**, 225-37.
268. Bucci, C., Wandinger-Ness, A., Lutcke, A., Chiariello, M., Bruni, C.B., Zerial, M. (1994) Rab5a is a common component of the apical and basolateral endocytic machinery in polarized epithelial cells. *Proc Natl Acad Sci U S A* **91**, 5061-5.
269. Barbero, P., Bittova, L., Pfeffer, S.R. (2002) Visualization of Rab9-mediated vesicle transport from endosomes to the trans-Golgi in living cells. *J Cell Biol* **156**, 511-8.
270. Bradley, R.L., Cleveland, K.A., Cheatham, B. (2001) The adipocyte as a secretory organ: mechanisms of vesicle transport and secretory pathways. *Recent Prog Horm Res* **56**, 329-58.
271. Kanzaki, M., Pessin, J.E. (2001) Insulin-stimulated GLUT4 translocation in adipocytes is dependent upon cortical actin remodeling. *J Biol Chem* **276**, 42436-44.
272. Kanzaki, M., Pessin, J.E. (2003) Insulin signaling: GLUT4 vesicles exit via the exocyst. *Curr Biol* **13**, R574-6.
273. Hashiramoto, M., James, D.E. (2000) Characterization of insulin-responsive GLUT4 storage vesicles isolated from 3T3-L1 adipocytes. *Mol Cell Biol* **20**, 416-27.

274. Martin, S.S., Haruta, T., Morris, A.J., Klippel, A., Williams, L.T., Olefsky, J.M. (1996) Activated phosphatidylinositol 3-kinase is sufficient to mediate actin rearrangement and GLUT4 translocation in 3T3-L1 adipocytes. *J Biol Chem* **271**, 17605-8.
275. Albiston, A.L., McDowall, S.G., Matsacos, D., Sim, P., Clune, E., Mustafa, T., Lee, J., Mendelsohn, F.A., Simpson, R.J., Connolly, L.M., Chai, S.Y. (2001) Evidence that the angiotensin IV (AT(4)) receptor is the enzyme insulin-regulated aminopeptidase. *J Biol Chem* **276**, 48623-6.
276. Ross, S.A., Scott, H.M., Morris, N.J., Leung, W.Y., Mao, F., Lienhard, G.E., Keller, S.R. (1996) Characterization of the insulin-regulated membrane aminopeptidase in 3T3-L1 adipocytes. *J Biol Chem* **271**, 3328-32.
277. Lampson, M.A., Racz, A., Cushman, S.W., McGraw, T.E. (2000) Demonstration of insulin-responsive trafficking of GLUT4 and vpTR in fibroblasts. *J Cell Sci* **113** (Pt 22), 4065-76.
278. Martin, O.J., Lee, A., McGraw, T.E. (2006) GLUT4 distribution between the plasma membrane and the intracellular compartments is maintained by an insulin-modulated bipartite dynamic mechanism. *J Biol Chem* **281**, 484-90.
279. Martin, S., Millar, C.A., Lyttle, C.T., Meerloo, T., Marsh, B.J., Gould, G.W., James, D.E. (2000) Effects of insulin on intracellular GLUT4 vesicles in adipocytes: evidence for a secretory mode of regulation. *J Cell Sci* **113 Pt 19**, 3427-38.
280. Chamberlain, L.H., Gould, G.W. (2002) The vesicle- and target-SNARE proteins that mediate Glut4 vesicle fusion are localized in detergent-insoluble lipid rafts present on distinct intracellular membranes. *J Biol Chem* **277**, 49750-4.
281. Pelham, H.R. (2004) Membrane traffic: GGAs sort ubiquitin. *Curr Biol* **14**, R357-9.
282. Karylowski, O., Zeigerer, A., Cohen, A., McGraw, T.E. (2004) GLUT4 is retained by an intracellular cycle of vesicle formation and fusion with endosomes. *Mol Biol Cell* **15**, 870-82.

283. Ewart, M.A., Clarke, M., Kane, S., Chamberlain, L.H., Gould, G.W. (2005) Evidence for a role of the exocyst in insulin-stimulated Glut4 trafficking in 3T3-L1 adipocytes. *J Biol Chem* **280**, 3812-6.
284. Satoh, S., Nishimura, H., Clark, A.E., Kozka, I.J., Vannucci, S.J., Simpson, I.A., Quon, M.J., Cushman, S.W., Holman, G.D. (1993) Use of bismannose photolabel to elucidate insulin-regulated GLUT4 subcellular trafficking kinetics in rat adipose cells. Evidence that exocytosis is a critical site of hormone action. *J Biol Chem* **268**, 17820-9.
285. Frevert, E.U., Bjorbaek, C., Venable, C.L., Keller, S.R., Kahn, B.B. (1998) Targeting of constitutively active phosphoinositide 3-kinase to GLUT4-containing vesicles in 3T3-L1 adipocytes. *J Biol Chem* **273**, 25480-7.
286. Zeigerer, A., McBrayer, M.K., McGraw, T.E. (2004) Insulin stimulation of GLUT4 exocytosis, but not its inhibition of endocytosis, is dependent on RabGAP AS160. *Mol Biol Cell* **15**, 4406-15.
287. Carey, A.L., Steinberg, G.R., Macaulay, S.L., Thomas, W.G., Holmes, A.G., Ramm, G., Prelovsek, O., Hohnen-Behrens, C., Watt, M.J., James, D.E., Kemp, B.E., Pedersen, B.K., Febbraio, M.A. (2006) Interleukin-6 increases insulin-stimulated glucose disposal in humans and glucose uptake and fatty acid oxidation in vitro via AMP-activated protein kinase. *Diabetes* **55**, 2688-97.
288. Larance, M., Ramm, G., James, D.E. (2007) The GLUT4 Code. *Mol Endocrinol*.
289. Barr, V.A., Malide, D., Zarnowski, M.J., Taylor, S.I., Cushman, S.W. (1997) Insulin stimulates both leptin secretion and production by rat white adipose tissue. *Endocrinology* **138**, 4463-72.
290. Roh, C., Thoidis, G., Farmer, S.R., Kandror, K.V. (2000) Identification and characterization of leptin-containing intracellular compartment in rat adipose cells. *Am J Physiol Endocrinol Metab* **279**, E893-9.
291. Shuldiner, A.R., Yang, R., Gong, D.W. (2001) Resistin, obesity and insulin resistance--the emerging role of the adipocyte as an endocrine organ. *N Engl J Med* **345**, 1345-6.

292. Hu, E., Liang, P., Spiegelman, B.M. (1996) AdipoQ is a novel adipose-specific gene dysregulated in obesity. *J Biol Chem* **271**, 10697-703.
293. Scherer, P.E., Williams, S., Fogliano, M., Baldini, G., Lodish, H.F. (1995) A novel serum protein similar to C1q, produced exclusively in adipocytes. *J Biol Chem* **270**, 26746-9.
294. Maeda, K., Okubo, K., Shimomura, I., Funahashi, T., Matsuzawa, Y., Matsubara, K. (1996) cDNA cloning and expression of a novel adipose specific collagen-like factor, apM1 (AdiPose Most abundant Gene transcript 1). *Biochem Biophys Res Commun* **221**, 286-9.
295. Nakano, Y., Tobe, T., Choi-Miura, N.H., Mazda, T., Tomita, M. (1996) Isolation and characterization of GBP28, a novel gelatin-binding protein purified from human plasma. *J Biochem (Tokyo)* **120**, 803-12.
296. Yamauchi, T., Kamon, J., Waki, H., Terauchi, Y., Kubota, N., Hara, K., Mori, Y., Ide, T., Murakami, K., Tsuboyama-Kasaoka, N., Ezaki, O., Akanuma, Y., Gavrilova, O., Vinson, C., Reitman, M.L., Kagechika, H., Shudo, K., Yoda, M., Nakano, Y., Tobe, K., Nagai, R., Kimura, S., Tomita, M., Froguel, P., Kadowaki, T. (2001) The fat-derived hormone adiponectin reverses insulin resistance associated with both lipoatrophy and obesity. *Nat Med* **7**, 941-6.
297. Tomas, E., Tsao, T.S., Saha, A.K., Murrey, H.E., Zhang Cc, C., Itani, S.I., Lodish, H.F., Ruderman, N.B. (2002) Enhanced muscle fat oxidation and glucose transport by ACRP30 globular domain: acetyl-CoA carboxylase inhibition and AMP-activated protein kinase activation. *Proc Natl Acad Sci U S A* **99**, 16309-13.
298. Yamauchi, T., Kamon, J., Minokoshi, Y., Ito, Y., Waki, H., Uchida, S., Yamashita, S., Noda, M., Kita, S., Ueki, K., Eto, K., Akanuma, Y., Froguel, P., Foufelle, F., Ferre, P., Carling, D., Kimura, S., Nagai, R., Kahn, B.B., Kadowaki, T. (2002) Adiponectin stimulates glucose utilization and fatty-acid oxidation by activating AMP-activated protein kinase. *Nat Med* **8**, 1288-95.
299. Arita, Y., Kihara, S., Ouchi, N., Takahashi, M., Maeda, K., Miyagawa, J., Hotta, K., Shimomura, I., Nakamura, T., Miyaoka, K., Kuriyama, H., Nishida, M., Yamashita, S., Okubo, K., Matsubara, K., Muraguchi, M., Ohmoto, Y., Funahashi, T., Matsuzawa, Y. (1999) Paradoxical decrease of an adipose-specific protein, adiponectin, in obesity. *Biochem Biophys Res Commun* **257**, 79-83.

300. Weyer, C., Funahashi, T., Tanaka, S., Hotta, K., Matsuzawa, Y., Pratley, R.E., Tataranni, P.A. (2001) Hypoadiponectinemia in obesity and type 2 diabetes: close association with insulin resistance and hyperinsulinemia. *J Clin Endocrinol Metab* **86**, 1930-5.
301. Heilbronn, L.K., Smith, S.R., Ravussin, E. (2003) The insulin-sensitizing role of the fat derived hormone adiponectin. *Curr Pharm Des* **9**, 1411-8.
302. Weiss, R., Dufour, S., Groszmann, A., Petersen, K., Dziura, J., Taksali, S.E., Shulman, G., Caprio, S. (2003) Low adiponectin levels in adolescent obesity: a marker of increased intramyocellular lipid accumulation. *J Clin Endocrinol Metab* **88**, 2014-8.
303. Pajvani, U.B., Scherer, P.E. (2003) Adiponectin: systemic contributor to insulin sensitivity. *Curr Diab Rep* **3**, 207-13.
304. Stepan, C.M., Lazar, M.A. (2002) Resistin and obesity-associated insulin resistance. *Trends Endocrinol Metab* **13**, 18-23.
305. Ukkola, O., Santaniemi, M. (2002) Adiponectin: a link between excess adiposity and associated comorbidities? *J Mol Med* **80**, 696-702.
306. Tschritter, O., Fritsche, A., Thamer, C., Haap, M., Shirkavand, F., Rahe, S., Staiger, H., Maerker, E., Haring, H., Stumvoll, M. (2003) Plasma adiponectin concentrations predict insulin sensitivity of both glucose and lipid metabolism. *Diabetes* **52**, 239-43.
307. Hotta, K., Funahashi, T., Arita, Y., Takahashi, M., Matsuda, M., Okamoto, Y., Iwahashi, H., Kuriyama, H., Ouchi, N., Maeda, K., Nishida, M., Kihara, S., Sakai, N., Nakajima, T., Hasegawa, K., Muraguchi, M., Ohmoto, Y., Nakamura, T., Yamashita, S., Hanafusa, T., Matsuzawa, Y. (2000) Plasma concentrations of a novel, adipose-specific protein, adiponectin, in type 2 diabetic patients. *Arterioscler Thromb Vasc Biol* **20**, 1595-9.
308. Statnick, M.A., Beavers, L.S., Conner, L.J., Corominola, H., Johnson, D., Hammond, C.D., Rafaeloff-Phail, R., Seng, T., Suter, T.M., Sluka, J.P., Ravussin, E., Gadski, R.A., Caro, J.F. (2000) Decreased expression of apM1 in omental and subcutaneous adipose tissue of humans with type 2 diabetes. *Int J Exp Diabetes Res* **1**, 81-8.

309. Lihn, A.S., Ostergard, T., Nyholm, B., Pedersen, S.B., Richelsen, B., Schmitz, O. (2003) Adiponectin expression in adipose tissue is reduced in first-degree relatives of type 2 diabetic patients. *Am J Physiol Endocrinol Metab* **284**, E443-8.
310. Fisher, F.M., McTernan, P.G., Valsamakis, G., Chetty, R., Harte, A.L., Anwar, A.J., Starcynski, J., Crocker, J., Barnett, A.H., McTernan, C.L., Kumar, S. (2002) Differences in adiponectin protein expression: effect of fat depots and type 2 diabetic status. *Horm Metab Res* **34**, 650-4.
311. Mohamed-Ali, V., Pinkney, J.H., Coppack, S.W. (1998) Adipose tissue as an endocrine and paracrine organ. *Int J Obes Relat Metab Disord* **22**, 1145-58.
312. Takatsu, H., Katoh, Y., Shiba, Y., Nakayama, K. (2001) Golgi-localizing, gamma-adaptin ear homology domain, ADP-ribosylation factor-binding (GGA) proteins interact with acidic dileucine sequences within the cytoplasmic domains of sorting receptors through their Vps27p/Hrs/STAM (VHS) domains. *J Biol Chem* **276**, 28541-5.
313. Misra, S., Puertollano, R., Kato, Y., Bonifacino, J.S., Hurley, J.H. (2002) Structural basis for acidic-cluster-dileucine sorting-signal recognition by VHS domains. *Nature* **415**, 933-7.
314. Nielsen, M.S., Madsen, P., Christensen, E.I., Nykjaer, A., Gliemann, J., Kasper, D., Pohlmann, R., Petersen, C.M. (2001) The sortilin cytoplasmic tail conveys Golgi-endosome transport and binds the VHS domain of the GGA2 sorting protein. *Embo J* **20**, 2180-90.
315. He, X., Chang, W.P., Koelsch, G., Tang, J. (2002) Memapsin 2 (beta-secretase) cytosolic domain binds to the VHS domains of GGA1 and GGA2: implications on the endocytosis mechanism of memapsin 2. *FEBS Lett* **524**, 183-7.
316. Puertollano, R., Randazzo, P.A., Presley, J.F., Hartnell, L.M., Bonifacino, J.S. (2001) The GGAs promote ARF-dependent recruitment of clathrin to the TGN. *Cell* **105**, 93-102.
317. Takatsu, H., Yoshino, K., Toda, K., Nakayama, K. (2002) GGA proteins associate with Golgi membranes through interaction between their GGAH domains and ADP-ribosylation factors. *Biochem J* **365**, 369-78.

318. Dell'Angelica, E.C., Puertollano, R., Mullins, C., Aguilar, R.C., Vargas, J.D., Hartnell, L.M., Bonifacino, J.S. (2000) GGAs: a family of ADP ribosylation factor-binding proteins related to adaptors and associated with the Golgi complex. *J Cell Biol* **149**, 81-94.
319. Boman, A.L. (2001) GGA proteins: new players in the sorting game. *J Cell Sci* **114**, 3413-8.
320. Zhu, Y., Doray, B., Poussu, A., Lehto, V.P., Kornfeld, S. (2001) Binding of GGA2 to the lysosomal enzyme sorting motif of the mannose 6-phosphate receptor. *Science* **292**, 1716-8.
321. Mattera, R., Arighi, C.N., Lodge, R., Zerial, M., Bonifacino, J.S. (2003) Divalent interaction of the GGAs with the Rabaptin-5-Rabex-5 complex. *Embo J* **22**, 78-88.
322. Wasiak, S., Legendre-Guillemain, V., Puertollano, R., Blondeau, F., Girard, M., de Heuvel, E., Boismenu, D., Bell, A.W., Bonifacino, J.S., McPherson, P.S. (2002) Enthoprotin: a novel clathrin-associated protein identified through subcellular proteomics. *J Cell Biol* **158**, 855-62.
323. Takatsu, H., Yoshino, K., Nakayama, K. (2000) Adaptor gamma ear homology domain conserved in gamma-adaptin and GGA proteins that interact with gamma-synergin. *Biochem Biophys Res Commun* **271**, 719-25.
324. Puertollano, R., Bonifacino, J.S. (2004) Interactions of GGA3 with the ubiquitin sorting machinery. *Nat Cell Biol* **6**, 244-51.
325. Elmendorf, J.S., Chen, D., Pessin, J.E. (1998) Guanosine 5'-O-(3-thiotriphosphate) (GTPgammaS) stimulation of GLUT4 translocation is tyrosine kinase-dependent. *J Biol Chem* **273**, 13289-96.
326. Simon, J.P., Ivanov, I.E., Adesnik, M., Sabatini, D.D. (2000) In vitro generation from the trans-Golgi network of coatomer-coated vesicles containing sialylated vesicular stomatitis virus-G protein. *Methods* **20**, 437-54.

327. Morinaga, N., Tsai, S.C., Moss, J., Vaughan, M. (1996) Isolation of a brefeldin A-inhibited guanine nucleotide-exchange protein for ADP ribosylation factor (ARF) 1 and ARF3 that contains a Sec7-like domain. *Proc Natl Acad Sci U S A* **93**, 12856-60.
328. Klausner, R.D., Donaldson, J.G., Lippincott-Schwartz, J. (1992) Brefeldin A: insights into the control of membrane traffic and organelle structure. *J Cell Biol* **116**, 1071-80.
329. Cherfils, J., Chardin, P. (1999) GEFs: structural basis for their activation of small GTP-binding proteins. *Trends Biochem Sci* **24**, 306-11.
330. Bogan, J.S., Lodish, H.F. (1999) Two compartments for insulin-stimulated exocytosis in 3T3-L1 adipocytes defined by endogenous ACRP30 and GLUT4. *J Cell Biol* **146**, 609-20.
331. Zhu, G., He, X., Zhai, P., Terzyan, S., Tang, J., Zhang, X.C. (2003) Crystal structure of GGA2 VHS domain and its implication in plasticity in the ligand binding pocket. *FEBS Lett* **537**, 171-6.
332. Guerre-Millo, M. (2004) Adipose tissue and adipokines: for better or worse. *Diabetes Metab* **30**, 13-9.
333. Klaus, S. (2004) Adipose tissue as a regulator of energy balance. *Curr Drug Targets* **5**, 241-50.
334. Marti, A., Berraondo, B., Martinez, J.A. (1999) Leptin: physiological actions. *J Physiol Biochem* **55**, 43-9.
335. Moran, O., Phillip, M. (2003) Leptin: obesity, diabetes and other peripheral effects--a review. *Pediatr Diabetes* **4**, 101-9.
336. Trayhurn, P. (2003) Leptin--a critical body weight signal and a "master" hormone? *Sci STKE* **2003**, PE7.

337. Minokoshi, Y., Kim, Y.B., Peroni, O.D., Fryer, L.G., Muller, C., Carling, D., Kahn, B.B. (2002) Leptin stimulates fatty-acid oxidation by activating AMP-activated protein kinase. *Nature* **415**, 339-43.
338. Couillard, C., Mauriege, P., Imbeault, P., Prud'homme, D., Nadeau, A., Tremblay, A., Bouchard, C., Despres, J.P. (2000) Hyperleptinemia is more closely associated with adipose cell hypertrophy than with adipose tissue hyperplasia. *Int J Obes Relat Metab Disord* **24**, 782-8.
339. Houseknecht, K.L., Baile, C.A., Matteri, R.L., Spurlock, M.E. (1998) The biology of leptin: a review. *J Anim Sci* **76**, 1405-20.
340. Diamond, F.B., Jr., Cuthbertson, D., Hanna, S., Eichler, D. (2004) Correlates of adiponectin and the leptin/adiponectin ratio in obese and non-obese children. *J Pediatr Endocrinol Metab* **17**, 1069-75.
341. Considine, R.V., Sinha, M.K., Heiman, M.L., Kriauciunas, A., Stephens, T.W., Nyce, M.R., Ohannesian, J.P., Marco, C.C., McKee, L.J., Bauer, T.L., et al. (1996) Serum immunoreactive-leptin concentrations in normal-weight and obese humans. *N Engl J Med* **334**, 292-5.
342. Kolaczynski, J.W., Nyce, M.R., Considine, R.V., Boden, G., Nolan, J.J., Henry, R., Mudaliar, S.R., Olefsky, J., Caro, J.F. (1996) Acute and chronic effects of insulin on leptin production in humans: Studies in vivo and in vitro. *Diabetes* **45**, 699-701.
343. Pappaspyrou-Rao, S., Schneider, S.H., Petersen, R.N., Fried, S.K. (1997) Dexamethasone increases leptin expression in humans in vivo. *J Clin Endocrinol Metab* **82**, 1635-7.
344. Lee, M.J., Wang, Y., Ricci, M.R., Sullivan, S., Russell, C.D., Fried, S.K. (2007) Acute and chronic regulation of leptin synthesis, storage, and secretion by insulin and dexamethasone in human adipose tissue. *Am J Physiol Endocrinol Metab* **292**, E858-64.
345. Russell, C.D., Petersen, R.N., Rao, S.P., Ricci, M.R., Prasad, A., Zhang, Y., Brodin, R.E., Fried, S.K. (1998) Leptin expression in adipose tissue from obese humans: depot-specific regulation by insulin and dexamethasone. *Am J Physiol* **275**, E507-15.

346. Cammisotto, P.G., Gelinas, Y., Deshaies, Y., Bukowiecki, L.J. (2003) Regulation of leptin secretion from white adipocytes by free fatty acids. *Am J Physiol Endocrinol Metab* **285**, E521-6.
347. Cammisotto, P.G., Gelinas, Y., Deshaies, Y., Bukowiecki, L.J. (2005) Regulation of leptin secretion from white adipocytes by insulin, glycolytic substrates, and amino acids. *Am J Physiol Endocrinol Metab* **289**, E166-71.
348. Trayhurn, P., Duncan, J.S., Rayner, D.V., Hardie, L.J. (1996) Rapid inhibition of ob gene expression and circulating leptin levels in lean mice by the beta 3-adrenoceptor agonists BRL 35135A and ZD2079. *Biochem Biophys Res Commun* **228**, 605-10.
349. Ricci, M.R., Lee, M.J., Russell, C.D., Wang, Y., Sullivan, S., Schneider, S.H., Brodin, R.E., Fried, S.K. (2005) Isoproterenol decreases leptin release from rat and human adipose tissue through posttranscriptional mechanisms. *Am J Physiol Endocrinol Metab* **288**, E798-804.
350. Donahoo, W.T., Jensen, D.R., Yost, T.J., Eckel, R.H. (1997) Isoproterenol and somatostatin decrease plasma leptin in humans: a novel mechanism regulating leptin secretion. *J Clin Endocrinol Metab* **82**, 4139-43.
351. Motoshima, H., Wu, X., Sinha, M.K., Hardy, V.E., Rosato, E.L., Barbot, D.J., Rosato, F.E., Goldstein, B.J. (2002) Differential regulation of adiponectin secretion from cultured human omental and subcutaneous adipocytes: effects of insulin and rosiglitazone. *J Clin Endocrinol Metab* **87**, 5662-7.
352. Halleux, C.M., Takahashi, M., Delporte, M.L., Detry, R., Funahashi, T., Matsuzawa, Y., Brichard, S.M. (2001) Secretion of adiponectin and regulation of apM1 gene expression in human visceral adipose tissue. *Biochem Biophys Res Commun* **288**, 1102-7.
353. Maeda, N., Takahashi, M., Funahashi, T., Kihara, S., Nishizawa, H., Kishida, K., Nagaretani, H., Matsuda, M., Komuro, R., Ouchi, N., Kuriyama, H., Hotta, K., Nakamura, T., Shimomura, I., Matsuzawa, Y. (2001) PPARgamma ligands increase expression and plasma concentrations of adiponectin, an adipose-derived protein. *Diabetes* **50**, 2094-9.

354. Yu, J.G., Javorschi, S., Hevener, A.L., Kruszynska, Y.T., Norman, R.A., Sinha, M., Olefsky, J.M. (2002) The effect of thiazolidinediones on plasma adiponectin levels in normal, obese, and type 2 diabetic subjects. *Diabetes* **51**, 2968-74.
355. Pajvani, U.B., Hawkins, M., Combs, T.P., Rajala, M.W., Doebber, T., Berger, J.P., Wagner, J.A., Wu, M., Knopps, A., Xiang, A.H., Utzschneider, K.M., Kahn, S.E., Olefsky, J.M., Buchanan, T.A., Scherer, P.E. (2004) Complex distribution, not absolute amount of adiponectin, correlates with thiazolidinedione-mediated improvement in insulin sensitivity. *J Biol Chem* **279**, 12152-62.
356. Xie, L., Boyle, D., Sanford, D., Scherer, P.E., Pessin, J.E., Mora, S. (2006) Intracellular trafficking and secretion of adiponectin is dependent on GGA-coated vesicles. *J Biol Chem* **281**, 7253-9.
357. Roh, C., Roduit, R., Thorens, B., Fried, S., Kandror, K.V. (2001) Lipoprotein lipase and leptin are accumulated in different secretory compartments in rat adipocytes. *J Biol Chem* **276**, 35990-4.
358. Weber, T., Joost, J., Simpson, I., Cushman, S (1988) Methods for assessment of glucose transport activity and the number of glucose transporters in isolated rat adipose cells and membrane fractions.
359. Livingstone, C., James, D.E., Rice, J.E., Hanpeter, D., Gould, G.W. (1996) Compartment ablation analysis of the insulin-responsive glucose transporter (GLUT4) in 3T3-L1 adipocytes. *Biochem J* **315** (Pt 2), 487-95.
360. Chardin, P., McCormick, F. (1999) Brefeldin A: the advantage of being uncompetitive. *Cell* **97**, 153-5.
361. Bonifacino, J.S. (2004) The GGA proteins: adaptors on the move. *Nat Rev Mol Cell Biol* **5**, 23-32.
362. Liljedahl, M., Maeda, Y., Colanzi, A., Ayala, I., Van Lint, J., Malhotra, V. (2001) Protein kinase D regulates the fission of cell surface destined transport carriers from the trans-Golgi network. *Cell* **104**, 409-20.

363. Ghanekar, Y., Lowe, M. (2005) Protein kinase D: activation for Golgi carrier formation. *Trends Cell Biol* **15**, 511-4.
364. Iglesias, T., Rozengurt, E. (1998) Protein kinase D activation by mutations within its pleckstrin homology domain. *J Biol Chem* **273**, 410-6.
365. Kitagawa, K., Rosen, B.S., Spiegelman, B.M., Lienhard, G.E., Tanner, L.I. (1989) Insulin stimulates the acute release of adiponin from 3T3-L1 adipocytes. *Biochim Biophys Acta* **1014**, 83-9.
366. Millar, C.A., Meerloo, T., Martin, S., Hickson, G.R., Shimwell, N.J., Wakelam, M.J., James, D.E., Gould, G.W. (2000) Adiponin and the glucose transporter GLUT4 traffic to the cell surface via independent pathways in adipocytes. *Traffic* **1**, 141-51.
367. Clarke, M., Ewart, M.A., Santy, L.C., Prekeris, R., Gould, G.W. (2006) ACRP30 is secreted from 3T3-L1 adipocytes via a Rab11-dependent pathway. *Biochem Biophys Res Commun* **342**, 1361-7.
368. Maeda, Y., Beznoussenko, G.V., Van Lint, J., Mironov, A.A., Malhotra, V. (2001) Recruitment of protein kinase D to the trans-Golgi network via the first cysteine-rich domain. *Embo J* **20**, 5982-90.
369. Hotamisligil, G.S. (2006) Inflammation and metabolic disorders. *Nature* **444**, 860-7.
370. Wellen, K.E., Hotamisligil, G.S. (2005) Inflammation, stress, and diabetes. *J Clin Invest* **115**, 1111-9.
371. Hauner, H. (2004) The new concept of adipose tissue function. *Physiol Behav* **83**, 653-8.
372. Bluher, M., Fasshauer, M., Tonjes, A., Kratzsch, J., Schon, M.R., Paschke, R. (2005) Association of interleukin-6, C-reactive protein, interleukin-10 and adiponectin plasma concentrations with measures of obesity, insulin sensitivity and glucose metabolism. *Exp Clin Endocrinol Diabetes* **113**, 534-7.

373. Zoccali, C., Mallamaci, F., Tripepi, G. (2003) Adipose tissue as a source of inflammatory cytokines in health and disease: focus on end-stage renal disease. *Kidney Int Suppl*, S65-8.
374. De Taeye, B., Novitskaya, T., McGuinness, O.P., Gleaves, L., Medda, M., Covington, J.W., Vaughan, D.E. (2007) Macrophage TNF- α contributes to insulin resistance and hepatic steatosis in diet-induced obesity. *Am J Physiol Endocrinol Metab*.
375. Ventre, J., Doebber, T., Wu, M., MacNaul, K., Stevens, K., Pasparakis, M., Kollias, G., Moller, D.E. (1997) Targeted disruption of the tumor necrosis factor- α gene: metabolic consequences in obese and nonobese mice. *Diabetes* **46**, 1526-31.
376. Stouthard, J.M., Oude Elferink, R.P., Sauerwein, H.P. (1996) Interleukin-6 enhances glucose transport in 3T3-L1 adipocytes. *Biochem Biophys Res Commun* **220**, 241-5.
377. Lagathu, C., Yvan-Charvet, L., Bastard, J.P., Maachi, M., Quignard-Boulange, A., Capeau, J., Caron, M. (2006) Long-term treatment with interleukin-1 β induces insulin resistance in murine and human adipocytes. *Diabetologia* **49**, 2162-73.
378. Beharka, A.A., Armstrong, J.W., Chapes, S.K. (1998) Macrophage cell lines derived from major histocompatibility complex II-negative mice. *In Vitro Cell Dev Biol Anim* **34**, 499-507.
379. Mora, S., Durham, P.L., Smith, J.R., Russo, A.F., Jeromin, A., Pessin, J.E. (2002) NCS-1 inhibits insulin-stimulated GLUT4 translocation in 3T3L1 adipocytes through a phosphatidylinositol 4-kinase-dependent pathway. *J Biol Chem* **277**, 27494-500.
380. Chapes, S.K., Beharka, A.A. (1995) Lipopolysaccharide is required for the lethal effects of enterotoxin B after D-galactosamine sensitization. *J. Endotoxin Res.* **2**, 263-271.
381. Kanzaki, M. (2006) Insulin receptor signals regulating GLUT4 translocation and actin dynamics. *Endocr J* **53**, 267-93.
382. Lacasa, D., Taleb, S., Keophiphath, M., Miranville, A., Clement, K. (2007) Macrophage-secreted factors impair human adipogenesis: involvement of proinflammatory state in preadipocytes. *Endocrinology* **148**, 868-77.

383. Guilbert, J.J. (2003) The world health report 2002 - reducing risks, promoting healthy life. *Educ Health (Abingdon)* **16**, 230.
384. Lazar, M.A. (2005) How obesity causes diabetes: not a tall tale. *Science* **307**, 373-5.
385. Marette, A., Richardson, J.M., Ramlal, T., Balon, T.W., Vranic, M., Pessin, J.E., Klip, A. (1992) Abundance, localization, and insulin-induced translocation of glucose transporters in red and white muscle. *Am J Physiol* **263**, C443-52.
386. Suganami, T., Nishida, J., Ogawa, Y. (2005) A paracrine loop between adipocytes and macrophages aggravates inflammatory changes: role of free fatty acids and tumor necrosis factor alpha. *Arterioscler Thromb Vasc Biol* **25**, 2062-8.
387. Miskolci, V., Rollins, J., Vu, H.Y., Ghosh, C.C., Davidson, D., Vancurova, I. (2007) NFkappaB is persistently activated in continuously stimulated human neutrophils. *Mol Med* **13**, 134-42.
388. Stephens, J.M., Pekala, P.H. (1991) Transcriptional repression of the GLUT4 and C/EBP genes in 3T3-L1 adipocytes by tumor necrosis factor-alpha. *J Biol Chem* **266**, 21839-45.
389. Long, S.D., Pekala, P.H. (1996) Lipid mediators of insulin resistance: ceramide signalling down-regulates GLUT4 gene transcription in 3T3-L1 adipocytes. *Biochem J* **319** (Pt 1), 179-84.
390. Niu, W., Huang, C., Nawaz, Z., Levy, M., Somwar, R., Li, D., Bilan, P.J., Klip, A. (2003) Maturation of the regulation of GLUT4 activity by p38 MAPK during L6 cell myogenesis. *J Biol Chem* **278**, 17953-62.
391. Fernandez-Veledo, S., Hernandez, R., Teruel, T., Mas, J.A., Ros, M., Lorenzo, M. (2006) Ceramide mediates TNF-alpha-induced insulin resistance on GLUT4 gene expression in brown adipocytes. *Arch Physiol Biochem* **112**, 13-22.
392. Sun, C., Zhang, F., Ge, X., Yan, T., Chen, X., Shi, X., Zhai, Q. (2007) SIRT1 improves insulin sensitivity under insulin-resistant conditions by repressing PTP1B. *Cell Metab* **6**, 307-19.

393. Wang, B., Trayhurn, P. (2006) Acute and prolonged effects of TNF-alpha on the expression and secretion of inflammation-related adipokines by human adipocytes differentiated in culture. *Pflugers Arch* **452**, 418-27.
394. He, A., Liu, X., Liu, L., Chang, Y., Fang, F. (2007) How many signals impinge on GLUT4 activation by insulin? *Cell Signal* **19**, 1-7.
395. Constant, V.A., Gagnon, A., Landry, A., Sorisky, A. (2006) Macrophage-conditioned medium inhibits the differentiation of 3T3-L1 and human abdominal preadipocytes. *Diabetologia* **49**, 1402-11.
396. Ruan, H., Hacoen, N., Golub, T.R., Van Parijs, L., Lodish, H.F. (2002) Tumor necrosis factor-alpha suppresses adipocyte-specific genes and activates expression of preadipocyte genes in 3T3-L1 adipocytes: nuclear factor-kappaB activation by TNF-alpha is obligatory. *Diabetes* **51**, 1319-36.
397. Suzawa, M., Takada, I., Yanagisawa, J., Ohtake, F., Ogawa, S., Yamauchi, T., Kadowaki, T., Takeuchi, Y., Shibuya, H., Gotoh, Y., Matsumoto, K., Kato, S. (2003) Cytokines suppress adipogenesis and PPAR-gamma function through the TAK1/TAB1/NIK cascade. *Nat Cell Biol* **5**, 224-30.
398. Xing, H., Northrop, J.P., Grove, J.R., Kilpatrick, K.E., Su, J.L., Ringold, G.M. (1997) TNF alpha-mediated inhibition and reversal of adipocyte differentiation is accompanied by suppressed expression of PPARgamma without effects on Pref-1 expression. *Endocrinology* **138**, 2776-83.
399. Rutherford, M.S., Witsell, A., Schook, L.B. (1993) Mechanisms generating functionally heterogeneous macrophages: chaos revisited. *J Leukoc Biol* **53**, 602-18.
400. McCormack, J.M., Leenen, P.J., Walker, W.S. (1993) Macrophage progenitors from mouse bone marrow and spleen differ in their expression of the Ly-6C differentiation antigen. *J Immunol* **151**, 6389-98.
401. Laskin, D.L., Weinberger, B., Laskin, J.D. (2001) Functional heterogeneity in liver and lung macrophages. *J Leukoc Biol* **70**, 163-70.

402. Stout, R.D., Suttles, J. (2004) Functional plasticity of macrophages: reversible adaptation to changing microenvironments. *J Leukoc Biol* **76**, 509-13.
403. Hansen, J.B., Kristiansen, K. (2006) Regulatory circuits controlling white versus brown adipocyte differentiation. *Biochem J* **398**, 153-68.
404. Adachi, K., Miki, M., Tamai, H., Tokuda, M., Mino, M. (1990) Adipose tissues and vitamin E. *J Nutr Sci Vitaminol (Tokyo)* **36**, 327-37.
405. Himms-Hagen, J. (1990) Brown adipose tissue thermogenesis: interdisciplinary studies. *Faseb J* **4**, 2890-8.
406. Csehi, S.B., Mathieu, S., Seifert, U., Lange, A., Zweyer, M., Wernig, A., Adam, D. (2005) Tumor necrosis factor (TNF) interferes with insulin signaling through the p55 TNF receptor death domain. *Biochem Biophys Res Commun* **329**, 397-405.
407. Permana, P.A., Menge, C., Reaven, P.D. (2006) Macrophage-secreted factors induce adipocyte inflammation and insulin resistance. *Biochem Biophys Res Commun* **341**, 507-14.
408. Mantovani, A., Allavena, P., Sica, A. (2004) Tumour-associated macrophages as a prototypic type II polarised phagocyte population: role in tumour progression. *Eur J Cancer* **40**, 1660-7.
409. Ghassabeh, G.H., De Baetselier, P., Brys, L., Noel, W., Van Ginderachter, J.A., Meerschaut, S., Beschin, A., Brombacher, F., Raes, G. (2006) Identification of a common gene signature for type II cytokine-associated myeloid cells elicited in vivo in different pathologic conditions. *Blood* **108**, 575-83.
410. Potts, B., Chapes, S. (2008) Functions of C2D macrophage cells after adoptive transfer. *J Leukoc Biol*.
411. Rodbell, M. (1964) Metabolism of Isolated Fat Cells. I. Effects of Hormones on Glucose Metabolism and Lipolysis. *J Biol Chem* **239**, 375-80.

412. Potts, B.E., Hart., M.L., Snyder , L.L., Boyle, D., Mosier, D.A., Chapes, S. (2008) Differentiation of C2D macrophage cells after adoptive transfer. *Clin. Vaccine Immunol.*
413. Leenen, P.J., Kroos, M.J., Melis, M., Slieker, W.A., van Ewijk, W., van Eijk, H.G. (1990) Differential inhibition of macrophage proliferation by anti-transferrin receptor antibody ER-MP21: correlation to macrophage differentiation stage. *Exp Cell Res* **189**, 55-63.
414. Stout, R.D., Suttles, J. (2005) Immunosenescence and macrophage functional plasticity: dysregulation of macrophage function by age-associated microenvironmental changes. *Immunol Rev* **205**, 60-71.
415. Stout, R.D., Jiang, C., Matta, B., Tietzel, I., Watkins, S.K., Suttles, J. (2005) Macrophages sequentially change their functional phenotype in response to changes in microenvironmental influences. *J Immunol* **175**, 342-9.
416. Rosen, E.D., MacDougald, O.A. (2006) Adipocyte differentiation from the inside out. *Nat Rev Mol Cell Biol* **7**, 885-96.
417. Canello, R., Tordjman, J., Poitou, C., Guilhem, G., Bouillot, J.L., Hugol, D., Coussieu, C., Basdevant, A., Bar Hen, A., Bedossa, P., Guerre-Millo, M., Clement, K. (2006) Increased infiltration of macrophages in omental adipose tissue is associated with marked hepatic lesions in morbid human obesity. *Diabetes* **55**, 1554-61.
418. Curat, C.A., Wegner, V., Sengenès, C., Miranville, A., Tonus, C., Busse, R., Bouloumie, A. (2006) Macrophages in human visceral adipose tissue: increased accumulation in obesity and a source of resistin and visfatin. *Diabetologia* **49**, 744-7.
419. Bouloumie, A., Curat, C.A., Sengenès, C., Lolmede, K., Miranville, A., Busse, R. (2005) Role of macrophage tissue infiltration in metabolic diseases. *Curr Opin Clin Nutr Metab Care* **8**, 347-54.
420. Liu, T., Jin, H., Ullenbruch, M., Hu, B., Hashimoto, N., Moore, B., McKenzie, A., Lukacs, N.W., Phan, S.H. (2004) Regulation of found in inflammatory zone 1 expression in bleomycin-induced lung fibrosis: role of IL-4/IL-13 and mediation via STAT-6. *J Immunol* **173**, 3425-31.

421. Lumeng, C.N., Deyoung, S.M., Bodzin, J.L., Saltiel, A.R. (2007) Increased inflammatory properties of adipose tissue macrophages recruited during diet-induced obesity. *Diabetes* **56**, 16-23.
422. Wellen, K.E., Hotamisligil, G.S. (2003) Obesity-induced inflammatory changes in adipose tissue. *J Clin Invest* **112**, 1785-8.
423. Koyama, Y., Yamanoha, B., Yoshida, T. (1990) A novel monoclonal antibody induces the differentiation of monocyte leukemic cells. *Biochem Biophys Res Commun* **168**, 898-904.
424. Armstrong, J.W., Chapes, S.K. (1994) Effects of extracellular matrix proteins on macrophage differentiation, growth, and function: comparison of liquid and agar culture systems. *J Exp Zool* **269**, 178-87.
425. Kennedy, D.W., Abkowitz, J.L. (1998) Mature monocytic cells enter tissues and engraft. *Proc Natl Acad Sci U S A* **95**, 14944-9.
426. Neels, J.G., Olefsky, J.M. (2006) Inflamed fat: what starts the fire? *J Clin Invest* **116**, 33-5.
427. Bose, A., Guilherme, A., Huang, S., Hubbard, A.C., Lane, C.R., Soriano, N.A., Czech, M.P. (2005) The v-SNARE Vti1a regulates insulin-stimulated glucose transport and Acp30 secretion in 3T3-L1 adipocytes. *J Biol Chem* **280**, 36946-51.